National Technical University of Athens

School of Civil Engineering

Institute of Steel Structures

Seismic actions and response of steel storage pallet racks- A numerical investigation

Doctoral Thesis of

Konstantinos P. Adamakos

Athens 2018

National Technical University of Athens
School of Civil Engineering
Institute of Steel Structures

Seismic actions and response of steel storage pallet racks- A numerical investigation

Doctoral Thesis of

Konstantinos P. Adamakos

ADVISORY COMMITTEE:
1. I. VAYAS, Professor N.T.U.A. (supervisor)
2. C. GANTES, Professor N.T.U.A.
3. C. MOUZAKIS, Assistant Professor N.T.U.A.

EXAMINATION COMMITTEE:
1. I. VAYAS, Professor N.T.U.A. (supervisor)
2. C. GANTES, Professor N.T.U.A.
3. C. MOUZAKIS, Assistant Professor N.T.U.A.
4. I. PSYHARIS, Professor N.T.U.A.
5. D. VAMVATSIKOS, Assistant Professor N.T.U.A.
6. C. CASTIGLIONI, Professor POLIMI
7. B. HOFFMEISTER, Professor RWTH AACHEN

Athens 2018

ΕΘΝΙΚΟ ΜΕΤΣΟΒΙΟ ΠΟΛΥΤΕΧΝΕΙΟ
ΣΧΟΛΗ ΠΟΛΙΤΙΚΩΝ ΜΗΧΑΝΙΚΩΝ
ΕΡΓΑΣΤΗΡΙΟ ΜΕΤΑΛΛΙΚΩΝ ΚΑΤΑΣΚΕΥΩΝ

«Αριθμητική διερεύνηση των σεισμικών δράσεων και της απόκρισης μεταλλικών βιομηχανικών ραφιών»

Διδακτορική διατριβή του

Κωνσταντίνου Π. Αδαμάκου

ΤΡΙΜΕΛΗΣ ΣΥΜΒΟΥΛΕΥΤΙΚΗ ΕΠΙΤΡΟΠΗ:
1. Ι. ΒΑΓΙΑΣ, Καθηγητής Ε.Μ.Π. (επιβλέπων)
2. Χ. ΓΑΝΤΕΣ, Καθηγητής Ε.Μ.Π.
3. Χ. ΜΟΥΖΑΚΗΣ, Επ. Καθηγητής Ε.Μ.Π.

ΕΠΤΑΜΕΛΗΣ ΕΞΕΤΑΣΤΙΚΗ ΕΠΙΤΡΟΠΗ:
1. Ι. ΒΑΓΙΑΣ, Καθηγητής Ε.Μ.Π. (επιβλέπων)
2. Χ. ΓΑΝΤΕΣ, Καθηγητής Ε.Μ.Π.
3. Χ. ΜΟΥΖΑΚΗΣ, Επ. Καθηγητής Ε.Μ.Π.
4. Δ. ΒΑΜΒΑΤΣΙΚΟΣ, Επ. Καθηγητής Ε.Μ.Π.
5. Ι. ΨΥΧΑΡΗΣ, Καθηγητής Ε.Μ.Π.
6. C. CASTIGLIONI, Καθηγητής POLIMI
7. B. HOFFMEISTER, Καθηγητής RWTH AACHEN.

Αθήνα 2018

To my parents' ethos

To my brother

To my wife

Στο ήθος των γονιών μου

Στον αδερφό μου

Στη γυναίκα μου

Nothing exists except atoms and empty space; everything else is opinion.

(Democritus)

Acknowledgments

First and foremost, I would like to express my sincere gratitude to my supervisor, Professor Ioannis Vayas not only for his scientific guidance and the constant encouragement throughout the course of this study, but also for the respect that he displayed to me and the continuous support and motivation that he offered to me.

I would also like to state that I am deeply thankful to my committee for their creative contribution to my dissertation through interesting and important comments, amendments and consultation.

Moreover I would like to express my sincere thanks to all my colleagues from the Universities and the industrial partners of the research Program Seisracks2, and especially to Prof. C.A.Castiglioni (POLIMI), Prof. Benno Hoffmeister (RWTH) and Prof. Herve Degee (ULIEGE), for the nice research trip that we did together. Special thanks to Stefano Sesana and Alper Kanyilmaz for the close collaboration and the assistance that they offered to me.

Next, I feel deeply thankful to the company that I worked to, ZPF Ingenieure AG, in Basel of Switzerland, for the time that it gave to me in order to accomplish my dissertation.

Moreover, I would like to express my sincere gratitude also to my everyday colleague Stella Avgerinou for the ideal climate that we create to work in, her personal advices and of course her sleepless second opinion that she offered to me.

Special thanks to my friends Vasilas A., Giannopoulos D., Dais N. and Kampitsis A. for our common trip to civil engineering, as well as to my longtime friends Giannis G., Konstantinos G., Christos Z. and Giannis K.

Finally, I would like to express my endless gratitude to my parents that strove to give me as much prospects and provisions as they could, to my wife Georgia that selfless and relentlessly supported me to reach my goals and my brother Theodoros, who always gives me the encouragement to go further and who stays for me a paragon for my present and my future.

Ευχαριστίες

Σε αυτό το σημείο θα ήθελα πρωτίστως να ευχαριστήσω τον καθηγητή κ. Βαγια τόσο για την επιστημονική του καθοδήγηση όσο και για τον σεβασμό με τον οποίον με αντιμετώπισε όλα αυτά τα χρόνια και μου πρόσφερε τις πολύτιμες συμβουλές του.

Επίσης θα ήθελα να ευχαριστήσω τόσο την τριμελή μου όσο και την επταμελή μου επιτροπή που συνέβαλε δημιουργικά στην ολοκλήρωση της διδακτορικής μου διατριβής, με ενδιαφέροντα σχόλια, διορθώσεις και συμβουλές.

Θα ήθελα ακόμα να ευχαριστήσω προσωπικά τους συναδέλφους με τους οποίους συνεργάστηκα στα πλαίσια του ερευνητικού προγράμματος SEISRACKS2, υπό την καθοδήγηση των καθηγητών κ. C.A. Castiglioni (POLIMI), B. Hoffmeister (RWTH) και H. Degee (ULIEGE). Ιδιαιτέρως θα ήθελα να ευχαριστήσω τον Stefano Sesana καθώς και τον Alper Kanyilmaz για την ενδιαφέρουσα συνεργασία και βοήθεια που μου προσέφεραν.

Νιώθω ακόμα την υποχρέωση να ευχαριστήσω την εταιρεία ZPF Ingenieure AG για την οποία δούλεψα και η οποία μου έδωσε τη δυνατότητα και τον χρόνο να ολοκληρώσω την διατριβή μου.

Στη συνέχεια θα ήθελα να ευχαριστήσω την φίλη και συνάδελφο μηχανικό και διδακτορική φοιτήτρια Στέλλα Αυγερινού για το δημιουργικό και ευχάριστο κλίμα στο οποίο δουλεύαμε και για την επιστημονική δεύτερη ματιά που μου πρόσφερε απλόχερα.

Θα ήθελα ακόμα να ευχαριστήσω τους φίλους μου Βασιλά Α., Γιαννόπουλο Δ., Δαή Ν. και Καμπίτση Α. για το κοινό μας ταξίδι στην επιστήμη του πολιτικού μηχανικου, και τους παιδικούς μου φίλους Γιάννη Γ., Κων/νο Γ., Χρήστο Ζ. και Γιάννη Κ. που με στήριξαν άμεσα ή έμμεσα κατά την διάρκεια της διατριβής μου.,

Τέλος, θα ευχαριστήσω τους γονείς μου, οι οποίοι μου έχουν προσφέρει όσα περισσότερα εφόδια μπορούσαν, τη γυναίκα μου Γεωργία η οποία κατάφερε να με στηρίξει αδιάκοπα από την αρχή μέχρι το τέλος του εγχειρήματος μου και τον αδερφό μου Θεόδωρο ο οποίος είναι το στήριγμα και πρότυπο μου σε ότι επιχειρώ.

National Technical University of Athens

School of Civil Engineering

Institute of Steel Structures

PhD Thesis by Konstantinos Adamakos

"Seismic actions and response of steel storage pallet racks- A numerical investigation"

Supervisor: Ioannis Vayas, Professor NTUA

Abstract

The present dissertation intends to convey the overall situation of steel storage pallet racking systems that are placed in areas of high seismicity. The seismic design of racks reaches nowadays a high level of reliability, but the theoretical background around that is not abundant. Thus, this dissertation comes to judge some provisions of the modern European norms and to note significant proposals for the amendment of the racks' seismic response.

The first chapter is a rough presentation of the racking systems that are not yet commonly known to all engineers, stating at the same time the existing research that is referring to the different specialties and peculiarities of such systems as well as to an efficient design against earthquake loading.

The second chapter presents the application of nonlinear static analyses, known as Pushover, to racking systems. The aim of this work is to predict and evaluate the seismic response of the systems. Nine real case studies, provided by the industrial partners of the European research program SEISRACKS2, are simulated in a conventional manner. Then, capacity curves for all the systems and for both main directions of the system are produced, calculating the available ductility of the systems and as a result proposing appropriate values of the behavior factor that could be used for this kind of configurations.

The third chapter is moving towards more reliable and advanced methods. Nonlinear dynamic analyses are performed for the developed models applying the methodology of FEMA p695 that is based on the Incremental Dynamic Analysis. Two of the models of the previous chapter are subjected to nonlinear dynamic analyses in the down aisle direction and four of them to the cross aisle direction. The objective of the chapter is once again to evaluate the used values of the behavior factor during the design procedure and to figure out the dynamic racks' behavior that is not yet extensively numerically investigated.

The fourth chapter has a different point of view. It focuses locally on the seismic design of the pallet beams investigating the interaction between pallet and pallet beams. During an earthquake the pallet beams face severe horizontal forces that are in this dissertation analytically determined, differently to the provisions of the corresponding norm. This norm considers that the examined interaction could have also a positive effect on the bending of the pallet beams and their buckling length out-of-plane; however, it is found that these specific provisions of the norm are deemed to be neither realistic nor conservative.

The fifth chapter states the main conclusions of this thesis and notes some ideas for further investigation and future research.

At the end of the thesis, in Appendix, experimental results that took place at the rest universities of the SEISRACKS2 project are used to calibrate the numerical models of the previous main chapters of the dissertation.

Publications

i. Journal publications

Adamakos K., Vayas I., "Tragverhalten von Palettenregalsystemen unter Erdbebenbeanspruchung", Stahlbau, Ernst & Sohn, 83 (1), 2014, p.36-46.

Adamakos K., Sesana S., Vayas I., "Interaction between pallets and pallet beams of steel storage racks in seismic areas", International Journal of Steel Structures, Springer, Vol 18 (3), 1018-1034, 2018.

ii. Conference papers

Adamakos K., Vayas I., Hoffmeister B., Heinemeyer C., Hervé D., Braham Donoël C., *Seismic Performance of Steel Storage Pallet Racks*, 7th European Conference on Steel Composite Structures, Eurosteel 2014, Naples, Italy.

Adamakos K., Avgerinou S., Vayas I., "Estimation of the behavior factor of steel sotrage pallet racks", Papadrakakis, M. et al (ed.), Proceedings COMPDYN 2013 Conference, Kos, Greece

Adamakos K., Vayas I., «Συμπεριφορά Βιομηχανικών μεταλλικών ραφιών υπο στατικές και σεισμικές καταπονήσεις», 8° Hellenic National Conference of Steel Structures, EEME, 2-4 Oct. 2014, Tripoli, Greece.

Adamakos K., Vayas I., "Seismic investigation of a pallet racking system including the influence of pallet sliding", 13th International conference on computational structures technology 2018, Elsevier, Sigtes, Barcelona, Spain

iii. Technical Reports

Castiglioni, C. A. et al, "EUR 27583 EN: Seismic behavior of steel storage pallet racking systems (SEISRACKS2), Final Report, RFSR-CT-2011-00031, European Commission, DG Research, 2014, Brussels, Belgium.

Εθνικό Μετσόβιο πολυτεχνείο
Σχολή Πολιτικών Μηχανικών
Εργαστήριο Μεταλλικών Κατασκευών

Διδακτορική διατριβή Κωνσταντίνου Π. Αδαμάκου

«Αριθμητική διερεύνηση των σεισμικών δράσεων και της σεισμικής συμπεριφοράς μεταλλικών βιομηχανικών ραφιών»

Επιβλέπων: Ιωάννης Βάγιας, Καθηγητής ΕΜΠ

Περίληψη

Η παρούσα διδακτορική διατριβή εκπονήθηκε με σκοπό να διερευνήσει και να εξηγήσει την τρέχουσα ερευνητική κατάσταση των ραφιών αποθήκευσης παλετών που είναι τοποθετημένα σε σεισμογενείς περιοχές. Αν και ο σχεδιασμός αυτού του είδους κατασκευών είναι πλέον σε αρκετά υψηλό επίπεδο, το θεωρητικό υπόβαθρο του είναι περιορισμένο. Έτσι η παρούσα διατριβή έρχεται να εξετάσει και να εντοπίσει τα προβλήματα των κατασκευών αυτών, αλλά και των αντίστοιχων ισχυόντων ευρωπαϊκών κανονισμών.

Στο πρώτο κεφάλαιο γίνεται μια παρουσίαση των μεταλλικών ραφιών, αφού αυτά δεν είναι ακόμα ευρύτατα γνωστά στην κοινότητα των μηχανικών. Ακόμα, παρουσιάζονται οι ιδιαιτερότητες τους και τα προβλήματα που έχουν εντοπιστεί έως σήμερα, μέσα από την διεθνή βιβλιογραφία.

Το δεύτερο κεφάλαιο περιγράφει την διαδικασία που πρέπει να ακολουθηθεί για τη διενέργεια στατικών υπερωθητικών αναλύσεων σε μεταλλικά ράφια. Εννέα ράφια που σχεδιαστήκαν στο πλαίσιο του ερευνητικού προγράμματος SEISRACKS2 προσομοιώνονται και εξετάζονται με την παραπάνω μέθοδο ώστε να εκτιμηθεί η συνολική πλαστιμότητα που διαθέτουν. Απώτερος σκοπός είναι να γίνει μια εκτίμηση του συντελεστή συμπεριφοράς που δύναται να χρησιμοποιηθεί με βάση τις ρεαλιστικές τιμές που προκύπτουν από αριθμητικές αναλύσεις.

Στο τρίτο κεφάλαιο ο σκοπός παραμένει η εύρεση του κατάλληλου συντελεστή συμπεριφοράς για τέτοιου είδους κατασκευές, χρησιμοποιώντας όμως δυναμικές αναλύσεις που θεωρούνται σήμερα περισσότερο αξιόπιστες. Για την επίτευξη του στόχου αυτού χρησιμοποιείται η μέθοδος που περιγράφει ο FEMA p695 και η όποια βασίζεται στην δυναμική επαυξητική μέθοδο (Incremental Dynamic Analysis).

Το τέταρτο κεφάλαιο αφήνει την συνολική σεισμική συμπεριφορά των ραφιών και εστιάζει στις δράσεις που αναπτύσσονται επί των δοκών κατά τη διάρκεια μιας σεισμικής διέγερσης. Με αφορμή τις διατάξεις του κανονισμού που θεώρει ότι μεταξύ των παλετών και των δοκών υπάρχει αλληλεπίδραση λόγω της αναπτυσσόμενης τριβής, υπολογίζονται , διαφορετικά από ότι στον κανονισμό, οι μέγιστες οριζόντιες δυνάμεις που αναπτύσσονται στις δοκούς όταν οι παλέτες ολισθαίνουν. Ακόμα, αντίθετα στις προβλέψεις του κανονισμού, με χρήση αριθμητικών μοντέλων συμπεραίνεται ότι η ύπαρξη των παλετών δεν προσφέρει πλήρη διαφραγματική λειτουργιά στο σύστημα. Έτσι το μήκος λυγισμού των δοκών και η κάμψη που αναπτύσσεται στις δοκούς εκτός του επίπεδου τους, πρέπει να υπολογίζονται χωρίς την χρήση μειωτικών συντελεστών, ακόμα και σε περίπτωση ύπαρξης παλετών.

Στο πέμπτο κεφάλαιο γίνεται μια περιληπτική παρουσίαση των συμπερασμάτων της παρούσας διατριβής και παρατίθενται κάποιες προτάσεις για περαιτέρω έρευνα.

Στο τέλος παρατίθεται υπόμνημα, όπου παρουσιάζεται η βαθμονόμηση των αριθμητικών μοντέλων, που χρησιμοποιήθηκαν στην διατριβή, με χρήση των πειραματικών αποτελεσμάτων που έλαβαν μέρος κατά την διάρκεια του ερευνητικού προγράμματος SEISRACKS2 στα άλλα συνεργαζόμενα πανεπιστήμια.

Εκτενής ελληνική περίληψη

Περιεχόμενα

1. Εισαγωγή

1.1 Εισαγωγή

Με την πάροδο των χρονών και την ανάπτυξη των ραφιών αποθήκευσης, οι αποθήκες αναγκάστηκαν να εφεύρουν λύσεις που να είναι απόλυτα συμβατές στις ανάγκες της εκάστοτε περιόδου και των εκάστοτε προϊόντων. Η αρχική ιδέα ήταν μια κατασκευή που να μπορούσε να προσαρμόζεται, σε όλα τα επίπεδα εύκολα και γρήγορα για να εξυπηρετήσει τις διαφορετικές ανάγκες που προέκυπταν. Η λύση αυτή μπορούσε να επιτευχτεί μόνο με μεταλλικά στοιχειά εύκολα αποσπώμενα και επανασυνδέσιμα. Έτσι κατέληξε η μορφή των ραφιών αυτών να αποτελείτε από μεταλλικά λεπτότοιχα στοιχειά και συνδέσεις μελών με γάτζους, αποφεύγοντας τις πολύπλοκες κοχλιωτές συνδέσεις. Αφού το σχήμα και η μορφή των μεταλλικών αυτών συστημάτων σταθεροποιήθηκε, η βιομηχανία παράγωγης ραφιών άρχισε να αναπτύσσεται και οι ερευνητές στις αρχές του 20ου αιώνα άρχισαν να μελετούν τα ράφια αποθήκευσης σαν κανονικές μεταλλικές κατασκευές. Πολλές χώρες μάλιστα, μεταξύ άλλων, οι ΗΠΑ, οι ευρωπαϊκές χώρες αλλά και η Νέα Ζηλανδία, η Κινά και η Ιαπωνία, ανέπτυξαν αρκετά την ερευνά τους πάνω στον τομέα αυτόν, δημοσιεύοντας κανονισμούς με τους οποίους θα έπρεπε τα ράφια αυτά να σχεδιάζονται. Οι κανονισμοί αυτοί ήρθαν βεβαίως όχι τόσο νωρίς όσο για τις συμβατικές κατασκευές, παρά μόνο στην δεκαετία του 1970.

Η Εικόνα 1 παρουσιάζει μια συνήθη διάταξη ενός ραφιού αποθήκευσης.

Εικόνα 1 Γενική άποψη συστήματος βιομηχανιών ραφιών

1.2 Κατασκευαστικές ιδιαιτερότητες των ραφιών

Τα βιομηχανικά ράφια είναι κατασκευές οι οποίες μοιάζουν αρκετά με κτιριακές μεταλλικές κατασκευές, παρόλα αυτά έχουν πολλές ιδιαιτερότητες τόσο όσον αφορά την στατική και δυναμική συμπεριφορά τους, όσο και στον τρόπο μοντελοποίησης τους.

Μια πρώτη ιδιαιτερότητα είναι το γεγονός ότι τα κινητά φορτία αποτελούν το μείζον φορτίο της κατασκευής, έως και 90%. Το γεγονός ότι ο φορέας πρέπει να παραμένει εύκολα μετατρέψιμος σε μια διαφορετική γεωμετρία, ανάλογα με τις ανάγκες της αποθήκης, οδηγεί σε ελαφρές διατομές και εύκαμπτες απλές συνδέσεις, γεγονός το οποίο οδηγεί συχνά σε πολύ εύκαμπτες κατασκευές.

Ένα άλλο χαρακτηριστικό των ραφιών είναι ο τρόπος με τον οποίο καλούνται να αναλάβουν τα ορίζονται, κυρίως σεισμικά, φορτία. Αυτό γίνεται είτε μέσω της πλαισιωτής λειτουργίας του φορέα, είτε μέσω χιαστί συνδέσμων δυσκαμψίας. Στην πρώτη περίπτωση οι κατασκευές είναι εξαιρετικά εύκαμπτες με αποτέλεσμα ακραίες αναμενόμενες μετατοπίσεις, ενώ στην δεύτερη περίπτωση οι χιαστί σύνδεσμοι τοποθετούνται στην πλάτη της κατασκευής, δημιουργώντας μια σημαντική εκκεντρότητα και επομένως στρεπτική απόκριση της κατασκευής.

Στην εγκάρσια διεύθυνση της κατασκευής τα διαγώνια μέλη είναι και αυτά συνδεδεμένα με απλές συνδέσεις, συνήθως με έναν απλό κοχλία. Κατ’ επέκταση δημιουργείται μια χαλάρωση στη σύνδεση, η οποία σε αφόρτιστη κατάσταση θεωρητικά έχει μηδενική δυσκαμψία μέχρι ο κοχλίας να φορτιστεί και να έρθει σε επαφή με την άντυτα των συνδεόμενων μελών.

Ακόμα μια ιδιαιτερότητα των ραφιών είναι η τιμή του συντελεστή ισοδύναμης απόσβεσης. Η απόσβεση που εμφανίζει η κατασκευή σε μια ταλάντωση της είναι συνάρτηση όχι μόνο από την ίδια την κατασκευή, όσο και από το παρόν φορτίο, το είδος των παλετών, το είδος των αποθηκευμένων προϊόντων κ.α. Ακολουθώντας τον κανονισμό ο συντελεστής απόσβεσης είναι παρόμοιος με μια μεταλλική κατασκευή.

Τέλος θα πρέπει να αναφερθεί ότι οι δοκοί των ραφιών που είναι εν δυνάμει τα ισχυρά στοιχεία της κατασκευής αποτελούν ευαίσθητα μέλη τα οποία φορτίζονται στον άνω πέλμα τους μέσω της τριβής μεταξύ παλέτας και δοκού. Η φόρτιση αυτή προκαλεί στρέψη στις δοκούς οι οποίες είναι στρεπτικά ευαίσθητες διατομές και οι οποίες όχου βρεθεί να αστοχούν λόγω αυτής της έκκεντρης φόρτισης.

1.3 Βιβλιογραφική αναφορά

Οι πρώτες συντονισμένες προσπάθειες για έρευνα γύρω από τα ράφια φαίνεται να γίνεται πριν το 1970 όπου εκδίδεται και ο πρώτος σχετικός κανονισμός. Όσον αφορά όμως την σεισμική απόκριση των ραφιών μόλις στις αρχές της δεκαετίας του 1980 δημοσιεύονται οι πρώτες εργασίες των Brown 1983 [1] Chen and Scholl (1980) [2], [3]. Την περίοδο εκείνη και λίγο νωρίτερα δημοσιεύονται εργασίες για λεπτότοιχες διατομές από τους Pekoz and Winter 1969 [4] , Pekoz (1973) [5]. (1975) [6], (1986) [7] (1988) [8] οι οποίες ευνοούν την περαιτέρω έρευνα πάνω στον λυγισμό των λεπτότοιχες διατομών των δοκών και των υποστυλωμάτων ενός ραφιού. Οι Hancock [9] (1985), Baldassino (1999) [10], ο Lewis (1991) [15] και Davies (1992) [16] ασχολήθηκαν στη συνέχεια με την ευστάθεια ολόκληρων ραφιών που έδωσε το έναυσμα για πιο λεπτομερή έρευνα της καθολικής συμπεριφοράς ενός ραφιού.

Στη συνέχεια οι Markazi (1997) [18], Sleczka και Kozlowski (2007) [19] και οι Baldassino et al. [20] ασχολούνται με τον χαρακτηρισμό και την συμπεριφορά των ημιάκαμπτων συνδέσεων δοκού-υποστυλώματος και οι Bajaria (2009) [21] και Abdel-Jaber (2005) [22] κάνουν αυτή την εφαρμογή στις συνδέσεις των ραφιών. Αργότερα και στο πλαίσιο ερευνητικών προγραμμάτων της ΕΕ, SEISRACKS and SEISRACKS2 (2007) [23], (2014) [24] διευρύνονται τα συμπεράσματα γύρω από την σεισμική απόκριση των ραφιών. Παράλληλα με αυτά τα προγράμματα ο Castiglioni(2008) [25], (2016) [26] και οι Hua and Rasmussen (2010) [27], Gilbert και Rasmussen (2009) [28] πραγματοποίησαν πολλά πειράματα τόσο σε μεμονωμένα μέλη της κατασκευής όσο και για τον προσδιορισμό του συντελεστή τριβής μεταξύ δοκού και παλέτας. Οι Rao et al. (2004) [29], Sajja et al. (2006) [30], (2008) [31] και οι Gilbert et al. (2012) [32] μελέτησαν τη διατμητική συμπεριφορά της εγκάρσιας διεύθυνσης των ραφιών και πως αυτή επηρεάζει την συνολική απόκριση του συστήματος. Οι Godley and Beale (2008) [33] μελέτησαν με ποιο τρόπο η χαλάρωση των διαγώνιων μελών της εγκάρσιας διεύθυνσης επηρεάζει την απόκριση του συστήματος. Ο Beattie (2001) [34] παρουσιάζει καταρρεύσεις και αστοχίες ραφιών κατά των σεισμό του Canterbury και οι Crosier et al. (2010) [35] κάνει μια αντίστοιχη παρουσίαση για τον σεισμό του Darfield και οι δυο στη Νέα Ζηλανδία. Αργότερο ο Bournas et al. (2014) [36] περιγράφει τις αστοχίες ραφιών από τον σεισμό στην Emilia Romagna της Ιταλίας, ενώ ο Plantes (2012) [37] κάνει μια ανασκόπηση διάφορων αστοχιών και καταρρεύσεων τέτοιου είδους κατασκευών.

Οι Adamakos and Vayas (2014) [38] δημοσίευσαν μια από τις πρώτες εργασίες για την σεισμική απόκριση ραφιών και πως αυτά πρέπει να μοντελοποιούνται για μια πιο ρεαλιστική πρόβλεψη της συμπεριφοράς. Οι Adamakos et al. (2014) [39], Degee και Denoel (2007) [40] και Degee et al. (2011) [41] μελετούν την δυναμική συμπεριφορά των ραφιών και οι Degee and Denoel (2009) [42] δημοσιεύουν μια πρώτη εργασία σχετικά με την αλληλεπίδραση παλέτας-κατασκευής. Οι Adamakos et al. (2018) [43] παρουσιάζουν εκτενώς μια εργασία πάνω στο ίδιο θέμα.

1.4 Σκοπός Διατριβής

Σκοπός αυτής της διατριβής είναι να αναδείξει τα προβλήματα και τις ιδιαιτερότητες των βιομηχανικών ραφιών και να προτείνει νέες μεθόδους μοντελοποίησης ή και νέες κανονιστικές προτάσεις. Απώτερος σκοπός είναι να εκτιμηθεί αν ο σχεδιασμός που προτείνεται από τους διαφόρους κανονισμούς και ιδιαιτέρως από τον ευρωπαϊκό κανονισμό EN16812 είναι επαρκής. Πιο συγκεκριμένα, ο συντελεστής συμπεριφοράς που χρησιμοποιείται στην πράξη θα εξεταστεί και θα σχολιαστεί με βάση αριθμητικά αποτελέσματα από στατικές αλλά και δυναμικές αναλύσεις. Τέλος εξετάζεται εκτενώς η αλληλεπίδραση των παλετών με το φέρον σύστημα και πως αυτή επηρεάζει τα σεισμικά χαρακτηριστικά των ραφιών αλλά και τα εντατικά μεγέθη των μελών τους.

2. Στατικές μη γραμμικές αναλύσεις μεταλλικών ραφιών υπό οριζόντιες σεισμικές δυνάμεις

2.1 Εισαγωγή

Διάφορες μελέτες και δημοσιεύσεις έχουν παρουσιάσει αστοχίες και καταρρεύσεις ραφιών μετά από ένα σεισμικό γεγονός. Ύστερα από ισχυρή σεισμική δόνηση, μεγέθους 6.5 βαθμών Ρίχτερ, που έλαβε χώρα στην Πάτρα στις 08.06.2008 μετρήθηκαν εδαφικές επιταχύνσεις οι οποίες ήταν χαμηλότερες από τις τιμές σχεδιασμού. Σύμφωνα όμως με το φάσμα της συγκεκριμένης δόνησης, οι επιταχύνσεις που αναπτύχθηκαν σε κατασκευές με ιδιοπερίοδο κοντά στο 1.1s ήταν της τάξεως του 0.33g και οι οποίες ήταν περίπου το 80% της τιμής σχεδιασμού. Κατασκευές όπως τα ράφια που θεωρούνται σχετικά εύκαμπτα και παρουσιάζουν ιδιοπεριόδους σε αυτήν την περιοχή υπέστησαν αρκετές αστοχίες. Οι αστοχίες αυτές παρουσιάζονται στην Εικόνα 2 και συνοψίζονται στις εξής:

a) τοπικός λυγισμός και κατ' επέκταση καθολικός λυγισμός των διαγώνιων μελών της εγκάρσιας διεύθυνσης
b) εκτενείς πλαστικές παραμορφώσεις της συνδεσμολογίας των διαγωνίων μελών του συστήματος δυσκαμψίας της επιμήκους διεύθυνσης
c) Αστοχία της συγκόλλησης των επιμέρους διατομών που διαμορφώνουν τις δοκούς έδρασης των παλετών.
d) Σύνθλιψη άντυγας στην περιοχή των γάτζων της σύνδεσης δοκού-υποστυλώματος
e) Εκτενείς πλαστικές παραμορφώσεις των παραπάνω συνδέσεων.

a

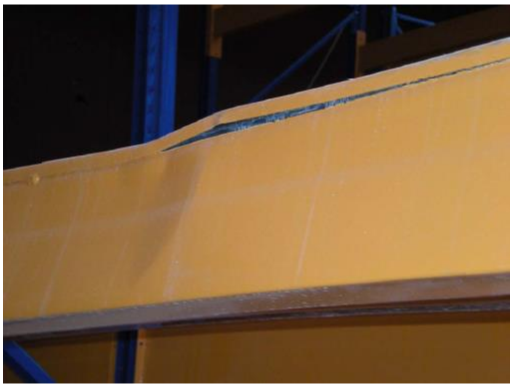

c

b

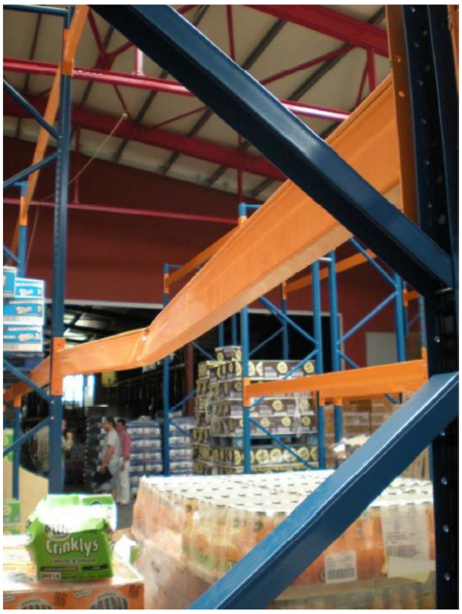

d

e

f

Εικόνα 2 Αστοχίες μετά από τον σεισμό της Πάτρας στις 08.06.2008

Με αφορμή τις αστοχίες αυτές και στα πλαίσια του ερευνητικού προγράμματος SEISRACKS2 έγιναν αναλύσεις σε πραγματικές κατασκευές τα δεδομένα των οποίων τα παρείχαν οι συμμετέχουσες στο ερευνητικό πρόγραμμα εταιρείες.

2.2 Η εφαρμογή των μη γραμμικών στατικών αναλύσεων για βιομηχανικά ράφια

Αν και οι σύγχρονοι κανονισμοί για τις συμβατικές κατασκευές έχουν υιοθετήσει τις γνωστές ως Pushover αναλύσεις εδώ και πολλά χρόνια και περιγράφουν ικανοποιητικά τον τρόπο εφαρμογής της μεθόδου, όσον αφορά στα μεταλλικά ράφια τα διαθέσιμα δεδομένα είναι ελλιπή. Όπως επισημαίνουν και οι κανονισμοί FEM

10.02.02 και FEM 10.02.08 τα πειράματα και τα πειραματικά δεδομένα είναι σχεδόν αναγκαία για τον χαρακτηρισμό της ακριβούς συμπεριφοράς των μελών ενός ραφιού.

Για την πραγματοποίηση αριθμητικών αναλύσεων χρειάζεται αρχικά να καθοριστούν εξαρχής οι θέσεις όπου αναμένονται οι αστοχίες και επομένως οι πλαστικές αρθρώσεις. Αυτές με βάση την εμπειρία, την βιβλιογραφία και την παρατήρηση πειραματικών δεδομένων και αστοχιών ορίζονται να είναι στις θέσεις που φαίνονται με κόκκινο στην Εικόνα 3. Πιο συγκεκριμένα οι πλαστικές αρθρώσεις ορίζονται για να περιγράψουν την αστοχία της σύνδεσης δοκού υποστυλώματος, την αστοχία του υποστυλώματος πάνω και κάτω από την προαναφερόμενη σύνδεση, και την αστοχία της βάσης στήριξης των υποστυλωμάτων. Εκτός αυτών των πλαστικών αρθρώσεων ορίζονται οι κατάλληλες πλαστικές αρθρώσεις για τα διαγώνια μέλη του συστήματος δυσκαμψίας τόσο για την επιμήκη όσο και για την εγκάρσια διεύθυνση. Στην παρούσα φάση οι δοκοί θεωρείται ότι παραμένουν ελαστικές.

Σε όλες τις αναλύσεις λαμβάνονται υπόψη τα φαινόμενα δευτέρας τάξεως, γνωστά ως P-Delta.

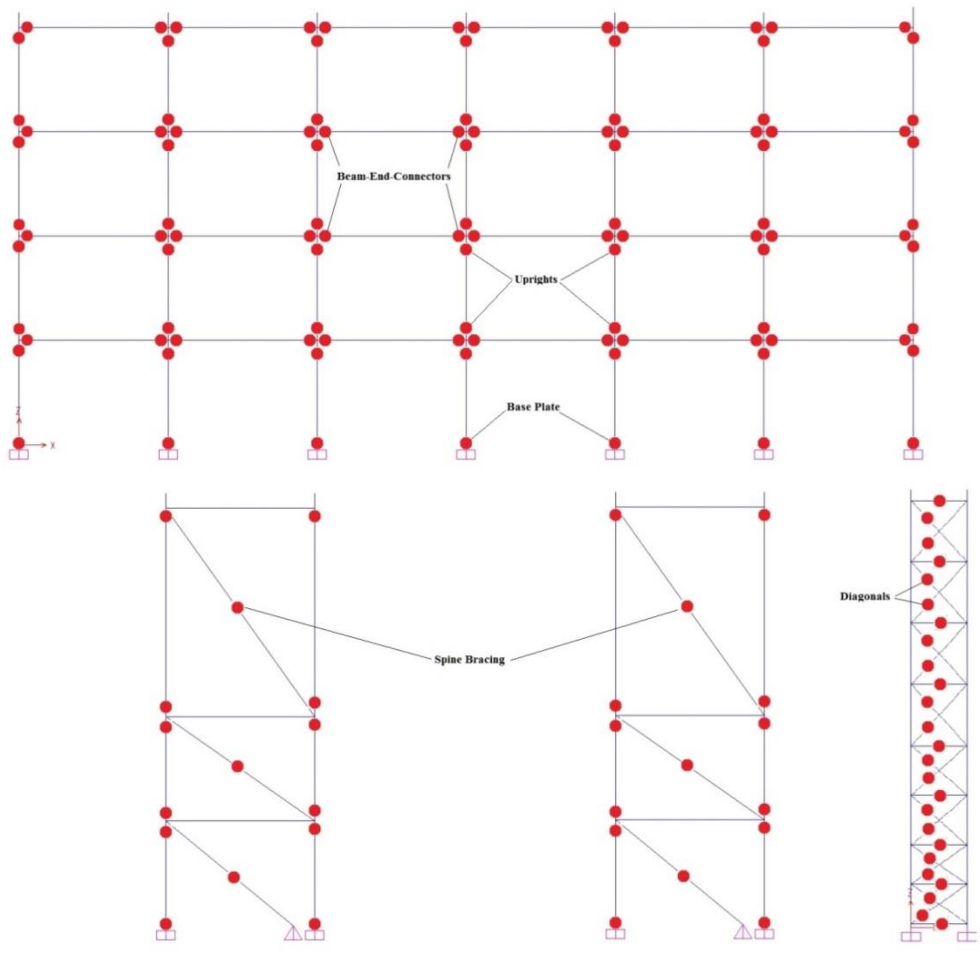

Εικόνα 3 Πιθανές θέσεις ανελαστικής συμπεριφοράς

2.3 Τοπολογίες υπό εξέταση

2.3.1 Γεωμετρία των κατασκευών

Οι εξεταζόμενες κατασκευές είναι μοντέλα που παρείχαν οι κατασκευάστριες εταιρείες του προγράμματος SEISRACKS2. Αυτές αναφέρονται ως IP-A, IP-B, IP-C and IP-D. Διατίθενται συνολικά 9 κατασκευές-μοντέλα. Πέντε πλαισιακές κατασκευές (L4) και 3 κατασκευές με χρήση χιαστί συστήματος δυσκαμψίας L1, L2 και L3. Στην εγκάρσια διεύθυνση όλες οι κατασκευές είναι διαφορετικές μεταξύ τους (Q1-Q9). Οι κατασκευές φαίνονται στην Εικόνα 4 και την Εικόνα 5. Το πλάτος της εγκάρσιας πλευράς κυμαίνεται μεταξύ 1.0 και 1.1μ. Το μήκος του κάθε φατνώματος στην επιμήκη διεύθυνση είναι περίπου 2.7μ. και το ύψος κάθε επιπέδου είναι περίπου 2.0μ.

Όνομα φορέα	Μορφολογία
L1	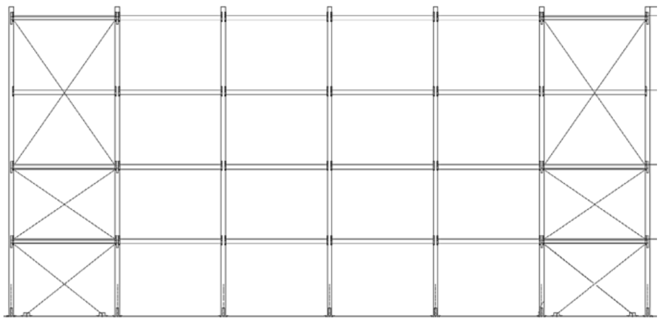
L2	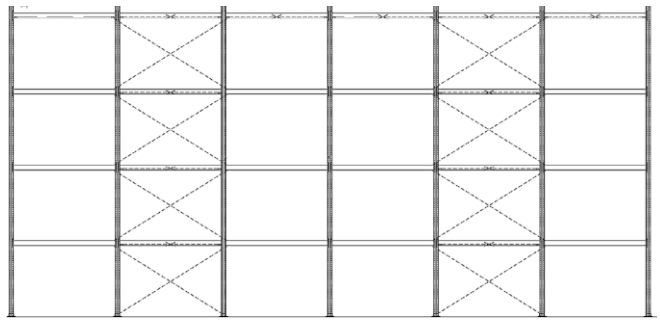

L3

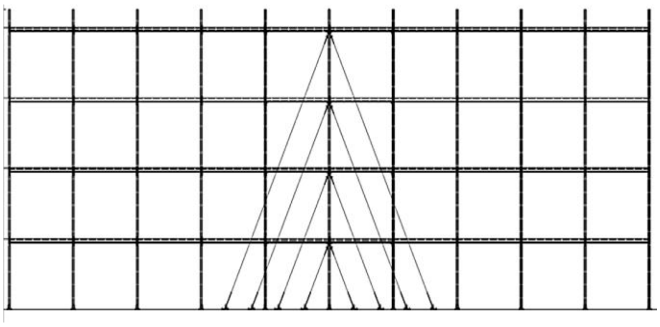

L4

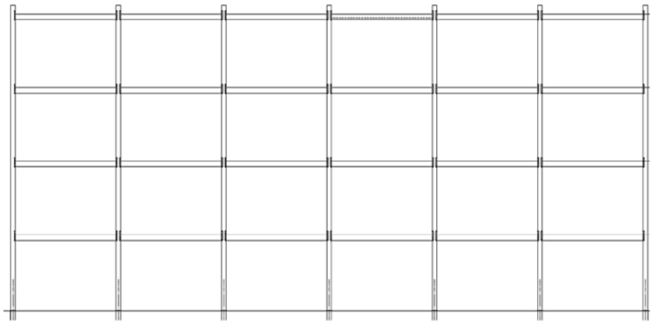

Εικόνα 4 Τοπολογία συστημάτων στην διαμήκη διεύθυνση

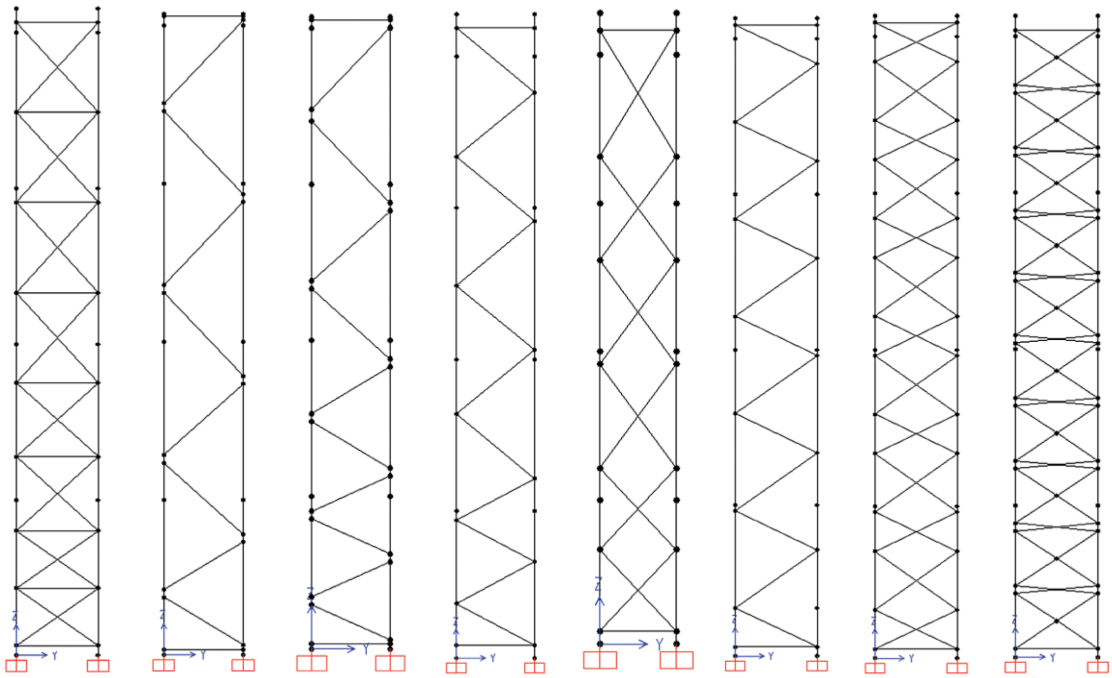

Q1 Q2 Q3 Q4 Q5 Q6 Q7 Q8

Εικόνα 5 Τοπολογία συστημάτων στην εγκάρσια διεύθυνση

Ο συντελεστής συμπεριφοράς που χρησιμοποιήθηκε για τις κατασκευές είναι 1.5 έως 2 και για τις δύο διευθύνσεις, ενώ σε κάποιες περιπτώσεις ο συντελεστής είναι διαφορετικός για κάθε διεύθυνση. Οι προτεινόμενες τιμές από τον κανονισμό είναι πολύ μεγαλύτερες, γεγονός που μαρτυρά την έλλειψη αυτοπεποίθησης και εμπιστοσύνης των μελετητών απέναντι στον κανονισμό.

2.3.2 Ανελαστικές ιδιότητες

Εδώ θα πρέπει να τονιστεί ότι ο όρος πλαστική άρθρωση στην παρούσα εργασία χρησιμοποιείται για να περιγράψει την ανελαστική συμπεριφορά των συμβαλλόμενων μελών και όχι κατά λέξη την πλαστικοποίηση κάποιο μέλους. Αυτό συμβαίνει γιατί τα μέλη της κατασκευής είναι συνήθως λεπτότοιχα και κατατάσσονται στην κατηγορία διατομών 3 ή 4 και δεν είναι σε θέση να αναπτύξουν τα πλαστικά τους χαρακτηριστικά. Κάποιο είδος τοπικού ή και καθολικού λυγισμού είναι πιο κρίσιμος και αυτή η συμπεριφορά καλείται να περιγραφεί με τη χρήση μια ισοδύναμης πλαστικής άρθρωσης κατά την μοντελοποίηση της κατασκευής. Οι πηγές πλαστιμότητας/ ανελαστικότητας των επιμέρους μελών περιγράφεται παρακάτω.

Μέλος	Πηγή ανελαστικότητας	Τύπος άρθρωσης
Σύνδεση δοκού-υποστυλώματος	αστοχία της δοκού στο σημείο της σύνδεσης, αστοχία της συγκόλλησης, αστοχία των γάτζων και της άντυγας γύρω από τις οπές τους υποστυλώματος.	Ροπής-στροφής
Βάση στήριξης	τοπικός λυγισμός διατομής, αστοχία της κοχλιωτής σύνδεσης με το έδαφος	Ροπής-στροφής
Υποστυλώματα	τοπικός ή/ και καθολικό λυγισμός (συνήθως στρεπτοκαμπτικός)	Ροπής-στροφής
Διαγώνια μέλη	λυγισμός του μέλους, διαρροή της διατομής, αστοχία της κοχλιωτής σύνδεσης.	Αξονικής δύναμης-μετατόπισης

Πίνακας 1 Πηγή ανελαστικότητα για τα διάφορα μέλη ενός τυπικού ραφιού

2.3.2.1 Σύνδεση δοκού-υποστυλώματος

Τα δεδομένα για τον ορισμό των πλαστικών αρθρώσεων βασίζονται στα παρακάτω πειραματικά αποτελέσματα.

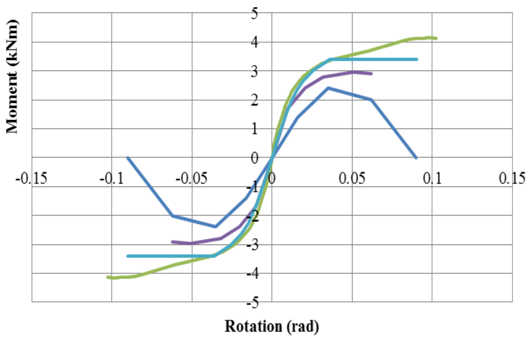

Εικόνα 6 Διαγράμματα ροπής-στροφής για διάφορες συνδεσμολογίες δοκού-υποστυλώματος

2.3.2.2 Βάση στήριξης

Αντίστοιχα πειραματικά δεδομένα χρησιμοποιήθηκαν για την βάση στήριξης των υποστυλωμάτων.

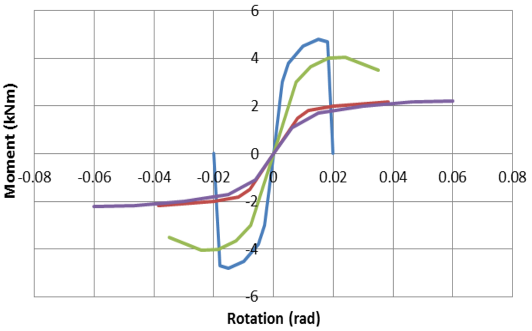

Εικόνα 7 Διαγράμματα ροπής-στροφής για διάφορες βάσης στήριξης

2.3.2.3 Υποστυλώματα

Όσον αφορά στις πλαστικές αρθρώσεις των υποστυλωμάτων αυτές ορίστηκαν με χρήση αριθμητικών αποτελεσμάτων λόγω έλλειψης πειραματικών διατάξεων και αποτελεσμάτων. Οι διατομές του εκάστοτε ραφιού, προσομοιώθηκαν με στοιχεία κελύφους στο λογισμικό ABAQUS και με μήκος 2μ, όσο δηλαδή και το ύψος των υποστυλωμάτων. Οι αναλύσεις για κάθε μέλος αφορούν σε γεωμετρικώς μη γραμμικές αναλύσεις με μη γραμμικότητα υλικού. Η Εικόνα 8 παρουσιάζει ένα τυπικό μοντέλο αναλύσεων και η Εικόνα 9 ένα τυπικό παραχθέν διάγραμμα και την γραμμικοποίηση του ώστε να είναι συμβατό με το λογισμικό.

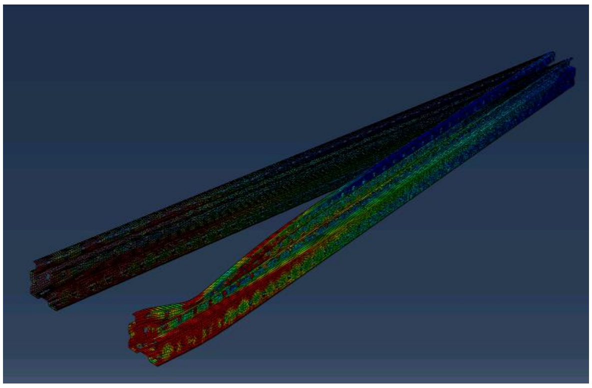

Εικόνα 8 Deformed shape of a numerically tested upright

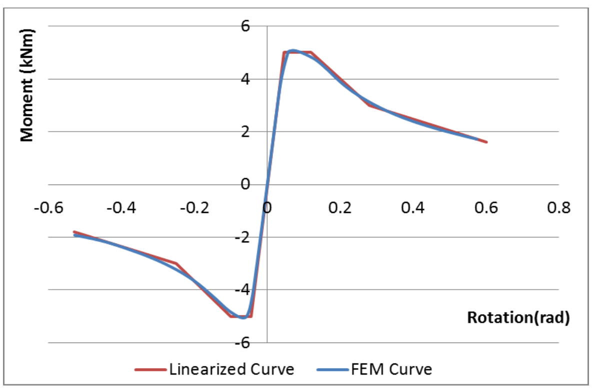

Εικόνα 9 Moment-rotation curve for a typical upright

Είναι γνωστό ότι για τα υποστυλώματα χρησιμοποιούνται πλαστικές αρθρώσεις που λαμβάνουν υπόψη την αλληλεπίδραση ροπής και αξονικής δύναμης. Στην περίπτωση των ραφιών τα υποστυλώματα δεν ακολουθούν τον κλασσικό νόμο αλληλεπίδρασης αφού ως λεπτότοιχα μέλη αστοχούν νωρίτερα από (τοπικό) λυγισμό με αποτέλεσμα ο νόμος αλληλεπίδρασης να είναι γραμμικός, αφού η διατομή παραμένει στην ελαστική περιοχή. Το κριτήριο αλληλεπίδρασης στην περίπτωση αυτή ταυτίζεται με το κριτήριο ευστάθειας του μέλους έναντι διαξονικής ροπής και ταυτόχρονης αξονικής δύναμης, όπως αυτός δίνεται στον ευρωκώδικα 3.

$$\frac{N_{Ed}}{\chi_{min}\cdot A_{eff}\cdot f_y/\gamma_M}+\frac{k_y\cdot M_{y,Ed}}{\chi_{LT}\cdot W_{eff,y}\cdot f_y/\gamma_M}+\frac{k_z\cdot M_{z,Ed}}{W_{eff,z2}\cdot f_y/\gamma_M}<1 \qquad (2\text{-}1)$$

2.3.2.4 Διαγώνια μέλη

Παρόμοια με τα μέλη των υποστυλωμάτων, τα διαγώνια μέλη των κατασκευών προσομοιώνονται αριθμητικά με το λογισμικό ABAQUS με σκοπό να παραχθούν ρεαλιστικά αποτελέσματα για το νόμο συμπεριφοράς των διαγώνιων μελών. Η συμπεριφορά των μελών αυτών ορίζεται ως μια πλαστική άρθρωση αξονικής δύναμης- αξονικής μετατόπισης. Η συμπεριφορά των μελών καθορίζεται από τον μηχανισμό αστοχίας που μπορεί να είναι είτε ο λυγισμός του μέλους, είτε η αστοχία της εκάστοτε σύνδεσης είτε ο συνδυασμός τους σε περίπτωση που οι μηχανισμοί αστοχίας εμφανίζουν παραπλήσια φορτία αστοχίας. Η Εικόνα 10 και η Εικόνα 11 δείχνουν κάποια από τα αριθμητικά μοντέλα που χρησιμοποιήθηκαν για τον ορισμό των ανελαστικών νόμων συμπεριφοράς κάθε μέλους.

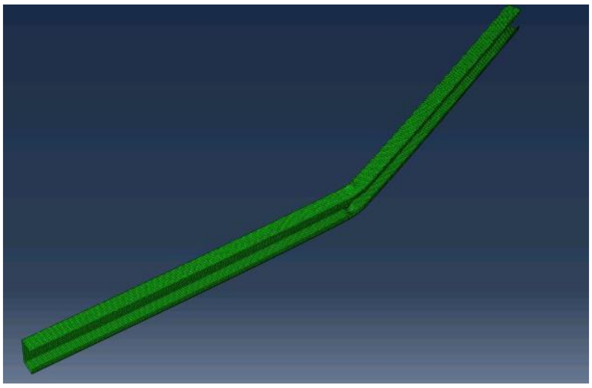

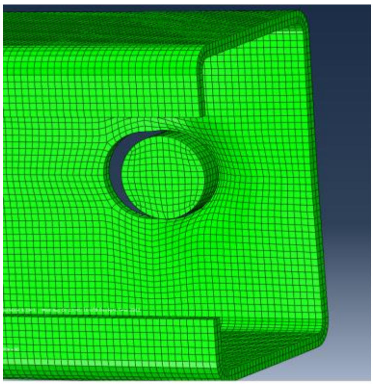

Εικόνα 10 Διαγώνιο μέλος διατομής C α) καθολικός λυγισμός (αριστ.) β) σύνθλιψη άντυγας (δεξ.)

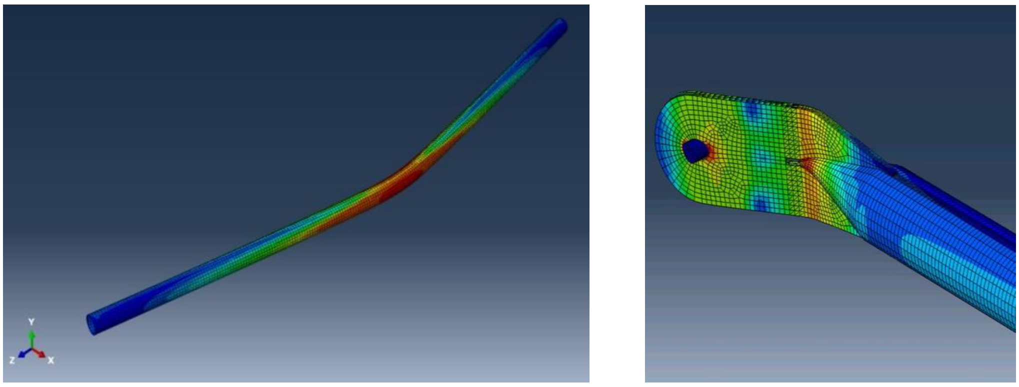

Εικόνα 11 Διαγώνιο μέλος κυκλικής διατομής α) καθολικός λυγισμός (αριστ.) β) τοπικός λυγισμός της ακραίας λεπτομέρειας του μέλους (δεξ.)

2.3.3 Εκτίμηση της μη γραμμικής απόκρισης

Στο σημείο αυτό και αφού οι ανελαστικές συμπεριφορές των μελών των ραφιών έχουν προσδιοριστεί είτε από πειραματικά αποτελέσματα είτε μέσω αριθμητικών μη γραμμικών αναλύσεων, οι 9 κατασκευές- μοντέλα φορτίζονται σταδιακά με οριζόντια φόρτιση τριγωνικής κατανομής και ταυτόχρονη κατακόρυφη πλήρη φόρτιση από τα κινητά φορτία/παλέτες μέχρι το σημείο κατάρρευσης. Ο σκοπός είναι η δημιουργία διαγραμμάτων για την ποσοτική εκτίμηση της απόκρισης του κάθε συστήματος. Στις επόμενες εικόνες παρατίθενται όλες μαζί οι αποκρίσεις των κατασκευών σε όρους οριζόντιας δύναμης- οριζόντιας μετατόπισης.

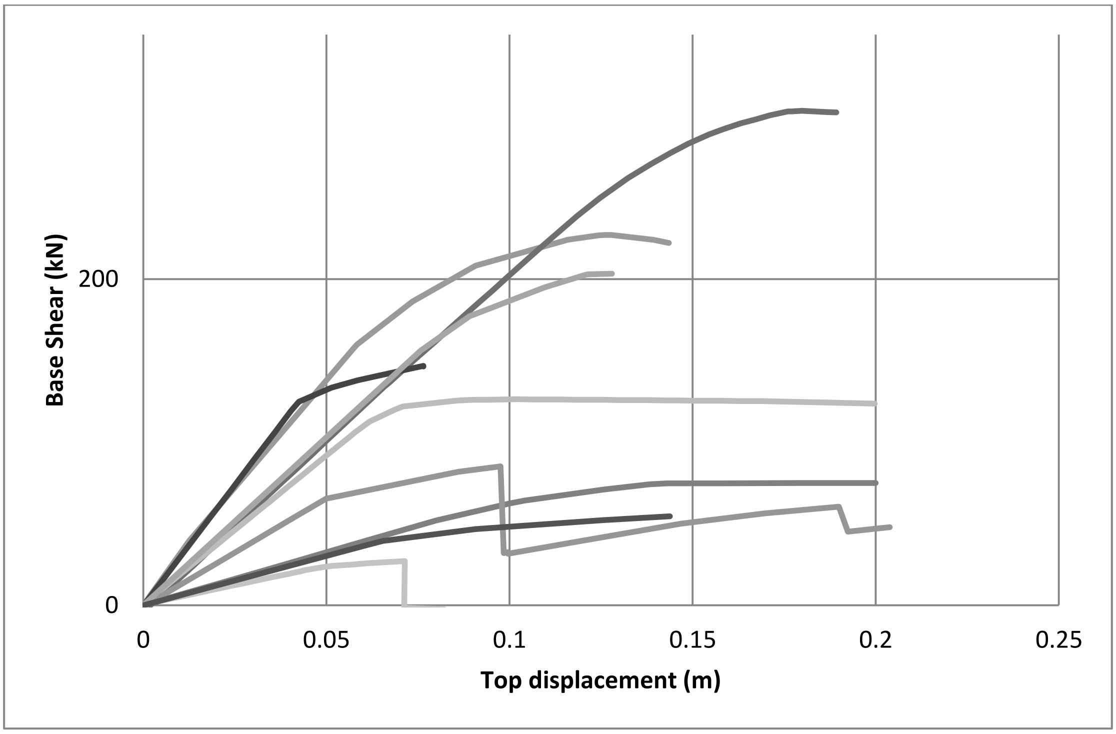

Εικόνα 12 Καμπύλες απόκρισης για όλα τα συστήματα για την εγκάρσια διεύθυνση

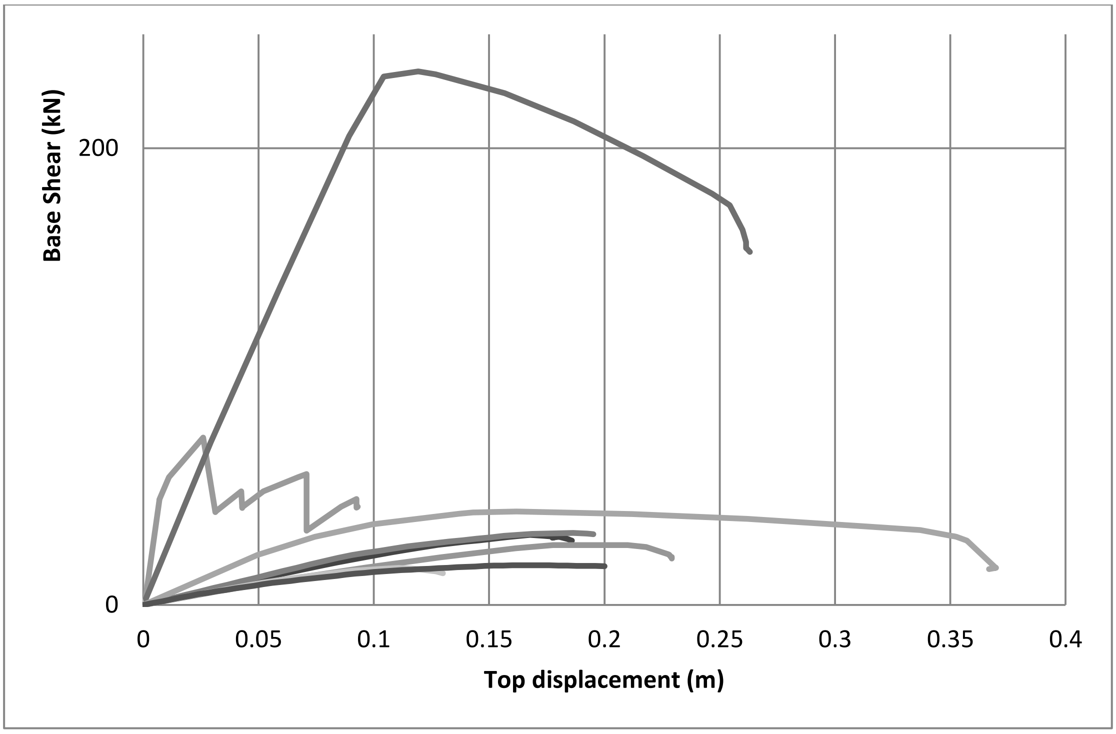

Εικόνα 13 Καμπύλες απόκρισης για όλα τα συστήματα για την διαμήκη διεύθυνση

Με την χρήση των διαγραμμάτων αυτών γίνεται μια εκτίμηση για τον συντελεστή συμπεριφοράς της κάθε κατασκευής. Για την εύρεση του διατιθέμενου συντελεστή συμπεριφοράς χρησιμοποιείται ο ορισμός του όπως δόθηκε από τον Uang (1992) [49], ενώ εξετάστηκαν και οι ορισμοί κατά Irzidinia et al. (2012) [48], The international building code [46] και το The American building code [47]. Εκτός από τον συντελεστή συμπεριφοράς υπολογίζεται αυτόματα με χρήση του λογισμικού SAP2000 οι συντελεστές επιτελεστικότητας και το σημείο απόκρισης. Για τον υπολογισμό του σε κάθε κατασκευή χρησιμοποιούνται οι ορισμοί των εξισώσεων 2 ως 6. Ως σημείο επιτελεστικότητας θεωρείται η αποφυγή κατάρρευσης, αφού δεν ορίζεται κάτι διαφορετικό από τον κανονισμό.

$$\mathbf{C_A=a_g \cdot S \cdot n} \tag{2}$$

$$\mathbf{C_V=2.5 \cdot a_g \cdot S \cdot n \cdot T_c} \tag{3}$$

$$\mathbf{\Omega=\frac{V_y}{V_1}=\frac{d_y}{d_1}} \tag{4}$$

$$\mathbf{q_0=\mu=\frac{d_{max}}{d_y}} \tag{5}$$

$$\mathbf{q=q_0 \cdot \Omega} \tag{6}$$

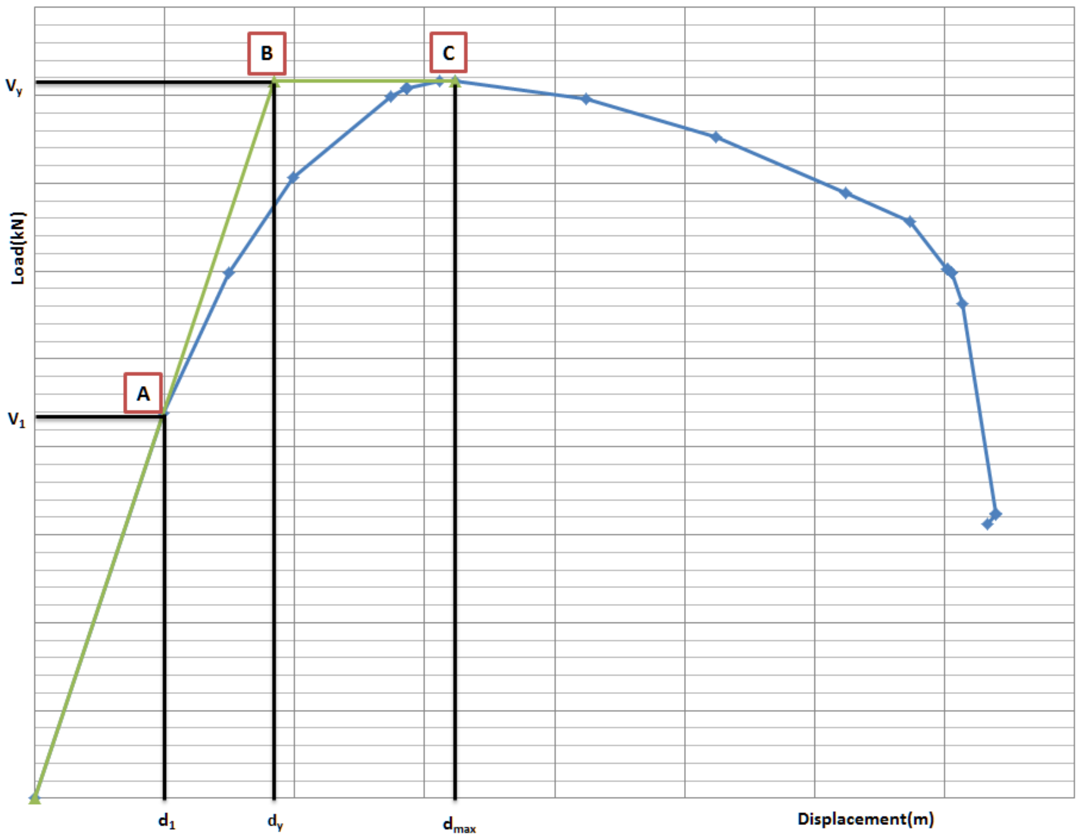

Εικόνα 14 Γραμμικοποίηση μιάς καμπύλης απόκρισης

Ο Πίνακας 2 παραθέτει συγκεντρωτικά την εκτιμώμενη απόκριση των κατασκευών Συμπεραίνεται ότι μια ασφαλής τιμή για του συντελεστή συμπεριφοράς για την επιμήκη διεύθυνση είναι 2 και για την εγκάρσια διεύθυνση 1.5. Τα συστήματα που διέθεταν σύστημα δυσκαμψίας με χρήση χιαστί συνδέσμων ή καλωδίων εμφάνισαν μεγαλύτερους συντελεστές συμπεριφοράς, με μέση τιμή το 3,5. Παρόλα αυτά όπως αναφέρει ο Beattie (2006) [50] η μέγιστη προτεινόμενη τιμή για τον συντελεστή συμπεριφοράς της εγκάρσιας διεύθυνσης πρέπει να είναι 1.25 ενώ για την επιμήκη διεύθυνση όταν αυτό δικαιολογείται πειραματικά μπορεί να πάρει μεγαλύτερες τιμές αλλά να μην ξεπερνάει την τιμή 3.5.

System/Zone	Direction	$q_0 = \mu$	Ω	q
A/High	Down	3.65	1.50	5.47
	Cross	1.47	1.2	1.76
A/Medium	Down	1.45	1.52	2.22
	Cross	1.72	1.44	2.48
B/High	Down	1.25	2.06	2.58
	Cross	1.54	1.17	1.81
B/Low	Down	1.25	1.59	2.00
	Cross	1.52	1.30	1.98
C/High	Down	1.24	3.27	4.07
	Cross	1.23	2.4	2.97
C/Medium	Down	1.90	2.90	5.51

	Cross	1.58	1.38	2.2
D/High	Down	2.34	1.59	3.72
	Cross	1.49	1.42	2.12
D/ Medium	Down	1.75	1.86	3.27
	Cross	1.29	1.30	1.68
D/Low	Down	1.30	2.18	2.84
	Cross	1.34	1.57	2.11

Πίνακας 2 Συγκεντρωτικός πίνακας του εκτιμώμενου συντελεστή συμπεριφοράς για όλα τα συστήματα

Ο Πίνακας 3 παραθέτει τις τιμές του συντελεστή συμπεριφοράς των κατασκευών όπως εκτιμήθηκαν από τις αναλύσεις της παρούσας εργασίας και τιμές που χρησιμοποιήθηκαν για τον σχεδιασμό.

Zone/IP		**A**		**B**		**C**		**D**	
	q-Factor	Down	Cross	Down	Cross	Down	Cross	Down	Cross
Low	Design	-	-	1.5	1.5	-	-	2	1.5
	Estimated	-	-	2	1.98	-	-	3.72	2.12
Medium	Design	1.5	1.5	-	-	1.5	1.5	2	1.5
	Estimated	2.22	2.48	-	-	5.51	2.2	3.27	1.68
High	Design	2	1.5	2	1.5	1.5	1.5	1.5	1.5
	Estimated	4.5	1.76	2.58	1.81	4.07	2.97	3.72	2.12

Πίνακας 3 Συγκεντρωτικός πίνακας του διαθέσιμου και του προτεινόμενου συντελεστή συμπεριφοράς για όλα τα συστήματα

2.3.4 Διαγράμματα απόκρισης για βαθμονομημένα μοντέλα της εγκάρσιας διεύθυνσης

Τα ίδια μοντέλα βαθμονομήθηκαν σύμφωνα με τα αποτελέσματα πού προέκυψαν στο πανεπιστήμιο της Λιέγης όπου πραγματοποιήθηκαν πειράματα πλήρους κλίμακας στην εγκάρσια διεύθυνση των προαναφερόμενων μοντέλων. Τα πειράματα εκτελέστηκαν χωρίς κατακόρυφα φορτία , ενώ στην παρούσα παράγραφο πραγματοποιήθηκαν νέες μη γραμμικές αναλύσεις με χρήση κατακόρυφων φορτίων, ώστε να ληφθεί υπόψη τα και τα φαινόμενα δευτέρας τάξης.

Ο Πίνακας 4 συγκεντρώνει τον συντελεστή συμπεριφοράς των βαθμονομημένων μοντέλων.

IP	**Seismic Zone**	**q factor**	**Bracing type**
IP A	Medium/High	1.1	X
IP B	Medium/High	1.8	D
IP C	High	2.2	X

	Low	1.1	D
IPD	High	1.2	D
	Medium	1.0	X
	Low	1.3	D

Πίνακας 4 Συγκεντρωτικός πίνακας του εκτιμώμενου συντελεστή συμπεριφοράς για όλα βαθμονομημένα συστήματα στην εγκάρσια διεύθυνση

3. Δυναμική απόκριση συστημάτων

3.1. Εισαγωγή

Αναζητώντας το επόμενο βήμα για την εκτίμηση της σεισμικής συμπεριφοράς των ραφιών, κρίνεται ως σκόπιμο να εφαρμοστεί η μέθοδος Incremental Dynamic Analysis, προσαρμοσμένη στα ιδιαίτερα χαρακτηριστικά των ραφιών. Η μέθοδος περιλαμβάνει την προσομοίωση των κατασκευών, την παραγωγή της πιθανότητας κατάρρευσης των κατασκευών και την ποσοτική εκτίμηση της συμπεριφοράς τους. Η μεθοδολογία εφαρμόζεται όπως περιγράφεται στο κανονιστικό κείμενο FEMA 695.

3.2. Σκοπός

Ο σκοπός του κεφαλαίου είναι η παραγωγή των αρχέτυπων μοντέλων που περιέχουν όλα τα βασικά χαρακτηριστικά των υπό εξέταση κατασκευών και η αξιολόγηση της συμπεριφοράς τους. Τα μοντέλα που δημιουργήθηκαν, είναι αυτά τα οποία είχαν διαθέσει οι συνεργαζόμενες εταιρείες του προγράμματος SEISRACKS2.

3.3. Προσαρμογή της μεθόδου για μεταλλικά ράφια

Τα βήματα της μεθόδου παρουσιάζονται στο διάγραμμα ροής στην Εικόνα 15. Η μοντελοποίηση των κατασκευών είναι όμοια με αυτήν που περιγράφηκε στο κεφάλαιο 2, με την διαφορά ότι εδώ χρειάζονται δεδομένα για τη συμπεριφορά των συνδέσεων/ μελών κ.α. υπό ανακυκλιζόμενη φόρτιση και όχι μόνο υπό στατικό μονοτονικό φορτίο. Δεδομένα σεισμικών δονήσεων είναι επίσης απαραίτητα και στην παρούσα διατριβή χρησιμοποιούνται οι καταγραφές που προτείνονται σαν βασικό σετ δονήσεων από το FEMA 695, και περιλαμβάνει 22 καταγραφές σε 2 διευθύνσεις. Συνολικά 44 καταγραφές οι οποίες περιέχουν την απαραίτητη ποικιλομορφία ώστε να εξεταστούν οι κατασκευές υπό διαφορετικά σεισμικά χαρακτηριστικά.

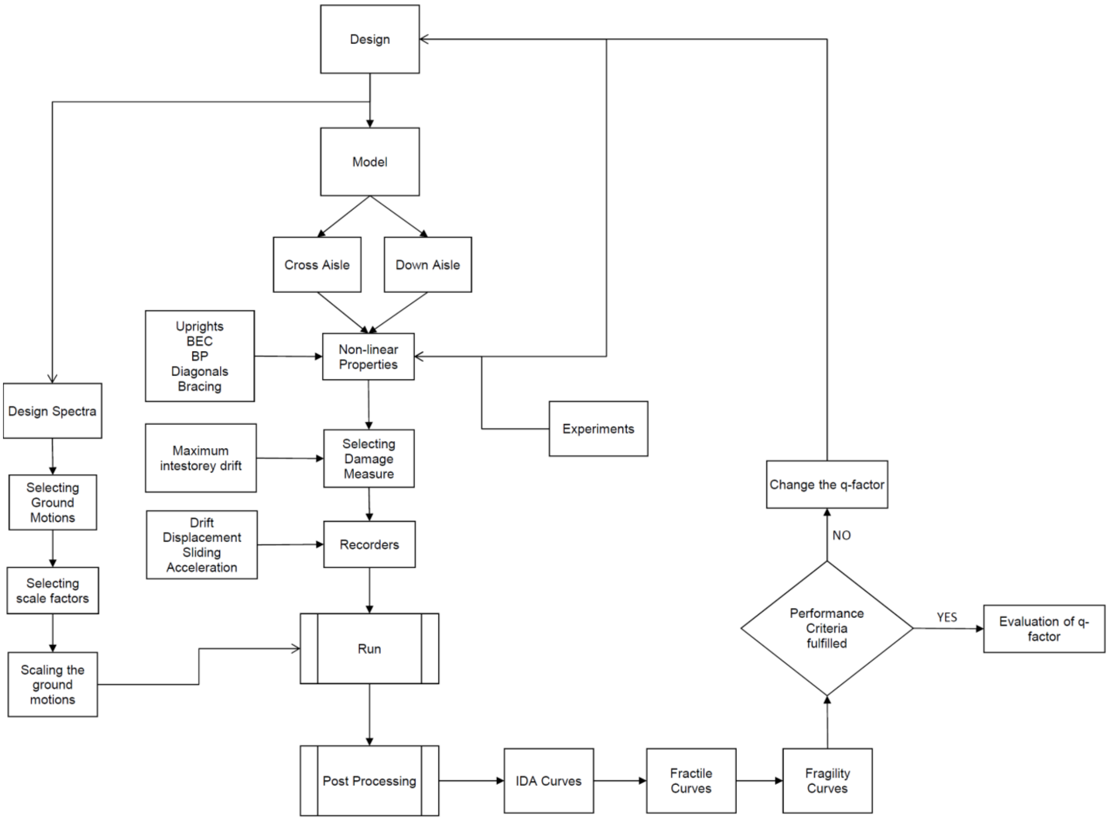

Εικόνα 15 Διάγραμμα ροής της μεθόδου IDA για βιομηχανικά ράφια

3.4. Προσομοίωση κατασκευών

Η προσομοίωση πραγματοποιείται στο λογισμικό OPENSEES, λόγω της δυνατότητας του να λαμβάνει υπόψη αρκετά υστεριτικά φαινόμενα χρησιμοποιώντας τα κατάλληλα εργαλεία του προγράμματος. Τα αποτελέσματα του είναι επίσης σε τέτοια μορφή που μπορούν με χρήση προγραμματιστικών εργαλείων να επεξεργαστούν και να παραχθούν τα επιθυμητά αποτελέσματα.

Οι εξεταζόμενες κατασκευές είναι δύο πλαισιωτές κατασκευές για την διαμήκη διεύθυνση και τέσσερεις δικτυωτές κατασκευές για την εγκάρσια διεύθυνση. Τα μοντέλα είναι δισδιάστατα και για αυτόν τον λόγο απορρίφτηκε το εγχείρημα να προσομοιωθούν οι κατασκευές που διέθεταν χιαστί συνδέσμους δυσκαμψίας. Στην διαμήκη διεύθυνση δεν προσομοιώθηκαν οι επιπλέον δύο πλαισιωτές κατασκευές που υπήρχαν διαθέσιμες, καθώς τα πειράματα που πραγματοποιήθηκαν στο Πολυτεχνείο του Μιλάνο, έδειξαν μία πλήρως ψαθυρή συμπεριφορά με αποτέλεσμα να κρίνεται μη σκόπιμη η περεταίρω διερεύνηση της ανελαστικής και μέτελαστικής τους συμπεριφοράς.

3.4.1. Αριθμητικά μοντέλα

Ένα τυπικό μοντέλο που αναπτύχθηκε παρουσιάζεται στην Εικόνα 16

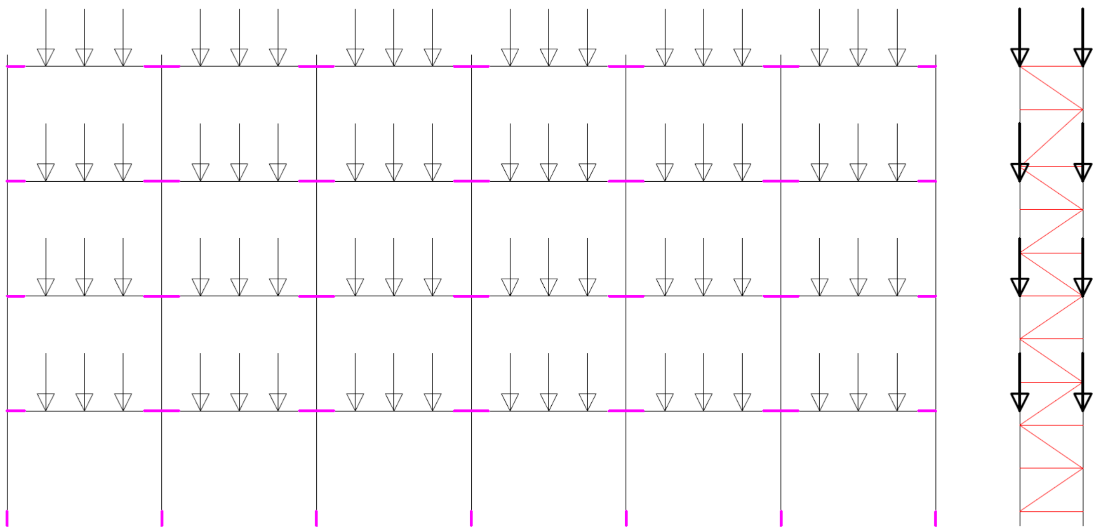

Εικόνα 16 Μορφή αριθμητικού μοντέλου

Οι κατασκευές μοντελοποιούνται με χρήση των εξής στοιχείων:

- Δοκοί: Ελαστικά στοιχεία δοκών
- Υποστυλώματα: Μη γραμμικά στοιχεία δοκού με μη γραμμικό υλικό (Hysteretic Material)
- Διαγώνια μέλη: Μη γραμμικά στοιχεία δικτυώματος
- Σύνδεση δοκού-υποστυλώματος: Μη γραμμικός ελαστικός κόμβος με μη γραμμικό υλικό
- Βάση υποστυλώματος: Μη γραμμικός ελαστικός κόμβος με μη γραμμικό υλικό

Το μη γραμμικό υλικό που χρησιμοποιείται ονομάζεται στο λογισμικό ως Hysteretic Material και δίνει τη δυνατότητα να λάβει υπόψη αρκετά υστεριτικά φαινόμενα.

3.4.2. Συντελεστής ισοδύναμης απόσβεσης

Η απόσβεση λαμβάνεται υπόψη με χρήση του μοντέλου Rayleigh. Ο συντελεστής απόσβεσης λαμβάνεται 3% όσο δηλαδή προτείνει και ο κανονισμός, παρότι πειραματικά δεδομένα έχουν δείξει ότι η τιμή αυτή δεν είναι αντιπροσωπευτική για καμία από τις δύο διευθύνσεις. Οι συντελεστές για τον ορισμό του μητρώου απόσβεσης κατά Rayleigh γίνεται για κάθε μοντέλο με χρήση των μεγεθών των πρώτων δεσποζουσών ιδιομορφών.

3.4.3. Επιλογή σεισμικών γεγονότων

Τα φάσματα των επιλεγμένων καταγραφών φαίνονται στην Εικόνα 17 σε σύγκριση με κάποια τυπικά φάσματα σχεδιασμού των υπό εξέταση ραφιών.

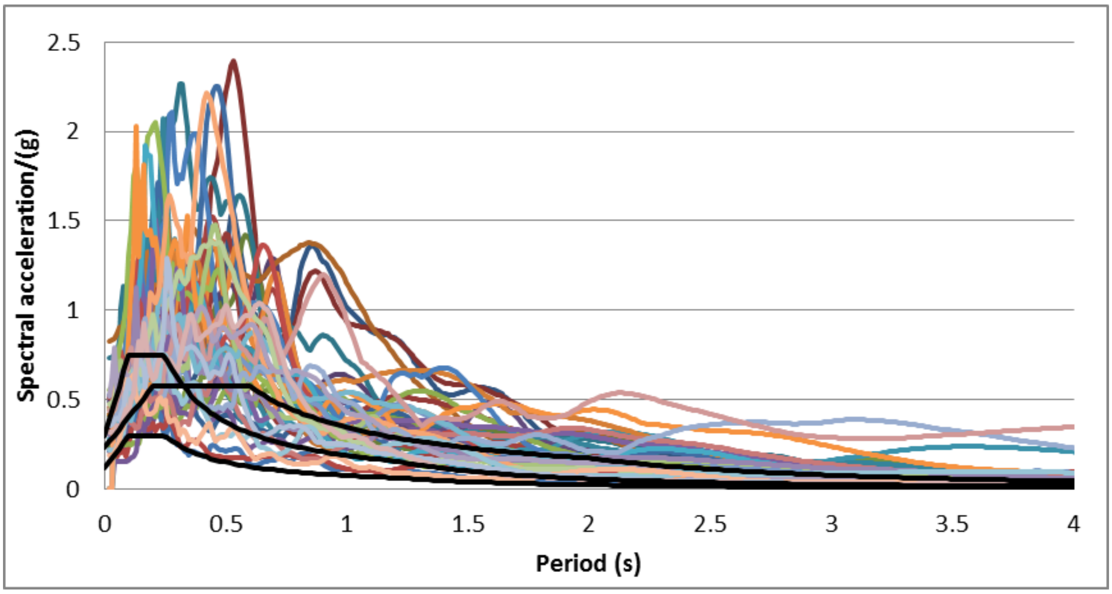

Εικόνα 17 Ελαστικά φάσματα των 44 καταγραφών (έγχρωμα) και κάποια ενδεικτικά φάσματα σχεδιασμού για χαμηλή και υψηλή σεισμικότητα

3.4.4. Επεξεργασία αποτελεσμάτων

Τα αποτελέσματα των δυναμικών αυτών αναλύσεων είναι διαγράμματα τα οποία ονομάζονται IDA-Curves, the fractile-curves και fragility curves. Το πρώτο διάγραμμα αποτελείται από 44 καμπύλες οι οποίες παρουσιάζουν τη μέγιστη απόκριση της κατασκευής (EDP, εδώ μέγιστη γωνία στροφής υποστυλώματος) για ένα δεδομένο μέγεθος έντασης (IM, εδώ επιτάχυνση πρώτης ιδιομορφής). Από το πρώτο διάγραμμα παράγονται οι στατιστικές καμπύλες απόκρισης για 16, 50 και 64%. Τέλος παράγεται η καμπύλη που δίνει την πιθανότητα κατάρρευσης της κατασκευής για μια δεδομένη τιμή της επιτάχυνσης της πρώτης δεσπόζουσας ιδιομορφής.

3.4.5. Αλληλεπίδραση παλέτας κατασκευής

Πιστεύεται ότι η αλληλεπίδραση παλέτας και κατασκευής δύναται να επηρεάσει τόσο τον σχεδιασμό όσο και την απόκριση ενός συστήματος. Σύμφωνα με τους Gilbert et al., (2011) η αλληλεπίδραση αυτή δεν επηρεάζει το σύστημα σημαντικά, εφόσον δεν υπάρξει ολίσθηση των παλετών. Η ολίσθηση θεωρείται ότι αλλάζει τα χαρακτηριστικά της κατασκευής και λειτούργει ως μια σεισμική μόνωση για την κατασκευή. Στη διαμήκη διεύθυνση η ολίσθηση δεν θεωρείται κρίσιμη, καθώς οι παλέτες έχουν γεωμετρικά το περιθώριο να ολισθήσουν χωρίς να πέσουν από τις δοκούς. Αντιθέτως, στην εγκάρσια διεύθυνση οι παλέτες έχουν μικρό περιθώριο ολίσθησης μετά το οποίο η παλέτα οδηγείται στην πτώση Η ολίσθηση επίσης μπορεί να επηρεάσει την απορρόφηση ενέργειας ακόμα και την απόσβεση της κατασκευής. Για να λάβουμε υπόψη την αλληλεπίδραση αυτή, υπάρχουν 2 βασικές μέθοδοι:

- Μη προσομοιωμένη αλληλεπίδραση και εκ των υστέρων επεξεργασία των αποτελεσμάτων για την εκτίμηση της επιρροής της. (Στατικό κριτήριο ολίσθησης)
- Προσομοίωση της αλληλεπίδρασης και καταγραφή της συμπεριφοράς σε πραγματικό χρόνο. (Δυναμικό κριτήριο ολίσθησης)

3.4.6. Στατικό κριτήριο ολίσθησης (NSC)

Στην μέθοδο αυτή δεν προσομοιώνεται άμεσα η ολίσθηση, αλλά καταγράφεται η επιτάχυνση κάθε ορόφου και γίνεται σύγκριση με το κριτήριο ολίσθησης του κανονισμού. Όταν η επιτάχυνση είναι $acc_i > \mu \cdot g$ τότε υπάρχει ολίσθηση. Η ανάλυση για την οποία μετρήθηκε μη αποδεκτή τιμή της επιτάχυνσης θεωρείται ότι οδήγησε σε κατάρρευση, αφού δεν μπορεί να γίνει ποσοτικός προσδιορισμός της ολίσθησης. Για τη συγκεκριμένη ανάλυση η αρχική καμπύλη τροποποιείται όπως φαίνεται στην Εικόνα 19 και λαμβάνει μια αριθμητικά άπειρη τιμή της απόκρισης και δημιουργεί έτσι μια οριζόντια γραμμή. Η Εικόνα 18 δείχνει γραφικά πώς γίνεται η καταμέτρηση των επιταχύνσεων ορόφου και ο εντοπισμός του σημείου ολίσθησης.

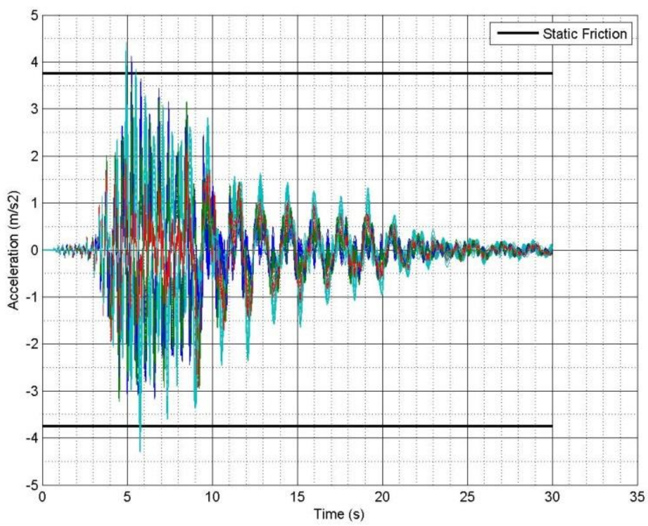

Εικόνα 18 Καταγραφές της επιτάχυνσης ορόφου για μία συγκεκριμένη τιμή του συντελεστή μεγέθυνσης και για μία ενδεικτική σεισμική δόνηση

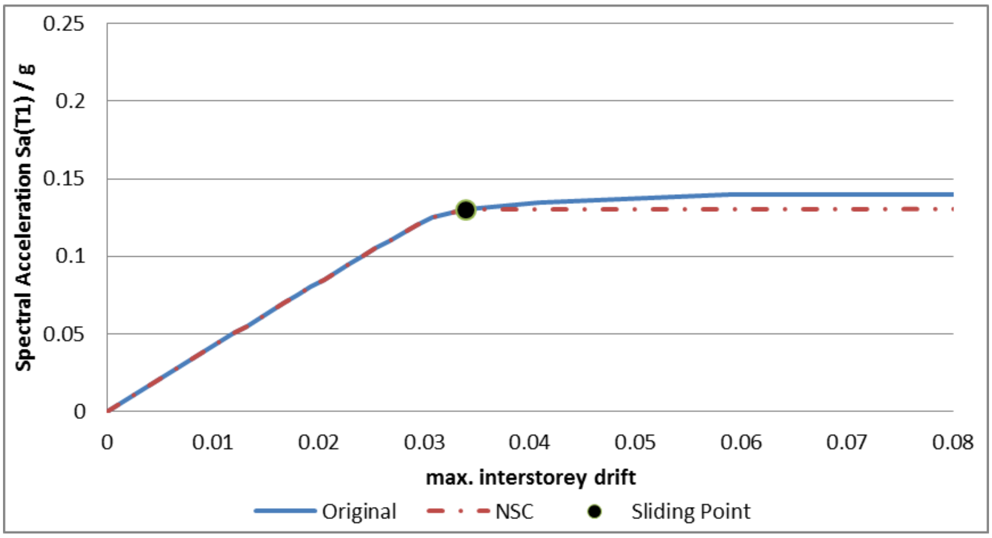

Εικόνα 19 Ενδεικτική καμπύλη απόκρισης λαμβάνοντας και μη το στατικό κριτήριο ολίσθησης

3.4.7. Δυναμικό κριτήριο ολίσθησης (SL)

Προσπαθώντας να γίνει η προσομοίωση της ολίσθησης και η επίδραση της στο σύστημα περισσότερο άμεσες και ρεαλιστικές προτείνεται ένα μοντέλο όπου το φαινόμενο της ολίσθησης περιλαμβάνεται στο αριθμητική προσομοίωση. Η παλέτα προσομοιώνεται σαν ένα πρακτικά άκαμπτο πλαίσιο με στοιχεία εφεδράνων στης βάση του (Flat slider bearing element). Τα στοιχεία εφεδράνων έχουν τη δυνατότητα να λάβουν υπόψη την δυσκαμψία του εφεδράνου (στην περίπτωση αυτή πρακτικώς άκαμπτα), αλλά και την τριβή του εφεδράνου μέσω του συντελεστή τριβής. Με το σύστημα αυτό γίνεται η καταγραφή της μετακίνησης του κάτω άκρου της παλέτας αλλά και η σχετική μετατόπισης του ως προς την δοκό στήριξης. Σε περίπτωση ολίσθησης η σχετική μετακίνηση παίρνει τιμές οι οποίες ελέγχονται με επεξεργασία των αποτελεσμάτων. Σε περίπτωση που η σχετική μετατόπιση είναι μεγαλύτερη από το περιθώριο που έχει μια θεωρητικώς συμμετρικά τοποθετημένη παλέτα, τότε θεωρείται αυτομάτως ως αστοχία και δίνεται στην συγκεκριμένη ανάλυση μία άπειρη τιμή για την απόκριση. Η Εικόνα 20 παρουσιάζει γραφικά το μοντέλο και η Εικόνα 21 τη σχετική μετατόπιση της παλέτας που καταγράφηκε για μια σεισμική δόνηση και έναν συντελεστή μεγέθυνσης για όλες τις παλέτες. Στην περίπτωση αυτή ναι μεν υπάρχει ολίσθηση, αλλά δεν είναι αρκετά μεγάλη ώστε να οδηγήσει σε πτώση της παλέτας. Ένα ακόμα πλεονέκτημα του προσομοιώματος είναι ότι εντοπίζεται ακόμα και μία πιθανή ανατροπή της παλέτας. Η Εικόνα 22 δείχνει την αντίδραση στη βάση των παλετών κάθε ορόφου. Όταν η αντίδραση γίνει αρνητική σημαίνει ότι η παλέτα ανατρέπεται. Στην παρούσα εργασία η παλέτες φαίνονται να ταλαντεύονται χωρίς όμως να ανατραπούν για καμία από τις εξεταζόμενες επιταχύνσεις.

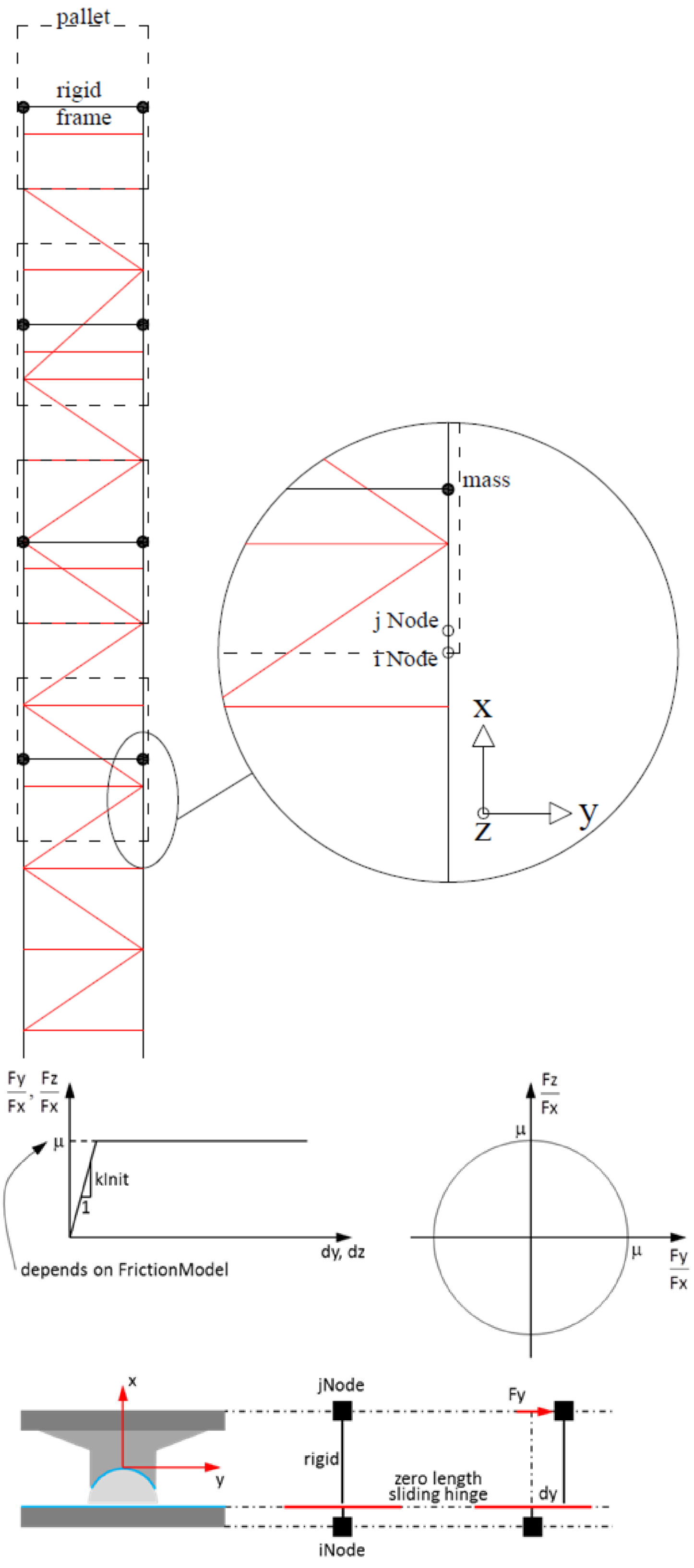

Εικόνα 20 Δισδιάστατο προσομοίωμα της εγκάρσιας διεύθυνσης με μοντέλο παλέτας πάνω σε στοιχεία εφεδράνων

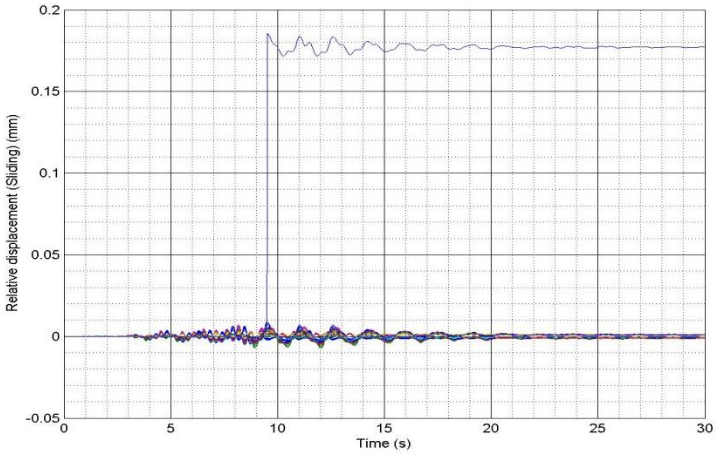

Εικόνα 21 Καταγραφή σχετικής μετακίνησης (ολίσθησης) παλέτας –δοκού

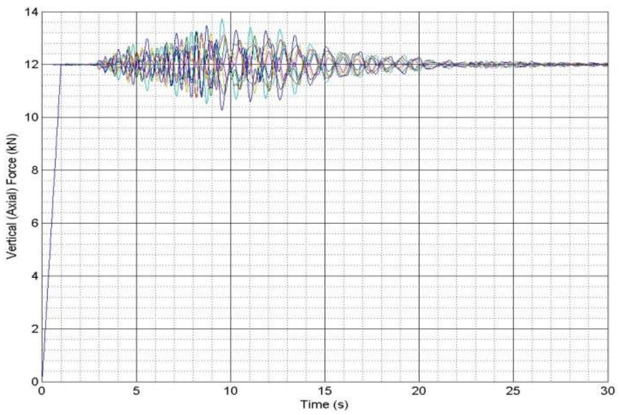

Εικόνα 22 Καταγραφή κατακόρυφης αντίδρασης της παλέτας

3.5. Αποτελέσματα

Στην παράγραφο αυτή παρουσιάζονται ενδεικτικά κάποια αποτελέσματα από τις μη γραμμικές δυναμικές αναλύσεις.

3.5.1. Διαμήκης διεύθυνση

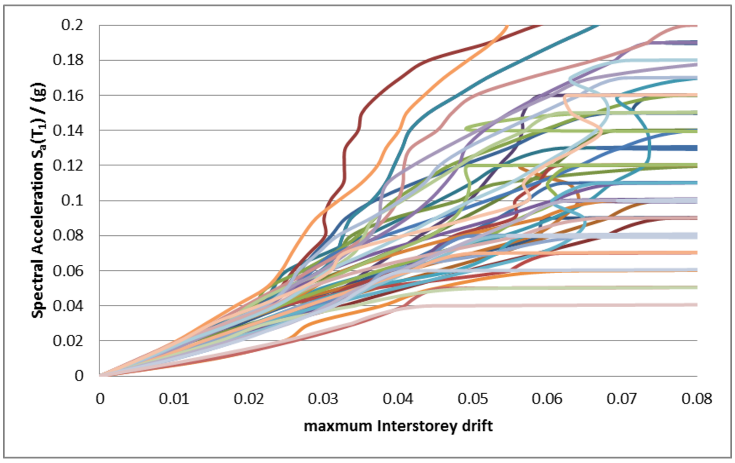

Εικόνα 23 Καμπύλες απόκρισης για το μοντέλο του κατασκευαστή Α

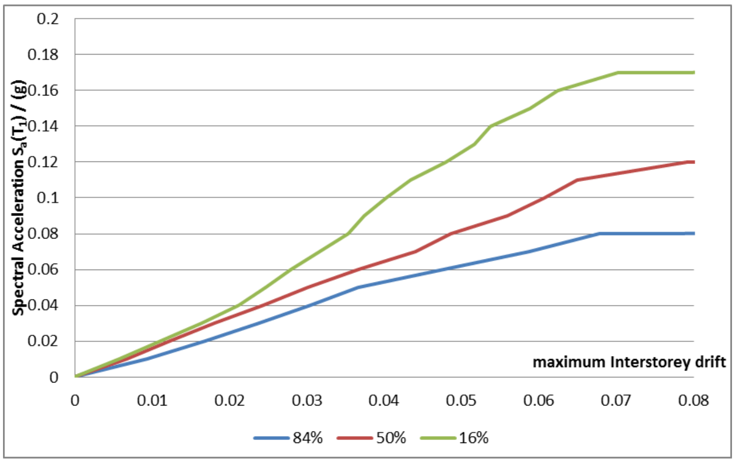

Εικόνα 24 Fractile Curves για τον κατασκευαστή Α

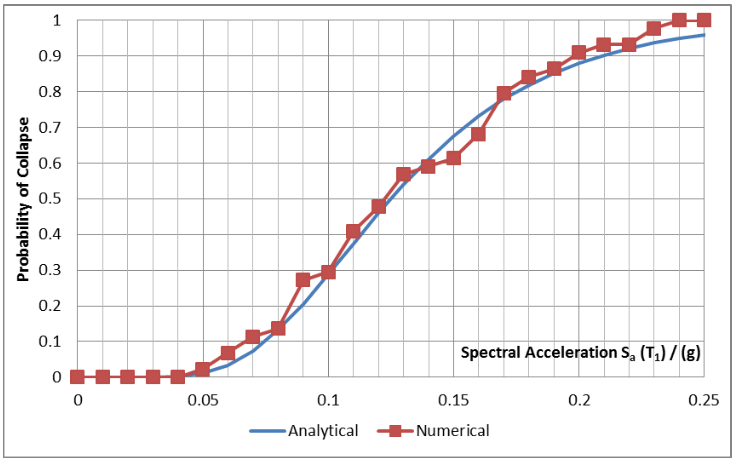

Εικόνα 25 Fragility Curve για τον κατασκευαστή Α

3.5.2. Εγκάρσια διεύθυνση

Ενδεικτικά παρουσιάζονται τα αποτελέσματα με την μέθοδο του στατικού κριτηρίου και του δυναμικού κριτηρίου ολίσθησης.

3.5.2.1. Στατικό κριτήριο ολίσθησης

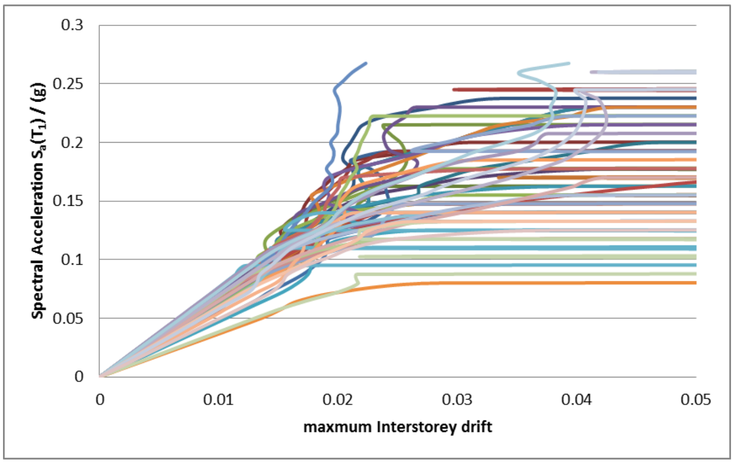

Εικόνα 26 Καμπύλες απόκρισης για το μοντέλο του κατασκευαστή D

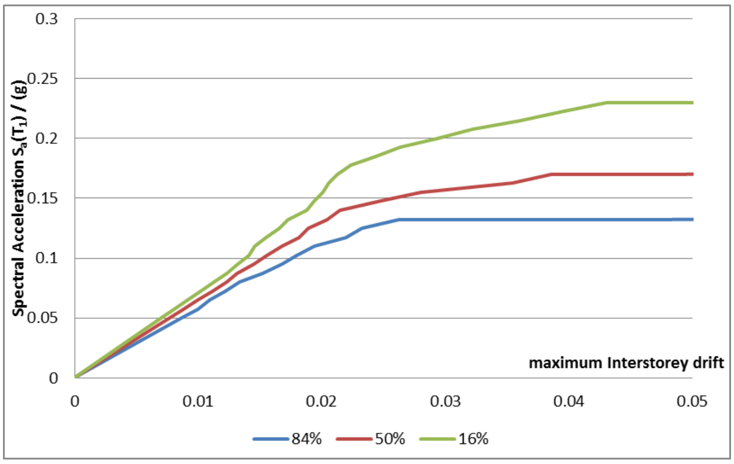

Εικόνα 27 Fractile Curves για τον κατασκευαστή D

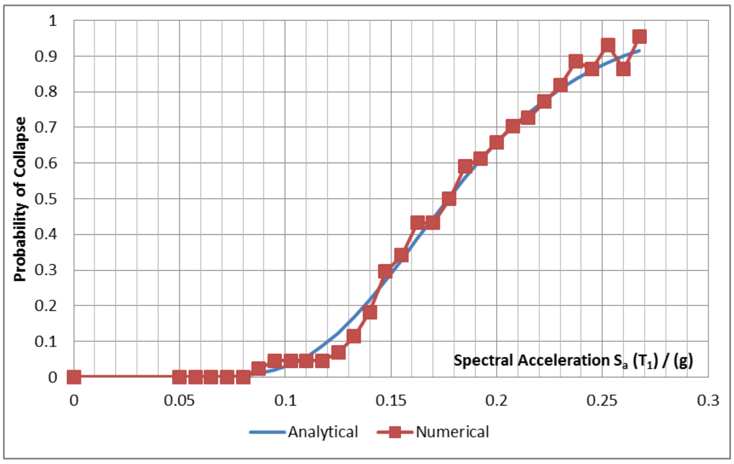

Εικόνα 28 Fragility για τον κατασκευαστή D

3.5.2.2. Δυναμικό κριτήριο ολίσθησης

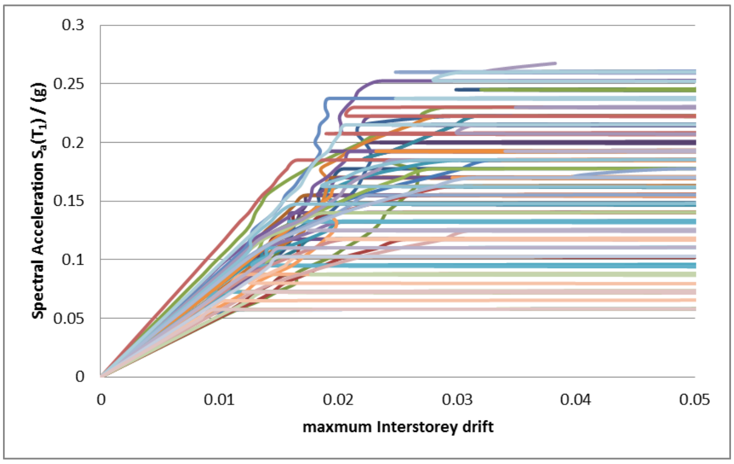

Εικόνα 29 Καμπύλες απόκρισης για το μοντέλο του κατασκευαστή D

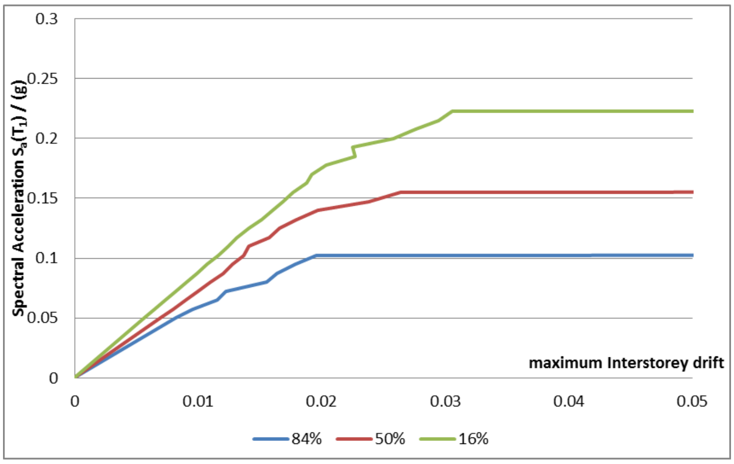

Εικόνα 30 Fractile Curves για τον κατασκευαστή D

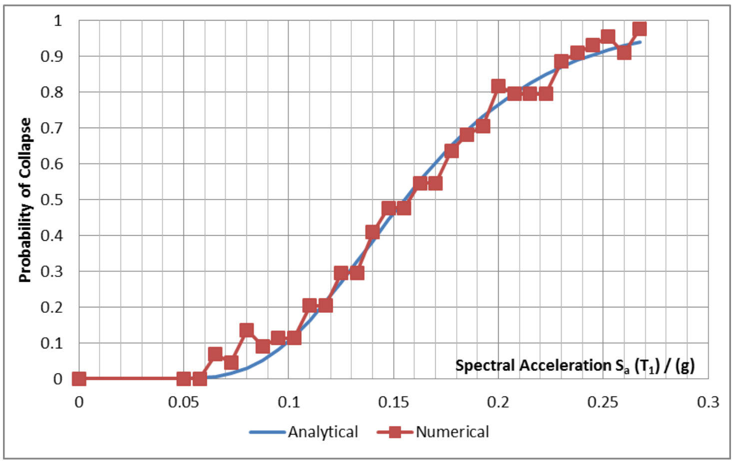

Εικόνα 31 Fragility Curve για τον κατασκευαστή D

3.5.3. Εκτίμηση απόκρισης των ραφιών

Οι επόμενοι πίνακες παρουσιάζουν τις τιμές των δεικτών που εισάγει το κανονιστικό κείμενο FEMA 695 για την εκτίμηση της τελικής δυναμικής απόκρισης των κατασκευών.

IP	**Διαμήκης διεύθυνση**			**Εγκάρσια διεύθυνση (NSC)**			**Εγκάρσια διεύθυνση (SL)**		
	S_{MT}	S_{CT}	CMR	S_{MT}	S_{CT}	CMR	S_{MT}	S_{CT}	CMR
A	0.027	0.120	2.963	0.052	0.115	1.474	0.052	0.120	1.538
B	0.039	0.150	2.538	0.100	0.200	1.333	0.100	0.200	1.333
C				0.290	0.515	1.184	0.290	0.400	0.920
D				0.054	0.170	2.099	0.054	0.155	1.914

Πίνακας 5 Τιμές του δείκτη CMR για τις εξεταζόμενες κατασκευές

IP-Direction	**ACMR**	β_{TOT}	**ACMR10%**	**ACMR20%**
A-Down	3.35	0.500	1.90	1.52
A-Cross	2.6	0.360	1.59	1.35
A-Cross SL	1.51	0.335	1.54	1.32
B-Down	1.76	0.500	1.90	1.52
B-Cross	1.41	0.390	1.65	1.39
B-Cross SL	1.41	0.390	1.65	1.39
C-Cross	1.28	0.407	1.68	1.41
C-Cross SL	1	0.461	1.80	1.47
D-Cross	2.22	0.424	1.72	1.43
D-Cross SL	2.02	0.461	1.80	1.47

Πίνακας 6 Τιμές δεικτών, κατά FEMA 695

3.6. Συμπεράσματα

Τα εξετασθέντα συστήματα βρέθηκαν να μην είναι ιδιαίτερα πλάστιμα με αποτέλεσμα οι τιμές που χρησιμοποιούν οι μελετητές για τον σχεδιασμό τους, οι οποίες φαίνονται αρχικά χαμηλές σε σύγκριση με τις προτεινόμενες από τον κανονισμό, να επιβεβαιώνονται. Με άλλα λόγια για την διαμήκη διεύθυνση προτείνεται η τιμή 1.5, ενώ για την εγκάρσια τιμές μέχρι 2.0. Παρ΄όλ΄αυτά προτείνεται σε κάθε περίπτωση η διενέργεια ικανοτικού σχεδιασμού ακόμα και για τις συγκεκριμένες τιμές του συντελεστή συμπεριφοράς που οδηγεί σε Low dissipative concept. Με τον τρόπο αυτό θεωρείται ότι η μετελαστική συμπεριφορά των συστημάτων μπορεί να εμφανιστεί περισσότερο πλάστιμη και στις δύο διευθύνσεις.

4. Αλληλεπίδραση παλέτας-κατασκευής

4.1. Εισαγωγή

Το παρόν κεφάλαιο ασχολείται με τρία διαφορετικά θέματα που αφορούν τις δοκούς των ραφιών και την αλληλεπίδραση που έχουν αυτά με τις παλέτες που στηρίζονται πάνω τους. Ο σκοπός είναι να ελεγχθεί αν οι διατάξεις του ευρωπαϊκού κανονισμού για τα ράφια είναι κατάλληλες για τον σχεδιασμό των δοκών. Τα τρία θέματα που αναλύει το παρόν κεφάλαιο είναι οι δυνάμεις που αναπτύσσονται στις δοκούς όταν οι παλέτες φορτίζονται με οριζόντιες δυνάμεις, που συνήθως προκαλούνται από σεισμικά φορτία. Ακόμα εξετάζονται οι ροπές κάμψης που αναπτύσσονται εξαιτίας των φορτίων αυτών και τέλος το φαινόμενο του λυγισμού των δοκών στην ασθενή τους διεύθυνση. Η Εικόνα 32 δείχνει εικόνες αστοχίας των δοκών μετά από σεισμικό γεγονός. Οι καταγεγραμμένες επιταχύνσεις ήταν παραπλήσιες μεν αλλά όχι μεγαλύτερες από τις τιμές σχεδιασμού.

Εικόνα 32 Εικόνες αστοχίας δοκών, με εκτενείς πλαστικές παραμορφώσεις προς το εξωτερικό της κατασκευής

4.2. Οριζόντιες εγκάρσιες σεισμικές δυνάμεις δοκών

4.2.1.Κανονιστικές διατάξεις

Οι διατάξεις του κανονιστικού κειμένου FEM 10.2.08 [25] ή του κανονισμού EN16681 [26] εισάγουν για τις οριζόντιες δυνάμεις των δοκών στην εγκάρσια διεύθυνση τους το γεγονός ότι οι μέγιστη δύναμη είναι το βάρος των παλετών πολλαπλασιασμένο με τον συντελεστή τριβής και πολλαπλασιασμένο με έναν συντελεστή $C_{\mu H} = 1.5$ ο οποίος χρησιμοποιείται για να καλύψει τις αβεβαιότητες στο σύστημα. Στη συνέχεια όμως της διατριβής ορίζεται με διαφορετικό τρόπο η μέγιστη αναπτυσσόμενη δύναμη στις δοκούς.

4.2.2.Αναλυτικό μοντέλο

Θεωρείται μια παλέτα που στηρίζεται συμμετρικά πάνω σε 2 δοκούς και ασκείτε στο κέντρο μάζας της μια αδρανειακή οριζόντια δύναμη H. Γίνεται η θεώρηση ότι η οριζόντια δύναμη παραλαμβάνεται εξίσου από τις δύο δοκούς. Αυτή η παραδοχή ισχύει μέχρις ότου συμβεί η ολίσθηση σε κάποια από τις δύο δοκούς. Η ολίσθηση όμως συμβαίνει πρώτα στην δοκό όπου είναι κατακόρυφα λιγότερο φορτισμένη. Αυτή είναι πάντα η εσωτερική δοκός σύμφωνα με την κατεύθυνση που δείχνει το βέλος της οριζόντιας δύναμης H. Η δοκός αυτή ονομάζεται Front beam ενώ η άλλη είναι η rear beam. Οι δυνάμεις που αναπτύσσονται και η γεωμετρία του συστήματος φαίνεται στην Εικόνα 33. Αφού συμβεί η ολίσθηση στην πρώτη δοκό τότε η οριζόντια δύναμη συνεχίζει να αυξάνεται αλλά η επιπλέον δύναμη παραλαμβάνεται εξολοκλήρου από την πίσω δοκό που είναι περισσότερο φορτισμένη. Το άθροισμα των αντιδράσεων των δύο δοκών είναι πάντα ίσο με την οριζόντια εξωτερική δύναμη H. Λύνοντας ένα σύστημα εξισώσεων λαμβάνοντας υπόψη τις παραπάνω παραδοχές υπολογίζονται οι μέγιστες δυνάμεις που μπορούν να αναπτυχθούν σε κάθε δοκό. Ο μηχανισμός της τριβής λειτουργεί ως μια σεισμική μόνωση που δεν επιτρέπει στην παλέτα να φορτιστεί περισσότερο από την στιγμή που ολισθαίνει πλήρως.

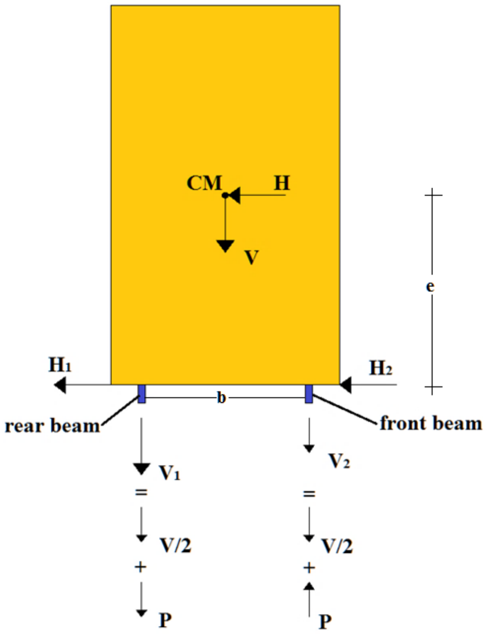

Εικόνα 33 Δράσεις και αντιδράσεις παλέτας υπό οριζόντια εγκάρσια φόρτιση

$$\boldsymbol{H_2} = \frac{V \cdot b \cdot \mu}{2(b + 2e \cdot \mu)} \tag{4-7}$$

Or:

$$\boldsymbol{H_1} = \frac{V \cdot b \cdot \mu}{4(b - e \cdot \mu)} \frac{2b + 5e \cdot \mu}{(b + 2e \cdot \mu)} \tag{4-8}$$

4.2.3.Αριθμητική μοντέλο

Για να επιβεβαιωθεί το αναλυτικό μοντέλο της προηγούμενης παραγράφου, δημιουργείται το παρακάτω αριθμητικό μοντέλο στο λογισμικό ABAQUS. Η παλέτα είναι ένα άκαμπτο σώμα, οι δοκοί αποτελούνται από στοιχεία κελύφους και η επαφή μεταξύ των σωμάτων ορίζεται μέσω στοιχείων επαφής με κριτήριο τριβής Coulomb. Η Εικόνα 34 δείχνει το αριθμητικό μοντέλο. Για την επαλήθευση ελέγχονται 3 διαφορετικές περιπτώσεις για να επιβεβαιώσει την επίδραση ή μη διάφορων παραμέτρων. Οι παράμετροι αυτοί είναι η δυσκαμψία των δοκών, η θέση της παλέτας και τέλος το βάρος της παλέτας. Για τις περιπτώσεις αυτές εμφανίζονται τα διαγράμματα με τα αποτελέσματα που εξήχθησαν από τα αριθμητικά μοντέλα για διάφορες τιμές του ύψους του κέντρου βάρους της παλέτας. Το ύψος αυτό θεωρείται ως εκκεντρότητα.

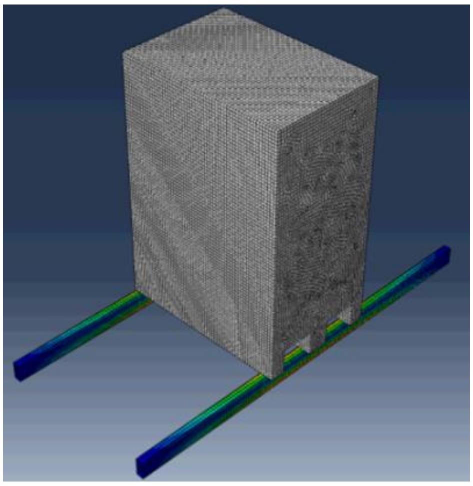

Εικόνα 34 Άποψη του αριθμητικού μοντέλου

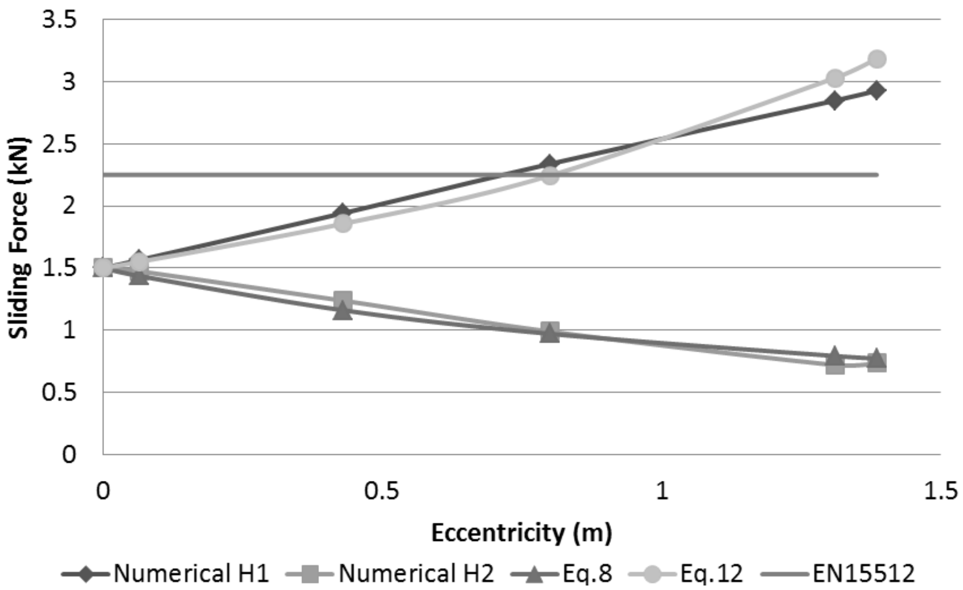

Εικόνα 35 Δύναμη ολίσθησης κατά τον κανονισμό, τις προτεινόμενες σχέσεις και το αριθμητικό μοντέλο, για διάφορες τιμές του ύψους του κέντρου μάζας της παλέτας

4.3. Καμπτικές ροπές λόγω οριζόντιων φορτίων στην εγκάρσια διεύθυνση

Ο κανονισμός EN16681 εισάγει την απομείωση των ροπών κάμψης γύρω από τον ασθενή άξονα των δοκών, λόγω της πιθανής διαφραγματικής λειτουργίας που προκαλείται από την ύπαρξη των παλετών. Για να ελεγχθεί η συγκεκριμένη διάταξη αναπτύσσονται επιπλέον αριθμητικά μοντέλα που εξετάζουν τις συγκεκριμένες ροπές μελετώντας πολλαπλές παραμέτρους όπως το πλήθος των παλετών, η θέση των παλετών, το βάρος των παλετών, η εκκεντρότητα του κέντρου μάζας των παλετών και τέλος τον συντελεστή τριβής. Ο Πίνακας 7 δείχνει την κατηγοριοποίηση των φορτιστικών περιπτώσεων και ο Πίνακας 8 τις περιπτώσεις και τις τιμές των παραμέτρων που χρησιμοποιήθηκαν.

Case	Configuration	Loading	Theoretical moment M^*
A		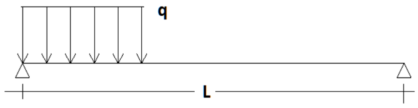	$25/648\ qL^2$
B		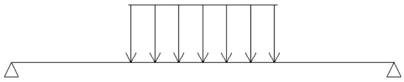	$5/72\ qL^2$
C	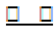		$1/18\ qL^2$
D		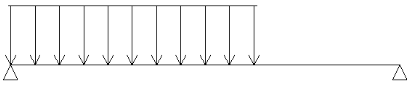	$8/81\ qL^2$
E		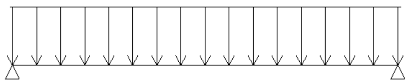	$1/8\ qL^2$

Πίνακας 7 Περιπτώσεις φόρτισης και τιμή της θεωρητικής ροπής κάμψης M*

No of case study	Friction coefficient μ	Pallet Weight Qp	Eccentricity of mass e
1	0.1	4	0.9
2	0.1	4	0.625
3	0.1	4	0.35
4	**0.1**	**8**	**0.9**
5	**0.1**	**8**	**0.625**
6	**0.1**	**8**	**0.35**
7	0.1	12	0.9
8	0.1	12	0.625
9	0.1	12	0.35
10	0.3	4	0.9
11	**0.3**	**4**	**0.625**
12	0.3	4	0.35
13	**0.3**	**8**	**0.9**

14	**0.3**	**8**	**0.625**
15	**0.3**	**8**	**0.35**
16	0.3	12	0.9
17	**0.3**	**12**	**0.625**
18	0.3	12	0.35
19	0.5	4	0.9
20	0.5	4	0.625
21	0.5	4	0.35
22	**0.5**	**8**	**0.9**
23	**0.5**	**8**	**0.625**
24	**0.5**	**8**	**0.35**
25	0.5	12	0.9
26	0.5	12	0.625
27	0.5	12	0.35

Πίνακας 8 Τιμές των παραμέτρων που χρησιμοποιήθηκαν στην παραμετρική ανάλυση

Τα αποτελέσματα επιβεβαιώνουν τη διαφραγματική λειτουργία και επομένως την απομείωση των ροπών μόνο πριν την, έστω τοπική, ολίσθηση κάποιας από τις παλέτες.

4.4. Λυγισμός δοκών εντός του εγκάρσιου επιπέδου

Με βάση τα ίδια αριθμητικά μοντέλα της προηγούμενης παραγράφου γίνεται μια προσπάθεια να διαπιστωθεί αν η μερική διαφραγματική λειτουργία που προσφέρουν οι παλέτες στην κατασκευή μπορεί να οδηγήσει τις δοκούς να λυγίσουν με κάποια από τις ανώτερες ιδιομορφές λυγισμού και όχι με τη μορφή της δεσπόζουσας ιδιομορφής. Αυτό θα σήμαινε αυτόματα αύξηση του φορτίου λυγισμού και μείωση του μήκους λυγισμού. Οι φορτιστικές περιπτώσεις του Πίνακας 8 εξετάζονται και εδώ και επιπλέον οι περιπτώσεις Α έως Ε εξετάζονται με μια μη ρεαλιστική τιμή του συντελεστή τριβής, μ=100, ώστε να ελεγχθεί μια περίπτωση που οι παλέτες είναι δυνητικά στερεωμένες πάνω στις δοκούς. Για όλες τις ρεαλιστικές τιμές του συντελεστή τριβής και για όλες τις φορτιστικές περιπτώσεις, οι δοκοί λύγισαν με την μορφή της πρώτης ιδιομορφήε και για το αντίστοιχο φορτίο. Η συμπεριφορά των δοκών παρουσιάζεται στην Εικόνα 36 και Εικόνα 37 σε όρους αξονικού φορτίου-μετατόπισης. Βρέθηκε ότι το φορτίο λυγισμού ήταν ανεπηρέαστο και το σχήμα λυγισμού επίσης.

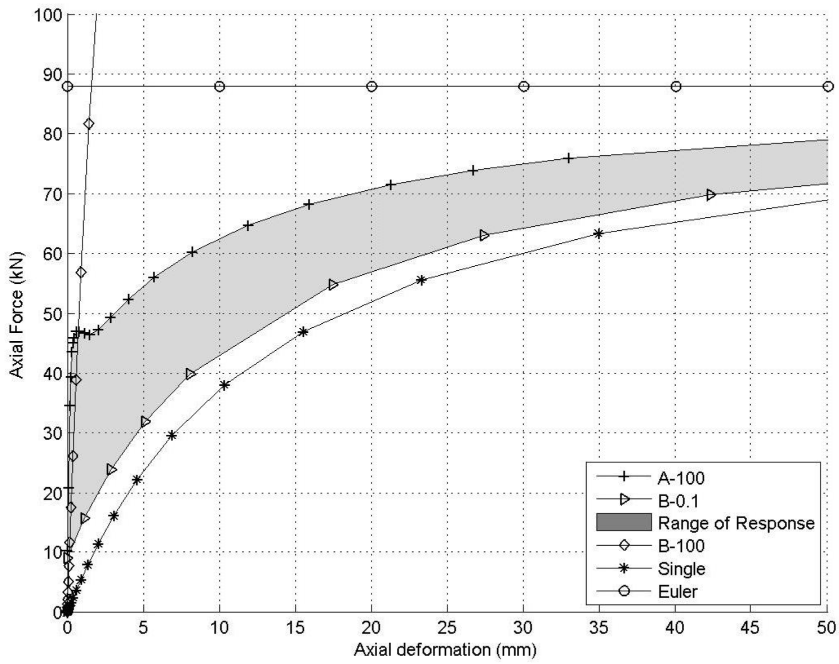

Εικόνα 36 Διάγραμμα αξονικού φορτίου-μετατόπισης δοκού για βάρος παλέτας 8 kN

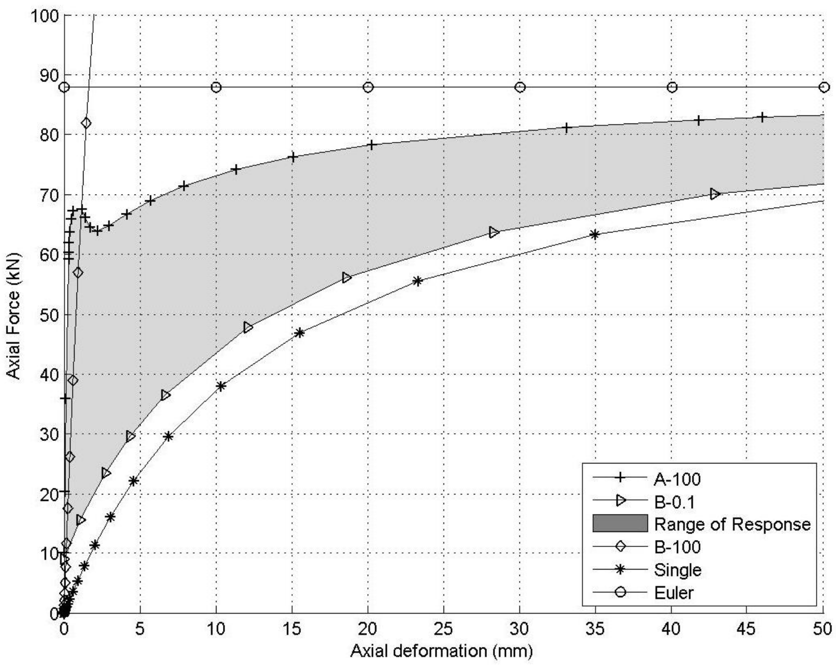

Εικόνα 37 Διάγραμμα αξονικού φορτίου-μετατόπισης δοκού για βάρος παλέτας 12 kN

4.5. Συμπεράσματα

Οι κανονισμοί υποεκτιμούν τις οριζόντιες δυνάμεις που αναπτύσσονται στις δοκούς. Η ύπαρξη των παλετών δεν είναι ικανή να δημιουργήσει μια πλήρη διαφραγματική λειτουργία στην κατασκευή και ως αποτέλεσμα οι αναπτυσσόμενες ροπές αλλά και ο λυγισμός των δοκών μένουν ανεπηρέαστα.

5. Συμπεράσματα & συμβολή διατριβής

5.1. Συμπεράσματα

Τα συμπεράσματα συνοψίζονται σε δύο ομάδες.

Συμπεράσματα για την απόκριση των συστημάτων:

a) Μοντέλα ραφιών που βασίζονται σε ονομαστικά χαρακτηριστικά των μελών τους δεν είναι ικανά να προβλέψουν την απόκριση του συστήματος.
b) Ακόμα και μη γραμμικές αναλύσεις που δεν βασίζονται σε πειραματικά δεδομένα υπερεκτιμούν την φέρουσα ικανότητα των συστημάτων
c) Μη γραμμικές δυναμικές αναλύσεις δείχνουν ότι η πλαστιμότητα των συστημάτων είναι εξαιρετικά περιορισμένη
d) Οι τιμές του συντελεστή συμπεριφοράς που χρησιμοποιούνται στην πράξη, είναι μεν χαμηλότεροι από τις προτεινόμενες, αλλά είναι ρεαλιστικές.
e) Υψηλές τιμές του συντελεστή συμπεριφοράς δικαιολογούνται κάποιες φορές, λογω της υπεραντοχής του συστήματος και όχι λόγω της πλαστιμότητας του.
f) Επειδή η υπεραντοχή αυτή δεν μπορεί να ποσοτικοποιηθεί, προτείνεται ένας εκ νέου ορισμός του συντελεστή συμπεριφοράς. Για την περίπτωση των ραφιών.
g) Η εφαρμογή ικανοτικού σχεδιασμού θεωρείται απαραίτητη για να οδηγηθεί η κατασκευή σε μια ελεγχόμενη μορφή κατάρρευσης που θα δώσει εν τέλει καλύτερες τιμές πλαστιμότητας στην κατασκευή.

Συμπεράσματα για τον σχεδιασμό των δοκών του εκάστοτε συστήματος:

a) Ο ευρωπαϊκός κανονισμός περιγράφει επαρκώς, αλλά με στατικό τρόπο το φαινόμενο της ολίσθησης.
b) Οι τιμές των ασκούμενων δυνάμεων στις δοκούς είναι συχνά αρκετά μεγαλύτερες από τις αντίστοιχες που δίνονται από τον κανονισμό.
c) Η τιμή των δυνάμεων αυτών επηρεάζονται από τη θέση του κέντρου βάρους της παλέτας και του αποθηκευμένου προϊόντος, το πλάτος της κατασκευής, το βάρος των παλετών και τον συντελεστή τριβής.
d) Οι διατάξεις του κανονισμού EN16681 για απομείωση των ροπών κάμψης γύρω από τον ασθενή άξονα των δοκών, δεν επιβεβαιώθηκαν.
e) Οι παλέτες εμφανίζουν τοπική ολίσθηση ή και πλήρη ολίσθηση με αποτέλεσμα να μην μπορούν να προσφέρουν πλήρη διαφραγματική λειτουργία.
f) Το μήκος λυγισμού των δοκών προτείνεται ίσο με το γεωμετρικό μήκος των δοκών.

5.2. Ιδέες για περεταίρω έρευνα.

Εφαρμογή της προτεινόμενης μεθοδολογίας για δυναμικές αναλύσεις σε περισσότερα μοντέλα-κατασκευές. Εφαρμογή των μεθόδων σε συστήματα με σύστημα δυσκαμψίας, με χρήση τρισδιάστατων αριθμητικών μοντέλων.

Πρόταση για έναν ικανοτικό κανονισμό που θα μπορούσε να αποδώσει στην κατασκευή καλύτερη ανελαστική συμπεριφορά.

Περιγραφή της αλληλεπίδρασης παλέτας –δοκών με δυναμικές αναλύσεις για να επιβεβαιωθούν οι τιμές της μέγιστης έντασης των δοκών από οριζόντια φορτία εκτός επιπέδου

Contents

List of figures

List of tables

List of Symbols

$a_{cc,i}$	Acceleration of floor i
ACMR	Adjusted Collapse margin ratio
a_{cr}	Critical buckling factor
A_{eff}	Effective section area
a_g	round acceleration
a_K	Factor for the stiffness matrix
a_M	Factor for the mass matrix
b	Width of the rack
BEC	Beam End Connector
BP	Base Plate
C_a, C_v	Demand spectrum factors
CMR	Collapse margin ratio
$C_{\mu H}$ $C_{\mu L}$	Correction factors for unit load-beam friction coefficient (lower and upper bound values)
d_1	Displacement for the first significant yield
DLE	Design level earthquake
d_{max}	Displacement for the ultimate load point
d_y	Displacement for the equivalent yield point
e	Eccentricity of the center of mass
F_{cr}	Critical buckling load
F_{Ed}	Applied load
f_y	Yield stress
H	Horizontal action
H_1	Horizontal reaction at the front pallet beam
H_2	Horizontal reaction at the rear pallet beam
IP	Industrial Partner
K_1, k_o	Factors depending on the geographic region of interest and ist seismicity
k_y,k_z	Factors for the flexural torsional buckling
L	Length
M	Bending Moment
M*	Theoretical bending Moments

$M_{b,Rd}$	Buckling resistance against lateral flexural buckling
MCE	Maximum considered earthquake
$M_{y,Ed}$, $M_{z,Ed}$	Acting bending moments in y and z axis
N	Normal Force
N_{Ed}	Acting normal force
P, P_1, P_2	Vertical reaction at pallet beams
PP	Performance point
Q	Behavior factor
q_o	
Q_P	Pallet weight
S	Soil factor
$S_a(T_1)$	Spectral acceleration for the first dominant eigenmode
$S_{a,DLE}$	Spectral acceleration for the design level earthquake
$S_{a,MCE}$	Spectral acceleration for the maximum considered earthquake
S_{CT}	Spectral acceleration for 50% collapse probability
S_{M1}	Elastic acceleration of the MCE for 1sec
S_{MS}	Acceleration of the MCE at the region of constant accelerations
S_{MT}	Spectral acceleration for the MCE
SSF	Spectral shape factor
T_1	Fundamental period
T_B T_C	Limits of the constant spectral acceleration branch
T_s	Transition period
V	Total base shear
V_1	Base shear for the first significant yield
V_y	Base shear for the equivalent yield point
$W_{eff,y}$ $W_{eff,z}$	Effective section modulus for the y and z axis
β_{DR}	Design requirements uncertainty
β_{MDL}	Modelling related collapse uncertainty
β_{RTR}	Record to record collapse uncertainty
β_{TD}	Test data collapse uncertainty
β_{TOT}	Total collapse uncertainty
γ_M	Safety factor
δ_y	Imposed experimental displacement

η	Damping correction factor
θ_p, θ	Rotation of the plastic hinge
λ	Mean annual frequency of exceedance
μ	Friction coefficient
μ	Ductility
μ_T	Period based ductility
ξ_i	Viscous damping ratio of eigenmode i
$\varphi(x)$	Plastic hinge's curvature at distance x
φ_u	Ultimate section curvature
φ_y	Yield curvature
χ_{min}, χ_{LT}	Buckling reduction factors
Ω	Overstrength
ω_i	Eigenvalue of eigenmode i

1. Introduction

1.1 History of steel storage pallet racking systems

Warehouses, in different forms, have been created as long as humans have had agriculture. Settling down in one spot meant that humans could harvest food rather than hunt for it. All this harvested food needs to be stored and so, humans have been using warehouses for 15,000 years. Still, the warehouse as we know it today is a recent invention and uses steel storage pallet racking systems. Pallet racking system is a material handling storage aid system designed to store different materials, mainly, on pallets. These pallets are placed on horizontal rows and multiple levels. The idea of racking systems actually imitates that of the multistory residential buildings. The need to accommodate a huge amount of goods due to the limitless development of the modern societies, especially after the industrial revolution, was led to adopt the idea of storing the goods in layers, one over the other, multiplying that way the available storage area. Since the World War II the most warehouses used these developing systems, increasing the storage density and as a result the efficiency of the warehouse and finally the profit from this business. The fact that many goods are really fragile, or of value, generated the need not to store the goods directly in touch one over the other, but safely on different levels and supported on stable beams. However, the variety of the goods, their dimensions, their weight etc. forced manufacturers to innovate new systems that could fully exploit the height of the storage systems. The solution beyond this thought was a system that could be fully adjustable in few minutes and that always comply the safety aspects. This flexibility in form of these systems was feasible only by steel elements which would be produced later massively by industry. Nowadays, these steel elements are completely industrialized by many manufacturers who produce steel elements in general or even they are specialized only on steel racks. As the amount and the value of the stored goods is increasing day by day, more and more warehouses intend to optimize their systems and to expand worldwide, in order to take advantage of all the developed and developing economies. This expansionism of the big manufacturers drove them to face an intense competition and a need to organize the way that a steel storage pallet rack is designed, studied, manufactured and used. In comparison to conventional structures which have started to be investigated from the beginning of the 19^{th} century, storage racks were been developing without any systematic intention of research and study. The Americans were the pioneers of this well-organized effort to investigate in depth the racking systems, as they were called to face first the increased demand on storage goods at the beginning of the 20^{th} century. Then, Europe, Australia and New Zealand initialized their researches in order to contribute to this effort. The result of this systematic research was the optimization of the racking systems and the increased interest of the industrial world to invent, to improve and to finance new systems, which are getting nowadays better and better. Today, this is a very interest research field and the numerous research papers could prove it.

1.2 Types of racking systems

Although the idea beyond the function of the pallet racks is a common one, there are different types of racks that present pros and cons, focusing on different parameters. The most widely known type of rack is the ***selective*** one. It is a universal system for direct access to each pallet of the rack, offering a complete control of the warehouse. It is highly adjustable to almost any kind of palletized good as it could carry pallets of different height and weight. The length and height of the system depends on the warehouses' characteristics, the available forklifts, etc. The main disadvantage is that it requires manual process for the management of the stored products. Figure 1-1 displays a so called back-to-back selective rack with one-sided access to the pallets. The term back to back rack is referred to two different racking systems which are connected to each other to their rear side.

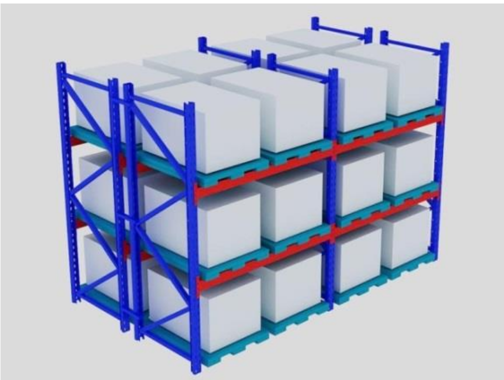

Figure 1-1 Selective type of rack

Another common type of racks is the ***cantilever*** type. It is a special type which stores the products on cantilever beams, offering free and direct access to all stored products; their major advantage is the fact that it can allow the storage of goods on its both sides. Figure 1-2a presents a cantilever rack with both-sided storage of goods and a one-sided storage system as well. Their typical characteristic is the massive single upright (highlighted with blue) that is repeated along the length of the system.

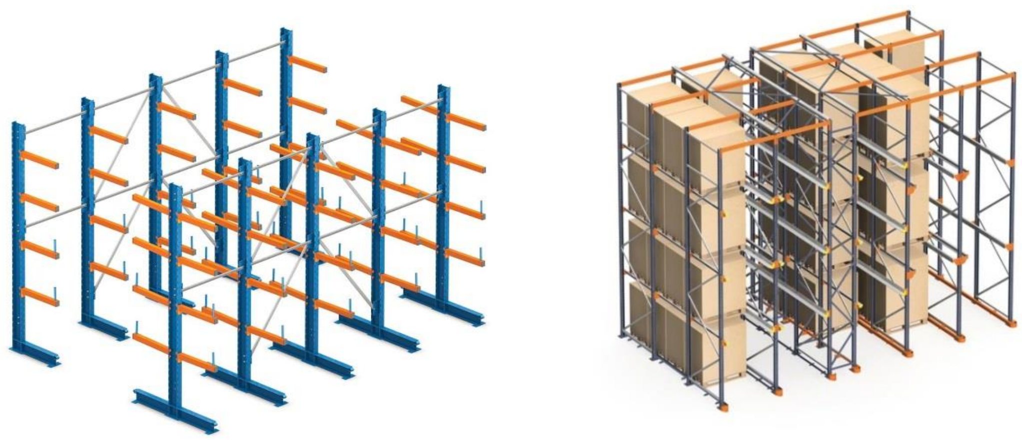

Figure 1-2 a) Cantilever type, b) Drive In Through type

The ***Drive-In*** or ***Drive-Through*** system is another very common option of the warehouses. These racks can accept more than one pallet at the same row and column, able to be used at First In- Last Out (FILO) and First In- First Out (FIFO) inventory control systems as well. This system is based on the storage by accumulation principle, which enables the highest use of available space in terms of either area or height. The Drive-In and Drive-Through systems service the same operational way with two different management systems: the drive-in system, with only one access aisle, and the drive-through system, with access to the load from both sides of the rack. Figure 1-2b shows such a system, whose disadvantage is the fact that not all the pallets are directly accessible.

Another similar type of rack is the ***Push Back*** system. As a pallet is loaded from the front, it pushes the pallet behind it back one position. The front pallet is removed when unloading and the rear pallets automatically come forward to the front picking position. This type of racks is ideal for easily accessible Last-In-First-Out (LIFO) inventory management. Operators can store product from 2-5 pallets deep, with front-only loading from a single aisle, a fact that is the main disadvantage of this rack type. An example of such a rack is shown in Figure 1-3a.

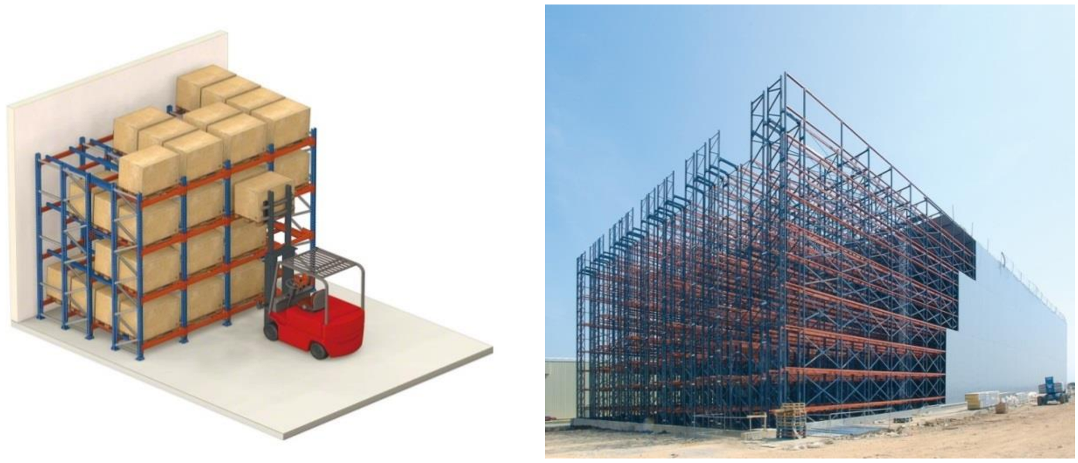

Figure 1-3 a) Push back type, b) Clad type

Though there are more different types of racks the last presented in this thesis is the ***clad*** system. It seems to the selective type of racks, but it carries itself part of the building that it is located in, like the ceiling, the side and roof cladding. Thus, the racking structure supports not only the actual goods and the different building elements but also the handling devices and external loads such as wind, snow, seismic actions, etc. The maximum height of clad-rack buildings is limited by local standards and by the reach height of stacker cranes or fork-lift trucks. Warehouses of more than 30m high can be built. Figure 1-3b shows a clad-rack during its construction.

All the previous figures present among others the similarities of the bearing structure that compose the racking systems. The present dissertation will extensively investigate the selective type of racks, as one of the most common types which are met all over the warehouses of the world.

1.3 Components of racking systems

Conforming to the basic properties of the racking systems, which are the lightness and adjustability, the components of such a system are not permanently fixed to each other. The beams that support the pallets, so called pallet beams, are usually closed sections composed by two facing welded channel sections. Figure 1-4a displays a typical cross section of a pallet beam, composed of two thin walled sections the one welded to each other. The pallet beams are single span beams, which obtain hooked connections at their ends, in order to be easily and quickly installed and uninstalled when it is required. These hooked connections should be able to be connected on each level of the racking system, being adjusted to the variable height of the palletized goods; such connector is known as beam-end-connector and it is shown in Figure 1-4b. This special connection governs partially the behavior of a racking system by its in-plane and out-of-plane stiffness as well as by its bending capacity.

Figure 1-4 a) Pallet beam's cross section b) Beam end Connector

The pallet beams are supported directly on the columns of the rack via the beam end connectors. The columns, commonly known as uprights, are composed of thin walled steel sections with stiffeners and perforations. Two typical upright sections and members are shown in Figure 1-5a and b.

Figure 1-5 Upright sections

a) with stiffened lips and **b) Unstiffened lips**

The uprights stand on concrete slabs that are anyway the base of industrial buildings. However, the uprights are not embedded in the concrete slabs but are anchored through their base plates, as shown in Figure 1-6. The lower part of the uprights is protected by a protective cover in order to reduce the risk of an accidental crash of the forklifts and different staff of the warehouse with the column and the base plate as well (Figure 1-6b).

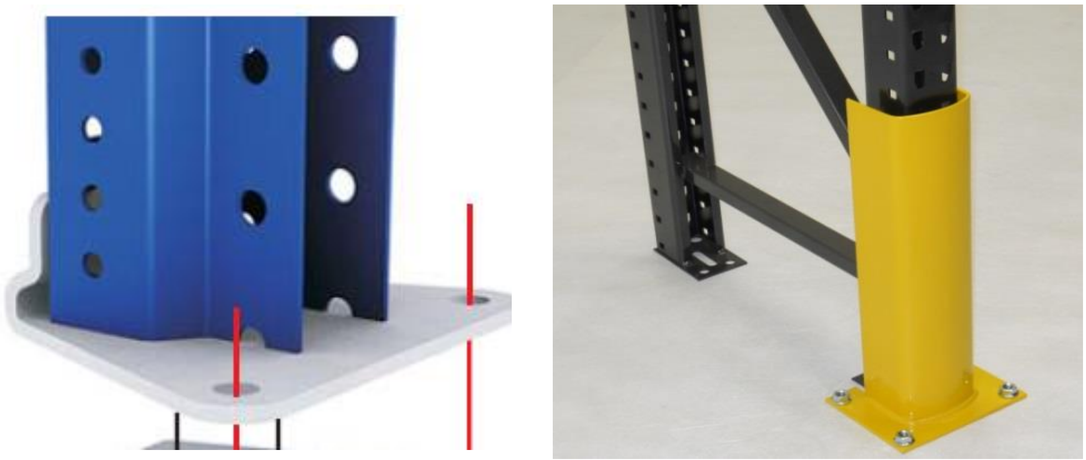

Figure 1-6 a) Base plate connector, b) Protective cover of base plate

As warehouses commonly include more than one racking system, they organize the racks parallel the one to each other, forming long aisles between them. The longitudinal side of racking systems which is parallel to these aisles is known as down-aisle direction, while the transverse side is called cross-aisle direction; this topology is presented in Figure 1-7. Usually, the cross aisle direction is a narrow side which connects the front and the rear longitudinal sides of the system; there are many different configurations, but the most common one in practice is a conventional bracing system. This bracing is made between two opposite uprights creating a planar truss-like frame, so called upright-frame. The members connecting the two opposite upright sections are the diagonals, which are usually composed of channel thin walled sections or small circular hollow sections with special end-connectors. The main characteristic of diagonals is the single bolt connections with the upright; the diagonals govern definitively the behavior of the upright frames. A typical assembly of the diagonals is presented in Figure 1-8; two channel sections back to back are connected at the same point, characteristically, with a single bolt. This is a very common assembly that forms an upright frame.

Figure 1-7 General view of pallet racking systems

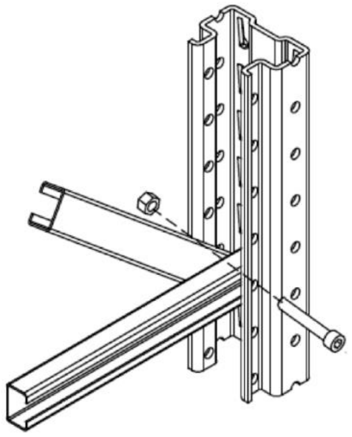

Figure 1-8 Upright frame bracing detail

The bracing of the upright frames is not the only bracing met in a racking system. A spine bracing is also used in cases of high horizontal loads, such as seismic loads. Many racking systems are placed in regions of medium to high seismic zones for which spine bracing seems to be almost necessary. Although there exist systems that can withstand high seismic loads by frame action, the high flexibility of such racks results in large deformations that are reduced, using a spine bracing system. A typical bracing system is illustrated in Figure 1-9. It should be mentioned that the spine bracing is always asymmetrically placed only on the rear side of the rack, since otherwise loading and unloading of the pallets would be unfeasible.

Figure 1-9 Spine Bracing in down aisle direction

Finally, a significant element of a racking system is the pallet, which loads the system and is presented in Figure 1-10; there are many types of pallets, however in everyday practice the presented one (Europallet) is the most commonly used. The palletized goods rest over this wooden pallet and then they are placed all together on the pallet beams.

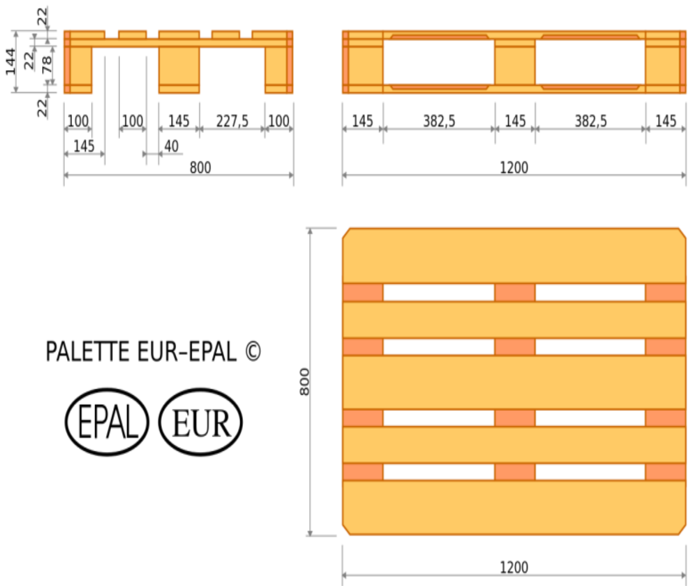

Figure 1-10 Europallet dimensions

1.4 Codes

Although normative documents arrived lately at the everyday practice, there were organizations all over the world which produced guidelines and recommendations for racking systems, as these were developing rapidly day by day. More specifically, the American organization Rack Manufacturers Institute (RMI) is an independent incorporated trade association affiliated with the Material Handling Industry (MHI) and it was established at 1964. This intended to provide useful information and guidance for owners, users, designers, purchasers and/or specifiers of material handling equipment or systems. In the opposite side of the Atlantic, the Europeans had already established their own association known today as European Materials Handling Federation (FEM) which the European Racking Federation (ERF) belongs to. FEM has represented European manufacturers of material handling, lifting and storage equipment since it was founded in 1953. FEM is a non-profit trade association (AISBL under Belgian law) permanently based in Brussels to better represent its members and their interests vis-à-vis the European institutions and European partners. FEM membership currently consists of 13 National Committees from Member States of the EU, as well as Switzerland and Turkey. They are the driving forces in promoting a common vision for FEM industries and in maintaining the European materials handling, lifting and storage industry’s position as leader on the world market. The European industry has an annual turnover of around 45 billion euros. In total, FEM represents more than 1,000 companies with about 160,000 employees, covering around 80% of all eligible European companies. It thus accounts for more than half of the world's total production. The associations above are considered one of the biggest to this field and they have produced normative documents, guidelines and worked examples, which are even adopted to other countries and continents. There is a big sequel of normative documents, which begun as FEM guidelines, and after a try-out period of application as Codes of practice, some of them hove become EN standards. In this dissertation, the European documents are studied more extensively, as it is intended to clarify their content and possibly amend them, in case that it is required. Next, some normative documents from different countries and organizations are epigrammatically presented.

European codes

- EN 15095: Power operated mobile racking and shelving, carousels and storage lifts – safety Equipment
- EN 15512: Steel static storage systems – adjustable pallet racking systems – principles for structural design FEM 10.2.02

- EN 15620: Steel static storage systems – adjustable pallet racking systems – tolerances
  deformations and clearances FEM 10.3.01
- EN 15629: Steel static storage systems – specification of storage equpment equipment FEM 10.2.03
- EN 15635: Steel static storage systems – application and maintenance of storage equipment FEM 10.2.04
- EN 15878: Steel static storage systems – adjustable pallet racking systems – terms and definitions
- FEM10.2.05 Guidelines for working safely with trucks in pallet racking installations.
- FEM 10.2.06 The design of hand loaded static steel shelving systems
- FEM 10.2.07 The design of drive in and drive through racking
- EN16681 Steel static storage systems: Seismic design FEM 10.2.08 Recommendations for the design of static steel storage pallet racks under seismic conditions
- FEM 10.2.09 The design of cantilever racking
- FEM 10.2.10 Rail dependent storage and retrieval systems- Interfaces
- FEM 10.2.11 Rail dependent storage and retrieval systems – Consideration of kinetic energy action due to a faulty operation in cross aisle direction, in compliance with EN 528- part 1: Pallet racking
- FEM 10.2.14 Warehouse Floors – Storage System Areas

American codes

- ANSI MH16.1: 2012 Specification for the Design, Testing and Utilization of Industrial Steel Storage Racks
- Rack Manufacturers Institute (RMI) Specification for the Design Testing and Utilization of Welded-Wire Rack Decking, ANSI 26.2-2007
- FEMA 490 Seismic Considerations for Steel Storage Racks Located in Areas Accessible to the Public

- ANSI MH16.2-1984 (R1996). American National Standard for the Use of Industrial and Commercial Steel Storage Racks: Manual of Safety Practices / A Code of Safety Practices. American National Standards Institute, Inc. 10 p.
- Rack Manufacturing Institute. 1973. Warehouse Storage Racks – What Are They? Building Standards, 5 p.
- RMI. 1990. Specification for the Design, Testing, and Utilization of Industrial Steel Storage Racks. Rack Manufacturers Institute, Charlotte, NC.
- RMI. 2004. Testing Guidelines for Pallet Stacking Frames. Rack Manufacturing Institute, Charlotte, NC, 4 p.

Australian codes

- AS4068: 1993 Flat pallets for materials handling
- AS4084: 2012 Steel storage racking
- AS4762: 2000 General purpose flat pallets, principal dimensions and tolerances

The aforementioned codes are used in the everyday practice; however they cannot stand on their own, as they must be complimented and referred to the general codes such as the corresponding codes on design of steel structures, the actions on structures, design of cold formed members, earthquake actions, etc. These could be either the Eurocodes for Europe or the AISC norms for USA or the AS/NZS ones for Australia and New Zealand. Here it should be noted that the Australian codes are sometimes referred to the European norms in case of special measurements regarding the racking systems.

1.5 Specialties and peculiarities of steel storage pallet racks

The racking systems generally follow the norms and the design's philosophy of normal buildings; however they remain by far different, with their own specialties and peculiarities in their behavior and their numerical simulation. These specialties are static and dynamic, global and local as well.

A first peculiarity of racks is the fact that their live loads (loads from the palletized goods) are about 90% of the total loads. The self-weight is just a very small portion of vertical loads, which are anyway the main loading situation of racks, while horizontal loads are secondary loads, resulted by eccentricities, imperfections and functional processes. This is the reason that these structures are composed by light weight, cold formed members with relative small dimensions. However, as the manufacturers were interested to supply any warehouse in every country with their products, they should face directly seismic loading which may impose large horizontal loads to the systems. This means that the systems in regions of high seismicity should be capable to withstand the seismic horizontal loads, either by frame action or bracing action, with both options to present peculiarities.

Although the frame action is already known, the stiffness of the system in both down and cross aisle direction is not yet clarified. The special beam end connectors are neither fixed nor pinned connections, thus, their current stiffness should be known in order to well predict the global response of the systems under horizontal loads. Unfortunately, the behavior and the stiffness of these hooked connections are governed by multiple parameters such as the thickness of the connected parts, the shape of the hooks and the perforations, the size and the shape of the connected sections, their stiffeners, even the looseness and the friction between the perforations and the beam end connectors. Although there are many modern researches that have already developed methods to calculate the static-monotonic stiffness and resistance of these connectors, all of them refer to specific types and they are not applicable to all types of connectors or even more to their behavior under cyclic loading.

The same peculiarity exists in respect to the horizontal response of the racks in cross aisle direction. This behaves as a truss structure, but the diagonals are usually single-bolt connected with high looseness and highly variable stiffness depending on the details of the assembly, such as the geometry of the bracing system, the relative position between two consecutive members, the cross section of the diagonals, the connection’s detail, etc. Hence, the stiffness and even more the cyclic response of the upright frames are not yet specified or categorized.

On the contrary, when designers decide for the use of spine bracing systems to resist horizontal loads, these systems can only be eccentrically placed in order to get free space for the forklifts to load and unload the palletized goods. This eccentricity generates two different issues on the rack’s behavior. First, the eccentricity creates an intensive torsion-behavior on the rack that is composed by open sections, really vulnerable to torsion effects. Moreover, the spine bracing is placed on an external system, like a bracing tower, or external uprights which then are connected to the main rack with special connectors. These connectors are usually weak and introduce local stresses and phenomena to the main rack. The light-weight cold-formed open sections of the uprights and the special beam end connectors and base plates are highly influenced by these phenomena, including torsion, warping, distortional buckling, etc.

Moreover, the aforementioned braced systems are not regular systems unlike the unbraced ones that are commonly regular in elevation and in plan. The regular unbraced racks are designed with conventional methods of analysis, as the response spectrum analysis of 3D or spatial models, or even the simplified lateral force method, described by the different codes. Despite the simplicity of the analysis method, the definition of the oscillated mass of these systems is a significant trouble in the earthquake design of racks. Since the self-weight of conventional structures is a very big part of the total seismic mass, the possibility of an eccentrically loaded structure in regard to the small live loads are covered by the use of accidental structural eccentricities which are defined in the norms. On the contrary, the seismic mass of racks is mainly composed of the pallets, whose existence and weight could be totally probabilistic and accidental. In racking systems, the move of the center of mass for different load cases could not be simply simulated with a percentage eccentricity of the mass, since it is completely unknown where it lies on. Theoretically the designer should examine the worst loading situation among the thousand different combinations; in common practice only some of them are examined when applying the provisions of normative documents.

Regarding the structural dynamic damping ratio which is defined to accomplish the seismic design of a rack, it is unlikely to make even a realistic approximation for a system whose dynamic characteristics depend on so many parameters. The amount of goods, the type of pallets, the type of goods, the conditions of the pallet and of the warehouse and many others, influence the total equivalent dynamic damping ratio of the structure. At the end, the damping ratio is conventionally adopted as for a normal steel structure in European norms, while in American codes it is made dependent also on the intensity of the expected seismic motion. In a more realistic simulation, the fact that the pallets are usually not fixed on the pallet beams may lead to the sliding of one or more of them. This sliding is a mechanism of energy dissipation that influences the dynamic properties of the system. A severe amount of energy is absorbed by the friction forces, a fact that could be helpful for the structure, but not for the goods themselves. Engineers focus on the sliding of the pallets not only to define the dynamic properties of the systems, but also to check whether a pallet falls down and either it is destroyed, or it damages the structure, or even more it hurts humans.

An additional specialty of racks is their connections. Although these are different than those for conventional structures, what is important is the fact that both beam end connectors and base plates exhibit a different stiffness and resistance in the two main directions. Both connections are fixed, with regard to the translational degrees of freedom, but they are partially fixed for bending around their major axis, and simply pinned for bending around the minor axis. Torsion is blocked, however warping is free. What worth to be noticed, is that these connections have usually different resistance in sagging and hogging bending and their cyclic behavior presents many special phenomena of hysteresis. The most important ones are pinching and degradation mainly due to the looseness of the bolted or hooked connections. In case that the rack is loaded in both directions, instantly the connections are unloaded when the forces alternate their direction and the structural tolerances are activated leading to the loss of stiffness. This makes the prediction of the dynamic characteristics of a rack extremely difficult.

From a local point of view, pallet beams present also peculiarities. These beams are loaded on their upper flange; vertically, directly by the pallets and horizontally by the friction forces between pallet and pallet beams. When these horizontal forces are perpendicular to the beams, torsion develops in the beam and an out of plane bending as well. These secondary effects result in the development of severe deformation for such flexible members, which could affect the buckling resistance of pallet beams, when they are simultaneously loaded in the longitudinal direction. These phenomena belong to the research field of the interaction between pallets and racking system. More specifically, the presence of the pallets could make buckling of the pallet beams more likely, but on the other hand it could offer a diaphragm-like action between two facing pallet beams. Although modern normative documents include provisions about this interaction between pallets and pallet beams, the background of these provisions is not abundant.

1.6 State of the art

As mentioned before, one can observe that research about racking systems begun early in order to be able to create norms on racks during the early 1970. However, one of the first known papers in the international bibliography about the seismic design of racks appears at the early 1980. In particular, Brown 1983 [1] presents a first systematic seismic design procedure for racks, while Chen and Scholl (1980) [2], [3] had already presented a research on the earthquake resistance of racks. All researches about racking systems were by that time included in the topic of cold-formed steel structures. Actually, research on cold formed structures and components was the ancestor of the racking systems research. Pekoz and Winter 1969 [4] created the strong background working on the torsional flexural buckling of cold formed steel sections in order to begin an intense research attempt that helped in the development of RMI, providing together significant papers about the design of steel storage pallet racks (1973) [5]. Pekoz continued after that also by testing full scale racks and individual components in Cornell University (1975) [6], investigating later also the design of general cold formed steel members (1986) [7] and moreover the design of perforated columns that are used in racking systems (1988) [8]. Next, Hancock [9] (1985) published his research about distortional buckling of steel storage rack's columns, an attempt that be continued together with Baldassino (1999) [10].

In the meanwhile, the textbooks by Timoshenko and Goodier (1969) [11] on theory of elasticity of Sokolnikoff (1983) [12] for the mathematical theory of elasticity, of Salmon, Schenker and Johnston (1955) [13], for the moment-rotation characterization and of Galambos (1960) [14] for the influence of the partial based fixity in the frame instability were keys to initialize an international and systematic investigation on the racking systems treating them as semi rigid, flexible, moment-resisting frames. Lewis (1991) [15] and Davies (1992) [16] working on stability of racking systems founded a new era for the global investigation of pallet racks, with Baldassino et al. (1998) [17] to continue in the numerically simulation of racking systems comparing them to experimental tests that have been performed.

With the development of the numerical tools and the computational power of modern computers, semi rigid racking systems have been investigating by Markazi (1997) [18], Sleczka and Kozlowski (2007) [19] and Baldassino et al. [20] to clarify finally the behavior of the rack's connections and especially that of the beam to columns semi-rigid connections. This kind of connections with semi-rigid behavior could influence the overall stability of racks as frame structures. Bajaria (2009) [21] and Abdel-Jaber (2005) [22] studied the stability of semi-rigid racking systems and how these are practically and numerically influenced by the non-rigidity of their connections.

At that time, a European coordinated research with the cooperation of many European universities and industrial partners begun in order to review the outcome of the previous researches and support the publication of the new European norms about the seismic design of racking systems. These projects were accomplished under the umbrella of the European Union and they were funded by RFCS (Research Fund for Coal and Steel). The projects are known as SEISRACKS and SEISRACKS2 and they gave some interesting reports (2007) [23], (2014) [24] investigating and solving many issues about the seismic design and the peculiarities of racks. Parallel to these research projects their coordinator Castiglioni summarized some of the most practical conclusions about the global seismic response of the racks as well as about the interaction of the palletized goods to the overall behavior of the racks (2008) [25], (2016) [26]. One of the most significant proposals of these projects was the determination of the friction coefficient that develops between the pallets and the pallet beams. Similar research was performed by Hua and Rasmussen (2010) [27] in Australia, where Gilbert and Rasmussen (2009) [28] have already executed many experiments on components of racking systems.

The reports from the above projects in Europe and Australia had also mentioned the significance and the difficulty to determine the shear stiffness of the racks in the cross aisle direction. Rao et al. (2004) [29], Sajja et al. (2006) [30], (2008) [31] and Gilbert et al. (2012) [32] investigated the shear stiffness of the upright frames, what it is affected from and how it affects the global behavior of the racks. One of the potential influencing parameters was found to be the looseness of the bracing connections that are composed of single bolts. This influence was examined extensively by Godley and Beale (2008) [33] who pointed out the influence of this looseness not only in respect to the shear stiffness but also to the final resistance of an upright frame.

Despite the numerous research projects and papers the everyday design practice around racking systems is not yet completely conclusive and clear. The corresponding norms are up-to-date but the seismic design for such vulnerable structures is still deemed weak. The evidence about is reports on damages after strong earthquake events worldwide. Some of the most important reports are the one by Uma and Beattie (2001) [34] that reported the damages during the Canterbury earthquake and the one of Crosier et al. (2010) [35] that refer to the collapses of storage racks in Darfield, both in New Zealand. Moreover, Bournas et al. (2014) [36] describe the observed damages, among others, to racking systems after the Emilia Romagna earthquake in Italy and Plantes (2012) [37] presents a summary of various collapses and damages met on pallet racks. These undesirable collapses gave the motivation to check the earthquake design of racking systems more deeply and specifically. Adamakos and Vayas (2014) [38] published numerical analyses to predict and review the seismic response of racking systems, focusing on the behavior factors that are used to the everyday practice, while Adamakos et al. (2014) [39], Degee and Denoel (2007) [40] and Degee et al. (2011) [41] presented an attempt to simulate the dynamic response of the systems under real earthquake excitations. Degee and Denoel (2009) [42] investigated also the influence of the pallet's potential sliding to the dynamic behavior of the racks; a likely phenomenon that could be dangerous for the goods and the human life as well. Thus, this phenomenon that is able to modify the dynamic characteristics of a rack and as a result its dynamic response was studied by many researchers and it is clarified by Adamakos et al. (2017) [43] in a very recent paper under publication.

Following the current research, modern norms that refer to racking systems are updated systematically in order to be always realistic, adequate and efficient. The objective is to offer a combination between theoretical knowledge and everyday practice.

1.7 Dissertation's goals

The present dissertation was partly supported by a research program of the European Union, with the name SEISRACKS2. This project was funded in order to perform research about the seismic behavior of steel storage pallet racking systems. This was the motivation to investigate static or pseudo static phenomena for these structures, as well as their dynamic-seismic behavior.

More specifically, the dissertation is divided into two main parts; the first part investigates the global behavior of the rack system, while the second part examined local phenomena to clarify the interaction between pallets and pallet beams.

As far as the global behavior of the racks is concerned, the seismic response was evaluated using a well-known numerical tool, the pushover analysis. The partners of the research program provided plans and details of some conventional racking systems in everyday practice that were designed according to the European norms. These constituted 9 case studies, which at the end of the program were examined in Full scale tests, giving the opportunity to compare the numerical results to experimental ones. Taking this opportunity, this dissertation expands the field of its research to the evaluation of the rack's dynamic response, performing a probabilistic analysis on the system's collapse using more advanced and modern tools, such as the Incremental Dynamic Analysis. The goal was to derive more general rules on the ductility of these structures and to propose more realistic values for the behavior factors q, used in Codes.

At the second part of the dissertation the racks are examined from a local point of view. The objective is to look into the interaction between the pallets and the pallet beams. First, the sliding phenomenon is attempted to be clarified, in order to provide a safer design against this possibility. The forces that apply on the pallet beams before, during and after the sliding effect are investigated and compared to the theoretical ones, aiming to provide a stronger background to this not intensively investigated field. Moreover this part of the thesis has the purpose to illuminate the accuracy of the proposed procedure about buckling of the pallet beams with the simultaneous existence of the pallets.

Finally, the thesis discusses experimental results performed by other universities, in order to highlight the vulnerable points of racking systems, their failure mechanisms and other important points.

1.8 References

1. Brown, B. J. 1983. Seismic Design of Pallet Racking Systems. Bulletin of the New Zealand National Society for Earthquake Engineering, 16(4), 291- 305.
2. Chen C. K., R. E. Scholl and J.A. Blume (1980), Seismic Study of Industrial Storage Racks, Report prepared for the National Science Foundation and for the Rack Manufacturers Institute and Automated Storage and Retrieval Systems (sections of the Material Handling Institute), John A. Blume & Associates, San Francisco, CA.
3. Chen C. K., Scholl R. R., Blume J. A., (1980), Earthquake Simulation Tests of Industrial Steel Storage Racks. Proceedings of the Seventh World Conference on Earthquake Engineering, Istanbul, Turkey, 379-386.
4. Peköz, T., Winter, G., "Torsional-Flexural Buckling of Thin-Walled Sections under Eccentric Load", Journal of the Structural Dijvision, ASCE, May 1969.
5. Peköz T., Winter G., Cold-formed steel rack structures, in: W.W. Yu (Ed.), 2nd Specialty Conference on Cold-Formed Steel Structures, St Louis, Missouri, USA, 1973, pp. 603- 615.
6. Peköz, T., (1975). Pallet Rack Tests, Report submitted to Rack Manufactures Institute, Cornell University, Ithaca, NY.
7. Pekoz, T., ‘Development of a Unified Approach to Design of Cold-Formed Steel Members’, AISI Report S.G.-86-4, November 1986.
8. Pekoz, T., ‘Design of Perforated Cold-Formed Steel Columns’ Proceeding of 9th International Specialty Conference, Cold-Formed Steel Structures, St. Louis, MO, November 1988.
9. Hancock G. J., (1985), “Distortional buckling of steel storage rack columns.” Journal of Structural Engineering, ASCE, vol. 111, no. 12, Dec. 1985
10. N. Baldassino ; G. Hancock, "Distortional Buckling of Cold-Formed Steel Storage Rack Sections including Perforations" in Ligth-weight steel and aluminium structures ICSAS'99, Elsevier, 1999, p. 131-138.
11. Timoshenko S. P., Goodier J.N., Theory of Elasticity, McGraw-Hill, New York, 1970
12. Sokolnikoff, I. S., (1983). Mathematical Theory of Elasticity, Krieger Publishing Company, Malabar, Florida.

13. Salmon, C. G., Schenker, L. and Johnston, B.G., (1955). "Moment Rotation Characteristics of Column Anchorages", Proceedings, ASCE, April 1955.
14. Galambos, T. V., 1960, ‘‘Influence of Partial Base-Fixity on Frame Stability.’’ Journal of the Structural Division, ASCE 86 (ST5) (May).
15. Lewis, G. M. (1991) “Stability of Rack Structures” Thin-Walled Structures, VOL. 12, pp. 163-174.
16. Davies, J. M., "Down-Aisle Stability of Rack Structures," Proceedings of the Eleventh Specialty Conference on Cold-Formed Steel Structures, St. Louis, Missouri, October 20-21, 1992.
17. Baldassino N., Bernuzzi C., Zandonini R., "Experimental and Numerical Studies on Pallet Racks" in Challenges and Perspectives for Steel Structures, Budapest: Akademiai Kiado, 1998, p. 61-83.
18. Markazi F. D., Beale R. G., Godley M. H. R., Experimental analysis of semi-rigid boltless connectors. Thin- walled structures 1997; 28(1):57–87.
19. Sleczka L, Kozłowski A. Experimental and theoretical investigations of pallet racks connections. Advanced Steel Construction 2007; 3(2) 607–610.
20. Baldassino N., Bernuzzi C., Zandonini R., (2000) Performance of joints in steel storage pallet racks. In proceedings of connections in steel structures IV: Steel Connections in the New Millennium, Roanoke, Virginia, USA.
21. Bajoria K. M., Sangl K. K., Talicotti R. S., stability analysis of 3-d conventional pallet rack structures with semi-rigid connections, International Journal of Advanced Structural Engineering, Vol. 1, No. 2, Pages 153-181, December 2009
22. Abdel-Jaber M., Beale R. G., Godley M. H. R., Numerical study on semi-rigid racking frames under sway, Computers & Structures 83 (28-30) (2005) 2463-2475.
23. SEISRACKS (2007), Storage Racks In Seismic Areas (SEISRACKS), Research Programme of the Research Fund for Coal and Steel RTD, Final Report, May 2007
24. Castiglioni, C. A. et al (2014). EUR 27583 EN: Seismic behavior of steel storage pallet racking systems (SEISRACKS2), Final Report, RFSR-CT-2011-00031, European Commission, DG Research, Brussels, Belgium.
25. Castiglioni, C. A.: Seismic behavior of steel storage pallet racking systems. Structural Engineering Department of Politecnico di Milano, Milano, 2008.

26. Castiglioni, C. A. (2016). Seismic behavior of steel storage pallet racking systems, Springer International Publishing, Switzerland.
27. Hua V., Rasmussen K. J. R. (2010), Static friction coefficient between pallets and beam rails and pallet shear stiffness tests, Research Report 914, School of Civil Engineering, The University of Sydney, Australia.
28. Gilbert B. P., Rasmussen K. J. R., (2009), Experimental tests on Steel storage rack components, Research Report No. R899, The University of Sydney
29. Rao S. S., Beale R. G., Godley M. H. R., Shear stiffness of pallet rack upright frames, in: 7th International Speciality Conference on Cold-Formed Steel Structures, Orlando, Florida, U.S.A., 2004, pp. 295-311.
30. Sajja S. R., Beale R. G., Godley M. H. R., Shear stiffness of pallet rack upright frames, Journal of Constructional Steel Research, 64 (2008) 867-874.
31. Sajja S. R., Beale R. G., Godley M. H. R., Factors affecting the shear stiffness of pallet rack uprights, Stability and Ductility of Steel Structures, Lisbon, Portugal, 2006, pp. 365-372.
32. Gilbert, B., Rasmussen, K., Baldassino, N., Cudini, T., Rovere, L. (2012). Determining the transverse shear stiffness of steel storage rack upright frames. Journal of Constructional Steel Research, 78, 107-116.
33. Godley M. H. R., Beale R. G., Investigation of the effects of looseness of bracing components in the cross-aisle direction on the ultimate load-carrying capacity of pallet rack frames, Thin-Walled Structures, 46 (2008) 848-854.
34. Uma S. R., Beattie G., Observed performance of industrial pallet rack storage systems in the Canterbury earthquakes. Bulletin of the New Zealand Society for Earthquake Engineering, 44 (2011), No. 4, pp. 388–393.
35. Crosier J., Hannah M., Mukai D., Damage to steel storage racks in industrial buildings in the Darfield earthquake. Bulletin of the New Zealand Society for Earthquake Engineering, 43 (2010), No. 4, pp. 425–428.
36. Bournas D. A., Negro P., Taucer F.F., Performance of industrial buildings during the Emilia earthquakes in Northern Italy and recommendations for their strengthening, Bulletin of Earthquake Engingeering (2014), 12: 2383.
37. Plantes J. P., Ahuja D., Chancey R. T., (2012), A Case Study on the Collapse of Industrial Storage Racks, Sixth Congress on Forensic Engineering, San Francisco, USA.

38. Adamakos K., Vayas I. (2014). “Tragverhalten von Palettenregalsystemen unter Erdbebenbeanspruchung.” Stahlbau, Ernst & Sohn, 83 (1), p.36-46.
39. Adamakos K., Vayas I., Hoffmeister B., Christoph H., Hervé D., Seismic Performance of Steel Storage Pallet Racks, 7th European Conference on Steel Composite Structures, Eurosteel 2014, Naples.
40. Degée H., Denoël V., (2009), Dynamic interaction between merchandizes and supporting structure in steel storage racking systems. Proceedings of the COMPDYN 2009 Conference (pp. 8).
41. Degée H., Rossi B., Jehin D., (2011), Geometrically nonlinear analysis of steel Storage racks submitted to earthquake loading. International Journal of Structural Stability & Dynamics, 11(5), 949-967.
42. Degée H., Denoël V., (2007), Numerical modelling of storage racks subjected to earthquake. Proceedings of COMPDYN 07, Conference on Computational Dynamics (pp. 11).
43. Adamakos K., Sesana S., Vayas I., Interaction between pallets and pallet beams of steel storage racks in seismic areas, International Journal of Steel structures, Springer, Vol.19, 2018

2. Static nonlinear response of steel storage pallet racks under the horizontal components of seismic actions

2.1 Introduction

Racks located in zones of middle to high seismicity face besides vertical loading from the pallets, severe horizontal loads that result in additional bending moments. That fact creates to the racks stability problems during strong ground motions, as they are primarily designed to withstand vertical forces. Inspections in the USA [1] after earthquakes detected minor damages to racks either because the earthquake was lighter than the design one, or because the racks were not fully loaded. In contrast to that optimistic scenario stand the observed performance of racks during the earthquakes of Darfield (2010) and Lyttleton (2011) in New Zealand [2], [3], where severe damages were recorded. In Greece, at 08.06.2008 a strong ground motion of 6.5R magnitude that took place in the Peloponnese, very close to the city of Patras (Greece) [4], produced also several damages, although its maximum recorded ground accelerations were between 0.09g and 0.17g, which are lower than the design acceleration 0.24g of that region. However, according to the spectral values which are depicted in Figure 2-1, the spectral acceleration in the long-period range was comparable to the design one. For example, a structure with fundamental period 1.1s was imposed to a spectral acceleration 0.33g that is ca. 80% of the design acceleration for common ground conditions. This is why flexible systems like racking systems developed extended failures.

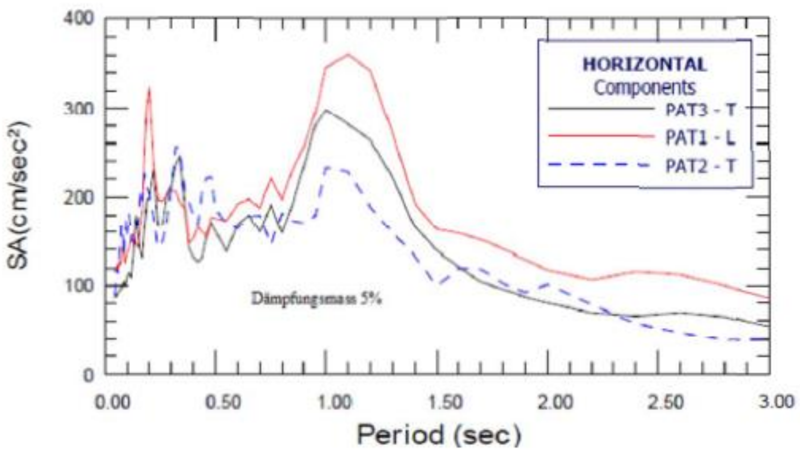

Figure 2-1 Spectrum of earthquake of Patras Greece, at 08.06.2008

The supervisor of the present thesis Prof. Vayas was called to inspect damages to racking systems in this region, and he did the following observations:

a. Local buckling in combination with global buckling of the diagonal members occurred in the cross aisle direction, weakening the bracing system in that direction. (Figure 2-2a)
b. Extensive local plastic deformations and buckling of the eccentrically placed spine bracing of the down aisle direction, leading to an insufficient bracing system. (Figure 2-2b)
c. Failure of the welding between the two channel sections that compose the pallet-beam section (Figure 2-2c). Hence, the initially closed section has been transformed to an open section, losing its torsional rigidity and resulting in torsional buckling of the beams. (Figure 2-2d)
d. Bearing failure of the uprights at the place of the hooked connections. (Figure 2-2Figure 2-2e)
e. Large deformations at the hooks of the beam-to-upright connections, leading to the reduction of the stiffness in down aisle direction. (Figure 2-2f)

a

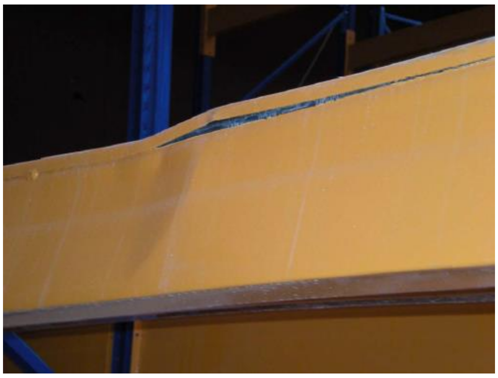

c

b

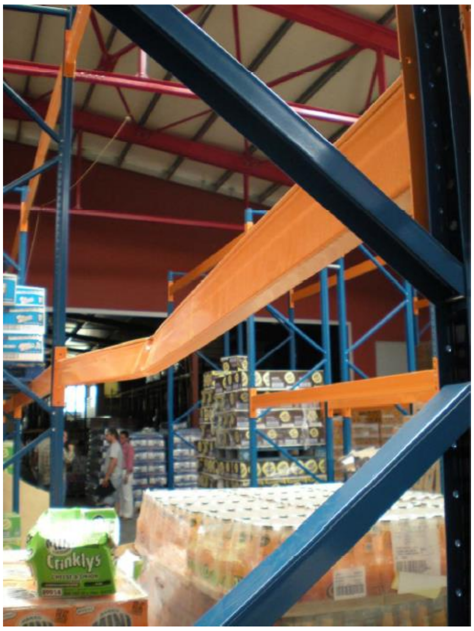

d

e

f

Figure 2-2 Observed damages after the earthquake of Patras at 08.06.2008

These damages and/or sliding of the pallets and their potential fall might drive the whole system to an entire collapse. In case of racking systems the consequences of a global or local collapse is not only the loss of human's life, which in case of automatic operated systems is unlikely, but also the loss of the palletized goods that may cost much more than the rack structure itself.

Designers and producers use common cross sections for the pallet beams and upright sections and try to avoid bracing the racks in the down aisle direction, in order to offer a lighter and more economical solution. Additionally, they take advantage, by using the behavior factor q, of all the possible inelastic capacities of the system in order to reduce the demanded seismic force and as a result to minimize the weight and the cost of the structure. Since the codes are still quite general and the racking systems so specially designed and produced by each specific producer, it is extremely difficult to assess if the used values of the behavior factors for such systems are too low or even too high. This is exactly the objective of this chapter of the present thesis; namely to evaluate the earthquake performance of racking systems with use of nonlinear static inelastic (nonlinear) analyses, the so called Pushover analyses. Participating in the research project SEISRACKS2 was an ideal opportunity to simulate real case studies from the everyday practice, been provided by the industrial partners of the project.

2.2 Pushover Analysis-A Brief State of the Art

The method of Pushover has begun from the early 1970 by Gulkan and Sozen (1974) [5] and Saiidi and Sozen (1981) [6], who introduced the use of inelastic static analysis in earthquake engineering, where a single degree of freedom system is derived to represent equivalently the multi degree of freedom structure. Notwithstanding the development of this method over the next decades, the pushover has no robust theoretical background [7]. Advantages and disadvantages of this method are extensively discussed by Kranwinkler and Seneviratna (1998) [8]. As those authors noticed, in an ideal world there would be no debate about the proper method of demand prediction and performance evaluation. Clearly, inelastic time history predicts with sufficient reliability the forces and cumulative deformation demands in every element of the structural system; that is the final "right" solution. However, the simplicity of the pushover method, in comparison to the inelastic nonlinear dynamic analyses, gives so many advantages to use it, especially if no abundant research background exists. On the same basis, Faella (1996) [9] compares the response of three, six and nine storey buildings subjected to artificial and real earthquakes with pushover analysis, and concludes that static analysis can, indeed, identify collapse mechanisms and critical regions, yielding reasonable estimates for the interstorey drifts.

Furthermore, considering that the objective is always to simulate the dynamic response of the structure, another question that arises is whether the displacement or the forces from a particular mode should be kept constant during a pushover analysis. Conceptually, the dynamic analysis is inertia force-driven, hence the constant force seems more appropriate, but storey forces in a dynamic analysis, even when one mode is dominant, do not exhibit a constant multiplier. It is however clear that fixing the displacement distribution may give seriously misleading results, notes Elnashai (2001) [10]. Adopting the conclusion of Elnashai a constant force pattern will be used to the present chapter to perform the nonlinear static inelastic analyses.

The question that is now arising is the distribution of the applied forces for the forthcoming pushover analyses in racking systems. During the last years there are many researchers among others Sasaki et al. (1998) [11] and Shakeri et al. (2007) [12] that observed the role of the higher modes at the final qualitative and quantitative results of the pushover analyses for the majority of the structures. Maniatakis et al. [13] present the different existent methods of performing a pushover analysis taking into account the influence of higher modes and compare them to the always realistic nonlinear dynamic analyses. Goel and Chopra [14] present also guidelines for a modal pushover analysis using more than the first significant eigenmode of the structure and Antoniou and Pinho (2004) present a force-based [15] and displacement-based [16] adaptive pushover analysis, comparing to the conventional one. However, not all the commercial software packages are implemented with sophisticated algorithms and tools in order to apply the aforementioned methods. Meanwhile, Aydinoglou [17] points out that although the major drawback of Pushover in its current form lies in the fact that it is essentially restricted with a single-mode response, the procedure can be reliably applied to (only) two-dimensional response of low-rise building structures regular in plan, where the seismic response is essentially governed by the first mode. This is exactly the case of the racking systems. They are usually, low-rise structures with a really dominant first eigenmode and regular in plan and in elevation, so that they usually are investigated with the use of 2D planar models. It is here, from now on, assumed that the use of modal pushover analysis (in its known simple form) offers sufficient reliability to apply this to the racking systems.

2.3 The Pushover Analysis method applied to racking systems

To perform nonlinear analysis at any structure the nonlinear behavior that governs each element's response should be explicitly defined. In case of conventional building structures the American codes ATC-40 [18] and FEMA 356 [19] give an excellent database and guidelines for the simulation of the inelastic behavior of almost every element of the structure. Since the elements of racking systems are not conventional-common elements, to determine an accurate behavior law for a member is practically inconvenient and surely not yet extensively analyzed by the norms.

In particular, the current norms for regular and seismic design of steel structures in Europe are regulated by EN1993 [20] (Eurocode 3), and EN 1998 [21] (Eurocode 8). Since racks are not conventional normal building structures, the aforementioned codes have limited applicability; thus, the *Federation Europeen de la Manutation* (FEM) issued two more specialized documents to implement and support design procedures for vertical loads, FEM 10.02.02 [22] and seismic loads, FEM 10.02.08 [23] in racking systems. These documents, later known as EN15512 [24] and EN16681 [25], respectively, are in complete conformity with the corresponding Eurocodes. Similar documents have been issued by RMI [26], the corresponding organization in the USA, and other countries with high seismic demands, like New Zeeland and Australia [27] and China [28].

FEM 10.02.02 and later FEM 10.02.08 have a common major outcome; they emphasize the necessity of experimental tests in order to determine the exact behavior of any specific element/product of any producer. The results of these tests are directly implemented in the static design of racks and they have been proven really helpful to the seismic design as well.

For that reason, the use of experimental results is one way direction. In that manner, using numerical, theoretical and experimental results the Pushover analysis helps to study the seismic performance of racks and to evaluate to what extend the inelastic reserves of the system have been exploited. The direct use and contribution of codes are apparently essential.

More specifically, a seismic design is performed according to EN16681 with the help of linear analyses and the use of a behavior factor q by which the seismic forces are reduced with that stems from the different sources of ductility and overstrength that are presented in such type of structures. However, to determine the seismic design forces assumptions concerning a lot of different parameters should be defined. Some of them are the filling ratio R_f of the rack, the friction coefficient between pallet and pallet beams, the damping ratio and the proper value of the behavior factor. The importance of those parameters, the range of their allowable values, their common values etc. were also examined in the scope of the project SEISRACKS and its subsequent SEISRACKS2. The interesting results of those research projects have been reported in [29] and [30] by the project's author's (among them the present author and the supervisor of the thesis) and later by the coordinator Professor Castiglioni in [31], [32].

Pallet racks are bearing systems that usually (not always) behave independently in their down and cross aisle directions. Therefore EN16681 recommends values of the behavior factor separately for the two different directions. The corresponding values for the down aisle direction are presented in Table 2-1, according to the EN 1998-1-1. Due to the fact that all components are made of thin-walled and cold-formed sections, a low dissipative concept design is adopted, following a conservative way. Table 2-2 presents here the recommended values for specific but common/conventional bracing systems of the upright frames (cross aisle direction). For non-conventional bracing systems the q factor should be reduced

Design Concept	**Ductility Class**	**Reference value of q factor**
Low dissipative structures	Low	$q \leq 1.5 \div 2$
Dissipative Structures	Medium	$q \leq 4$
	High	$q \geq 4$

Table 2-1 Maximum value of q factor in down aisle direction

	X-Braced with horizontal elements	Partially Braced	D-Braced
	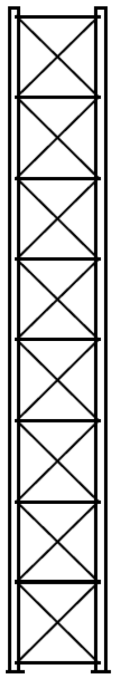	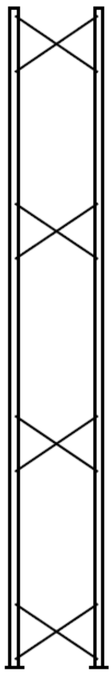	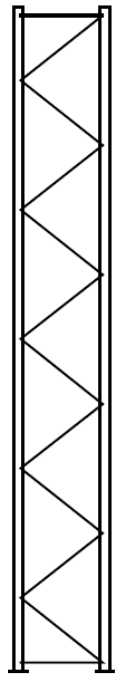
Only active tension diagonals (dissipative design concept)	**According EN 1998-1 (q=4)**	**-**	**-**
Only active tension diagonals (low dissipative design concept)	**q = 2.0**	**q = 1.0**	**q = 1.5**
Active Compression & Tension diagonals (low dissipative design concept)	**q = 2.0**	**q = 1.0**	**q = 1.5**

Table 2-2 Maximum value of q factor in cross aisle direction

In order to perform a nonlinear inelastic analysis the potential inelastic zones should be predefined. The available inelasticity of any specific system differs from each other, however herein a topological proposal of the potential inelastic zones is proposed for common and conventional racking systems. Figure 2-3 shows the zones that are selected as potentially inelastic for a typical configuration in the down aisle and the cross aisle direction, as well as for a typical bracing system. In particular, based on the results of the previous project SEISRACKS and on the damages that were reported at the inspections-reports mentioned at the beginning of this chapter, the potential inelasticity was found to be developed at the bracing members (spine bracing & diagonals), the beam-to-upright connections (beam end connectors), the base plates and the uprights ends.

2.3.1 Sources of inelastic behavior

It should be noted that the profiles in racking systems are usually cold formed and/or thin walled so that their plastic properties cannot develop. Thus, the term inelastic from now on is referred either to the indeed plastic properties (yielding) of the elements, if this is applicable, or (more likely) to an equivalent nonlinearity which is resulted by local deformations or local buckling.

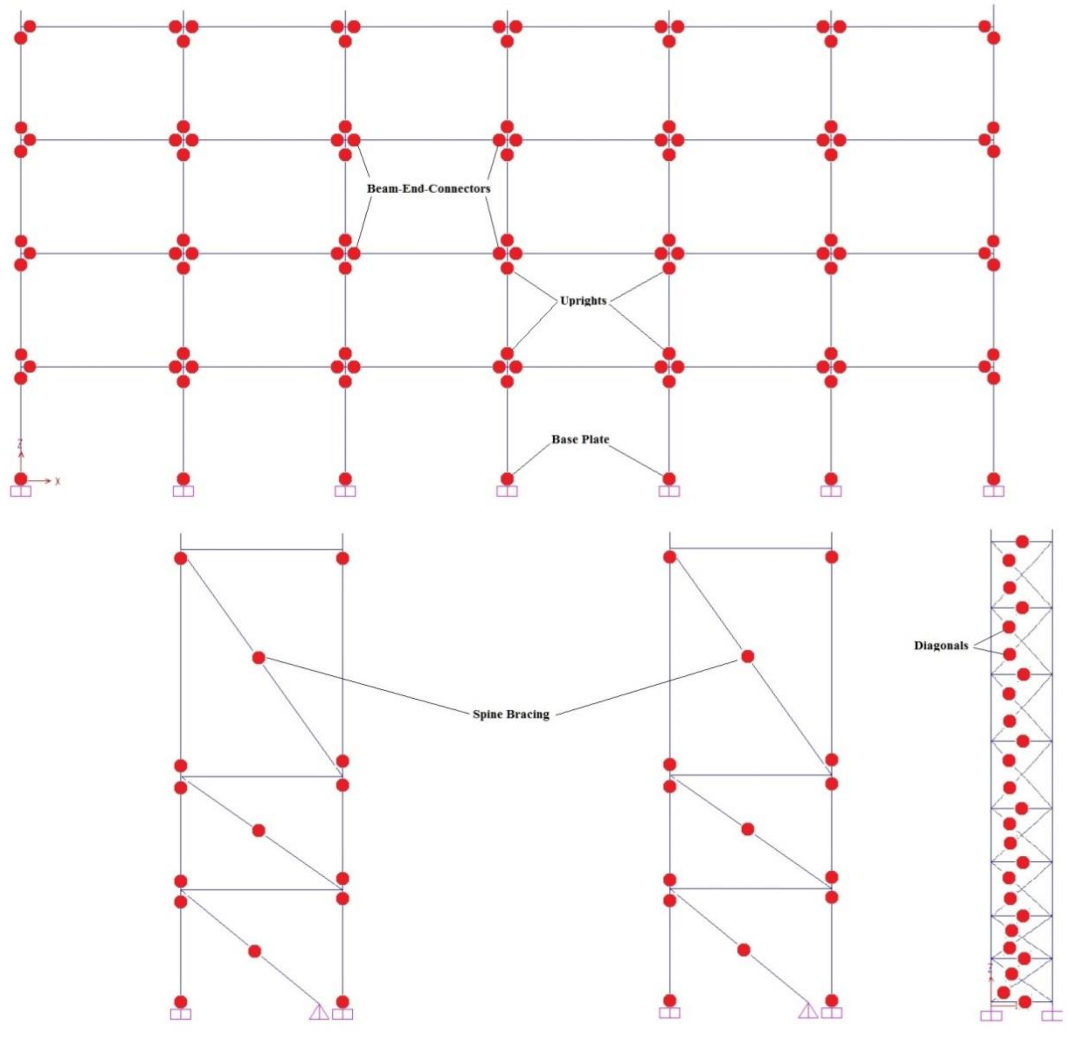

Figure 2-3 Potential Inelastic zones of a typical racking system

The inelastic properties of each element are introduced to the software either with the use of nonlinear spring elements, or directly with plastic hinges at the extremities of the elements (for beam elements) or at their middle (for truss elements).

The principles of how to define the inelastic properties of any member is next summarized for each potentially nonlinear element.

2.3.1.1 Diagonals & Spine Bracing members

Diagonals and spine bracing members are truss elements and their plastic properties are introduced with the use of axial hinges (axial force vs. axial displacement). A diagonal member could fail either due to buckling (under compression) and/or yield (under tension), or due to connection's failure. Buckling occurs to diagonals of the upright frames under axial forces and secondary bending moments due to potential eccentricities of the special assemblies. Yield occurs when members under tension reach their yield stress. The connection's failure, usually these are bolted connections, occurs when the forces on the connections exceed the bearing capacity of the connected members and/or the shear strength of the bolts. Sometimes more than one failure mechanisms coexist; as a result more complicated analysis is required to well-describe the entire failure mechanism. Finally, there are connections' details that are not directly norm-described and so numerical analyses with finite elements software are strongly recommended to derive the exact behavior of the assemblies.

2.3.1.2 Uprights

The uprights are usually subjected to biaxial bending moments and axial forces. Their plastic properties are determined using the combined capacity of the member to lateral-flexural buckling, and/ or the section's capacity under axial force and biaxial bending. The fact that the uprights consist of thin walled cold formed sections with stiffeners and perforations along their whole length, makes the use of numerical and/or experimental results a necessity. For a sufficient definition of the uprights' inelastic behavior an interaction surface between axial force and biaxial bending moment should be taken into account. To define the desired moment-curvature curve of each element for any level of axial force and any combination My-Mz, nonlinear numerical analyses are required. Usually the upright sections are classified as Class 3 or Class 4; that means that the upright members suffer from local or global buckling. Therefore, the norm proposed formula for combined compression and biaxial bending is strongly recommended to be introduced as an interaction surface. Each code proposes this formula, in a slightly different form and uses different factors.

2.3.1.3 Beam-end-connectors

As it is seen in Figure 2-1a and Figure 2-1f the beam end connectors are very special connections, where a beam hangs on to the perforations of the upright. Although there are multiple modern researchers, among others Ayhan and Schafer (2012) [33], Sarawit and Peköz (2003) [34], Gilbert and Rasmussen (2009) [35], Baldassino et al. (2000) [36], Cardoso and Rasmussen (2016) [37] and Ślęczka and Kozłowski (2007) [38], that attempt to define analytically the properties of those connections, the experimental tests remain always more reliable, as the normative document FEM10.2.02 also points out. Figure 2-4 shows such a typical moment vs. rotation diagram derived from experiments executed in RWTH in the frame of SEISRACKS 2 [30] for different level of vertical pay-load. In case of fully loaded pallet-beams the stiffness of the beam end connector is higher and that of the whole system too. This means that the stiffness and the final bearing capacity of the connectors are directly influenced by the level of the vertical loading. In case that a moment-rotation curve is to be derived from an experimental procedure, care should be taken that the pay load should correspond to the one that charges the beam end connector at the earthquake combination. Another interesting point about the beam end connectors is the fact that their behavior for sagging and hogging bending is not identical, due to the no-symmetry of the assembly. This is seen in Figure 2-4, where the moment-rotation curve is not symmetric. If possible, this should be taken into account at the definition of the nonlinear behavior of the connectors.

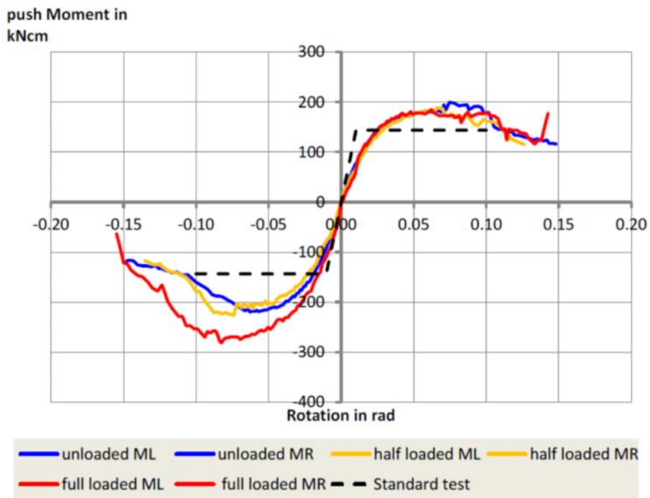

Figure 2-4 Experimental Moment-rotation curves for sagging and hogging bending of a beam-end-connector

2.3.1.4 Base Plates

The base plates are also special connections, whose capacity may not be determined theoretically, but experimental results should be used to determine their inelastic properties. Such results have shown that the pay load applied is significant for the overall capacity and stiffness of the component test (similar to the beam end connectors). The curves that are derived from experiments and are used to describe the nonlinear behavior of the base plates assemblies should be correspond to tests that were performed for vertical loads similar to those calculated by linear elastic analyses for the earthquake combination.

2.3.1.5 Pallet beams

Theoretically pallet beams could also be potentially nonlinear sources for the system; however, their bending capacity is that higher in comparison to that of the beam end connectors, so that it could be neglected in order to simplify the model. Apparently, this assumes a sufficient design of the beams in respect to the bending and torsion capacity and the adequacy of the welding between the component-sections used for the manufacturing of the typical hollow pallet-beam sections.

2.4 P-Delta Effect

P-delta effects have a known and significant influence to the overall behavior and design of structures. Taking this into account, 2^{nd} order analysis is more accurate than 1^{st} order analysis but it is sometimes complicated to apply it. Eurocode-3 indicates when it is considered necessary to perform 2^{nd} order analysis taking into consideration P- delta effect and when it is allowed to neglect it. Linear buckling analysis on the global structure has to be performed, to indicate whether or not it is necessary to perform 2^{nd} order analysis. If the critical buckling factor is greater than 10, 2^{nd} order effects may be neglected. Figure 2-5 presents and compares the resulted response curves derived from two different models with and without 2^{nd} order effects. The two models present different extreme values of the critical buckling factor α_{cr}, which is defined as:

$$a_{cr}=\frac{F_{cr}}{F_{Ed}} \tag{2-1}$$

where F_{cr} is the critical buckling load for the fundamental buckling mode and F_{Ed} the design vertical load of the structure.

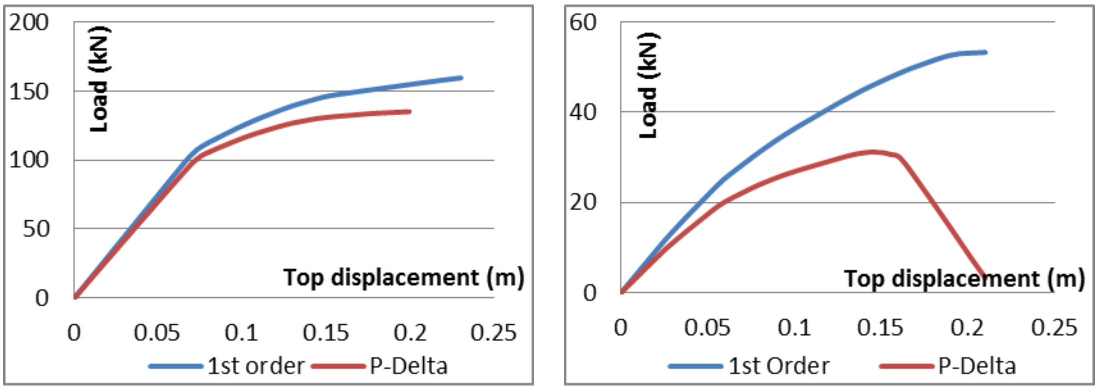

a) Braced system: Buckling Factor a_{cr}=13 b) Unbraced system: Buckling Factor a_{cr}=4

Figure 2-5 Pushover curves with and without P-delta effects

As far as unbraced racking systems are concerned, it is clearly and strongly recommended that P-Delta effects should be taken into consideration; otherwise the results may be unreliable.

2.5 Investigated case studies

Investigating nine case studies, two different software packages were used to perform pushover analyses. The commonly used software SAP2000 [39] was used to perform global and final pushover analyses, while the ABAQUS [40] software was used to perform more complicated analyses at local level of each member to define the exact nonlinear laws for the upright sections and the diagonal members. As far as the beam end connectors and the base plates are concerned, experimental results were used. The procedure for each potentially inelastic member towards the global pushover analysis is described further down.

2.5.1 Configurations

In the frame of SEISRACKS2 nine racks have been investigated, that were provided by four different producers of the project. For confidentiality reasons the presented data and results are usually dimensionless or general without revealing which one belongs to whom. The different producers are denoted by the abbreviations IP-A, IP-B, IP-C and IP-D. The different topologies of the provided racks are depicted in Figure 2-6. Systems L1, L2 and L4 consist of six spans of 2.7m length and a total length of 16.2m, while system L3 consists of 10 spans of 2.7m. All the racks have four levels, 2m each, and a total height about 8.2m. In the down aisle direction only three racks are braced: L1, L2 and L3 (Figure 2-6). The topology L1 allocates bracing in two different positions and it braces the two lower levels separately and the two higher levels together. The topology L2 has also two bracing systems that brace each level separately. The third braced topology, L3, uses a non-conventional bracing system composed of eight non-prestressed cables (4+4 symmetrically placed) connected to a central upright that stands behind the main rack. The rest bracing systems are assembled together in a so called bracing tower that is eccentrically connected (40-50cm) to the rear side of the main rack. The topology L4 represents the six remaining unbraced racks; these have similar configurations with no bracing system, although they are designed for low, medium or even high seismic zones. This system works like a moment-resisting frame, while the braced racks considered activate only the tension diagonals of their bracing system.

Name	Topology
L1	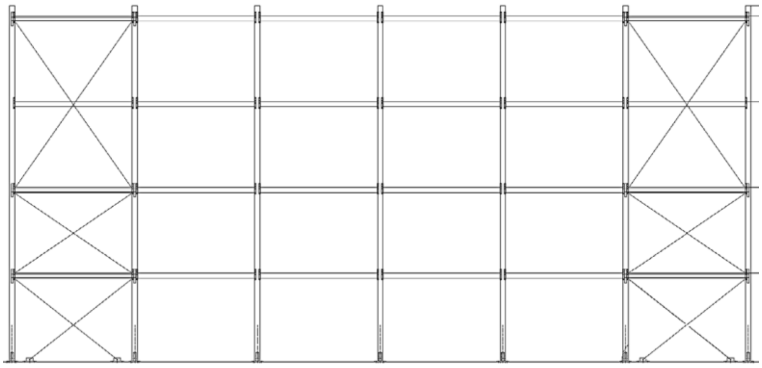
L2	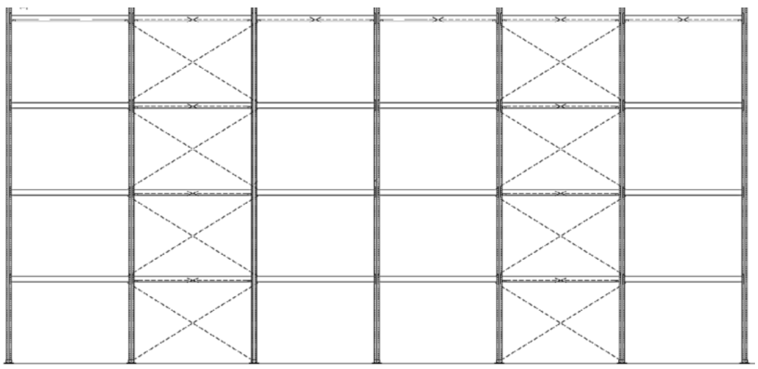

L3

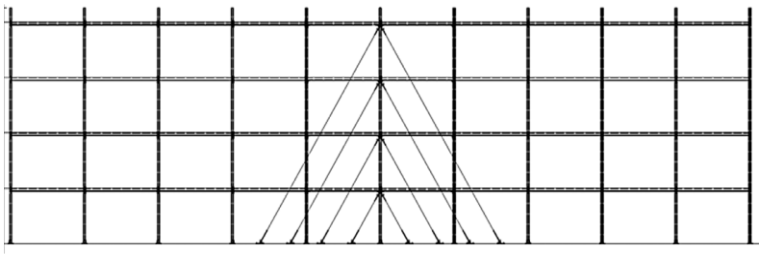

L4

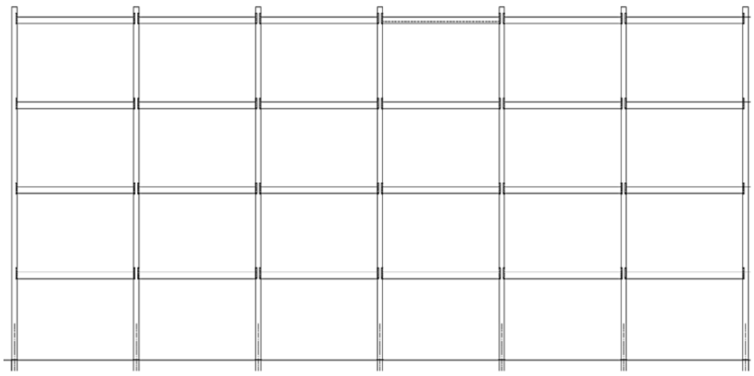

Figure 2-6 Topology of the provided configurations for the down aisle direction

In cross aisle direction which has a width between 1m and 1.1m, the producers provided several solutions for the bracing of the upright frame. The different configurations are presented in Figure 2-7. Topology Q1 is used twice for low/medium and medium/high seismic zones.

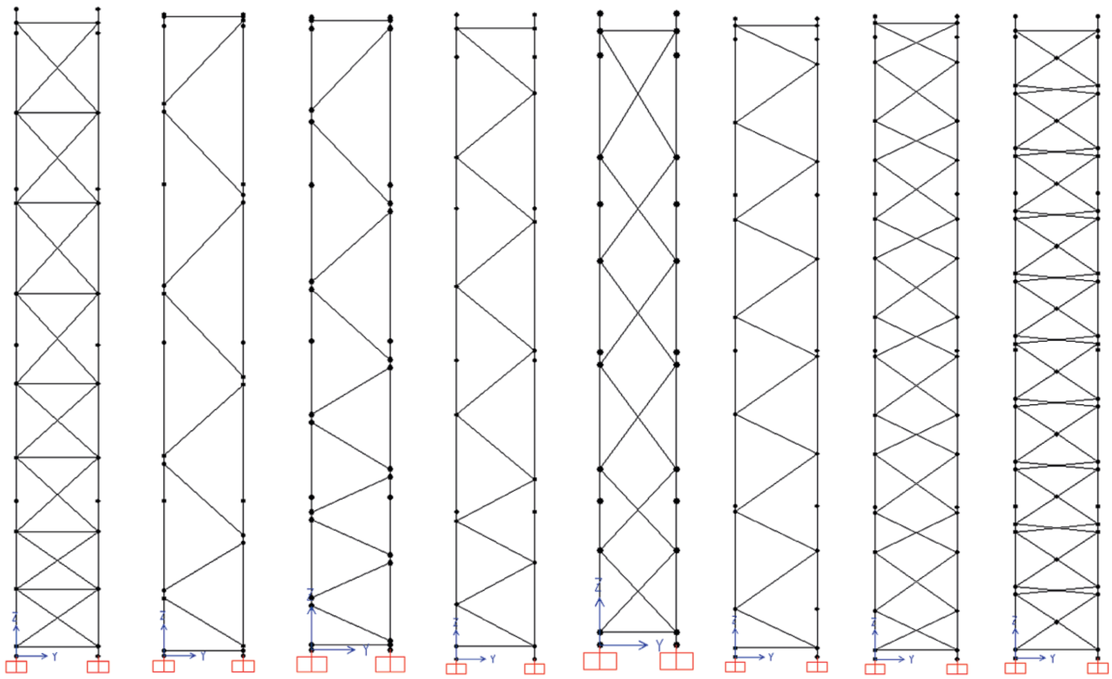

Q1 Q2 Q3 Q4 Q5 Q6 Q7 Q8

Figure 2-7 Topology of the provided configurations for the cross aisle direction

The examined systems were designed for low, medium and high seismic zones, according to the provisions of FEM 10.02.08 or EN16681. Generally in cross aisle direction the behavior factor that was selected is q=1.5. This value conforms to the code rules for the system Q2, Q4, Q5, Q6 and Q7. For the systems Q1 and Q8 this value is much lower than the maximum allowable one (for only tension diagonals, the behavior factor could take the value of q=4).

In the down aisle direction according to Table 2-2 the behavior factor ranges from 1.5 to 2, applying FEM 10.02.08 for low dissipative concept. It is apparent the fact that the producers use different values of the behavior factor for generally similar systems. This shows the lack of confidence to use the relatively high values recommended by the codes.

2.5.2 Inelastic Properties

2.5.2.1 Beam End Connector

The curves used for these connectors were derived by experiments that were performed at the University of Aachen (RWTH, Aachen, Germany). Both monotonic and cyclic tests were executed; however in this chapter only results from the monotonic test will be presented.

The stiffness and the strength of each connector vary for each Industrial Partner (IP) and each assembly. Thus, each IP provided independently the properties of his connector, as derived from experimental tests. Figure 2-8 presents indicatively the nonlinear properties of the used connectors, as initially provided by the IPs.

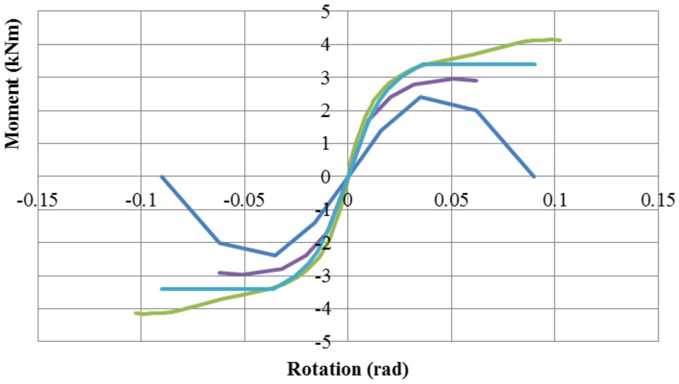

Figure 2-8 Adopted moment-rotation curves for the beam end connectors for the different case studies

These nonlinear properties are introduced as a multi-linear inelastic link-element with length equal to the half upright-width. This link element is free to rotate about the minor axis of the pallet-beam and it has the translational degrees of freedom fixed. The initial stiffness is used for the linear analyses, while the full moment-rotation curve is used for the nonlinear Pushover analyses.

2.5.2.2 Base- Plates

Experimental results of the selected base-plate assemblies were provided by the industrial partners for different levels of axial force. Since the average stiffness and strength of these connections under different axial loads differ, the results that selected to be used have been derived for levels of axial forces similar to the axial forces that correspond to a fully loaded rack. Figure 2-9 presents the used moment-rotation curves of the base plates for each IP. The inelastic properties were introduced by using plastic hinges at the base point of the lower uprights.

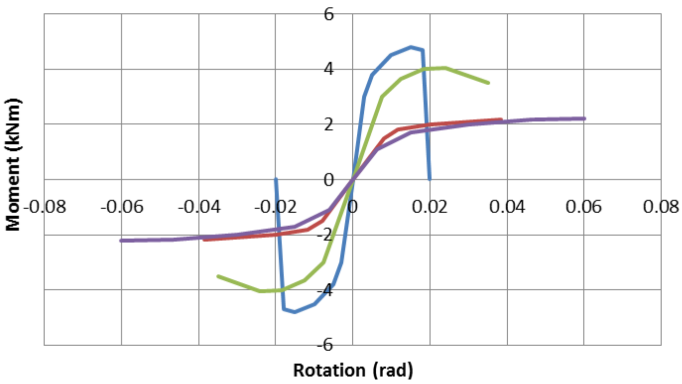

Figure 2-9 Adopted experimental moment-rotation curves for the base plate for the different case studies

2.5.2.3 Uprights

The uprights o rack systems are usually made of class 3 or class 4 sections and are sensitive to any kind of buckling (flexural, torsional, distortional, local). These sections are not capable to develop plastic properties; however, buckling as a failure mechanism may be introduced as an equivalent plastic hinge at the most vulnerable column’s point, which is close to the beam-to-column connection as bending moments are maximal in this region due to horizontal seismic loads. The required properties are the yielding point, the ultimate point and the exact path before, between and after them. This path is defined by the moment-rotation curve of the member.

The exact definition of an equivalent plastic hinge for the uprights of a racking system might be the trickiest part of this endeavor. Many researchers have applied a big effort to clarify the capacity for such peculiar upright sections. The et al. (2004) [41] noted that conventional 2D, even 3D beam element models of commercial software packages cannot estimate properly the buckling load of an upright. Freitas et al. (2005) [42] presented some numerical models of uprights, using shell and solid elements in Finite Element Software. The outcome of these models in terms of ultimate buckling load and buckling mode were in good agreement compared with experimental results. This conclusion offered the confidence to use such numerical models to predict the behavior of such members. Ungureanu and Dubina (2013) [43] came to the conclusions that the ECBL method (Erosion of Critical Bifurcation Load [44]) could sufficiently estimate the final buckling load of an upright member, taking into account special imperfections for the examined member. Such imperfections or the combination of these imperfections could be those of a global buckling mode, of a distortional buckling mode, etc. Finally Koen (2008) [45] presented in his master thesis an extended series of numerical and experimental results for upright members, concluding that the numerical model (Finite Element) could be used for the calculation of the upright's design; however the actual capacity of such a member is influenced by many parameters that are not deterministically defined. Such a typical parameter is the existence of the diagonal bracing of the upright frames; as Koen refers for a braced upright: "The capacity of the uprights using FEA is up to 50% greater than the design strength predictions for the 3150mm long uprights. This indicates that the discrete torsional restraint of the bracing has a significant effect on the upright strength".

Since, an accurate FEM analysis is required to provide the exact pre- and post-failure behavior of these members, a nonlinear static analysis was performed for an upright member of 2m height, constraining the translation along the major axis at the points where diagonal members are connected to the upright. The one upright-end is pinned, the opposite one is free to be translated longitudinally and both points are constrained regarding torsion. An axial load is applied in a first step, and then in a second step a horizontal load is applied and gradually increased, producing bending moment. Two cases are examined here: a) the load is applied in such a horizontal direction that produces bending around the major axis, and b) the load is applied in the other horizontal direction in order to produce bending around the minor axis. The objective is to evaluate the final capacity and to produce moment-rotation curve of the member which will be used subsequently as plastic-hinge properties in the global numerical model, using software SAP2000.

The upright members are simulated by shell elements taking into account the exact section-geometry (both radius and perforations), using an elastic-plastic material behavior with the nominal yield stress of each member. Figure 2-10 presents a typical numerical model, for an upright member implemented in the ABAQUS software. Figure 2-11 shows the deformed shape of an upright at the end of the analysis while Figure 2-12 shows the resulting moment-rotation curve for bending moments with different sign.

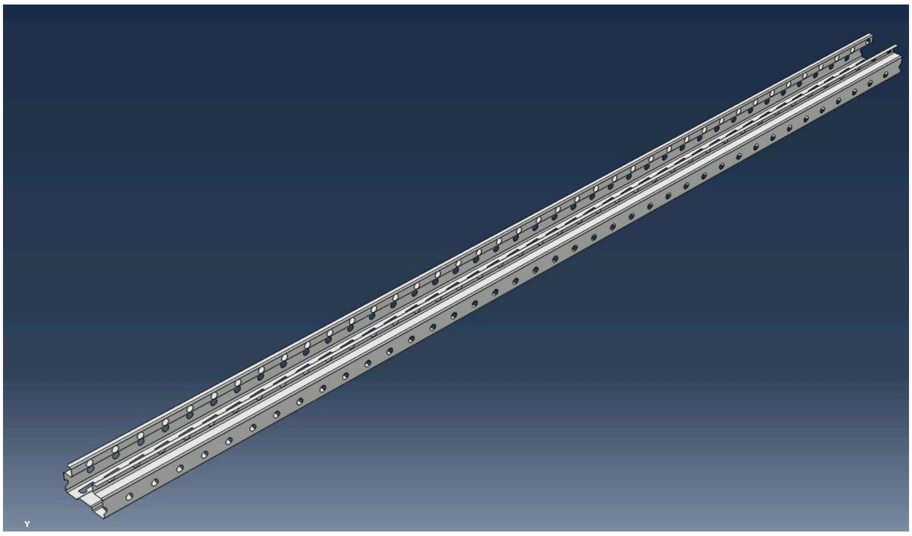

Figure 2-10 Typical ABAQUS numerical model of upright

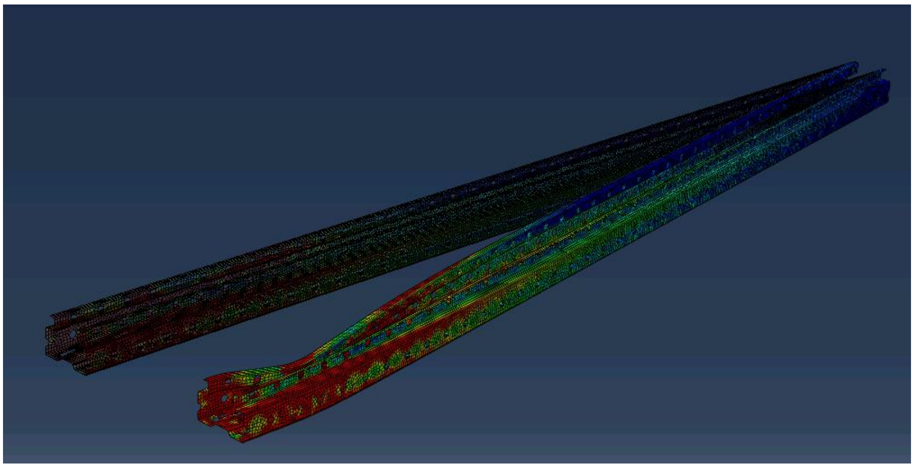

Figure 2-11 Deformed shape of a numerically tested upright

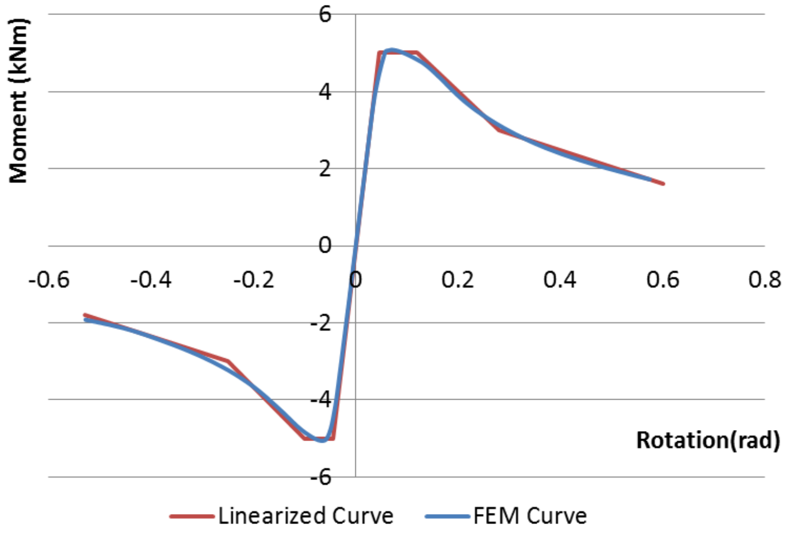

Figure 2-12 Moment-rotation curve for a typical upright

The objective is to introduce an equivalent multi-linear moment-rotation law as plastic hinge, in the global numerical model, using SAP 2000. All the different curves for each direction were normalized and linearized to create a compatible curve with the required one by SAP2000, as depicted in Figure 2-12.

The problem arising is that the upright's "plastic hinges" are not uniquely described by one moment rotations curve. This has a strong dependence on the axial force and the bending moment of the other direction. This means that a three dimensional interaction surface N-M_z-M_y is required. Here the interaction formula of EN1993-1-1 for biaxial bending and coexistent axial force is used. The formula is shown in Eq.(2-2) in a form that takes into account also the global stability of the member.

$$\frac{N_{Ed}}{\chi_{min}\cdot A_{eff}\cdot f_y/\gamma_M}+\frac{k_y\cdot M_{y,Ed}}{\chi_{LT}\cdot W_{eff,y}\cdot f_y/\gamma_M}+\frac{k_z\cdot M_{z,Ed}}{W_{eff,z2}\cdot f_y/\gamma_M}<1 \qquad \textbf{(2-2)}$$

The above relation represents all the interaction N-M_y surfaces; the one that corresponds to uniaxial bending and compression is shown in Figure 2-13. The axes of the diagram are dimensionless, dividing by $N_{b,Rd}$ that is the corresponding buckling load against flexural buckling and $M_{b,Rd}=W_{eff,y}\cdot f_y/(\gamma_M\cdot k_y)$.

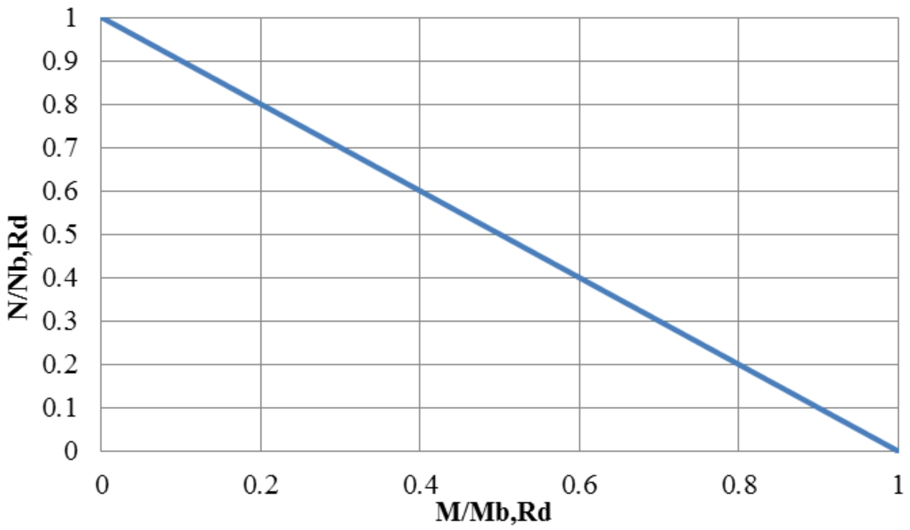

Figure 2-13 Interaction curve for axial force and bending moment

2.5.2.4 Diagonals

2.5.2.4.1 Channel Diagonals

Diagonals are represented by truss elements in the global numerical model and their inelastic properties are introduced as axial plastic hinges. The yield strength of these "plastic hinges" should be chosen as the smallest value among the buckling capacity of the member, the yield strength of the cross section, the bolts' shear strength and the bearing resistance of the connection plates. However, these failure modes interact in case of a ductile and/or hardening post-failure behavior of the diagonal. Thus, a further numerical investigation is necessary in order to clarify the exact behavior of the diagonals, including the unique members' and connections' characteristics.

Diagonal channel members are simulated in ABAQUS by shell elements investigating initially the member's buckling resistance. The load is applied on the web of the channel section producing a secondary bending moment due to the connection's eccentricity. Analysis considering geometrical imperfections is performed using the shape of the fundamental buckling mode, determined by a linear buckling analysis and an imperfection magnitude according to EC3. Figure 2-14 shows the member's buckling mode under compression loading.

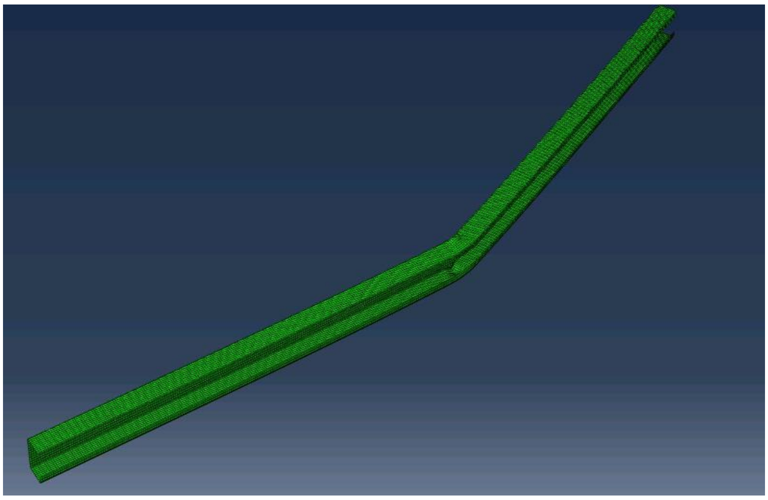

Figure 2-14 Deformations of a diagonal member from channel section at ultimate loading, ABAQUS simulation

Subsequently, the simulation of the bolted connection was performed with ABAQUS software. A contact model is used with solid elements in order to be more realistic, although the computation time needed and the model's numerical instability make the calculation much difficult. The expected local buckling, leads to the necessity to use a great amount of solid elements, a problem that can be abbreviated by using half of the model -taking advantage of the symmetry. The appropriate boundary conditions are introduced to the half model, thus it is easier to increase the number of elements around the connection's hole. The load on the diagonal is applied via a displacement control of the bolt. The model is loaded to both tension and compression. The results show that bearing failure appears first independently to the load direction. Figure 2-15 presents the compression response of an isolated member, shown before, together with the local response at its end for tension and compression (all in absolute values).

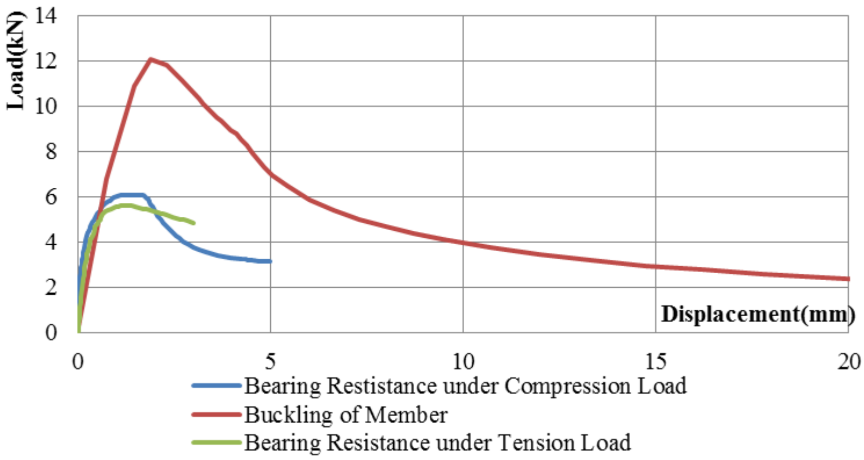

Figure 2-15 Response of the global member and its local ends to loading

It may be seen that although the bearing resistance is highly ductile, this thin walled channel members could not display this property fully as local buckling around the hole occurs. Figure 2-16 shows the numerical model before loading and Figure 2-17 the failure modes for the two different load directions (tension and compression). It may be seen for both load directions that local buckling of the web in front of the bolt and due to bearing take place. The plastic hinge properties that were used in the pushover analyses are produced by diagrams such as in Figure 2-15, when the exact properties of the diagonals were known.

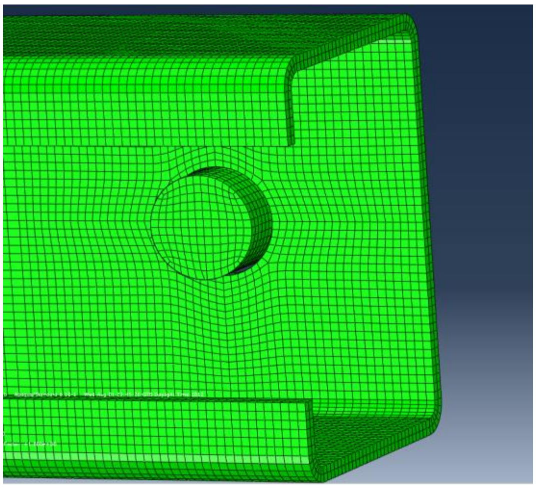

Figure 2-16 Numerical model of a bolted connection to the diagonal in ABAQUS

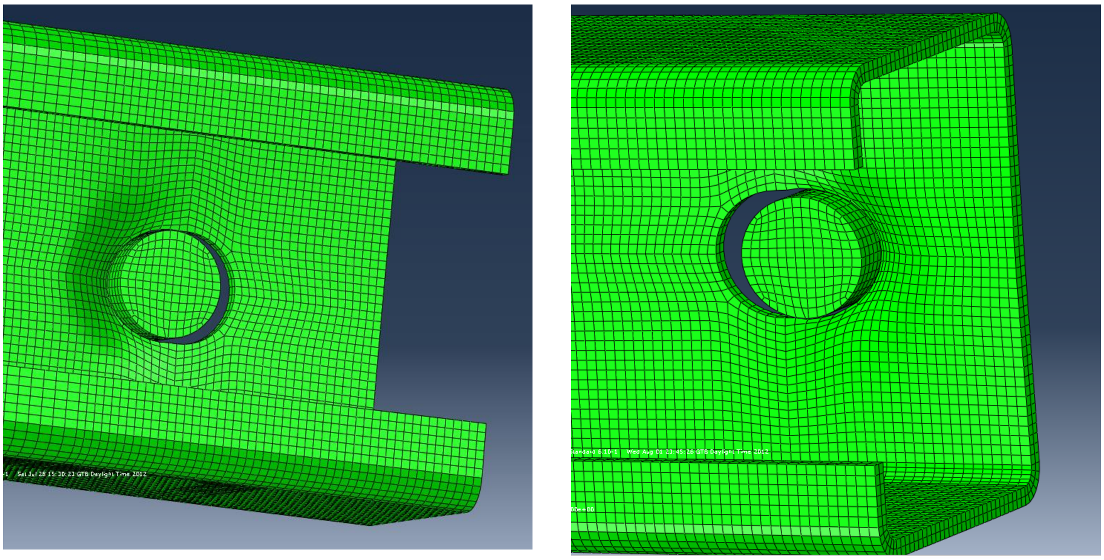

a) compression load

b) tension load

Figure 2-17 Bearing failure and local buckling due to compression and tension loads

2.5.2.4.2 CHS diagonal

The same advanced analyses were performed for another type of diagonal made by circular hollow section, whose ends are formed with special turnbuckles. This specific geometry under investigation is shown in Figure 2-18.

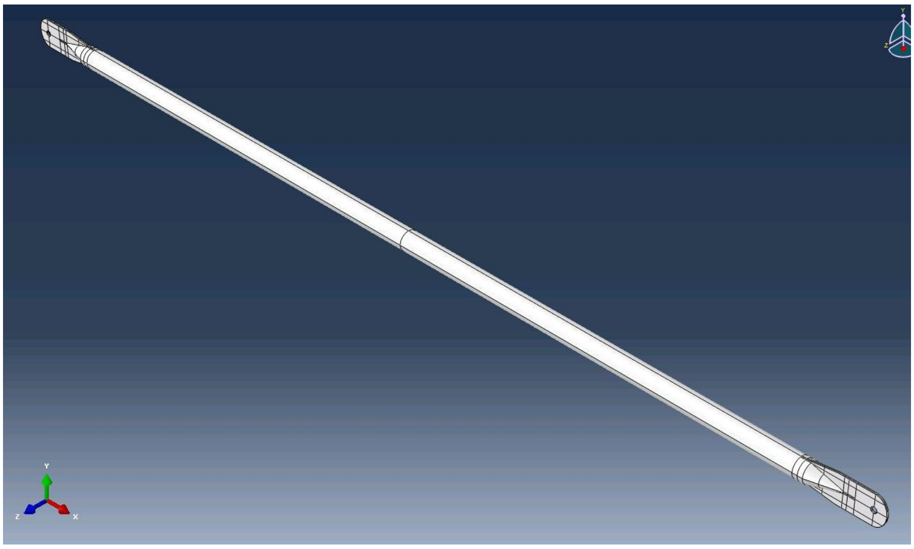

Figure 2-18 Numerical model for circular hollow section with turnbuckles used as diagonal members in ABAQUS

This model is simulated in ABAQUS software, to determine the member's compression response and the connection's strength. In Step-1, the member is studied isolated without the turnbuckles and its deformed shape at the end of the analysis is shown in Figure 2-19.

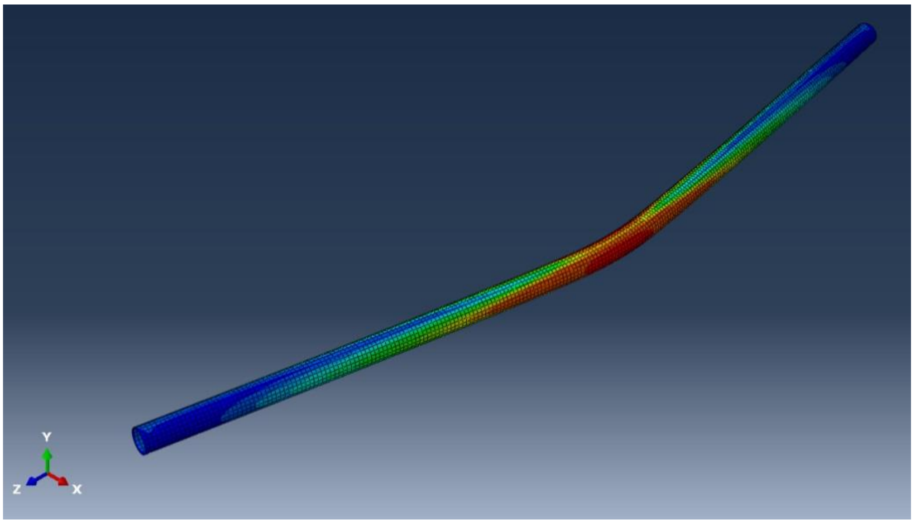

Figure 2-19 Buckling of an isolated diagonal members from CHS section

At Step-2, the whole model including the turnbuckles is simulated, with two rigid pins at the holes of the turnbuckles. Loading is introduced by displacing one pin while the other one was kept fixed and so producing compression. Figure 2-20 shows buckling of the turnbuckles and simultaneously circular-hole ovalization at maximum loading.

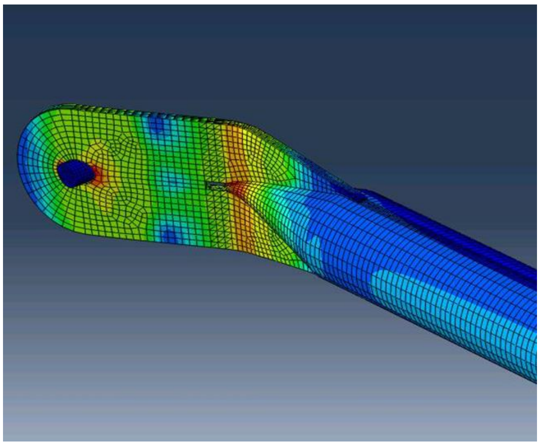

a- Buckling at flatten ends

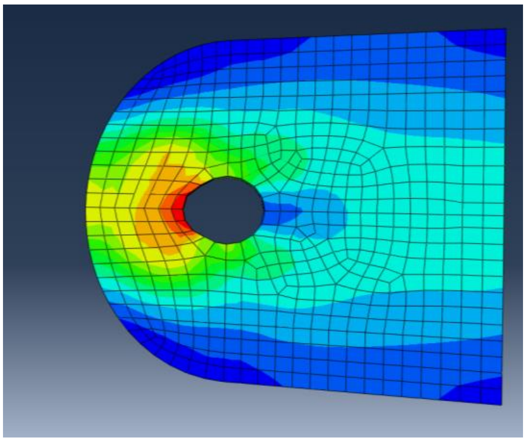

b- Ovalization of pin hole

Figure 2-20 Local deformations of the beam ends at ultimate loading

The failure mode in compression for the selected CHS member is a coupled one, between bearing resistance, global buckling of the member and buckling of the flatten ends. Figure 2-21 shows load-displacement curves for the isolated member (Step-1) and the complete diagonal including its ends (Step-2). Finally, the curve of the completed diagonal which is more critical is introduced in SAP2000 as plastic hinges property.

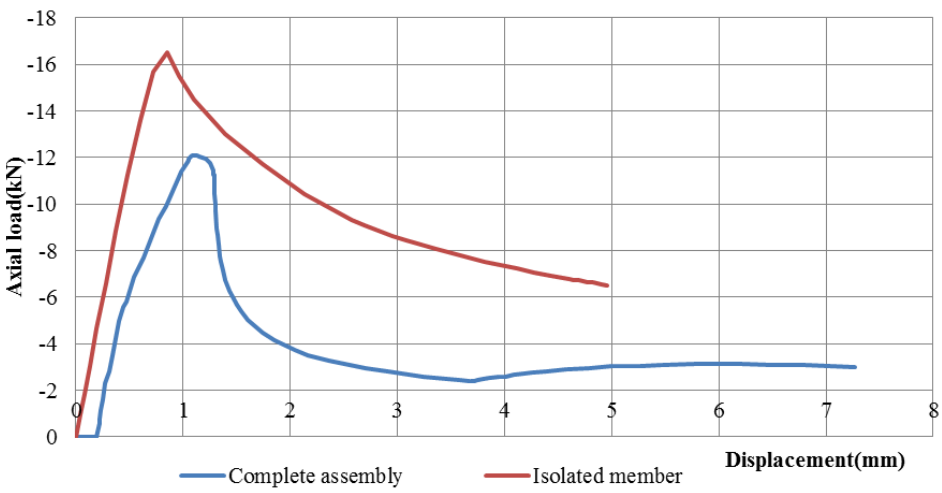

Figure 2-21 Load displacement curves for simulation of the isolated CHS member and the whole assembly

2.6 Global analyses and behavior factors

After the inelastic properties of all members were defined, all nine studied rack configurations were investigated by static nonlinear analysis in SAP 2000 software. The analyses were performed in two different steps. In the first step the vertical loads are applied in order to consider the stiffness of the deformed/loaded system as well as the P-Delta effects that are important. The applied load corresponds to 3 pallets of 800kg pro compartment. Subsequently, in the second step a horizontal load is applied that is gradually increased up to collapse of the system. The analyses are performed separately for the down and the cross aisle direction.

The distribution of the horizontal forces over the height of the rack remains always a questionable issue. Here, a load distribution following the fundamental mode-shape was selected for the pushover analyses, considering that the first mode is highly dominant for the unbraced racks (about 90% participating mass ratio) and simply dominant for the braced one (about 65% participating mass ratio).

The result of such analyses is the capacity curves for each configuration. These curves feature the base shear force vs. the horizontal top displacement of the rack and are shown for all systems in Figure 2-22 and Figure 2-23 for the cross and the down aisle direction, respectively. The different systems are designated with the use of letters that represent the different producers and with the term low, medium or high that indicates the seismic zone which the systems are designed for. No further information is provided, due to confidentiality reasons.

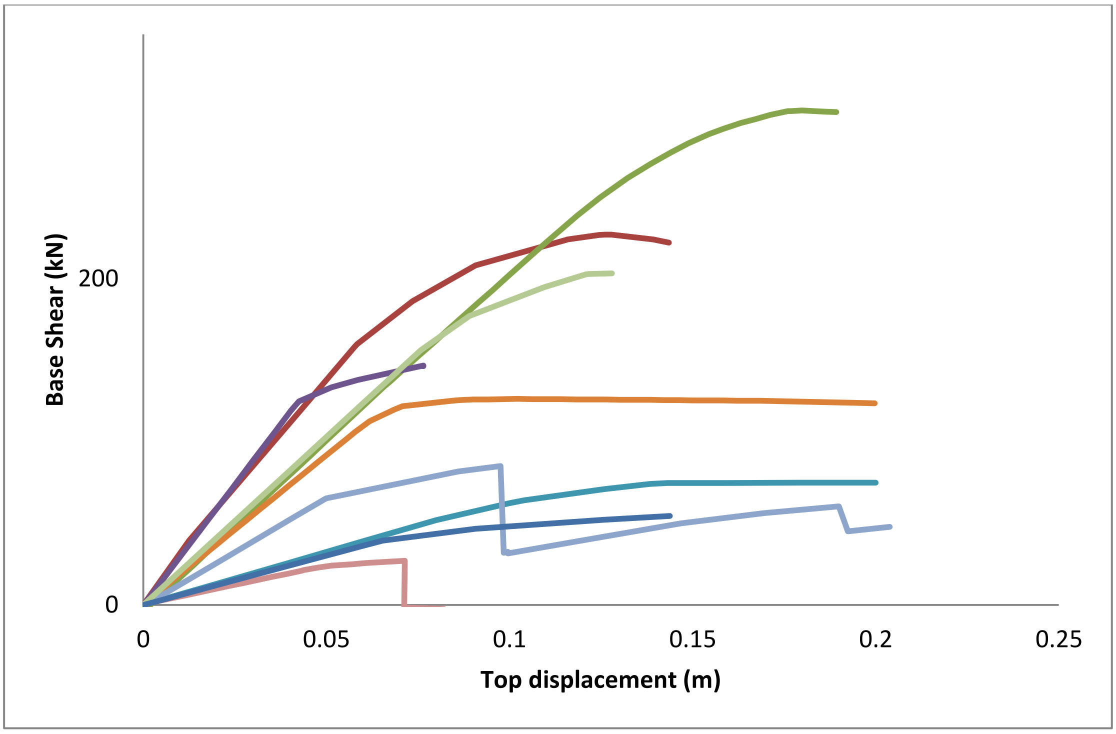

Figure 2-22 Pushover curves for all studied configurations in the cross aisle direction

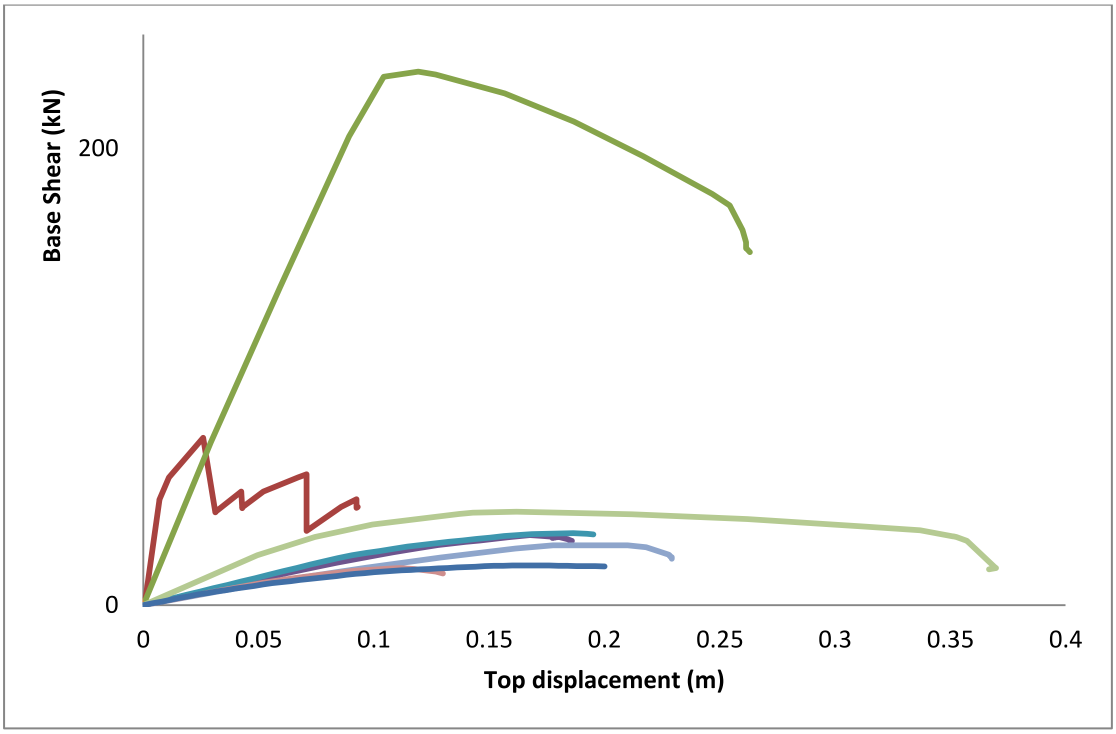

Figure 2-23 Pushover curves for all studied configurations in the down aisle direction

With the use of the capacity curves, the behavior factor of each system is estimated. For this purpose the capacity curves are linearized according to Figure 2-24. The system is idealized as bilinear (elastic-perfectly plastic system) defining the characteristic points A, B and C that indicates the first significant failure of the system, the equivalent yield point of the system and the ultimate load point, respectively. Then the behavior factor-q may be calculated. The definition of the behavior factor troubles the researchers for many years. It is even harder because the different international building codes use different definitions, looking that from another point of view. The international building code [46] and the American building code [47] use two different factors to introduce the energy dissipation capacity of a system in the design procedure; in particular, the force modification factor and the displacement modification factors are used. Irzidinia et al. (2012) [48] point out that the different proposed method for derivation of the behavior factor fall into two main categories; the European and the American one. Here one of the most known American methods is adopted as proposed by Uang (1992) [49]. This method is expressed by Eq. (2-7) as the product of ductility q_0 (Eq. (2-6)) and overstrength factor Ω (Eq. (2-5)).

In order to estimate the demand imposed by the design earthquake, the performance points for each structure and earthquake have to be determined as the section point between the capacity curve and the elastic design spectrum. The relevant calculations are made by SAP2000 on basis of the procedure described in ATC-40. The parameters C_A (Eq. (2-3)) and C_V (Eq. (2-4)) that define the elastic spectrum are determined from:

$$\mathbf{C_A = a_g \cdot S \cdot n} \tag{2-3}$$

$$\mathbf{C_V = 2.5 \cdot a_g \cdot S \cdot n \cdot T_c} \tag{2-4}$$

$$\mathbf{\Omega = \frac{V_y}{V_1} = \frac{d_y}{d_1}} \tag{2-5}$$

$$\mathbf{q_0 = \mu = \frac{d_{max}}{d_y}} \tag{2-6}$$

$$\mathbf{q = q_0 \cdot \Omega} \tag{2-7}$$

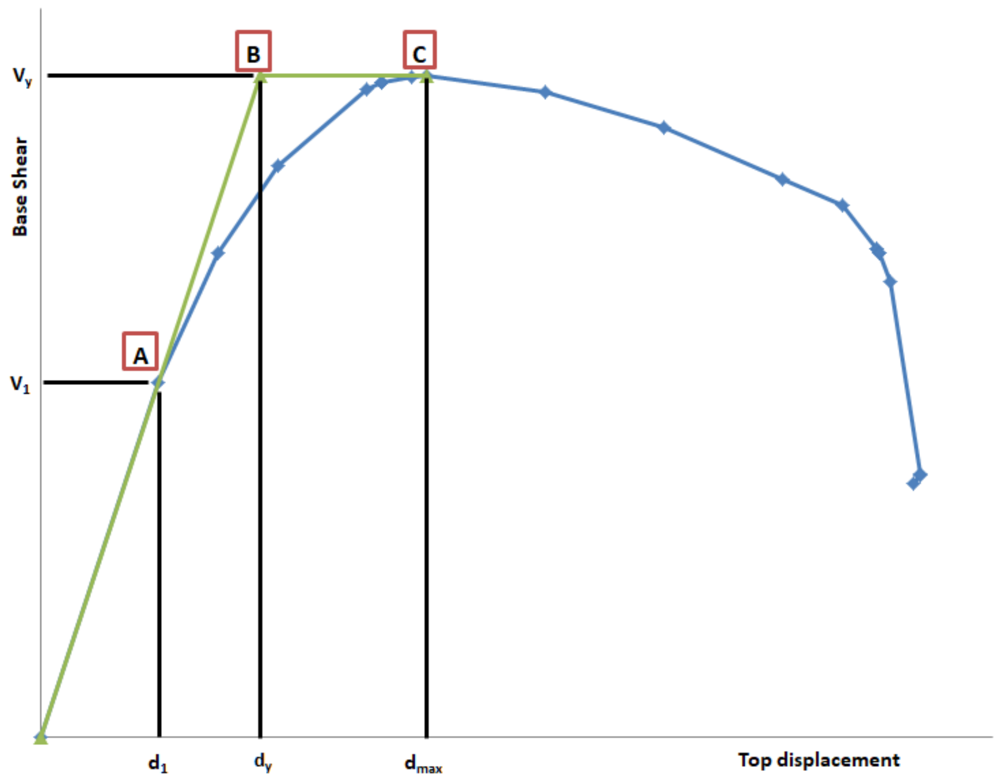

Figure 2-24Linearization of a pushover curve

The ultimate point C is selected to represent the ultimate limit state collapse prevention, as no other limit states are defined in the normative documents. In Figure 2-25 to Figure 2-33 all capacity curves (in blue) with the corresponding bilinear idealized curves (in green), the first significant failure point (in purple) and the performance point (in red) are presented. The position of the performance point registers how the system would respond to the design earthquake. For example in Figure 2-26 the performance point of system A for both directions stays under the first significant yielding that means that the structure remains in the elastic region. On the contrary, the performance point of System D in Figure 2-31a exceeds even the maximum capacity point of the system. The first case could show that the system is over-dimensioned, while the second one shows the opposite, namely that the system is under-dimensioned. Furthermore with use of the capacity curves and of the performance point the producer and/ or the user of the rack could decide if the displacements of the system are acceptable for the design earthquake.

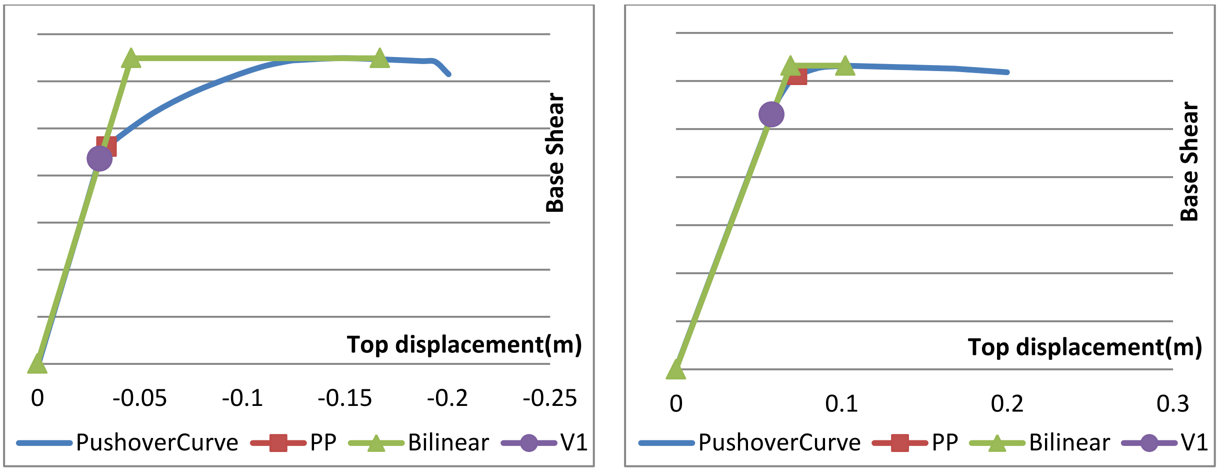

a) Down aisle

b) Cross aisle

Figure 2-25 System A, high seismic zone

The ductility, the overstrength and the q- factor of each system are presented in Table 2-3 to Table 2-11.

	μ	Ω	q
Down	3.65	1.50	5.47
Cross	1.47	1.2	1.76

Table 2-3 Ductility, overstrength and q- factor for system A-high seismic zone

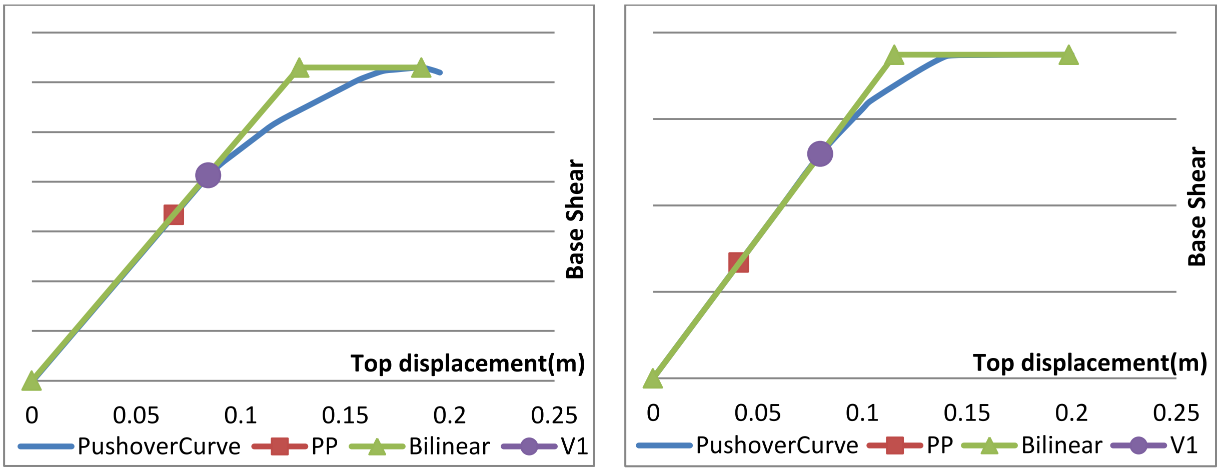

a) down aisle

b) cross aisle

Figure 2-26 System A, Medium Seismic Zone

	μ	Ω	q
Down	1.45	1.52	2.22
Cross	1.72	1.44	2.48

Table 2-4 Ductility, Overstrength and q- factor for the case study A-Medium seismic zone

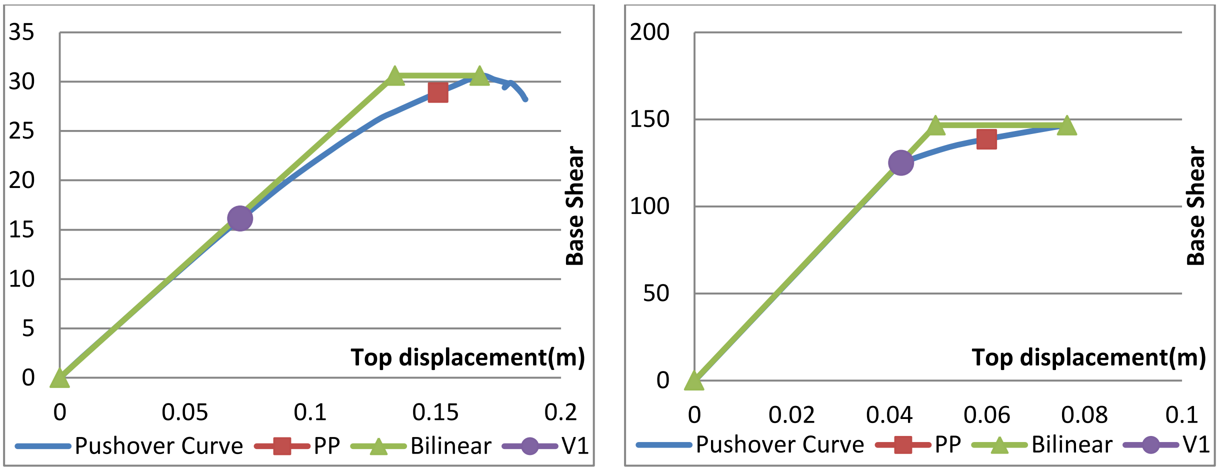

a) down aisle b) cross aisle

Figure 2-27 System B, High Seismic Zone

	μ	Ω	q
Down	1.25	2.06	2.58
Cross	1.54	1.17	1.81

Table 2-5 Ductility, Overstrength and q- factor for the case study B-high seismic zone

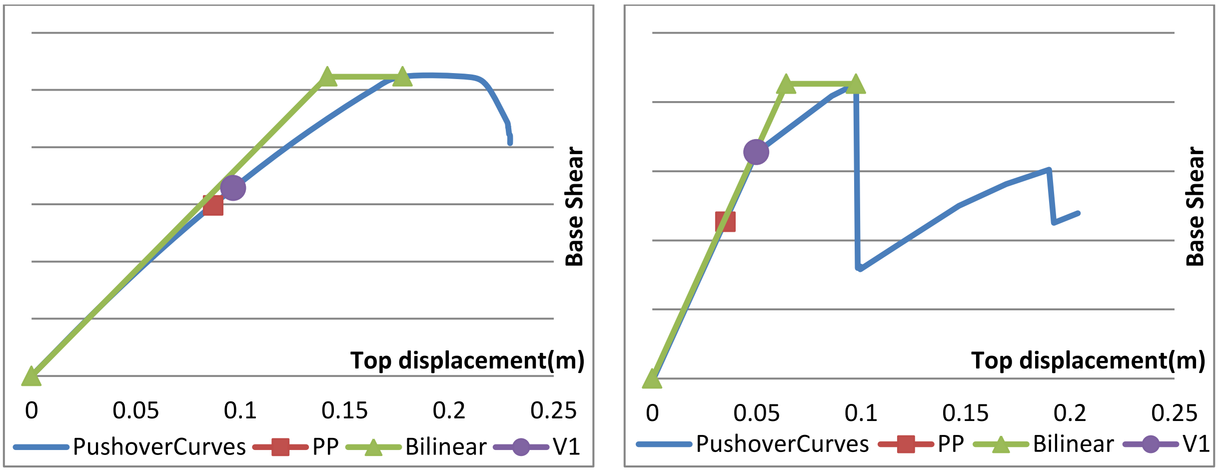

a) down aisle b) cross aisle

Figure 2-28 System B, Low seismic zone

	μ	Ω	q
Down	1.25	1.59	2.00
Cross	1.52	1.30	1.98

Table 2-6 Ductility, Overstrength and q- factor for the case study B-Low seismic zone

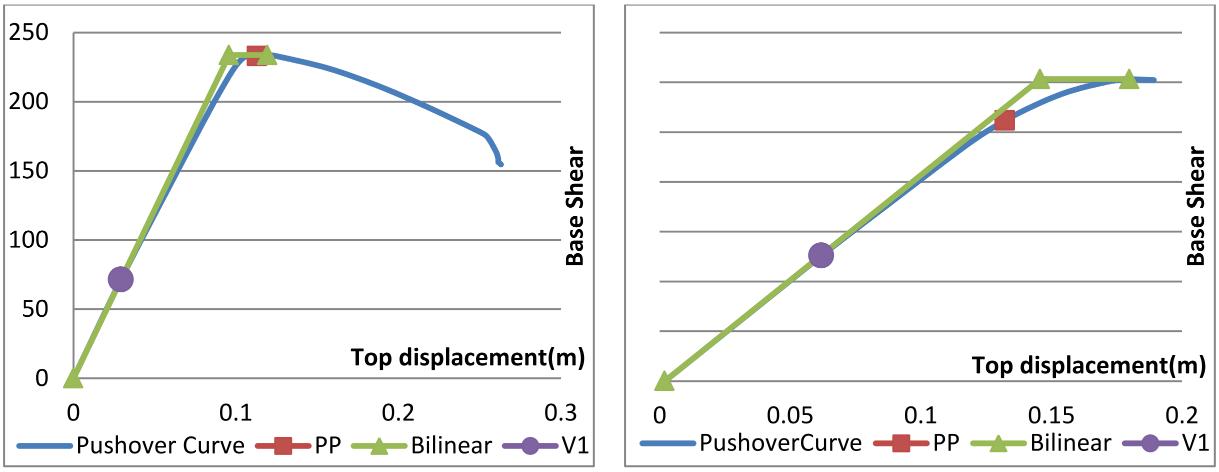

a) down aisle b) cross aisle

Figure 2-29 System C, High seismic zone

	μ	Ω	q
Down	1.24	3.27	4.07
Cross	1.23	2.4	2.97

Table 2-7 Ductility, Overstrength and q- factor for the case study C-high seismic zone

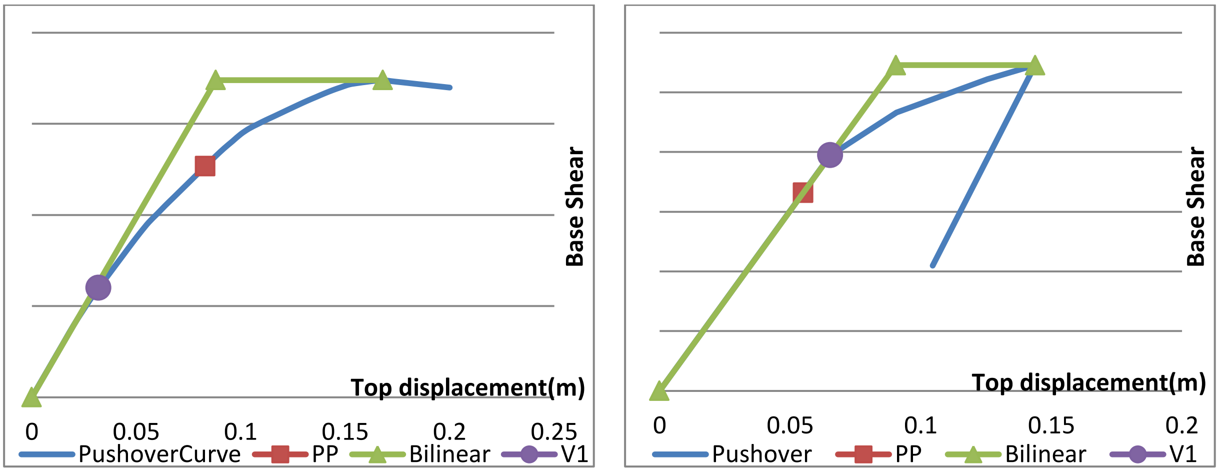

a) down aisle b) cross aisle

Figure 2-30 System C, Medium seismic zone

	μ	Ω	q
Down	1.90	2.90	5.51
Cross	1.58	1.38	2.2

Table 2-8 Ductility, Overstrength and q- factor for the case study C- Medium seismic zone

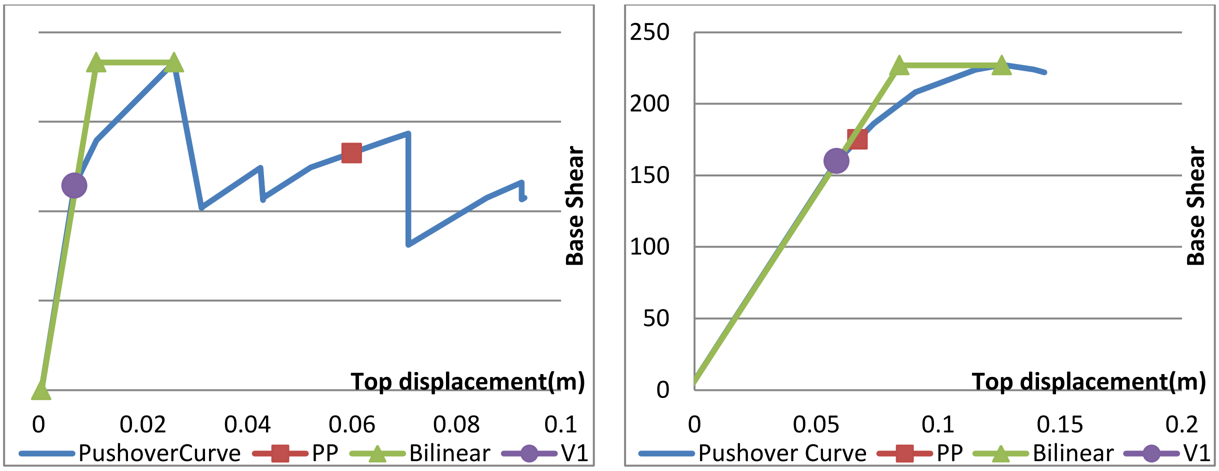

a) down aisle b) cross aisle

Figure 2-31 System D, High seismic zone

	μ	Ω	q
Down	2.34	1.59	3.72
Cross	1.49	1.42	2.12

Table 2-9 Ductility, Overstrength and q- factor for the case study D-high seismic zone

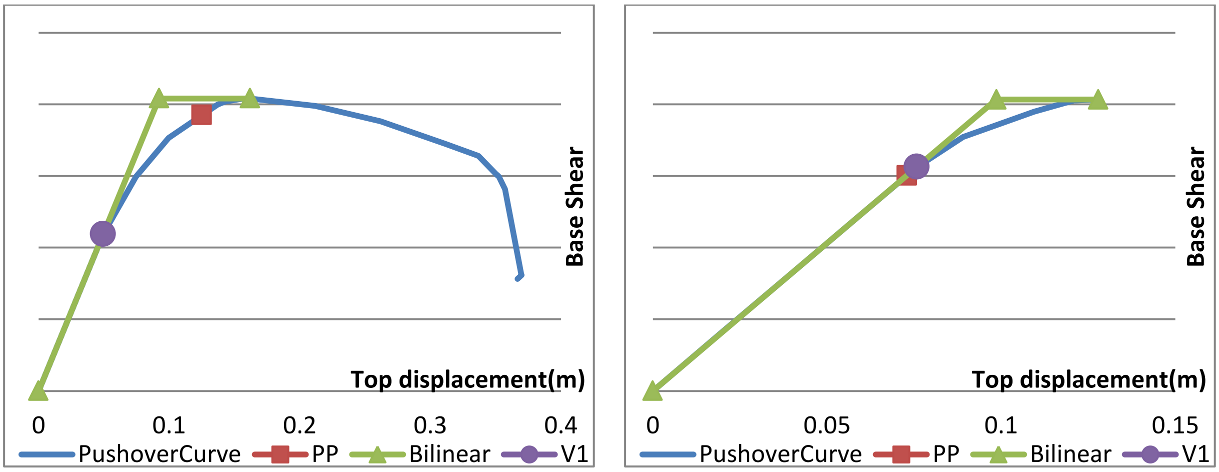

a) down aisle b) cross aisle

Figure 2-32 System D, Medium seismic zone

	μ	Ω	q
Down	1.75	1.86	3.27
Cross	1.29	1.30	1.68

Table 2-10 Ductility, Overstrength and q- factor for the case study D- Medium seismic zone

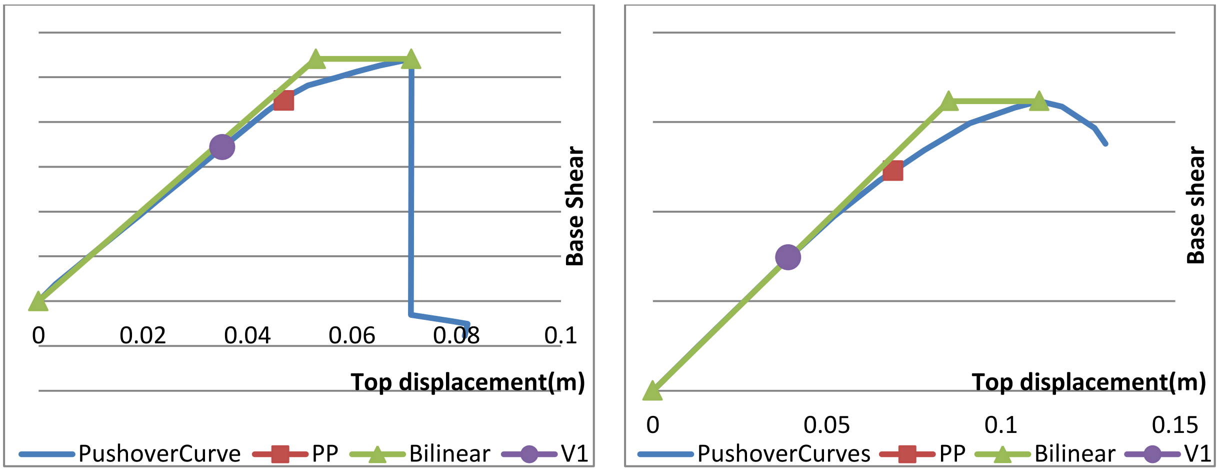

a) down aisle

b) cross aisle

Figure 2-33 System D, Low seismic zone

	μ	Ω	q
Down	1.30	2.18	2.84
Cross	1.34	1.57	2.11

Table 2-11 Ductility, Overstrength and q- factor for the case study D- Low seismic zone

Table 2-12 summarizes the calculated behavior factors, the ductility and the overstrength factors of each system. Considering the extreme differences between the calculated values, it may be concluded that this definition of the q-factor is probably not the most suitable for racking systems. It is seen that the overstrength in the down aisle direction is on average higher than in cross aisle direction. A safe outcome would be a behavior factor q=1.5 for the cross aisle direction and q=2 for the down aisle direction. One more difference could be seen between the braced and the unbraced configurations at the down aisle direction. The braced models seem to have higher ductility reserves, leading to a behavior factor of 3.5. Beattie (2006) [50] however proposed a design guideline for steel storage racks where he suggested that for both cross aisle and down aisle directions the maximum ductility used for design should be 1.25. In down aisle direction, if the performance of the connections has been investigated experimentally, the ductility could take higher values and in no cases should it go beyond 3.0 except detailed studies suggest otherwise.

System/Zone	Direction	$q_0 = \mu$	Ω	q
A/High	Down	3.65	1.50	5.47
	Cross	1.47	1.2	1.76

A/Medium	Down	1.45	1.52	2.22
	Cross	1.72	1.44	2.48
B/High	Down	1.25	2.06	2.58
	Cross	1.54	1.17	1.81
B/Low	Down	1.25	1.59	2.00
	Cross	1.52	1.30	1.98
C/High	Down	1.24	3.27	4.07
	Cross	1.23	2.4	2.97
C/Medium	Down	1.90	2.90	5.51
	Cross	1.58	1.38	2.2
D/High	Down	2.34	1.59	3.72
	Cross	1.49	1.42	2.12
D/ Medium	Down	1.75	1.86	3.27
	Cross	1.29	1.30	1.68
D/Low	Down	1.30	2.18	2.84
	Cross	1.34	1.57	2.11

Table 2-12 Summary of the estimated behavior fators

Table 2-13 presents a summary and comparison of the estimated (available) behavior factors and the used ones during the design procedure. It is concluded that the calculated values of the behavior factor with the adopted definition are higher, even much higher than the used ones in everyday practice. However, the calculated pushover curves and performance points allow an easy determination of the q-factor by any modified definition of it.

Zone/IP		**A**		**B**		**C**		**D**	
	q-Factor	Down	Cross	Down	Cross	Down	Cross	Down	Cross
Low	Design	-	-	1.5	1.5	-	-	2	1.5
	Estimated	-	-	2	1.98	-	-	3.72	2.12
Medium	Design	1.5	1.5	-	-	1.5	1.5	2	1.5
	Estimated	2.22	2.48	-	-	5.51	2.2	3.27	1.68
High	Design	2	1.5	2	1.5	1.5	1.5	1.5	1.5
	Estimated	4.5	1.76	2.58	1.81	4.07	2.97	3.72	2.12

Table 2-13 Comparison of the available and the used behavior factors

2.7 Pushover curves for fully calibrated models in cross aisle direction

In this section of this chapter numerical models in the cross aisle direction are presented once again. These models differ from the previous ones, as they include just one upright frame and not the whole racking system. These models are investigated and presented separately because they are fully calibrated to experimental tests that were performed at the University of Liege in the frame of the research project SEISRACKS2. Their configurations are identical to the ones presented in Figure 2-7 Topology of the provided configurations for the cross aisle direction. With a calibration procedure that is described in Appendix A, the numerical models for these configurations were calibrated in order to perform new Pushover analyses for real assemblies that are more realistic compared to both experimental on partial subassemblies and numerical ones on complete assemblies but lacking the material properties. The current numerical investigations go beyond the experimental ones since in the experiment tests of Liege gravity loads were not considered. Although upright frames are not that flexible, P-Delta effects highly affect the final capacity of the systems, as upright members are extremely vulnerable to compression forces, due to the flexural and/or the distortional buckling.

The models are 2D models and the pushover analyses use the same loading protocol with the full scale tests (triangular distribution over the height), which is very similar to the fundamental mode-shape of the system. The results from these analyses are presented for all systems from Figure 2-34 to Figure 2-40 in terms of Base Shear force vs. Top displacement. The new curves have lower initial stiffness compared to the experimental ones, due to the presence of the gravity loads due to pallet loading and consequently due to higher P-delta effects. The symmetric configurations are investigated only in one direction, while the non-symmetric configurations are investigated for loading to both horizontal directions; the two directions are differentiated by the positive and negative sign.

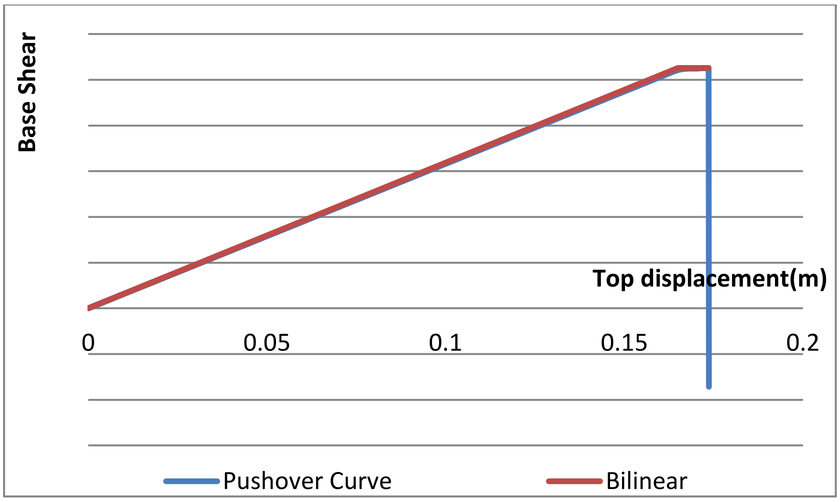

Figure 2-34 Base Shear- Top displacement diagram for IP-A

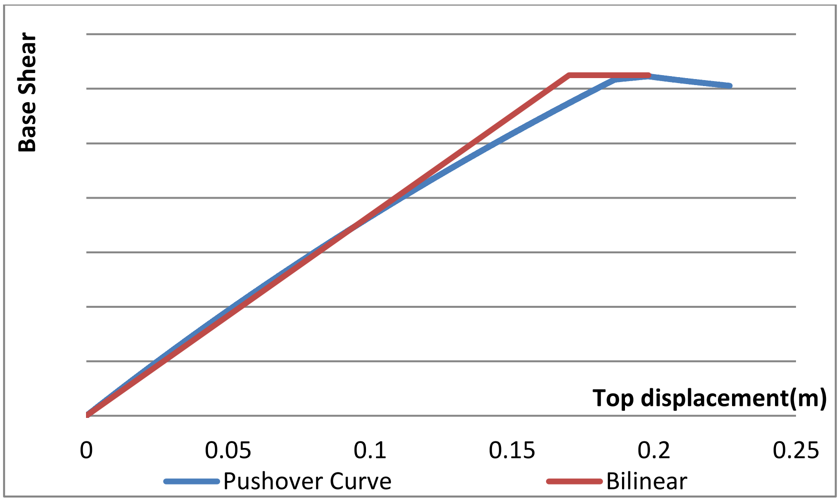

Figure 2-35 Base Shear- Top displacement diagram for IP-B

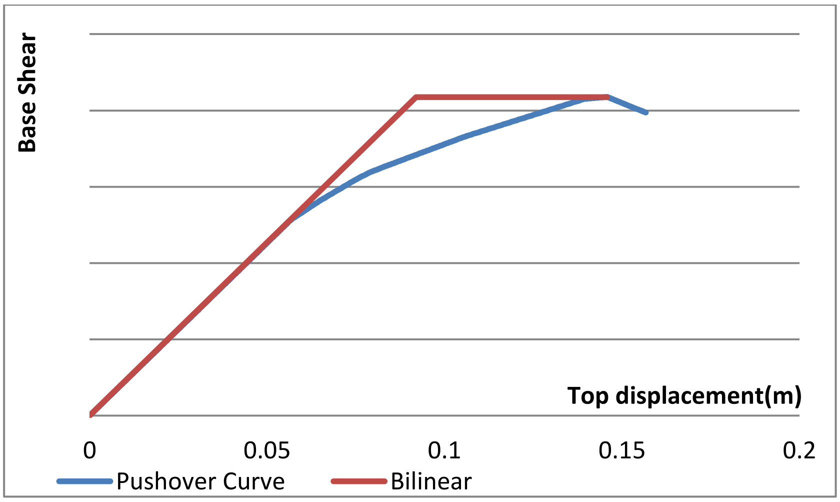

Figure 2-36 Base Shear- Top displacement diagram for IP-C-High Seismicity

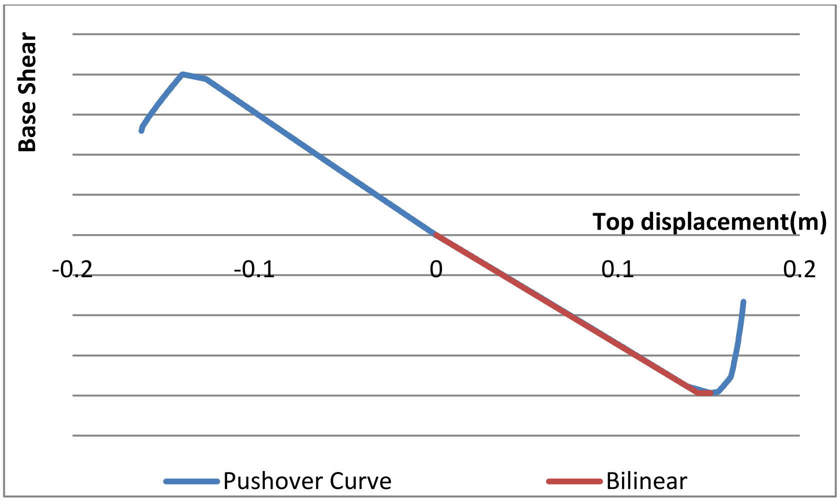

Figure 2-37 Base Shear- Top displacement diagram for IP-C-Medium Seismicity

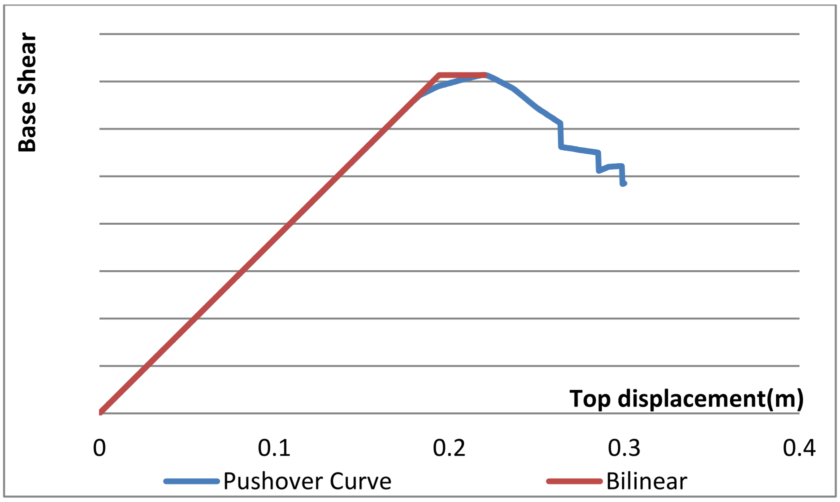

Figure 2-38 Base Shear- Top displacement diagram for IP-D-High Seismicity

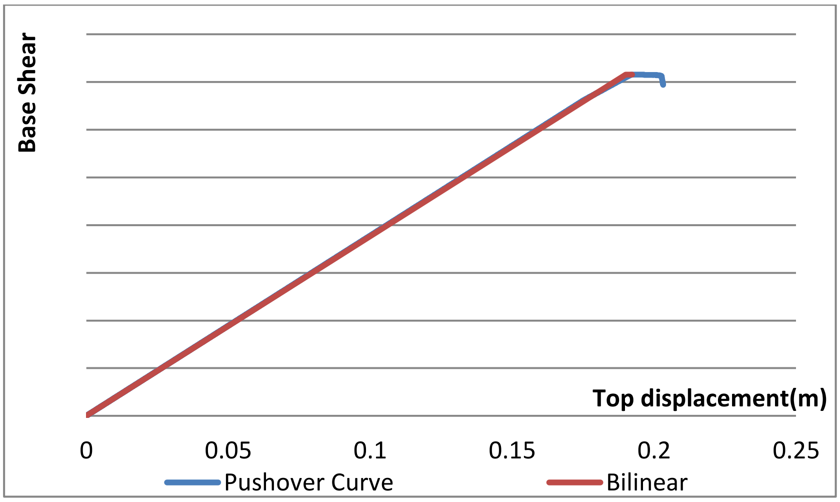

Figure 2-39 Base Shear- Top displacement diagram for IP-D-Medium Seismicity

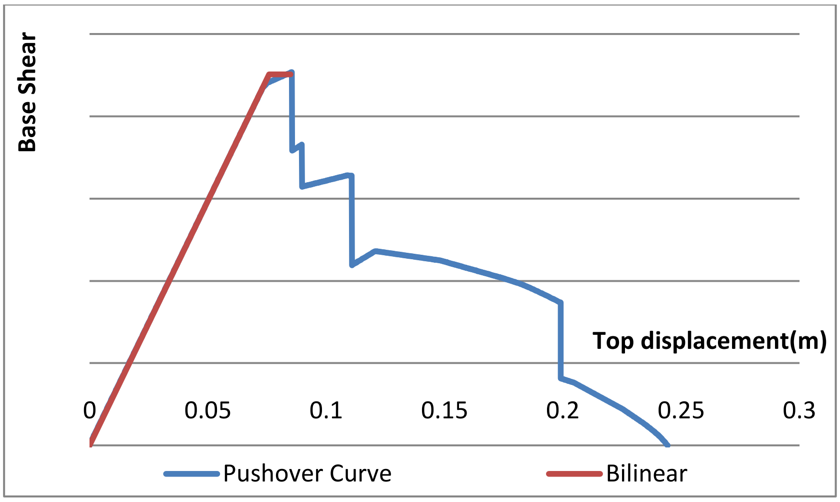

Figure 2-40 Base Shear- Top displacement diagram for IP-D-Low Seismicity

Using the definition of the behavior factor q given by Eq. (2-7) the new derived values for the upright frames are here presented. It is seen that the values differ from the corresponding ones that have been derived using the theoretical and nominal data provided by the industrial partners. Indeed, they differ in an extremely noticeable manner.

IP	Seismic Zone	q factor	Bracing type
IP A	Medium/High	1.1	X
IP B	Medium/High	1.8	D
IP C	High	2.2	X
	Low	1.1	D
IPD	High	1.2	D
	Medium	1.0	X
	Low	1.3	D

Table 2-14 Calculated q factor values for the fully loaded upright bracing systems of each IP

2.8 Conclusions

In this chapter nonlinear static pushover analyses were performed to study the seismic response of real racking systems, braced or unbraced, designed for low or high seismic zones, whose data were provided by the industrial partners of the SEISRACKS2 project. A first significant outcome is the development of procedures which should be followed to perform pushover analyses for racking systems. This includes a number of experimental and numerical investigations on isolated members and/or subassemblies. In other words, herein is specified what kind of inelasticity should be taken into account, how one could define the exact inelastic properties of each member and how one could annotate the results.

Nine configurations were investigated in order to determine their behavior factor. It was found that the usual values that are used in the everyday practice for the behavior factor are safe and sometimes conservative. However, very high values such as q=4 for braced racks in the down aisle direction, could not be verified. Moreover, the fully calibrated models to the full scale tests on single upright frames that were performed by University of Liege proved that in reality the available ductility for such systems is not that high as calculated using only numerical results and nominal material properties for the component elements. These fully calibrated models were of two different types of bracing system, X bracing and D bracing. However, there was found no indication that one system is more ductile than the other. The actual q factors as derived from the calibrated numerical results were randomly distributed.

In other words, it was shown that the numerical models, even if the partial data about their components is available, could not efficiently predict the real behavior of the system.

However, the limits of the nonlinear inelastic static analyses to the racking systems have to be noticed. Important phenomena like sliding of the pallets, the looseness of the bolted and hooked connections, etc. can be investigated with the use of nonlinear dynamic analyses.

2.9 References

1. FEMA 460: Seismic considerations for Steel Storage Racks. Federal Emergency Management Agency, 2005.
2. Uma, S. R.: Beattie Graeme: Observed performance of industrial pallet rack storage systems in the Canterbury earthquakes. Bulletin of the New Zealand Society for Earthquake Engineering, 44 (2011), No. 4, pp. 388–393.
3. Crosier, J., Hannah, M., Mukai, D.: Damage to steel storage racks in industrial buildings in the Darfield earthquake. Bulletin of the New Zealand Society for Earthquake Engineering, 43 (2010), No. 4, pp. 425–428.
4. ITSAK. (2008).“The earthquake of Achaia-Ilia 8.6.2008. Institute of Technical Seismology and Aseismic Structures, Thessaloniki, Greece.

5. Gulkan, P. and Sozen, M. A., “ In-elastic Responses of Reinforced Concrete Structures to Earthquake Motions”, Proceedings of the ACI, Vol. 71, No. 12, Dec. 1974, pp605-610
6. Saiidi M. and Sozen A.M. "Simple nonlinear analysis of rc structures", ASCE, Struct. Div., Vol. 107(ST5), pp. 937-951, 1981.
7. Menjivar M. A. L., (2004) “A Review of Existing Pushover Methods for 2-D, Reinforced Concrete Buildings”, Dissertation Thesis, University of Pavia.
8. Kranwinkler H. & Seneviratna G. D. P. K. (1998) "Pros and cons of a pushover analysis of seismic performance evaluation", Engineering Structures, vol. 20, No. 4-6, 452-464, 1998.
9. Faella G., Evaluation of the R/C Structures Seismic Response by Means of Nonlinear Static Pushover . Eleventh Word Conference on Earthquake Engineering. Paper No.1146,1996
10. Elnashai A. S. (2001). Advanced inelastic static (pushover) analysis for earthquake applications. Structural Engineering and Mechanics 12:1, 51-69.
11. Sasaki K. K, Freeman S. A, Paret T. F. Multi-mode pushover procedure (MMP) — a method to identify the effects of higher modes in a pushover analysis. Proceedings of the Sixth U.S. National Conference on Earthquake Engineering; 1998.
12. Shakeri, K., Shayanfar, M. A., and Mohebbi, M. (2008). “A spectrabased multi modal adaptive pushover procedure for seismic assessment of buildings.” *Proceedings of the 14th World Conference on Earthquake Engineering*, Beijing, China.
13. Maniatakis, C. A., Psycharis, I. N., and Spyrakos, C. C. (2013). “Effect of higher modes on the seismic response and design of moment resisting RC frame structures.” *Engineering Structures*, Vol. 56, pp. 417–430
14. Goel, R. K. and Chopra, A. K. (2005). “Role of higher-“mode” pushover analyses in seismic analysis of buildings.” *Earthquake Spectra*, Vol. 21, No. 4, pp. 1027–1041
15. Antoniou S. and Pinho R. [2004] "Advantages and limitations of adaptive and non-adaptive force-based pushover procedures," Journal of Earthquake Engineering, Vol. 8, No 4, pp. 497-522.

16. Antoniou S. and Pinho R. [2004] "Development and verification of a displacement-based adaptive pushover procedure," Journal of Earthquake Engineering, Vol. 8, No. 5, pp. 643-661.
17. Aydinoglu, M. N., 2004b. Incremental Response Spectrum Analysis (IRSA) procedure for multimode pushover including p-delta effects. Proceeding of the 13th World Conference on Earthquake Engineering, Vancouver, B.C., Canada, Paper No. 1440
18. ATC, (1996), Seismic Evaluation and Retrofit of Concrete Buildings, ATC-40, Applied Technology Council, Redwood City, California.
19. Federal Emergency Management Agency (2000). FEMA 356: Prestandard and commentary for the seismic rehabilitation of buildings, Washington, USA.
20. EN 1993, (2003). Eurocode 3: Design of Steel Structures, European Committee for Standardization, Belgium.
21. EN 1998-1-1, (2004). Eurocode 8. Earthquake resistant design of structures. Part 1-1 General rules and rules for buildings, European Committee for Standardization, Belgium.
22. FEM 10.2.02, (2001). The Design of Static Steel Pallet Racking, Federation Europeenne de la Manutention Section X, Version 1.02, England.
23. FEM 10.2.08 (2011), Recommendations for the design of static steel pallet racks in seismic conditions, Federation Europeenne de la Manutention, Version 1.04, England.
24. EN 15512, (2009). Steel static storage systems - Adjustable pallet racking systems - Principles for structural design. European Committee for Standardization, Belgium.
25. EN 16681, (2016). Steel static storage systems — Adjustable pallet racking systems — Principles for seismic design, European Committee for Standardization, Belgium.
26. RMI: Specifications for the design, testing and utilization of industrial steel storage racks. Rack Manufactures Institute, 2002.
27. AS/NZS 40841 2012. Steel storage racking, standards Australia/Standards New Zealand, Sydney, Australia.
28. CECS23:90, 1991. The Specification for design of steel storage racks. Beijing, China Association for Engineering Construction Standardization.

29. SEISRACKS (2007), Storage Racks In Seismic Areas (SEISRACKS), Research Programme of the Research Fund for Coal and Steel RTD, Final Report, May 2007
30. Castiglioni, C. A. et al. (2014). Seismic behaviour of steel storage pallet racking systems (SEISRACKS2), EUR 27583 EN, Publications Office of the European Union, Luxemburg.
31. Castiglioni, C. A. (2016). Seismic behavior of steel storage pallet racking systems, Springer International Publishing, Switzerland.
32. Castiglioni, C. A.: Seismic behavior of steel storage pallet racking systems. Structural Engineering Department of Politecnico di Milano, Milano, 2008.
33. Ayhan, D., and Schafer, B. W. (2012). Moment-rotation characterization of cold-formed steel beams, Research Report CFS-NEES, RR02, April 2012,
34. Sarawit, A. T. and Peköz, T., "Cold-formed Steel Frame and Beam-column Design", Report of a Research Project AISI-RMI, Report 03-03, 2003, pp. 330.
35. Gilbert B. P., Rasmussen K. J. R., 2009. Experimental test on steel storage rack components. Research Report No R899, School of civil engineering, The university of Sydney, Australia.
36. Baldassino N, Bernuzzi, C., Zandonini, R. (2000) Performance of joints in steel storage pallet racks. In proceedings of connections in steel structurs IV: Steel Connections in the New Mellennium, Roanoke, Virginia, USA.
37. Henriques De Sena Cardoso, F., Rasmussen, K. (2014). FE modelling of storage rack frames. Applied Mechanics and Materials, 553, 631-636.
38. Lucjan Ślęczka and Aleksander Kozłowski, "Experimental and theoretical investigations of pallet racks connections", Advanced Steel Construction Vol. 3, No. 2, pp. 607-627 (2007)
39. Computers and Structures Inc., CSI Analysis Reference Manual for SAP2000®, ETABS®, and SAFE®, Berkeley, California, USA, 2010.
40. ABAQUS. (2008). ABAQUS User's Manual. Version 6.8, Vol II, Dassault Systèmes Simulia Corp., Providence, RI, USA.
41. Teh, L. H., Hancock, G. J. & Clarke, M. J. (2004). Analysis and design of double-sided high-rise steel pallet rack frames. Journal of Structural Engineering, 130 (7), 1011-1021.

42. Freitas A. M. S., Freitas M. S. R., Souza F. T., “Analysis of steel storage rack columns”. Journal of Constructional Steel Research 61 (2005) 1135–1146
43. Ungureanu V., Dubina D., (2013). “Sensitivity to Imperfections of Perforated Pallet Rack Sections”, Mechanics and Mechanical Engineering, Vol. 17, No. 2 207–220.
44. Dubina, D.: The ECBL approach for interactive buckling of thin–walled steel members, Steel & Composite Structures, 1(1), pp. 75–96, 2011.
45. Koen D., (2008). Master of engineering: “Structural Capacity of Light Gauge Steel Storage Rack Uprights”, The University of Sidney.
46. International Building code (IBC), 2009, International Code Council, USA
47. ASCE-7-2005: Standard-Minimum Design Loads for Building and Other Structures. American Society of civil engineers, 2005.
48. Irzidinia M., Rahgozar M. A.,Mohammadrezaei O., Response modification factor for steel moment-resisting frames by different pushover analysis methods, Journal of Constructional Steel Research, Volume 79, December 2012, Pages 83–90.
49. Uang C. M., 1992. “Seismic force reduction and displacement amplification factors”, Earthquake Engineering, 10th World Conference, Rotterdam.
50. Beattie G. J., 2006. A Design Guide for High Level Storage Racking with Public Access, Paper No. 40, Proceedings 2006 NZSEE Conference, New Zealand.

3. Collapse probability and check of the behavior factor of racking systems

3.1 Introduction

Looking deeper into the new modern methods that assess the seismic performance of structures, it is noticed that the nonlinear static analysis is a conservative deterministic method. The new trend for evaluation of the seismic performance of structures is the combination of dynamic nonlinear analyses and probabilistic theories. All these are included in the frame of the Incremental Dynamic Analysis (IDA), developed by Vamvatsikos and Cornell, 2002, [1]. Based on such analyses, ATC 63 [2], after the compilation of FEMA p695 [3], proposes a process for the “Quantification of Building Seismic Performance Factors”. The proposed process is similar to, but distinct from the concept of IDA, as initially developed by Vamvatsikos and Cornell. Examples of the proposed methodology are given by Deierlein et al., [4] and Haselton et al. [5]. Following an overview of the assessment methodology, this chapter reviews specific aspects related to a) modeling collapse assessment of structures by nonlinear time-history analysis, b) development of collapse fragility curves, including uncertainties, c) ground motion characteristics with adjustment for spectral shape effects for collapse assessment, d) evaluation and acceptance criteria for archetype racking system models. The current methodology is based on the minimum design criteria proposed in ASCE/SEI 7 [6].

The principles of the new methodology have been introduced as early as 1977 by Bertero [7]. The idea of the pushover analysis for scaling the lateral loading on the structure till the collapse level passed also unforced to the dynamic analyses. Seismic loading is also scaled continuously to the response from the early elastic region to the entire collapse. This concept has been incorporated in the work of many researchers (as cited by Vamvatiskos and Cornell), among others Luco and Cornell [8], Bazzuro and Cornell [9], [10], Yun and Foutch [11], Mehanny and Deierlein [12], Dubina et al. [13], De Matteis et al. [14], Nassae and Krawinkler [15], and Phsycharis et al. [16].

3.2 Objective

The objective of this chapter is to apply the aforementioned methodology to the special steel storage pallet racking systems. The first step is to develop the so-called archetype models that reflect the general characteristic and general behavior of the systems as well as the peculiarities that affect the seismic response and the collapse capacity of such systems. Then some specific issues around the peculiarities of the racking systems are clarified and described to propose guidelines for an IDA in racking systems. The models that are investigated for that purpose are always real case studies coming from the everyday practice and designed by industrial partners according to the latest European norms, EN1998 [17], EN15512 [18] and EN16681 [19]. The final objective is to review the dynamic response and the design of these selected systems and to evaluate whether the used behavior factors' values were correctly selected or not.

3.3 Step-by-Step Methodology for Steel Storage Pallet Racks

The current methodology is summarized in the next flow chart of Figure 3-1 that presents all steps from the design procedure until the final evaluation of the seismic performance of the system. The archetype models are supposed to be well designed according to the actual norms and so the final designed systems are ready to be subjected to numerical dynamic analyses. The methodology is strongly influenced by many parameters that should be selected for each individual system.

As long as the system is already designed, the nonlinear properties of its component members should be defined as described in chapter 2. The main difference here is that the nonlinear behavior of the components should include also their behavior under cyclic loading. One should focus on the peculiarities of each member, the general experience, the literature and the experimental results that are necessary to build a reliable model that would be capable to run properly nonlinear dynamic analyses.

Subsequently, the ground motions that will be used for the numerical analyses should be selected. The selection should be appropriate to cover a big range of representative ground motions that could lead the system to collapse and could be recorded at the specific region that the rack is located to. Thus, the ground motions are depended on the initially design spectrum, namely the soil type, the peak ground acceleration of the geographical area, the spectral acceleration at the dominant time periods of the structure etc. The selection of the ground motion is a tricky part where many researchers' opinions contradict.

Finally, numerous nonlinear dynamic analyses are performed and their results are visualized, forming different diagrams that characterize the seismic response of a structure. These charts are formed by a post processing procedure whose outcome are three diagrams that each one emerges from the previous one. These diagrams are the so called IDA curves, the fractile curves and the fragility curves, which give qualitative and quantitative information about the response of the structure. If this information fulfills the performance criteria that are defined by FEMA p695, the seismic design is evaluated. Finally, this method could be converted to an assessment about the used behavior factor.

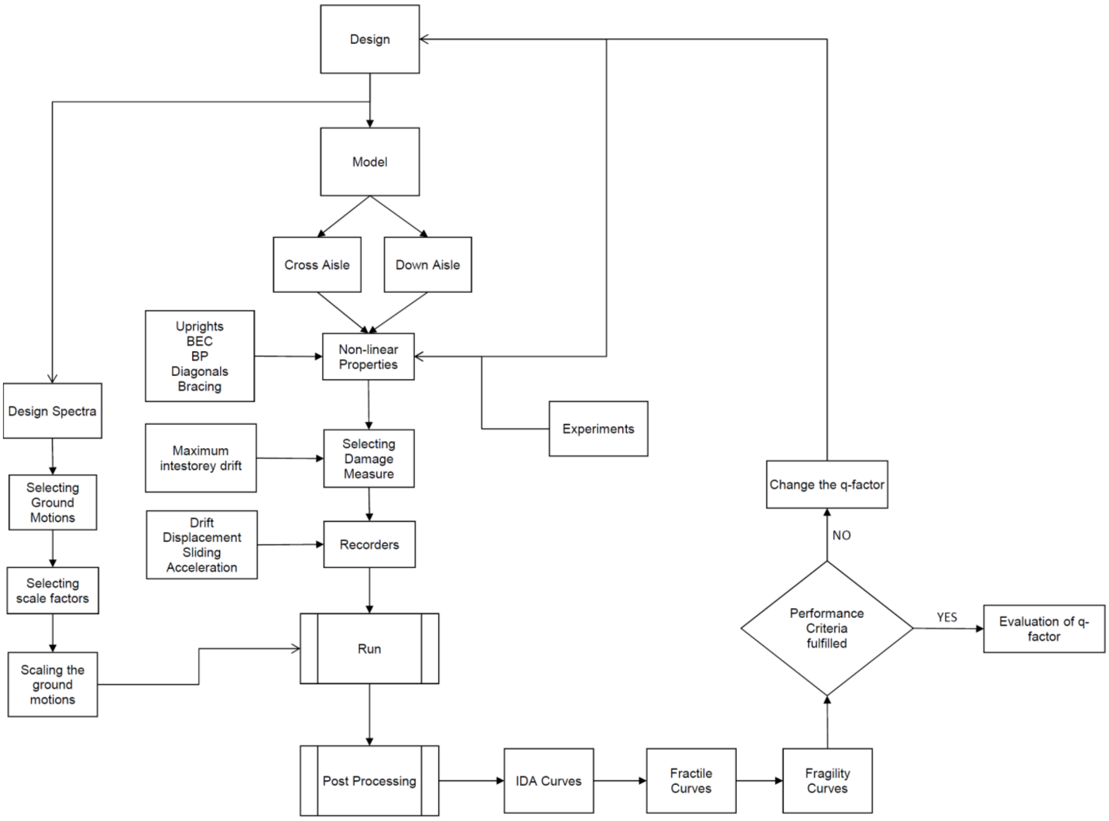

Figure 3-1 Flow chart for the application of IDA

3.4 Simulation of the investigated configurations

Since the IDA method requires numerous dynamic analyses, the use of commercial software is not appropriate, as it does not offer many capabilities for the post processing of results. Thus, the open source research software OPENSEES [20] developed initially in Berkeley University and subsequently widely implemented in researches appears as the most suitable. In this thesis pre- and post-processing took place using self-developed tools in MATLAB that did the calculations rapidly, providing automatic visual results. Moreover, the components of the racking systems present very special hysteretic phenomena that may not easily be taken into account with the conventional hysteretic models included in commercial software packages.

The examined configurations are two unbraced racking systems in down aisle direction and four single upright frames in the cross aisle direction. The examined models in the down aisle direction are based on the calibrated models; however they consist of 6 bays and 4 levels and are identical to the configurations of previous chapter 2. The reason that only two models are examined in the down aisle direction is that the other unbraced racks did not exhibit experimentally any ductility and additionally are extremely flexible (more than 4s dominant first period), a fact that is approaching the limit of the method's applicability. In the cross aisle direction the systems were examined that exploited a minimum level of ductility according to the experimental results and the nonlinear static analyses of the previous chapter. There are two types of bracing systems for the upright frames; the X and the D bracing type; two configurations of each type are included in the examined ones. The braced models in down aisle direction were not included in this study due to the fact that they request 3D models in order to consider also their torsional behavior. The application of the method to racking systems is in a preliminary level, and so the complexity of the 3D models was considered a parameter that would give no reliable results.

3.4.1 Numerical models

The developed models were composed of beam, truss and link elements. In particular, the exact position of each element is depicted in Figure 3-2. For the down and the cross aisle direction, beam elements are shown with black lines, truss elements with red and link elements with purple.

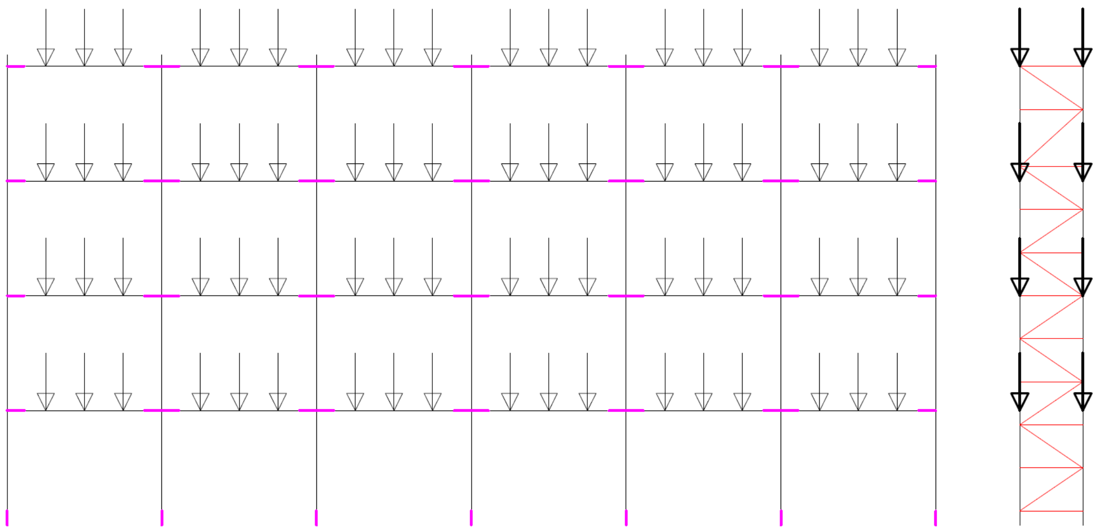

Figure 3-2 Simulated topology with different types of elements

Based on the results of chapter 2 that describes how the potential inelasticity sources of the system can be simulated, structural elements of the system are represented as following:

- Pallet Beams: Elastic beam elements
- Uprights: Nonlinear beam elements (defined by Hysteretic Material)
- Diagonals: Nonlinear truss Elements
- Beam-End-Connectors: nonlinear two-node Link Elements (defined by Hysteretic Material)
- Base plates: nonlinear two-node Link Elements (defined by Hysteretic Material)

Vertical loading of the system is introduced as concentrated loads and masses. For the models in down aisle direction these are applied to 3 points along the pallet beams; each point represents the middle of a pallet, on an assumption of three pallets/ compartment. For the models in cross aisle direction the masses/loads are applied on the joints of the uprights that are on the level of the pallet beams. In this case, the imposed masses correspond to the loads that are resulted by two consecutive fully loaded compartments, on the in-between upright frame, see Figure 3-2.

The elastic and inelastic behavior of the potential nonlinear elements is introduced by application of the *Hysteretic Material* provided in the Opensees library. This material is used to construct a uniaxial multilinear hysteretic material object with pinching of force and deformation, damage due to ductility and energy dissipation, and degraded unloading stiffness based on ductility. All these special phenomena are presented in racking systems and this is another reason that Opensees was preferred against other software packages. Each element is characterized by the skeleton curve and the hysteretic parameters, as they are presented in Appendix A for all industrial partners.

3.4.2 Damping Ratio

The last parameter that has to be fixed before the IDA performance is the damping parameter. A lot of questions arise about this parameter, e.g. how large is the equivalent damping ratio, how it is taken into account, etc. The peculiar connections of racks, the merchandize goods, the potential sliding of the pallets over the pallet beams and numerous other parameters, led Chen et al.(1980) [21], [22] to perform experiments on real racks in the shaking table of the Berkeley University. The outcome was that for these specific systems the damping ratio was on average 5.7% of the critical for the down aisle direction and just 1.3% of the corresponding critical for the cross aisle direction. Similar conclusion extracted Brown (1983) [23] and Filiatrault and Wanitkorku (2004) [24] also by shaking table tests. However, the European codes propose a value of 3% for the damping ratio, similar to bolted steel structures. Thus, this value was considered for the present models for both directions using the Rayleigh damping model [25]. This provided a source of energy dissipation in the nonlinear dynamic analyses that required for the IDA. The Rayleigh damping in a finite element model consists of a mass-proportional and a stiffness-proportional part, given by Eq. (3- 1).

$$[C] = a_M \cdot [M] + a_K \cdot [K] \tag{3- 1}$$

where a_M and a_K are constants with units of s^{-1} and s, respectively, and [K] is the linear stiffness matrix of the structure derived from the initial tangent stiffness of the structure. The misuse of this damping encounters many problems, as Hall (2005) [26] pointed out.

Thus, the matrix [C] consists of a mass-proportional term and a stiffness-proportional term.

The factors a_M and a_K are defined using appropriate values of damping for the dominant eigenmodes of the linear system. Damping of a mode *i* is quantified by the damping ratio ξ_i; the ratio of the mode's damping to the critical value [27]. If a_M and a_K are known, ξ_i can be found from Eq. (3- 2) and vice versa.

$$\xi_i = \frac{1}{2\omega_i} a_M + \frac{\omega_i}{2} a_K \qquad \textbf{(3- 2)}$$

The inverse procedure is followed to estimate the factors a_M and a_K. The damping factor for the first and second significant modes have been fixed to 3%, and so with the expressions of ξ_1 and ξ_2 one could define the values of these factors; where ω_i is the natural frequency (rad/s) of mode *i*. Thus, a_M and a_K can be set to give any damping ratio to any two modes. Other modes will receive default amounts of damping that can be computed directly from Eq. (3- 2).

3.4.3 Selection of ground motions

The selection of the ground motion to perform the IDA is of major importance. An extensive comparison of the different methods of selection is made by Katsanos et al. [28]. Since the present thesis is one of the first attempts to apply IDA to racking systems, it would be considered more reasonable not to complicate the whole undertaking. Thus, the selected ground motions are those proposed by ATC-63, as the set for Far Field Ground Motions. This set includes the accelerograms of 22 earthquake events. Each earthquake is described by two different accelerograms in the two different horizontal directions, recorded at the same station. Accordingly the total used ground motions are 44, which is considered a sufficient large number with checked variability and reliability. This specific set of ground motions conforms to some specific criteria regarding the seismic characteristics of the seismic events [29]. These are summarized as:

- Moment magnitude greater than 6.5
- Source to site distance greater than 10km
- PGA>0.2g and PGV>15cm/sec
- Soil shear wave velocity in upper 30m of soil greater than 180m/s. Note that all the selected records are on C or D site (according to the ATC norm).
- Limit of two records from single seismic even

- Lower bound of useable frequency range less than 0.25Hz in order to ensure that the low frequency content was not removed by the ground motion filtering procedure.
- Strike slip and thrust faults.
- No consideration of spectra shape
- No consideration of station housing, but PEER-NGA records were selected to generally be "free-field".

As FEMA p695 says, this ground motion record set includes a sufficient number of records to permit evaluation of record-to-record (RTR) variability and calculation of median collapse intensity. Large-magnitude events dominate collapse risk and generally have longer durations of shaking, which is important for collapse evaluation of nonlinear degrading models.

The primary function of the Far-Field record set is to provide a fully-defined set of records for use in a consistent manner to evaluate collapse across all applicable Seismic Design Categories located in any seismic region and founded on any soil site classification. Actual earthquake records are used, in contrast to artificial or synthetic records, to address a regional variation of ground motions.

Due to the limited number of very large earthquakes and the frequency ranges of ground motion recording devices, the ground motion record sets are primarily intended for buildings with natural (first-mode) periods less than or equal to 4 seconds. Thus, the record set is not necessarily appropriate for tall buildings or too flexible structures with fundamental periods of vibration greater than 4 seconds.

Baker and Cornell (2006) [30] have noted that rare ground motions in the Western United States, such as those corresponding to the MCE, have a distinctive spectral shape that differs from the shape of the design spectrum used for structural design in ASCE/SEI 7-05. In essence, the shape of the spectrum of rare ground motions is peaked at the period of interest, and drops off more rapidly (and has less energy) at periods that are longer or shorter than the period of interest. Where ground motion intensities are defined based on the spectral acceleration at the first-mode period of a structure and where structures have sufficient ductility to inelastically soften into longer periods of vibration, this peaked spectral shape and more rapid drop at other periods causes rare records to be less damaging than would otherwise be expected based on the shape of the standard design spectrum. The most direct approach to account for spectral shape would be to select a unique set of ground motions that have the appropriate shape for each site, hazard level, and structural period of interest. This, however, is not feasible in a generalized procedure for assessing the collapse performance of a class of structures with a range of possible configurations, located in different geographic regions, with different soil site classifications. To remove this conservative bias, simplified spectral shape factors, SSF, are used instead.

The selected ground motions are used in their original form as well as in a scaled down or scaled up form. According to Haselton et al. [29], the ground motion set is independent from the scaling procedure and, thus, any scaling method is applicable. The method that is applied to this set follows the proposal by Kircher [31]. For reasons of completeness, it should be cited the proposals of Ye and Wang [32] about the methods of matching the selected ground motions, keeping at the same time the proper energy content.

The spectra of the 44 used ground motions are shown in Figure 3-3; these are derived from the original ground motions and for statistical reasons are no matched to the specific design spectra of the different systems in order not to eliminate the original motions’ characteristics. Three typical design spectra for high, medium and low seismic zones are included also in this figure (in black) to compare visually the intensity of the selected ground motions with the expected ones by the norm. It is seen that the mean spectra of the 44 ground motions are over the design spectra; however, there are several cases where the spectral acceleration of an individual ground motion for a specific period of the structure remains below the design spectra.

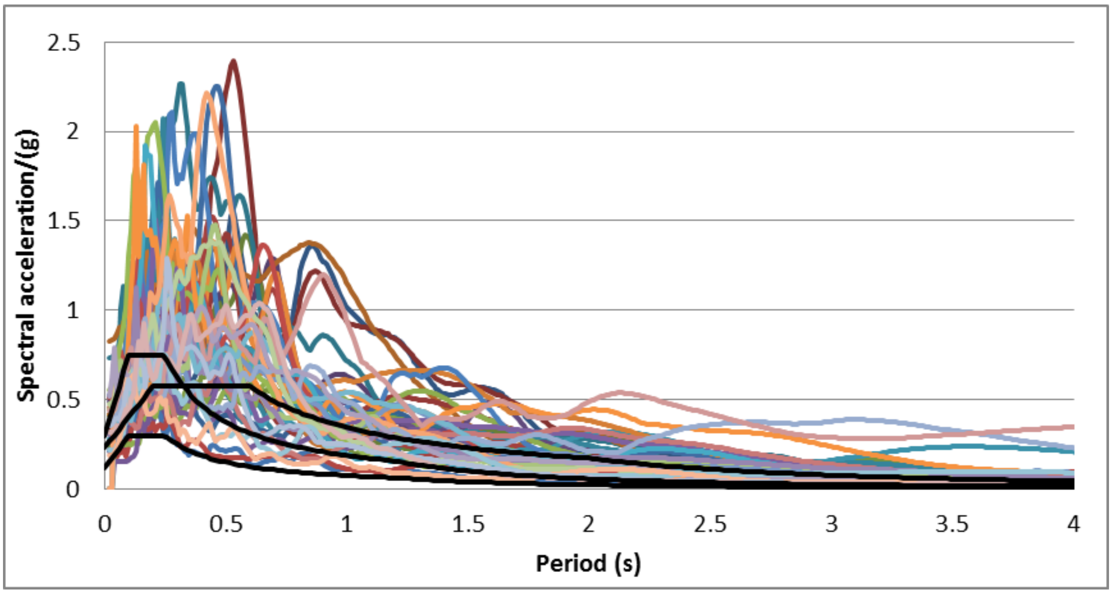

Figure 3-3 Elastic Spectra for the 44 ground motions (colored) and some indicative EC8 design spectra (black) for low and high seismic zones

3.4.4 Post-processing

Post processing is called the procedure, which one edits the recorded results with and builds the results in a visual-graphical form. The final presented results are the IDA-Curves, the fractile-curves and the fragility curves. The first ones are presented in a diagram with 44 different lines, where each line represents the response of the structure against one specific ground motion. The points of each line depict the maximum developed damage measure (EDP) (here, interstorey drift among the 4 levels) of each rack for a specific level of the intensity measure (IM) (here, the spectral acceleration $S_a(T_1)$). Thereafter, the fractile curves figure out the percentile response of the structure. The selected percentile curves are referred to the 16, 50 and 84%. The meaning of these curves is that each point of a percentile curve, with coordinates (EDP, IM), indicates that for a specific value of IM the structure developed at least the corresponding value of the EDP for the given percentage of the ground motions. The last step is the calculation of the Fragility curve. This curve indicates the cumulative probability of collapse of the structure for any likely value of the IM and is formed by points of IM vs. a given probability of collapse. This probability is estimated counting the number of the presented flatlines for any level of IM, out of 44 (the 44 different ground motions). The fragility curve was confirmed to follow the analytical lognormal distribution.

3.4.5 Intensity and Damage Measure

The different results of IDA used the terms of IM vs. DM. The exact definition of IM and DM is given by Vamvatsikos and Cornell [33]. The DM parameter is also known as EDP meaning Engineering Demand Parameter and is used here.

A review for the different possible IM that one could select to representatively describe the behavior of a system is made by authors of the University of Pavia in the research program SYNER-G [34]. Steel storage racking systems are however not included in this document and thus, the spectral acceleration $S_a(T_1)$ commonly used for conventional building structures is selected as a representative IM.

The selected EDP in that case is the maximum interstorey drift among the 4 levels of the rack. In conventional building structures the EDP is an objective or subjective criterion of response. Modern norms have introduced limit states for the response of structures, like the Immediate Occupancy, Life Safety and Collapse Prevention limit states. These are determined as a restriction on the maximum allowable value of the interstorey drift (i.e. for flexure critical columns in EC8 the maximum allowable interstorey drift is for IO 0.66%, for LF 2.17% and for CP 2.89%), The sources of these limits are not always static, but also constructional, aesthetic or architectural. In case of racks, there are not yet such limits. Thus, the only rational limit state is the collapse prevention. This is translated into prevention of falling of the pallet, breaking of the hooks of the beam-end-connectors (resulting in the falling of the beams), buckling (global, torsional, distortional, etc.) of the uprights, etc.

It is apparent that all these limit states are either simulated in a numerical model or are included in the so-called non-simulated collapse mechanisms. The first are directly detected by the software during nonlinear dynamic analyses; the latter should be introduced sometimes even manually to the final results. In the present study there are two different simulated damages; the dynamic instability and the maximum allowable rotation of the beam-end connectors, in case that the experiments of the provided components showed such a limit, due to the breaking off of the beam-end-connectors that subsequently resulted in fall of the pallet beams.

Furthermore, there is also a very significant collapse mechanism that conventionally is assigned to the non-simulated damages, namely sliding of the pallets. The fact that the pallets lie on the pallet beams results in an interaction between the rack and the pallets. In case that the pallets are fixed on the pallet-beams with the use of special clips, this interaction could be neglected. In any other case, it should be investigated.

3.4.6 Interaction Pallets - Structure

It is believed that the interaction between pallets and pallet beams might influence significantly the behavior of the whole rack. However, Gilbert et al., (2011) showed that the numerical simulation of that interaction does not affect the final design of the system in cross aisle direction [35], while it does slightly influence the design in down aisle direction (about 4%) [36]. This conclusion is true under certain circumstances that the friction coefficient between pallets and pallet beams of a drive-in racking system is sufficient not to let the pallet free to slide. However, in case of conventional racking systems the friction coefficient is not always high enough to protect the pallets from sliding. As far as the seismic response of a racking system is concerned, sliding could affect it changing the dynamic characteristics and subsequently the final response of the system. In particular, the aforementioned potential sliding of pallets could result in the fall of the pallets and damage of the rack, or injury of people that are moving in the surrounding area. Previous seismic events and rack-collapses showed that the fall of pallets is dangerous mostly for the cross aisle direction. In the down aisle direction, the pallets could slide, move and change position without falling down and without changing that much the inertial masses and properties of the system. Thus, here it is preferred to neglect sliding of pallets in the down aisle direction. However, in the cross aisle direction the overhang of the pallets amounts to about 5cm outside the pallet beams and there are not enough margins for the pallet to slide over. Moreover, friction forces between pallets and pallet beams develop and transmit the seismic forces from the pallets center of mass to the racking system and they might be a source of energy absorption, especially when the pallets slide, intervening in the total damping of the system.

3.4.7 Non Simulated sliding Criterion (NSC)

There are two different methods for simulating the aforementioned interaction (friction-sliding). The first one has no numerical impact, as it does not include directly this interaction in the simulation; thus it is named Non Simulated Criterion (NSC). The procedure is as follows: The acceleration at each pallet-level is recorded together with the displacement of each level and the reaction forces. Then, with the post-processing procedure the recorded (absolute) acceleration is compared to the theoretical acceleration that causes sliding of the pallet. This acceleration is mentioned by numerous researchers, among others, Degee and Denoel [37], and apparently by the norm EN16681. In particular, the sliding criterion is fulfilled when $acc_i > \mu \cdot g$ that would mean that the pallet slides instantaneously; however this is not translated directly to the fall of the pallet. It is very likely, that the pallet starts to slide over the pallet beams and then it sticks again. Without the direct simulation of the pallet it is not possible to quantify the range of the sliding and as a result to figure a realistic failure criterion. Thus, conservatively, it is considered that when the acceleration exceeds the value of the sliding acceleration ($\mu \cdot g$), this is automatically a collapse point and so an infinite value is given to the EDP, for the current ground motion and scale factor. Graphically, the check of this criterion is illustrated in Figure 3-4. The different colored lines are the real-time recorded acceleration of each level for a specific ground motion and different scale factors. The horizontal black lines show the non-simulated limit state, for “static” sliding. Although, most of the lines remain between the upper and lower limit, there are recorded accelerations to some levels of the rack that indicate sliding of the pallet as the scale factor is increasing. The ground motion and the scale factor that result in sliding of the pallet are recorded and in that case the initial IDA curve of this ground motion is modified manually, introducing an artificial flatline after the supposed sliding point. This modification is presented for one ground motion in Figure 3-5. The initial line is highlighted as “Original” and the modified one as “NSC”.

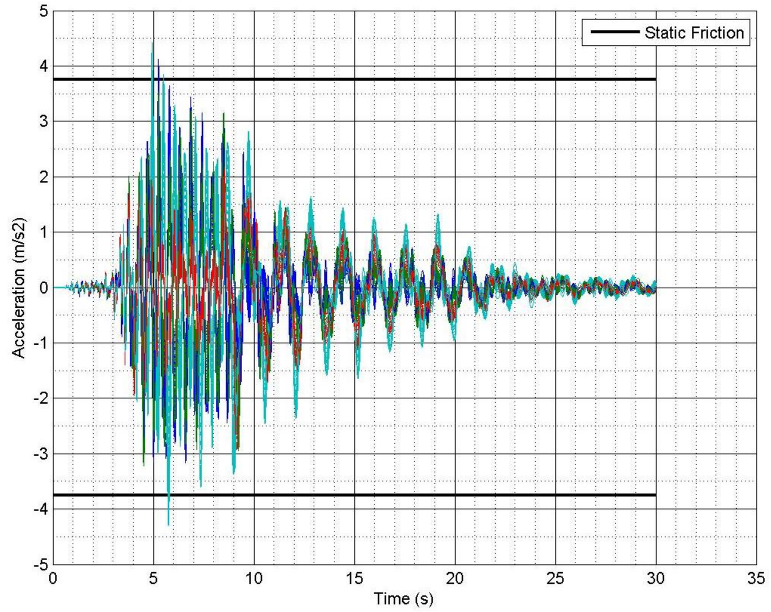

Figure 3-4 Recorded acceleration to different levels of the structure for different scale factors of a typical ground motion

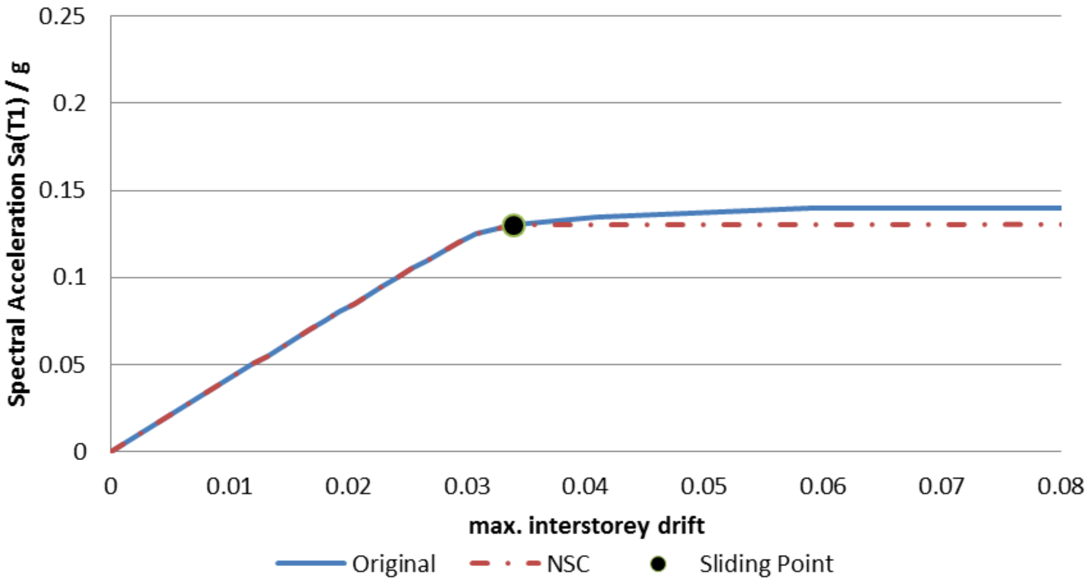

Figure 3-5 Typical IDA-curve with and without the NSC of the sliding effect

Although this procedure that considers the sliding effect with a non-simulated manner is numerically fast, this could not be considered reliable enough. The criterion is extremely conservative and the incremental dynamic analyses with scaled imposed ground motions are not always compatible to this criterion. In case that the imposed spectral acceleration is higher than the sliding acceleration, the dynamic analyses above the corresponding scale factor are commonly senseless and the current criterion invalidates the whole method anymore. Thus, this method is not here applied, but only stated for the sake of completeness.

3.4.8 Simulated sliding Criterion (SL)

Improving the numerical models for a more reliable analysis, the pallets are simulated as a practically rigid frame (numerically extreme high stiffness values). This is the second more detailed and promising method that has been roughly presented by Adamakos et al. [38]. The masses are positioned in the corners of this rigid-frame and rest on bearing elements provided by Opensees software (Flat slider bearing element). What is important for a proper simulation of the friction is to assign appropriate values to all the different parameters. The slider elements follow the Coulomb friction model which is defined by the initial shear stiffness, the friction coefficient, the down- and upward (axial) stiffness and the bending stiffness as presented schematically with the corresponding parameters in Figure 3-6. In the following presented models the initial shear stiffness and the axial stiffness are numerically infinite, the bending stiffness numerically zero and the friction coefficient equal 0.375 that is a typical value.

The bearing element should take into account, that the pallets are likely to overturn (rocking effect). This means that one foot of the pallet moves away from the pallet beam with regard to the gravity direction; thus when the pallet stays on the air has no contact with the structure and as a result the axial stiffness becomes zero. This could be better approached using a compression-only material; however against the numerical cost of such a model a conventional one was used, introducing the need to check whether the vertical reactions of the pallets on the beams remain always against the gravity direction. Such a graphical check is presented in Figure 3-7.

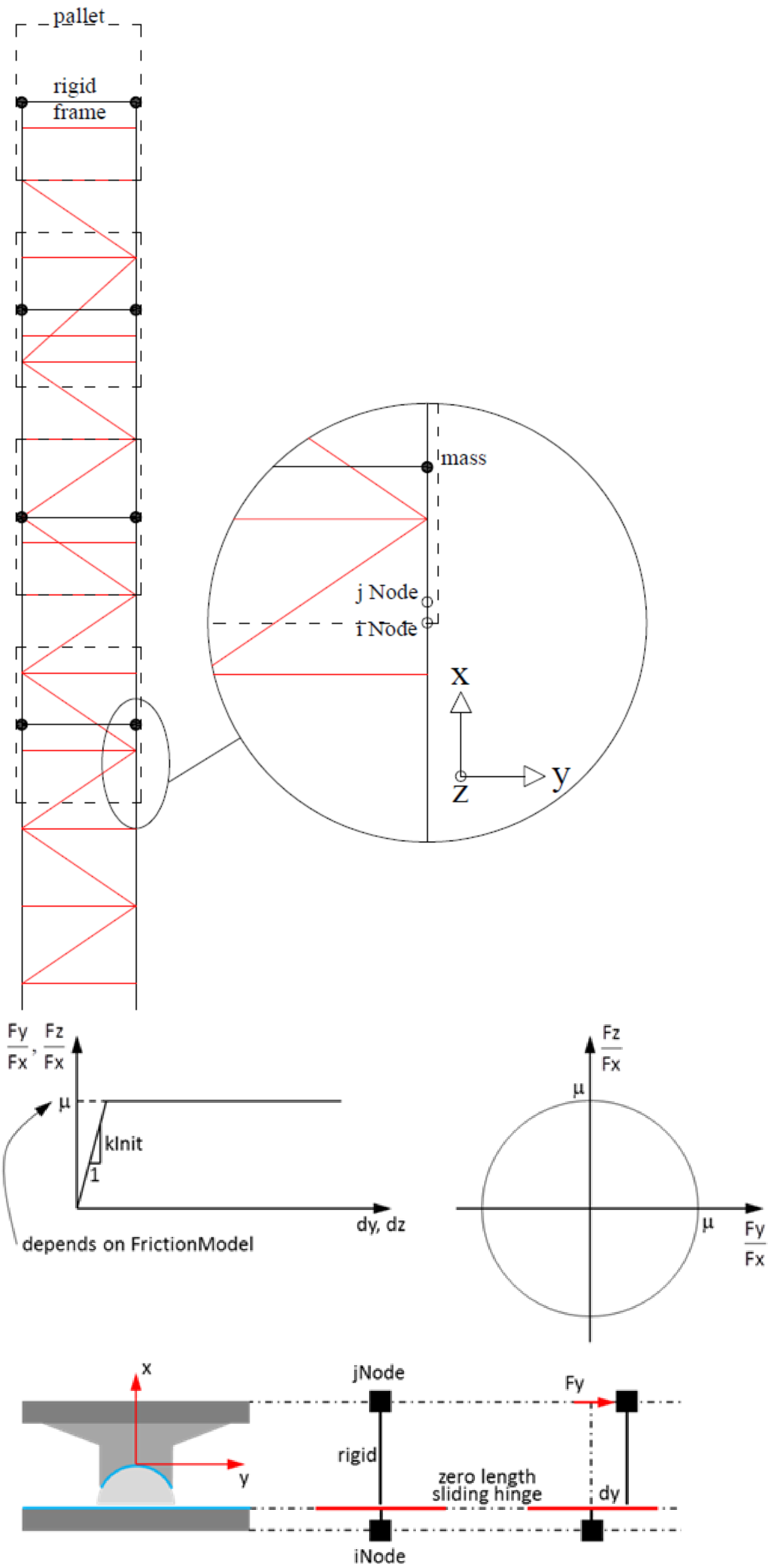

Figure 3-6 Upright Frame model and detail of Bearing (Flat Slider Bearing) Element of Opensees software

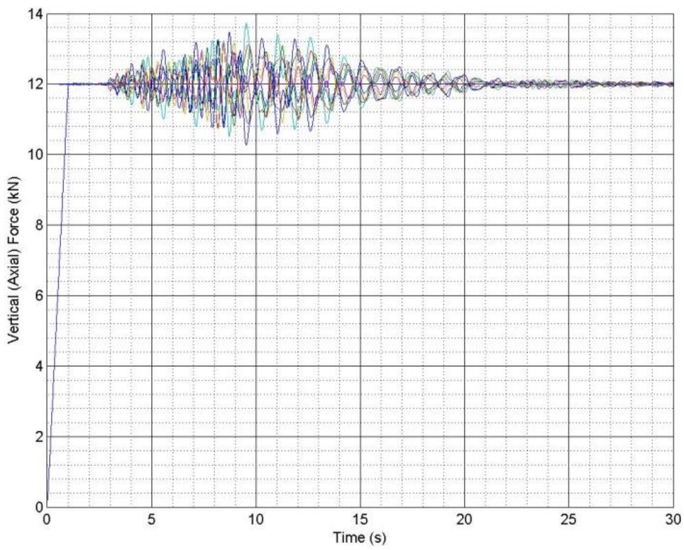

Figure 3-7 Recorded vertical reaction of a simulated pallet on the pallet beam

The vertical force is 12kN due to the self-weight of the pallets and it oscillates, since the inertial seismic forces that are applied to the center of mass of the pallets are eccentrically introduced. The aforementioned eccentricity is taken into account by adjusting the height of the pallet's sub-model to the center of mass of the merchandized goods. Here, the selected value of the eccentricity is 75cm that corresponds to a pallet of 1.5m height with uniform weight. It should be noted here that for any case (any ground motions and any scale factor) the vertical force (similar to those presented in Figure 3-7) did not exceed the zero line that would mean that the pallet does not overturn. In an opposite case, an artificial flatline would be sketched (by post-processing), since it is considered as a possible collapse mechanism of the system.

Supposing that no overturning occurs and that the analysis is performed till the end of the earthquake event, the final check that has to be done is that of sliding. The bearing element is able to slide and this potential sliding is recorded during the time of the ground motion. The advantage of this model is that the pallet is able to slide over the pallet beams without discarding directly the dynamic response of the system for this analysis (this specific ground motion and scale factor). Instead, a check is provided in order to measure whether the likely sliding of the pallet has exceeded the overhang of the pallet or not. If yes, it means that the pallet falls down and the system has been practically and/or structurally collapsed. Figure 3-8 depicts such a graphical check for the range of sliding. The lines shown in the diagram correspond to all different bearing elements of the four levels, for different scale factors of a typical ground motion. It is here observed that there is indeed sliding of a pallet, however its magnitude (relative displacement between the two nodes of the bearing element) is only 0.17mm, much less than the 50mm that is a typical limit for a Europallet and the specific geometry of the provided configurations. These 50mm have been derived from the fact that the Europallet is 1200mm wide, while the pallet beams are in a distance of 1100cm. Of course such a complicated and multiparametric model is sensitive to the actual parameters of a specific system. In case of a narrower or wider rack or in case of different pallet types (with another friction coefficient, or dimensions) the criteria as well as the results may change.

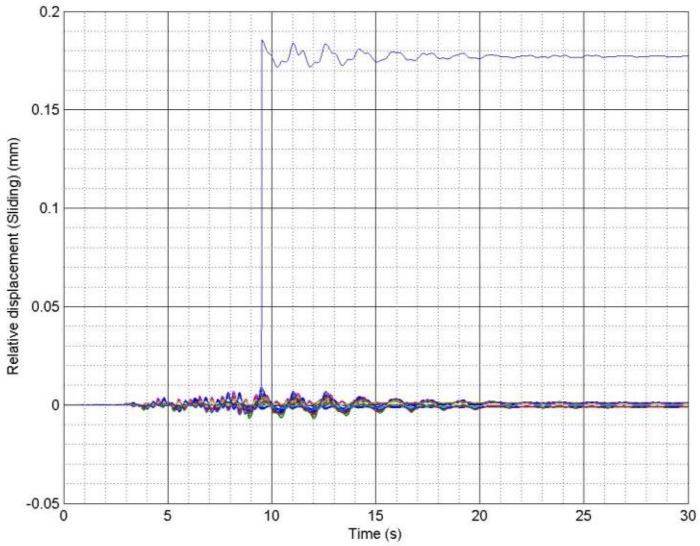

Figure 3-8 Relative displacement (sliding) of a simulated pallet

3.4.9 Performance Criteria

After all the previously described processes, the results of IDA can be built. These results are referred to the IDA- curves, the fractile curves and the fragility curves. From these diagrams, significant parameters of the methodology are calculated. The objective is to define the structure’s collapse margin ratio (CMR) that is defined as:

$$CMR=S_{CT}/S_{MT} \qquad \textbf{(3- 3)}$$

where :

S_{CT} is the spectral acceleration which corresponds to a probability of collapse 50% and it is actually the level of IM which the 50% fractile curve presents its flatline for.

S_{MT} is the spectral acceleration that corresponds to the maximum considered earthquake (MCE) given in FEMA p695 by:

$$S_{MT}=S_{M1}/T_1, \qquad \text{if } T_1>T_s$$
$$S_{MT}= S_{MS}, \qquad \text{if } T_1<T_s, \tag{3- 4}$$

where:

T_1 is the fundamental period

S_{M1} is the elastic acceleration of the MCE for 1sec in the elastic design spectrum

T_s is the transition period and

S_{MS} is the acceleration of the MCE at the region of the constant accelerations.

According to FEMA p695 and ASCE 07-05 the maximum considered earthquake is 1.5 times the design level earthquake, namely the elastic design spectrum. In Europe, where Eurocode 8 is applied, this simplified value of 1.5 is not applicable.

Considering that the MCE is defined as the earthquake that has 2% probability of exceedance in 50 years, the mean annual frequency of exceedance (MAF) is given as:

$$\lambda= \text{MAF}=k_0 S_a^{-K_1} \tag{3- 5}$$

where:

k_0 and K_1 are factors that depend on the geographic region of interest and its seismicity.

If one applies the Eq.(3- 5) for both the MCE and DLE (design level earthquake) and divide the two expressions, it results in the next relation:

$$\frac{\lambda_{10\%-50years}}{\lambda_{2\%-50years}}=\frac{S_{a,DLE}^{-K_1}}{S_{a,MCE}^{-K_1}} \tag{3- 6}$$

The MAF is 0.0021 for probability of 10% and 0.000404 for probability 2% in 50 years. Thus, the ratio of MAF for MCE over the one for DLE is constant and equal to 0.0021/0.000404=5.215. Finally, considering the generally proposed in Eurocode value, K_1=3 (Medium Seismic Zone), the ratio is given as:

$$\frac{S_{a,MCE}}{S_{a,DLE}}=\sqrt[K_1]{5.125}=1.73 \tag{3- 7}$$

Next, the estimated CMR is modified in order to take into account the spectral shape of any ground motion, using the parameter SSF, which is a tabulated parameter given in FEMA p695. Then, the Adjusted Collapse Margin Ratio (ACMR) is calculated as:

$$ACMR = SSF \cdot CMR \tag{3- 8}$$

Subsequently, the performance-criteria that are used to evaluate the seismic response of an archetype or a performance group (a group that includes many similar and representative archetype models) are checked. This is the final step of the procedure described in the flow chart that was presented in Figure 3-1. These performance criteria are presented extensively in FEMA p695, with all the possible parameters and exceptions of any investigated system and they are fulfilled, if:

- The probability of collapse for MCE ground motion is approximately 10% or less, on average across a performance group.
- The probability of collapse for MCE ground motion is approximately 20% or less, for each index archetype within the performance group
- The average value of the adjusted collapse margin ratio for each performance group exceeds $ACMR_{10\%}$
- Individual values of adjusted collapse margin ratio for each index archetype within a performance group exceed $ACMR_{20\%}$

If the above criteria, individually, or on average for a performance group, are fulfilled the performance of the racking system is acceptable and therefore the q factor, used during the design procedure is deemed to be appropriate. The appropriate values of $ACMR_{i\%}$ are given in a tabulated format in FEMA p695, based on a total uncertainty β_{TOT}. The definition of this total system's collapse uncertainty is given as:

$$\beta_{TOT} = \sqrt{\beta_{RTR}^2 + \beta_{DR}^2 + \beta_{TD}^2 + \beta_{MDL}^2} \tag{3- 9}$$

where:

β_{RTR} is the record-to-record collapse uncertainty
β_{DR} is the design requirements collapse uncertainty
β_{TD} is the test-data related collapse uncertainty and
β_{MDL} is the modelling related collapse uncertainty.

3.5 Results

In this paragraph the graphical results of the performed IDA are presented. These results are presented for the down aisle and the cross aisle direction separately. For the cross aisle direction the results are presented twice; once for the original models and once for the modified models that include the simulated pallet-sub-model as described in section 3.4.8. The results always display three diagrams: the IDA-curves, the fractile curves and the fragility curves for each model with respect to the industrial partner (IP).

3.5.1 Down aisle direction

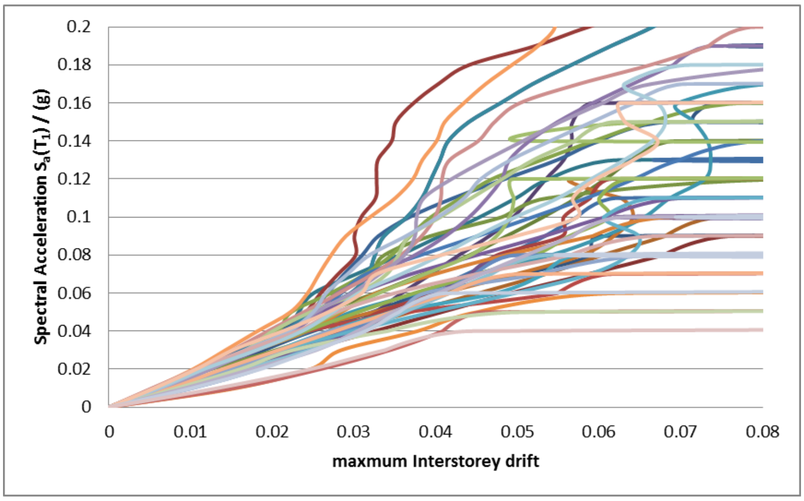

Figure 3-9 IDA Curves for IP-A

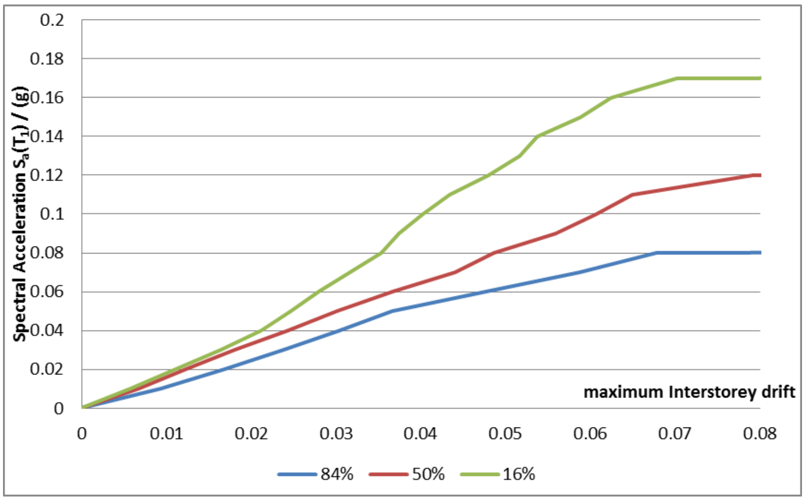

Figure 3-10 Fractile Curves for IP-A

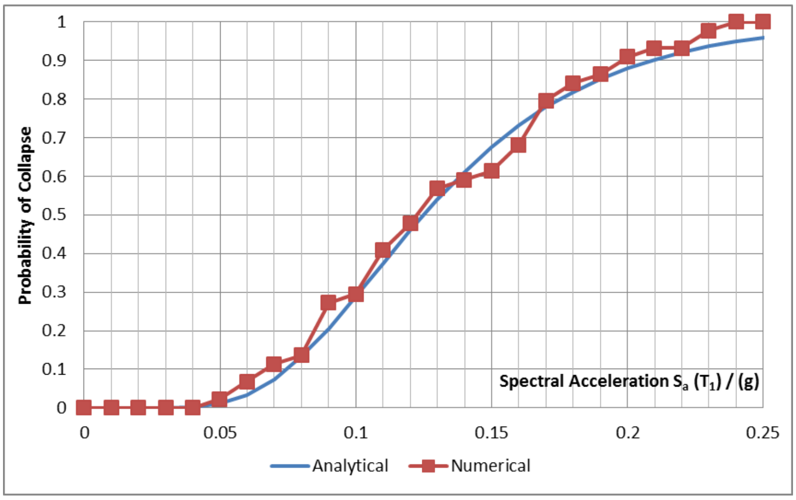

Figure 3-11 Fragility Curve for IP-A

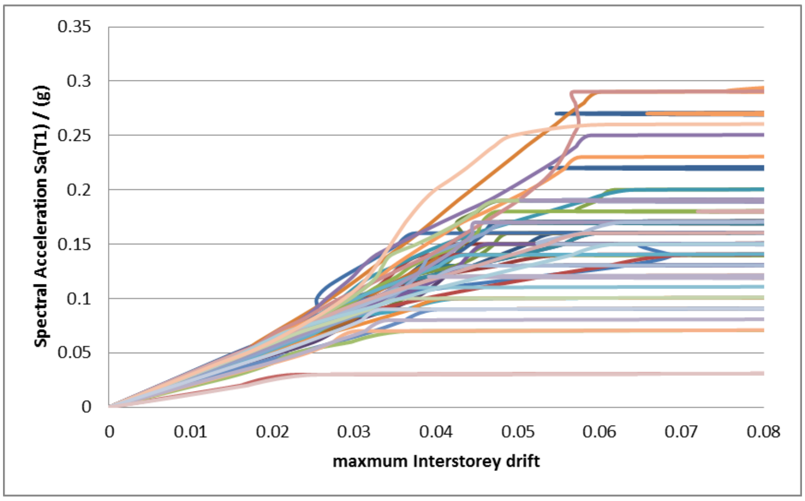

Figure 3- 1 IDA Curves for IP-B

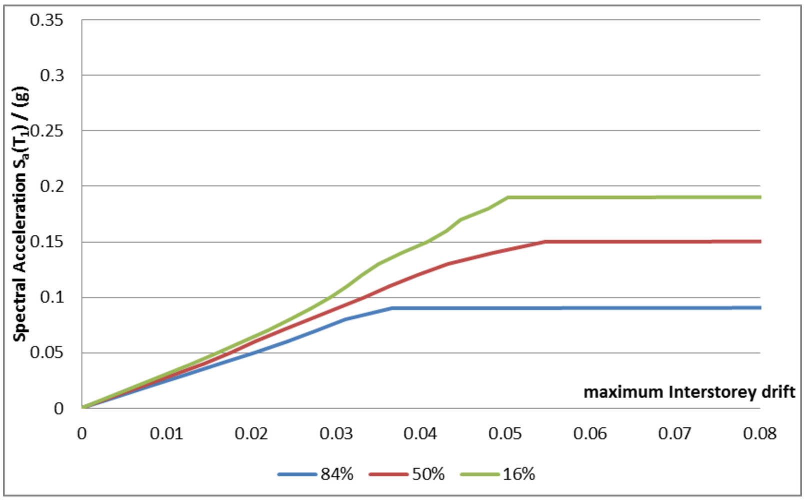

Figure 3-12 Fractile Curves for IP-B

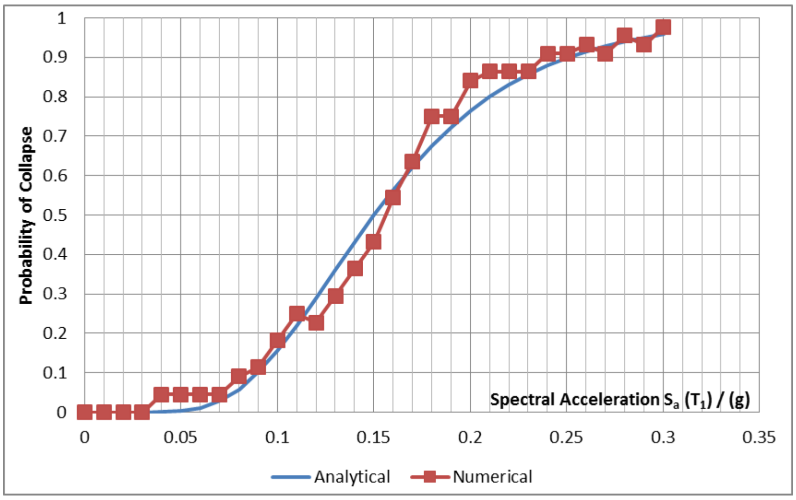

Figure 3-13 Fragility Curve for IP-B

3.5.2 Cross aisle direction

In this paragraph the results that concern the cross aisle direction are designated as "No explicit sliding" for the numerical models that do not simulate explicitly the sliding effect and as "Simulated Sliding", for the advanced numerical models that simulate explicitly this effect.

3.5.2.1 No explicit sliding

These results have been derived by the original models not taking the sliding into consideration.

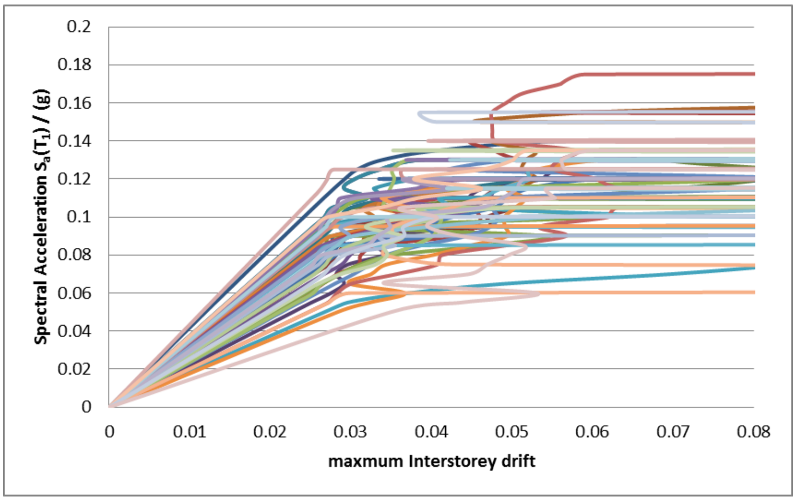

Figure 3-14 IDA Curves for IP-A

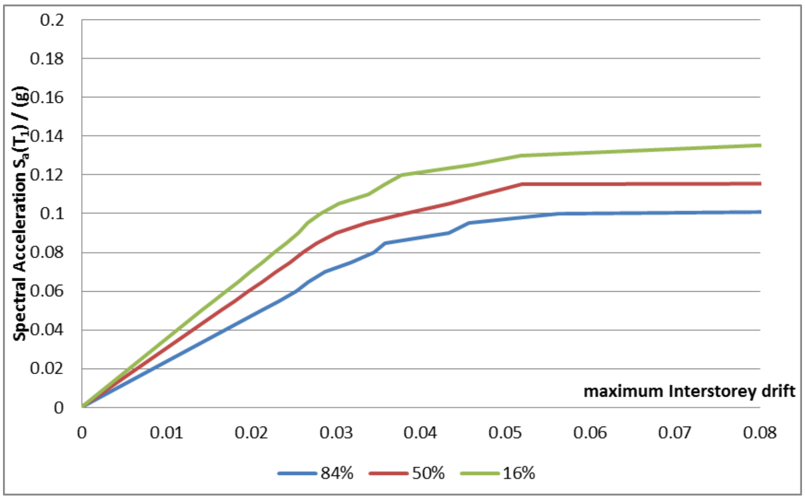

Figure 3-15 Fractile Curves for IP-A

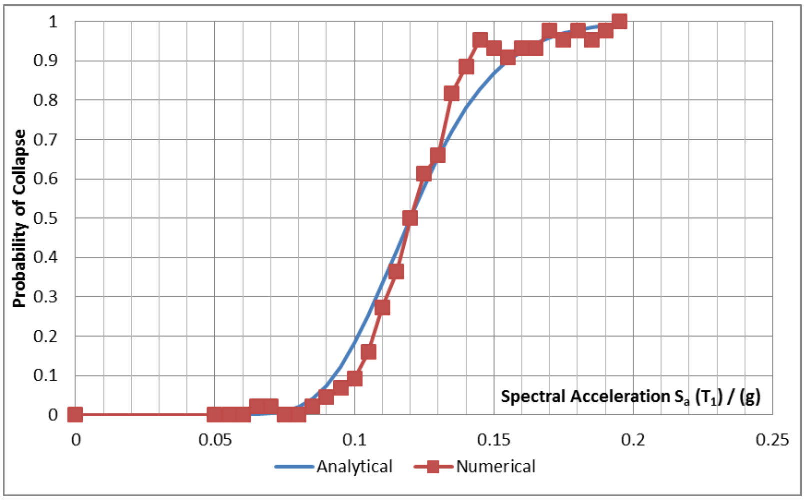

Figure 3-16 Fragility Curve for IP-A

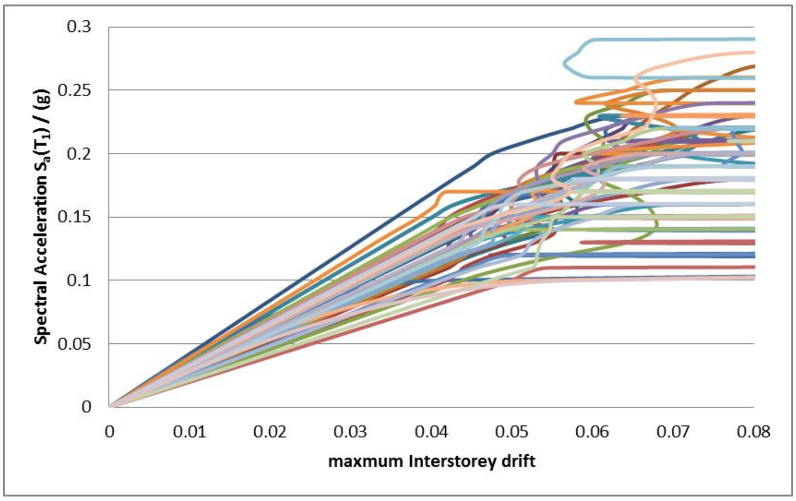

Figure 3-17 IDA Curves for IP-B

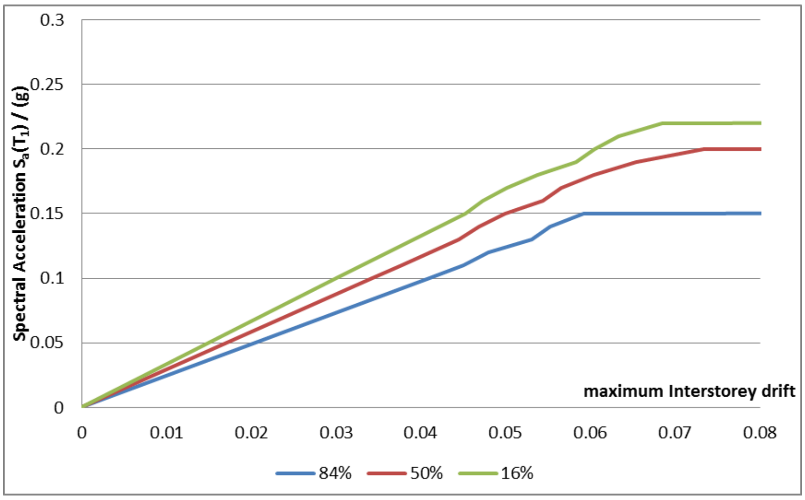

Figure 3-18 Fractile Curves for IP-B

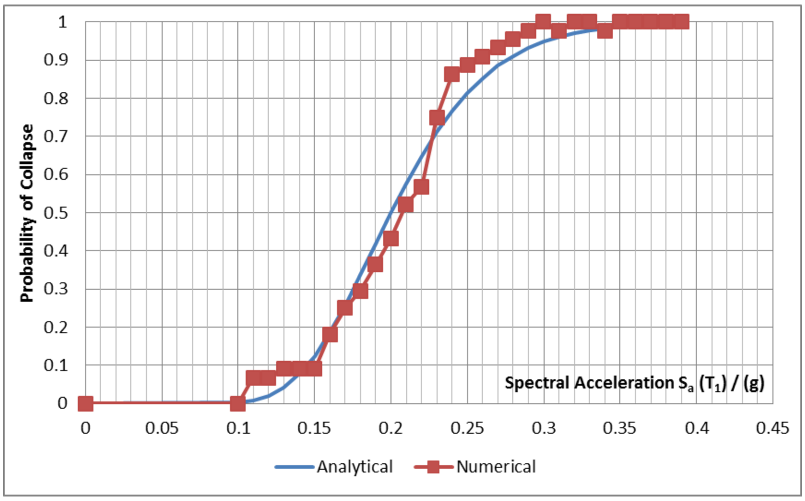

Figure 3-19 Fragility Curve for IP-B

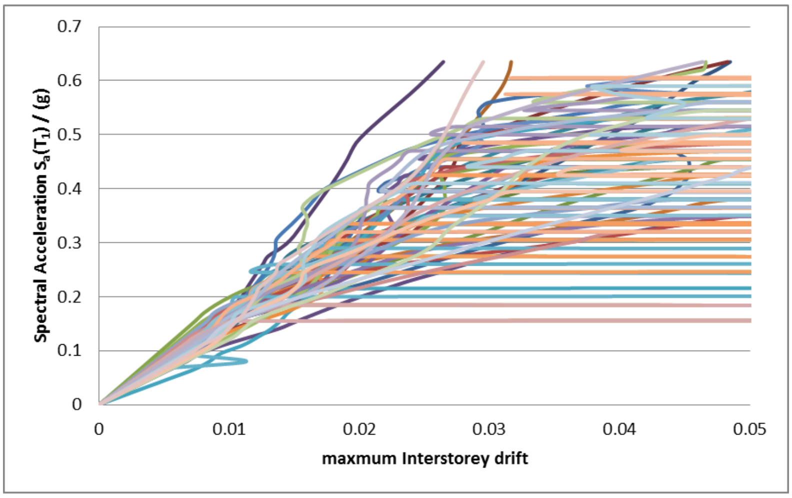

Figure 3-20 IDA-Curves for IP-C

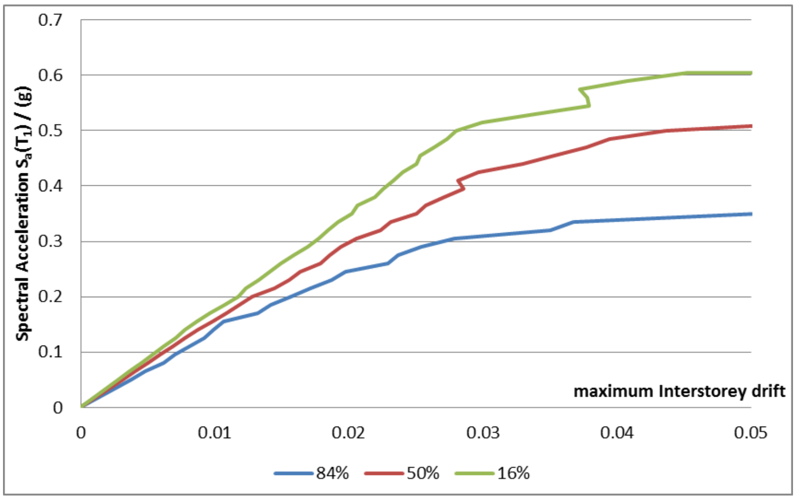

Figure 3-21 Fractile Curves for IP-C

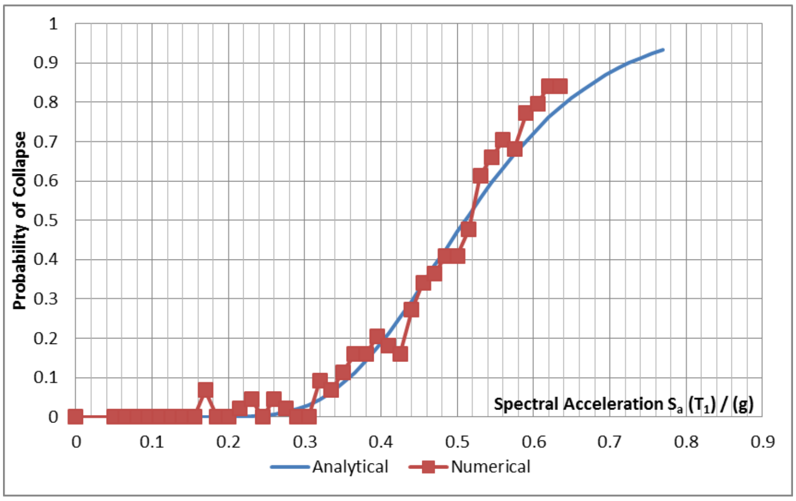

Figure 3-22 Fragility Curve for IP-C

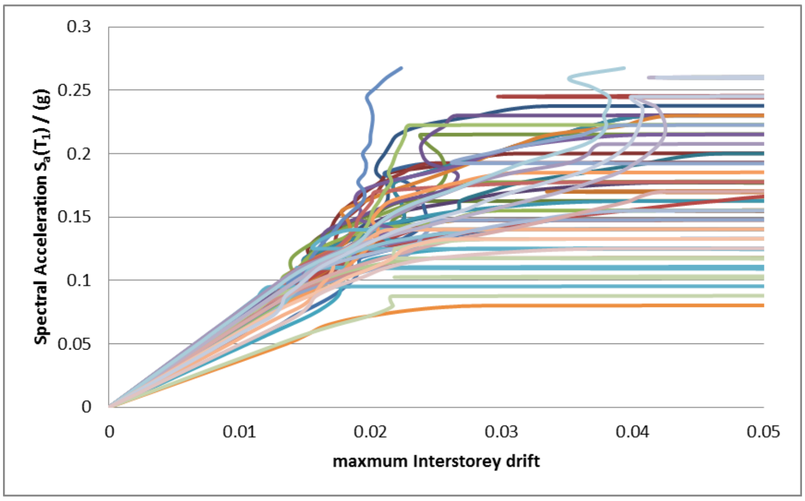

Figure 3-23 IDA Curves for IP-D

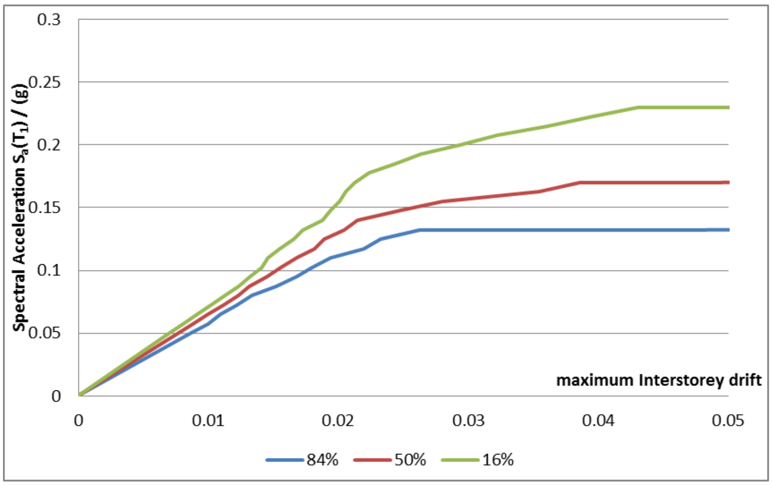

Figure 3-24 Fractile curves for IP-D

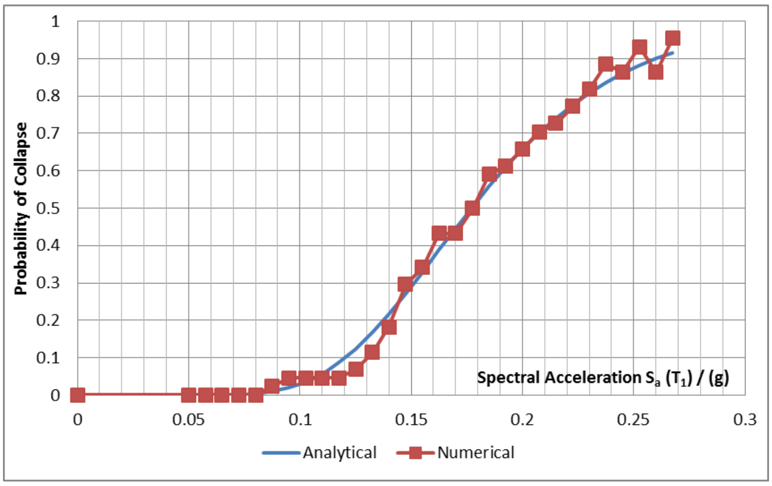

Figure 3-25 Fragility Curve for IP-D

3.5.2.2 Simulated Sliding

These results have been obtained by the method outlined in section 3.4.8.

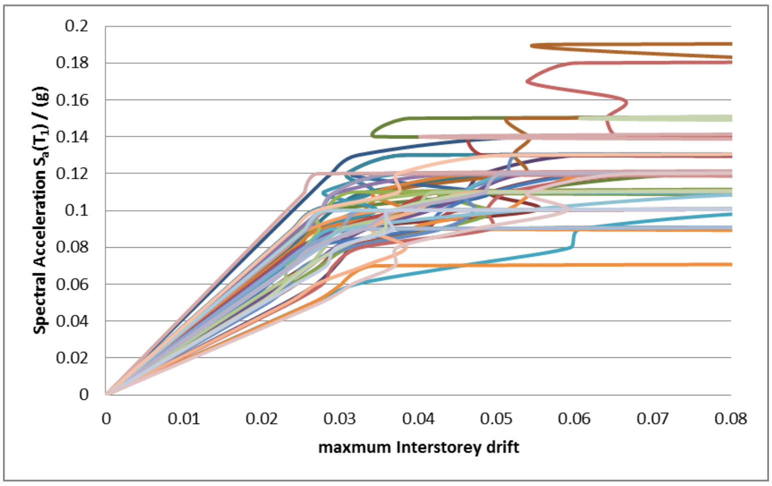

Figure 3-26 IDA Curves for IP-A

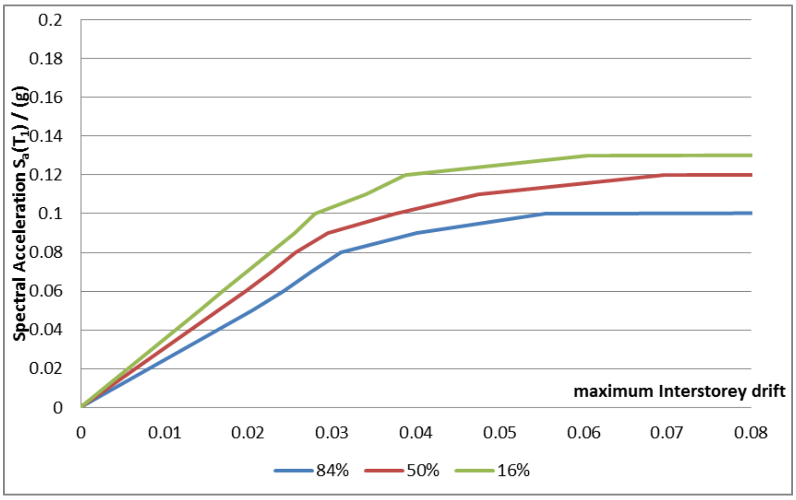

Figure 3-27 Fractile Curves for IP-A

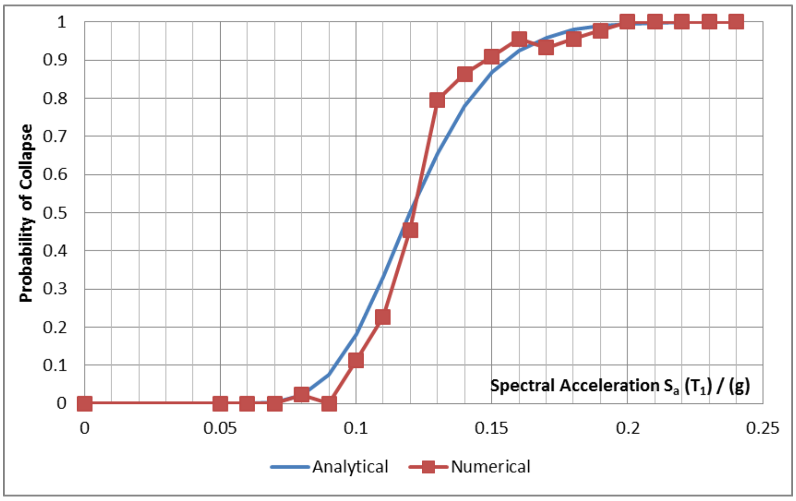

Figure 3-28 Fragility Curves for IP-A

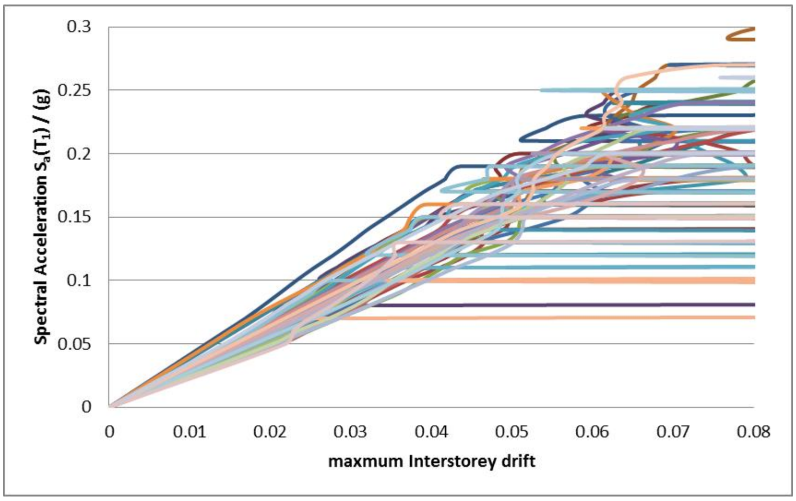

Figure 3-29 IDA Curves for IP-B

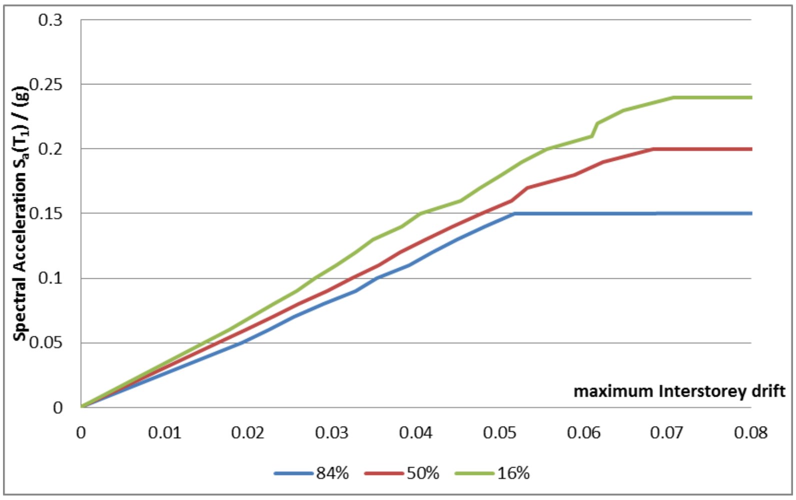

Figure 3-30 Fractile Curves for IP-B

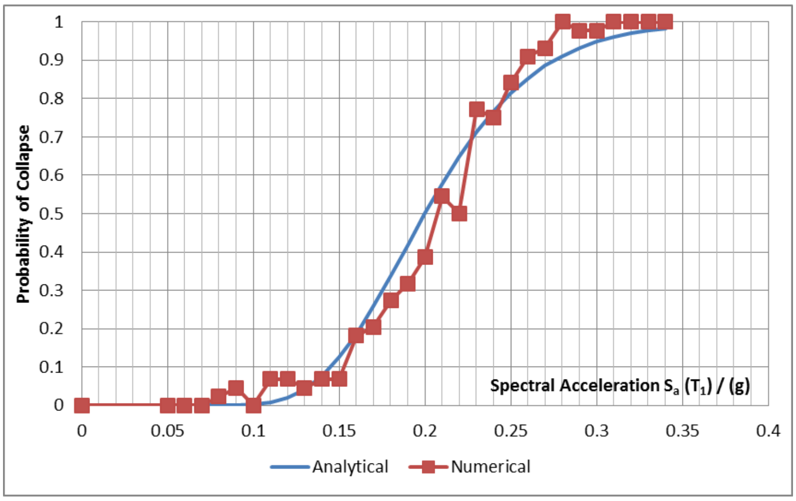

Figure 3-31 Fragility Curves for IP-B

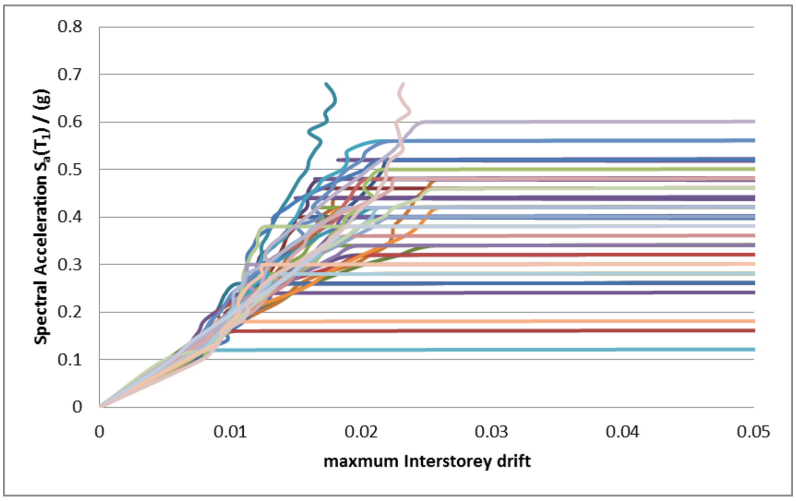

Figure 3-32 IDA Curves for IP-C

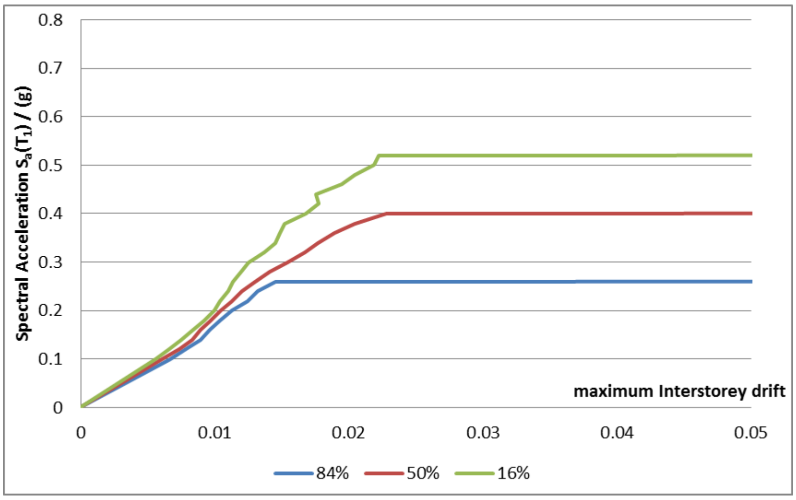

Figure 3-33 Fractile Curves for IP-C

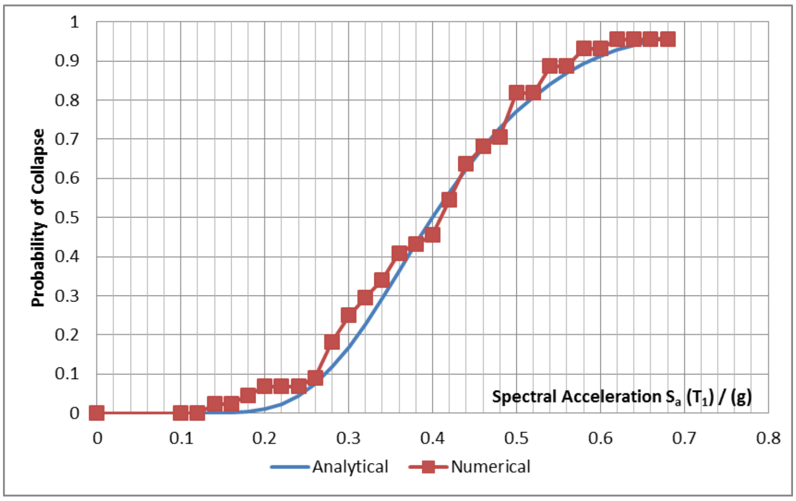

Figure 3-34 Fragility Curves for IP-C

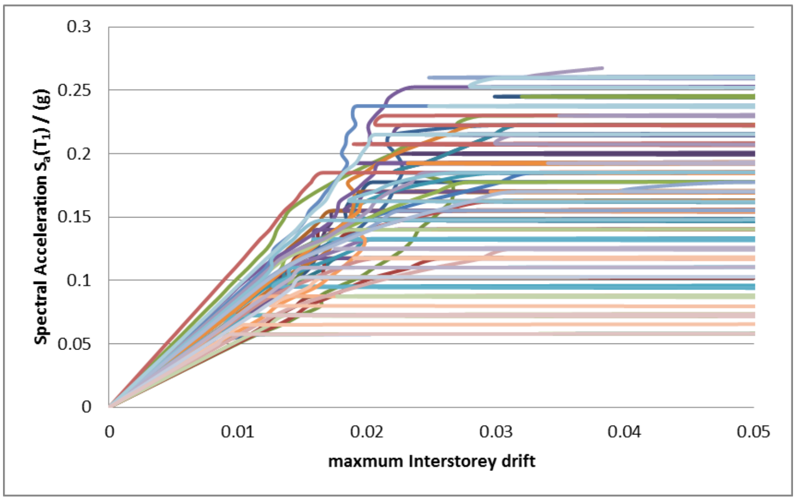

Figure 3-35 IDA Curves for IP-D

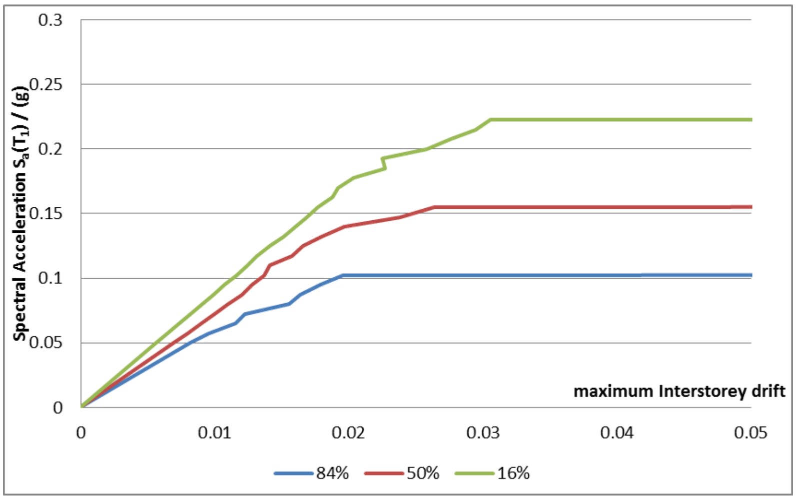

Figure 3-36 Fractile Curves for IP-D

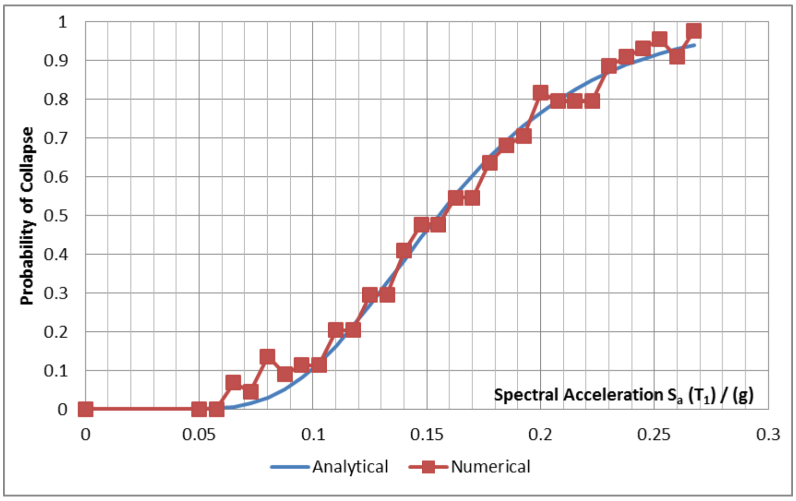

Figure 3-37 Fragility Curve for the IP-D

3.5.3 Influence of the friction coefficient

All the previous diagrams correspond to numerical models that include a friction coefficient between the pallets and the pallet beams equal to 0.375. This is a value proposed in EN16681 for normal conditions of the warehouse, the pallet itself and the rack. However, for any reason the friction coefficient could take any other value. Thus, it is perceptible that the actual value of the friction coefficient could modify the results of the applied methodology. A typical example is here presented, for the case of IP D. The IDA for this configuration in the cross aisle direction is examined again for two different values of the friction coefficient, namely μ=0.2 and μ=0.5. Indicatively the mean curves in cross direction that correspond to the 50% fragility curve are superimposed for the -non simulated criterion model- (NSC Models, section

3.4.7), and the models that simulate the sliding effect (SL-Model, section 3.4.8), with friction coefficient values of μ=0.375, μ=0.2 and μ=0.5. These results in Figure 3-38 show that the value of the friction coefficient 0.5 and 0.375 is high enough to not allow sliding of the pallets before the structural failure and the collapse of the structure. The mean curves for μ=0.5 and μ=0.375 exceed the curve of the original (NSC) model, as the directly simulated sliding effect gives more realistic and non-conservative results, as the static equivalent criterion does. On the contrary, as the friction coefficient takes lower values (i.e. μ=0.2), the mean curve promote a lower value of the mean spectral acceleration for which the system collapses.

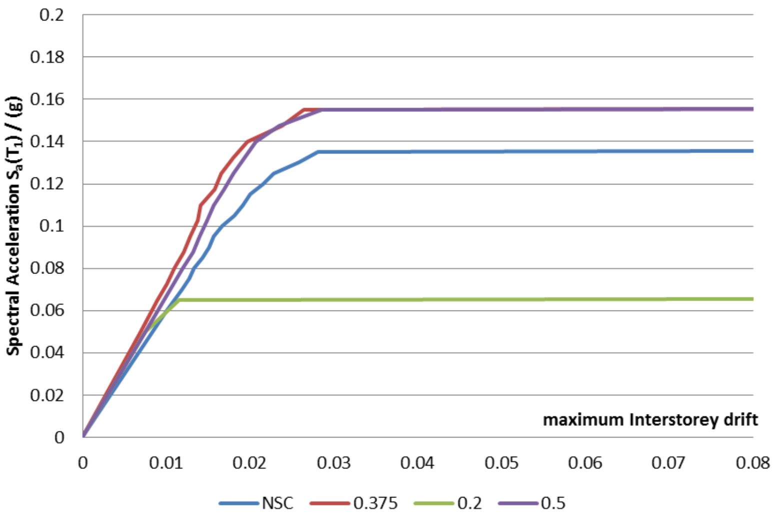

Figure 3-38 Mean (50%) fractile curves for different values of the friction coefficient and no simulated sliding (NSS)

3.5.4 Evaluation of the behaviour factor

Here, all necessary parameters to evaluate the performance of the systems have been calculated derived from the results of sections 3.5.1, 3.5.2.1 and 3.5.2.2. These parameters are used to finally calculate the CMR that is calculated with the use of Eq. (3- 3) and is presented in Table 3-1.

IP	Down Aisle			Cross aisle (Original)			Cross aisle (SL)		
	S_{MT}	S_{CT}	CMR	S_{MT}	S_{CT}	CMR	S_{MT}	S_{CT}	CMR
A	0.027	0.120	2.963	0.052	0.115	1.474	0.052	0.120	1.538
B	0.039	0.150	2.538	0.100	0.200	1.333	0.100	0.200	1.333
C				0.290	0.515	1.184	0.290	0.400	0.920
D				0.054	0.170	2.099	0.054	0.155	1.914

Table 3-1 Calculated values of the CMR for the different examined configurations

The calculated values of CMR in the table above should be adjusted (ACMR), to take into account the Record to Record uncertainties and the spectral shape, as well, that affects the response of a system. This is done with the use of SSF and Eq.(3- 5). The values of SSF are tabulated values in FEMA p695 and they are presented in Figure 3-39. The values of ACMR are presented for each IP and each system in Table 3-2

IP-Direction	T	μ_T	SSF	ACMR
A-Down	3.20	1.76	1.13	3.35
A-Cross	2.11	1.05	1.025	2.6
A-Cross SL	2.11	1.05	1.025	1.51
B-Down	2.41	1.90	1.142	1.76
B-Cross	2.02	1.16	1.06	1.41
B-Cross SL	2.00	1.16	1.06	1.41
C-Cross	1.05	1.59	1.085	1.28
C-Cross SL	1.10	1.59	1.085	1
D-Cross	1.56	1.12	1.057	2.22
D-Cross SL	1.50	1.12	1.057	2.02

Table 3-2 Calculated Values of ACMR for the different examined configurations

Here, the standard values of the adjusted collapse margin ratio ($ACMR_{i\%}$) are given in tabulated format as in FEM p695 and are presented in Figure 3-40. The values of the calculated ACMR for each one of the investigated configurations are mentioned in Table 3-3 next to the corresponding values of $ACMR_{10\%}$ and $ACMR_{20\%}$ that correspond to 10% and 20% collapse probability, respectively. The value of the total collapse uncertainty is given according to Eq.(3- 9).

IP-Direction	ACMR	β_{TOT}	ACMR10%	ACMR20%
A-Down	3.35	0.500	1.90	1.52
A-Cross	2.6	0.360	1.59	1.35
A-Cross SL	1.51	0.335	1.54	1.32
B-Down	1.76	0.500	1.90	1.52
B-Cross	1.41	0.390	1.65	1.39
B-Cross SL	1.41	0.390	1.65	1.39
C-Cross	1.28	0.407	1.68	1.41
C-Cross SL	1	0.461	1.80	1.47
D-Cross	2.22	0.424	1.72	1.43
D-Cross SL	2.02	0.461	1.80	1.47

Table 3-3 Tabulated values for the Performance criteria

The results of Table 3-3 indicate that just one configuration does not fulfill the performance criterion described in 3.4.9. This is the case of IP-C in Cross aisle direction. All other examined models could confirm the behavior factors they have been designed for.

T (sec.)	Period-Based Ductility, μ_T							
	1.0	1.1	1.5	2	3	4	6	≥ 8
≤ 0.5	1.00	1.02	1.04	1.06	1.08	1.09	1.12	1.14
0.6	1.00	1.02	1.05	1.07	1.09	1.11	1.13	1.16
0.7	1.00	1.03	1.06	1.08	1.10	1.12	1.15	1.18
0.8	1.00	1.03	1.06	1.08	1.11	1.14	1.17	1.20
0.9	1.00	1.03	1.07	1.09	1.13	1.15	1.19	1.22
1.0	1.00	1.04	1.08	1.10	1.14	1.17	1.21	1.25
1.1	1.00	1.04	1.08	1.11	1.15	1.18	1.23	1.27
1.2	1.00	1.04	1.09	1.12	1.17	1.20	1.25	1.30
1.3	1.00	1.05	1.10	1.13	1.18	1.22	1.27	1.32
1.4	1.00	1.05	1.10	1.14	1.19	1.23	1.30	1.35
≥ 1.5	1.00	1.05	1.11	1.15	1.21	1.25	1.32	1.37

Figure 3-39 SSF values according to FEMA p695

Total System Collapse Uncertainty	Collapse Probability				
	5%	10% ($ACMR_{10\%}$)	15%	20% ($ACMR_{20\%}$)	25%
0.275	1.57	**1.42**	1.33	**1.26**	1.20
0.300	1.64	**1.47**	1.36	**1.29**	1.22
0.325	1.71	**1.52**	1.40	**1.31**	1.25
0.350	1.78	**1.57**	1.44	**1.34**	1.27
0.375	1.85	**1.62**	1.48	**1.37**	1.29
0.400	1.93	**1.67**	1.51	**1.40**	1.31
0.425	2.01	**1.72**	1.55	**1.43**	1.33
0.450	2.10	**1.78**	1.59	**1.46**	1.35
0.475	2.18	**1.84**	1.64	**1.49**	1.38
0.500	2.28	**1.90**	1.68	**1.52**	1.40
0.525	2.37	**1.96**	1.72	**1.56**	1.42
0.550	2.47	**2.02**	1.77	**1.59**	1.45
0.575	2.57	**2.09**	1.81	**1.62**	1.47
0.600	2.68	**2.16**	1.86	**1.66**	1.50
0.625	2.80	**2.23**	1.91	**1.69**	1.52
0.650	2.91	**2.30**	1.96	**1.73**	1.55
0.675	3.04	**2.38**	2.01	**1.76**	1.58
0.700	3.16	**2.45**	2.07	**1.80**	1.60
0.725	3.30	**2.53**	2.12	**1.84**	1.63
0.750	3.43	**2.61**	2.18	**1.88**	1.66
0.775	3.58	**2.70**	2.23	**1.92**	1.69
0.800	3.73	**2.79**	2.29	**1.96**	1.72
0.825	3.88	**2.88**	2.35	**2.00**	1.74
0.850	4.05	**2.97**	2.41	**2.04**	1.77
0.875	4.22	**3.07**	2.48	**2.09**	1.80
0.900	4.39	**3.17**	2.54	**2.13**	1.83
0.925	4.58	**3.27**	2.61	**2.18**	1.87
0.950	4.77	**3.38**	2.68	**2.22**	1.90

Figure 3-40 Values of ACMR10% and ACMR20%, given in FEMA p695

3.6 Conclusions

The presented analyses indicate that the actual values of the behavior factor for design of the investigated racks were adequately selected. Although the proposed values for such configurations by the normative provisions are much higher, the actual values used in the everyday practice are low and somehow conservative. The dynamic analyses did not detect a comfortable ductile response that could justify the use of higher values of q. In other words, the behavior factor of 1.5 for the cross aisle direction and 1.5÷2 for the down aisle direction is proposed as safe and reasonable. These notable low values of the behavior factor are deemed to correspond to the use of Ductility Class Low (DCL) design. The use of such low values of behavior factor absolves the engineers from applying a capacity design for the different component members of the rack; as a result a progressive and desirable failure progress is not achieved and the available ductility of the systems is limited.

Finally, the proposed simulation in the present dissertation of the potential sliding effect gives new potentials for the even more realistic simulation of such numerical models. By this simulation, it is also seen that the sliding event could significantly limit, as performance level, the available ductility of the system.

3.7 References

1. Vamvatsikos, D. and C. A. Cornell (2005). "Direct estimation of seismic demand and capacity of multidegree-of-freedom systems through incremental dynamic analysis of single degree of freedom approximation." Journal of Structural Engineering 131(4): 589-599.
2. ATC, 2009. Quantification of Building Seismic Performance Factors, FEMA P695, ATC-63 Project Report, Applied Technology Council, Redwood City, CA.
3. Federal Emergency Management Agency (FEMA) (2009). Recommended Methodology for Quantification of Building System Performance and Response Parameters, FEMA P695, Prepared for the Federal Emergency Management Agency, Prepared by the Applied Technology Council, Redwood City, CA
4. Deierlein, G., Liel A. B., Haselton C. B., and Kircher C. A., (2008). "ATC-63methodology for evaluating seismic collapse safety of archetype buildings," Proceedings of ASCE-SEI Structures Congress, Vancouver, Canada, April 24-26, 2008, 10 pp.
5. Haselton, C. B., Liel A. B. and Deierlein G., “Example Evaluation of the ATC-63 Methodology for Reinforced Concrete Special Moment Frame Buildings,” Crossing Borders: ASCE Structures Congress, Vancouver, British Columbia, April, 2008, 10 pg.
6. ASCE/SEI, 2005. Minimum Design Loads for Buildings and Other Structures (ASCE/SEI 7-05), American Society of Civil Engineers/Structural Engineering Institute, Reston, VA.
7. Bertero V. V. Strength and deformation capacities of buildings under extreme environments. In Structural Engineering and Structural Mechanics, Pister KS (ed.). Prentice Hall: Englewood Cliffs, NJ, 1977; 211–215.
8. Luco N, Cornell C. A. Effects of connection fractures on SMRF seismic drift demands. ASCE Journal of Structural *Engineering* 2000; **126**:127–136.
9. Bazzurro P, Cornell C. A. Seismic hazard analysis for non-linear structures. I: Methodology. *ASCE Journal of Structural Engineering* 1994; **120**(11):3320–3344.
10. Bazzurro P, Cornell C. A. Seismic hazard analysis for non-linear structures. II: Applications. *ASCE Journal of Structural Engineering* 1994; **120**(11):3345–3365.

11. Yun S. Y, Hamburger R. O, Cornell C. A, Foutch D. A. Seismic performance for steel moment frames. *ASCE Journal of Structural Engineering* 2002; (submitted).
12. Mehanny S. S, Deierlein G. G. Modeling and assessment of seismic performance of composite frames with reinforced concrete columns and steel beams. *Report No. 136*, The John A.Blume Earthquake Engineering Center, Stanford University, Stanford, 2000.
13. Dubina D, Ciutina A, Stratan A, Dinu F. Ductility demand for semi-rigid joint frames. In *Moment resistant connections of steel frames in seismic areas*, Mazzolani F. M (ed.). E & F. N Spon: New York, 2000; 371–408.
14. De Matteis G, Landolfo R, Dubina D, Stratan A. Influence of the structural typology on the seismic performance of steel framed buildings. In *Moment resistant connections of steel frames in seismic areas*, Mazzolani FM (ed.). E & FN Spon: New York, 2000; 513–538.
15. Nassar A. A, Krawinkler H. Seismic demands for SDOF and MDOF systems. *Report No. 95*, The John A.Blume Earthquake Engineering Center, Stanford University, Stanford, 1991.
16. Psycharis I. N, Papastamatiou D. Y, Alexandris A. P. Parametric investigation of the stability of classical comlumns under harmonic and earthquake excitations. *Earthquake Engineering and Structural Dynamics* 2000; **29**:1093–1109.
17. EN 1998-1-1, (2004). Eurocode 8. Earthquake resistant design of structures. Part 1-1 General rules and rules for buildings, European Committee for Standardization, Belgium.
18. EN 15512, (2009). Steel static storage systems - Adjustable pallet racking systems - Principles for structural design. European Committee for Standardization, Belgium.
19. EN 16681, (2016). Steel static storage systems — Adjustable pallet racking systems — Principles for seismic design, European Committee for Standardization, Belgium.
20. McKenna, F., Fenves, G. L., Scott, M. H., and Jeremic, B., (2000). Open System for Earthquake Engineering Simulation (OpenSees). Pacific Earthquake Engineering
21. Chen C. K., Scholl R. E. and Blume J. A. (1980a), Seismic Study of Industrial Storage Racks, Report prepared for the National Science Foundation and for the Rack Manufacturers Institute and Automated Storage and Retrieval Systems

(sections of the Material Handling Institute), John A. Blume & Associates, San Francisco, CA.

22. Chen C. K., R. E. Scholl and J. A. Blume (1980b) Earthquake Simulation Tests of Industrial Steel Storage Racks. Proceedings of the Seventh World Conference on Earthquake Engineering, Istanbul, Turkey, 379-386.
23. Brown, B. J. 1983. Seismic Design of Pallet Racking Systems. Bulletin of the New Zealand National Society for Earthquake Engineering, 16(4), 291- 305.
24. Filiatrault, A., and Wanitkorkul, A. 2004. Shake-Table Testing of Frazier Industrial Storage Racks, Report No. CSEE-SEESL-2005-02, Structural Engineering and Earthquake Simulation Laboratory, Departmental of Civil, Structural and Environmental Engineering, University at Buffalo, State University of New York, 83 p.
25. Rayleigh, L. “Theory of Sound (two volumes)”, 1954th ed., Dover Publications, New York, 1877
26. Hall, J. F. “Problems Encountered from the Use (or Misuse) of Rayleigh Damping” Earthquake Engineering and Structural Dynamics 2005; 35(5): 525-545.
27. Clough, R. W. and Penzien, J. (1995), Dynamics of Structures, McGraw-Hill, New York.
28. Katsanos E. I., Sextos A. G., Manolis G. D., Selection of earthquake ground motion records: A state-of-the-art review from a structural engineering perspective, Soil Dynamic and Earthquake engineering 30 (2010) 157-169.
29. Haselton C. B., Liel A. B., Deierlein G. G., Kircher C., “ATC-63 EARTHQUAKE, GROUND MOTION SET: FAR-FIELD”, May 26, 2006,
30. ATC-63 Nonlinear Dynamic Analysis Working Group. Baker, J.W. and Cornell, C.A., 2006, “Spectral shape, epsilon and record selection,” Earthquake Engineering and Structural Dynamics, 34 (10), pp. 1193-1217.
31. Kircher, C. A., 2006, “Seismically isolated structures,” *NEHRP Recommended Provisions: Design Examples,* Chapter 11 of FEMA 451, prepared by the Building Seismic Safety Council for the Federal Emergency Management Agency, Washington, D.C.
32. Ye, X. & Wang, Selection of real earthquake accelerograms for structural dynamic analysis and energy evaluation, D. Sci. China Technol. Sci. (2011) 54: 2878.

33. Vamvatsikos, D., Cornell A., (2002). "Incremental dynamic analysis." Earthquake Engineering and Structural Dynamics 31(3): 491-514.
34. Weatherill G., Crowley H., Pinho R., “Efficient Intensity Measures for Components Within a Number of Infrastructures”, Deliverable of WP2 D2.12 of the research project SYNER-G, FP7-ENV-2009-1, Project No. 244061, University of Pavia, 2011.
35. GILBERT, B. P., TEH, L. H., BADET, R. X. & RASMUSSEN, K. J. R. The influence of pallets on the behaviour and design of drive-in steel storage racks – Part I Behaviour. Fifth International Conference on Structural Engineering, Mechanics and Computation, 2013a Cape Town, South Africa.
36. Gilbert, B. P., Teh, L. H., Badet, R. X. & Rasmussen, K. J. R. (2013). The influence of pallets on the behaviour and design of steel drive-in storage racks - Part II Design. Research and Applications in Structural Engineering, Mechanics and Computation - Proceedings of the 5th International Conference on Structural Engineering, Mechanics and Computation, SEMC 2013 (pp. 1285-1290). CRC Press.
37. Degée, H., Denoël, V., (2006). “An investigation on the sliding of pallets on storage racks subjected to earthquake”. Proc. 7th National Congress on Theoretical and Applied Mechanics, Faculté Polytechnique de Mons, Belgium.
38. Adamakos K., Vayas I., Hoffmeister B., Christoph H., Hervé D., Seismic Performance of Steel Storage Pallet Racks, 7th European Conference on Steel Composite Structures, Eurosteel 2014, Naples.

4. Interaction between pallets & pallet beams

4.1 Introduction

This chapter focuses on the seismic design of pallet beams in pallet racking systems and concentrates on three issues in order to verify or improve rules of European Codes on racks: the horizontal seismic forces on the pallet beams, the developing horizontal bending moments and whether the buckling length of the beams on horizontal plane may be reduced due to diaphragmatic action offered by the pallets. Investigations are based on theoretical and numerical analyses. It is found that opposite to Code provisions the lateral seismic forces are not equal distributed between the two pallet beams and, confirming field observations, that the forces directed towards the outside of the rack are higher compared to those directed towards the inner side. Concerning the horizontal bending moments appropriate correction coefficients are proposed that deviate from the codified values. Finally, it was found that pallet friction does not affect so much the buckling length to safely reduce its buckling length.

Accordingly, this chapter targets to clarify the influence of the pallets to the global and local behavior of the rack. There is an interaction between pallets and pallet-beams, or between pallets and racks' response which is likely to affect the design of a racking system. Although the behavior of a rack is so sensitive to small parametric changes and as a result it is quite difficult to examine all different parameters, there are several researchers that tried to clarify this interaction. This is usually investigated separately for the cross and the down aisle direction. Gilbert et al. (2013) [1] concluded that the influence of the pallets on the design of the rack for the cross aisle direction does not influence the final design. The same authors (2013) [2] investigated the problem also for the down aisle direction. In particular, they examined an issue that is also extensively examined in the current chapter; this is whether or not the friction forces developed in the interface of a pallet and the upper flange of the steel pallet beams are sufficient to provide a partial or entire diaphragm between the opposite pallet beams in the horizontal plane. This would affect the whole stiffness of the system and as a result the modal analyses and the final seismic design. The previous authors finally stated that the down aisle direction is slightly affected by the existence of the pallets. This holds as long as the pallets do not slide over the pallet beams. Hua and Rasmussen (2010) [3] and Castiglioni et al. (2007) [4] found out the practical values of the friction coefficient that exist between different interfaces and conditions of the steel beams and the wooden pallets which prevent sliding; thus developing a diaphragm action to the system. It is clearly seen that the friction forces and the selected friction model govern and state the whole problem.

The first systematic description of the friction phenomenon has been done by Coulomb. Although it was historically the first model about friction and the simplest one, the Coulomb model (1776) [5] is still a really useful and almost accurate model, under circumstances. In the Coulomb model, the main idea is that friction is independent of velocity and contact area and shows opposite direction than that of motion. The main disadvantage of this model is that it does not specify the magnitude of the friction for zero velocity. The friction coefficient takes values in the interval [-Fc Fc]. Morin (1833) [6] introduced a model where the friction at rest is higher than the Coulomb friction force at movement, however Stribeck (1902) [7] found out that the friction does not decrease discontinuously from this higher value but continuously, depending on the velocity. These authors specified the problem at the very beginning. At a very later time, other researchers among others Karnopp (1985) [8], Armstrong et al. (1994) [9] and Olsson et al. (1998) [10] introduced new friction models. The disadvantage of those models was that all have described the phenomenon from the static point of view.

Results showed that loading history is an important factor for characterizing the magnitude of the static friction force. It was found that the existence of a stop-restart motion acts to increase the static friction force. In contrast, the existence of a stop-inversion motion acts to reduce the magnitude of static friction force.

The observations by Yang, Zhang, and Marder [11] certainly further solidify the idea that static friction is not truly static and it is intriguing that their observations can be cast into a simple and thus elegant rate-state model, which would require interfaces to slip before they stick.

Lately an interest in dynamic models arose. Dahl (1968) [12], (1975) [13] and (1976) [14] introduced a dynamic model where friction depends only on the relative displacement of the contact surfaces. The last model is a generalized model of the Coulomb one, but does not include the observations of Stribeck that it is a rate dependent phenomenon and as a result it does not capture stiction. Bliman and Sorine (1991) [15], (1993) [16], (1995) [17] developed several also dynamic friction models based on the investigations of Rabinowicz (1951) [18].

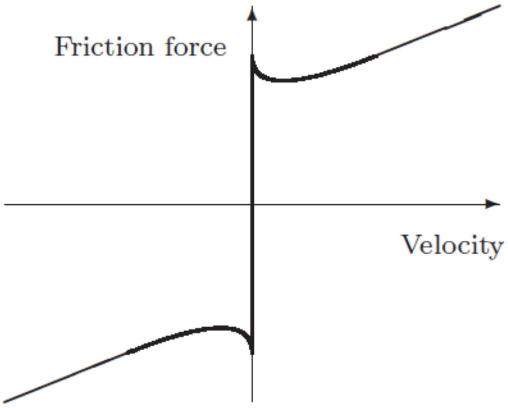

Figure 4-1 Friction model according to Stribeck

A more analytical and mathematical attempt was done by Degée et Denoël (2006) [19]. They produced the differential equations that give an analytical solution of the sliding effect, and more specifically referring to the dynamic aspect of the problem using the model of the mathematical Deck, developed by Yang (1996), for bridges [20]. However, these equations have no analytical solutions for every parameter that affect the phenomenon, and thus, there are no closed form equations that could lead to a complete solution of the problem.

In May 2012 a series of earthquakes, the highest of magnitude M_w 5.9 and spectral accelerations more than twice as large as the values provided in the Italian seismic code, struck the Emilia Romagna region in Northern Italy (2013) [21]. The earthquake resulted in collapse to many buildings, especially precast industrial buildings, with a large economic loss. Since Emilia is one of the most industrial regions of Europe with large numbers of storage buildings and warehouses, it is not surprising that lots of racking systems suffered light to serious damages, partly due to sliding and falling of pallets so that a number of lessons could be learned from the designer's point of view [22].

Another earthquake relates to the subject hit Northwestern Peloponnese, Greece in June 2008 [23]. This earthquake was of magnitude M_w 6.5 and had smaller spectral accelerations than the codified one in the low period range. However, in the long period range typical for racking systems it had similar spectral accelerations with the Emilia one, with values between 0.30 and 0.40 g. As reported in [23], this earthquake resulted in damage in many racking systems, many of them almost new. In this chapter we concentrate on the damages on pallet beams. Figure 4-2 shows large permanent lateral deformations of the pallet beams in the outside direction of the rack that endangers falling of the pallet due to insufficient overhang.

Figure 4-2 Large lateral deformations of pallet beams after an earthquake

Figure 4-3 shows that this type of damage affected a large number of beams and that these lateral deformations were systematically directed to the outer side of the rack. This magnified the distance between pallet beams and resulted in falling of pallets and accordingly to damage or collapse of the rack. It is reported here that pallets fell down primarily not due to excessive sliding of pallets but as a result of the increasing distance between the supporting beams that suffered plastic lateral deformations in opposite direction outside the rack.

Figure 4-3 Lateral deformations of the pallet beams towards the outer side of the rack

Another type of failure for pallet beams is shown in Figure 4-4. The cross section of the pallet beams is usually composed of two U-shaped cold formed sections stuck together and connected at certain distances by spot welds to form a hollow section. Figure 4-4 shows that spot welds failed so that the two sections separated from each other and the cross section was transformed to an open section with small resistance to torsion. This occurred not over the entire length of the beam but rather in the central part, see Figure 4- 3, and resulted in eventually failure of the pallet beams due to lateral torsional buckling.

Figure 4-4 Opening of the closed section due to failure of spot welds connecting its two parts

All failure modes as described above indicate that the pallet beams were adequately designed against vertical live loading but not sufficiently designed against lateral seismic loading. Indeed, no pallet beams showed permanent vertical deflections indicating that neither the live loads were excessive nor analysis and design for gravity loading was inappropriate. Accordingly, one task of the SEISRACKS2 project that is reported in this chapter was to investigate this effect, i.e. analysis and design of pallet beams due to seismic loading. This includes among others the answer to the question why the permanent deformations of the beams were always directed towards the outer side of the rack resulting in an increased danger to pallet's falling and the rack's safety.

4.2 Seismic horizontal lateral forces on pallet beams

4.2.1 Code provisions and research methodology

Pallet-beams support the pallets and are subjected to gravity loading. Seismic forces introduce horizontal forces (directly to the pallets) which are transmitted to the upper flange of the pallet-beams. These forces are caused only by the friction due to the fact that the pallets are not mechanically connected to the beams. They have accordingly an upper limit, since they cannot exceed the maximum friction force which develops between the pallet and the pallet beam. The lack of mechanical connection between pallets and beams acts therefore as a seismic isolation for the racking system but creates possible sliding of the pallets which can cause damage or collapse in case of pallet falling.

According to FEM 10.2.08 [24] pallet beams are to be checked for the internal forces and moments arising from global analysis of the system, combining a) vertical forces due to the weight of the pallets and the effect of pallet overturning due to seismic action in cross aisle direction (transverse direction), b) horizontal seismic forces in cross aisle direction, equally divided between the two compartment beams, limited by the capacity of the pallet-beam friction, i.e. with a maximum value of μ-times the pallet weight, where μ is the friction coefficient and c) axial forces for beams that are part of a vertical bracing system.

EN16681 [25] does not substantially differ from [24], but enhances the upper limit of horizontal forces introducing a safety factor $C_{\mu H}$ = 1.5, so that the maximum horizontal seismic force is equal to $C_{\mu H} \cdot \mu$ – times the pallet weight. Accordingly, in both specifications the seismic horizontal forces in cross aisle are equally distributed to the two pallet beams, each beam being subjected to a force H/2, where H is the total seismic horizontal force of the pallets.

In the following, the maximum horizontal seismic forces that develop on a pallet-beam during seismic loading are investigated as well as to what extend they create sliding of the pallets. The first part of the study refers to the development of analytical formulae that are based on an analytical model. In the second part the analytical formulae are evaluated with the use of numerical models via nonlinear finite elements (FEM) analyses, taking into account different parameters of the system. The examined system is composed of a single rigid pallet supported by a pair of separate pallet beams and subjected to horizontal forces in cross aisle direction. The different parameters that are taken into consideration in this chapter and which are supposed to influence the sliding forces, are: 1) the eccentricity e of the mass, i.e. the elevation of the center of gravity of the pallet in respect to the beam top flange 2) the axial distance b between the pallet beams, 3) the friction coefficient μ between pallet and pallet-beams and 4) the pallet's weight V.

4.2.2 Analytical model

Assuming a pallet of weight V and the fact that it is supported symmetrically by two pallet-beams (Figure 4-5), the vertical reaction on each beam is $V/2$. In case that an extra horizontal load, indicated with H, is applied at the centroid of the pallet, which is at a distance e from the upper flange of the beams, a reaction $H1$ develops on the left beam (front beam) and a reaction $H2$ on the right beam (rear beam). The force of an earthquake loading can always act either to the right or to the left; here the direction is indicative. As front beam is defined always the beam whose seismic forces act towards the inside of the pallet beams; the rear beam is the other one.

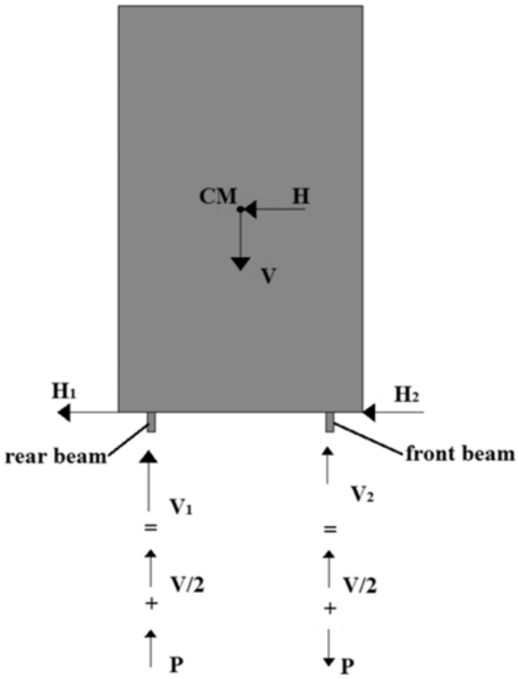

Figure 4-5 Forces on pallet beams after sliding

The pallet weight V is equally shared between the two pallet beams, each of which is loaded by a vertical force $V/2$. Due to seismic action a horizontal force H develops in the pallet which is applied at its centroid “CM”. The eccentricity e between the seismic force H and the top of the beams creates an overturning moment and a pair of vertical forces “P” in the pallet beams, determined from:

$$\boldsymbol{P = \frac{H \cdot e}{b}} \tag{4-8}$$

The force P is added to the force due to gravity loading in the rear beam and subtracted in the front beam. The total vertical forces on the two pallet beams are then equal to:

Rear beam: $$\boldsymbol{V_1 = \frac{V}{2} + \frac{\mathrm{H \cdot e}}{\mathrm{b}}} \tag{4-9}$$

Front beam: $$\boldsymbol{V_2 = \frac{V}{2} - \frac{\mathrm{H \cdot e}}{\mathrm{b}}} \tag{4-10}$$

Eq. (4-9) and Eq. (4-10) are valid when both forces V_1 and V_2 are positive, i.e. there is no rocking of the pallets. This is the only case examined here that corresponds to field observations where no rocking of the pallets was reported. Rocking starts when V_2 becomes zero, i.e when $H = \frac{V \cdot b}{2 \cdot e}$.

As the vertical forces on the two pallet beams are unequal, so are the corresponding friction forces at sliding. According to Coulomb’s friction law, the maximum friction forces at the instance of sliding that remain unchanged also during sliding are equal to:

Rear beam: $$\boldsymbol{H_1 = \mu \cdot V_1 = \mu \cdot (\frac{V}{2} + \frac{H \cdot e}{b})} \quad \textbf{(4-11)}$$

Front beam: $$\boldsymbol{H_2 = \mu \cdot V_2 = \mu \cdot (\frac{V}{2} - \frac{H \cdot e}{b})} \quad \textbf{(4-12)}$$

It may be seen that oppositely to the Code provisions [24], [25], the maximum horizontal seismic forces are not equally shared between the two pallet supporting beams. The forces on rear beam that are directed to the outside of the rack are larger than the corresponding ones on the front beam that are directed on the inner side of the rack. As the direction of the seismic forces is changing the front beam becomes rear and its seismic horizontal forces, directed this time to the outside of the rack, get larger. Accordingly, the Codes underestimate the horizontal seismic forces on the pallet beams although they ensure equilibrium for the sum of forces. Such an equilibrium is also provided by equations Eq. (4-11) and Eq. (4-12), the sum of which gives Eq. (4-13) that indicates that sliding starts when the total horizontal force is μ-times the total pallets weight.

$$\boldsymbol{H = H_1 + H_2 = \mu \cdot V} \quad \textbf{(4-13)}$$

The fact that the horizontal seismic forces on the pallet beams directed to the outside of the rack are larger than the corresponding ones directed to the inside of the rack explains the observed plastic deformations of the beams to the outside that is shown in Figure 4-2 and Figure 4-3.

Since the pallet is examined as rigid body, the horizontal action, before the sliding, is symmetrically transferred to the pallet beams. The horizontal reactions on each beam are equal to each other and specifically equal to H/2. Solving Eq. (4-12) for H/2, it is redefined as:

$$\boldsymbol{H_2 = \frac{H}{2} = \frac{V}{2}\mu - \frac{He}{b}\mu \rightarrow \ H(b + 2e\mu) = Vb\mu \rightarrow \frac{H}{2} = \frac{Vb\mu}{2(b+2e\mu)}} \quad \textbf{(4-14)}$$

Thus, the expression of H_2 is written:

$$\boldsymbol{H_2 = \frac{V \cdot b \cdot \mu}{2(b+2e \cdot \mu)}} \quad \textbf{(4-15)}$$

After the first sliding of the pallet, over the front beam, the magnitude of the lower reaction H_2 remains constant at its maximum value given by Eq. (4-15), while the total action H could be further increased. Considering that $H=H_1+H_2$, and that after the sliding H_1 and H_2 are not equal anymore, Eq. (4-11) is rewritten as:

$$\boldsymbol{H_1 = \frac{V}{2}\mu + \frac{(H_1+H_2)e}{b}\mu \rightarrow 2H_1 b = Vb\mu + 2H_1 e\mu + 2H_2 e\mu} \tag{4-16}$$

Eliminating H_2, using Eq. (4-15) the Eq. (4-16) is written as:

$$\boldsymbol{2H_1(b - e\mu) = Vb\mu + \frac{Vbe\mu^2}{(b+2e\mu)}} \tag{4-17}$$

The expression of H_1 is then written as:

$$\boldsymbol{H_1 = \frac{Vb\mu}{2(b-e\mu)}\left[1 + \frac{e\mu}{2(b+2e\mu)}\right]} \tag{4-18}$$

Or:

$$\boldsymbol{H_1 = \frac{V\cdot b\cdot \mu}{4(b-e\cdot\mu)}\frac{2b+5e\cdot\mu}{(b+2e\cdot\mu)}} \tag{4-19}$$

H_1 is the higher force that acts on both pallet beams and it is proposed as design force.

4.2.3 Numerical model

In order to evaluate the analytical formulae, a numerical study is performed using quasi-static geometric nonlinear analysis with FEM models in ABAQUS Code [26]. The numerical model as shown in Figure 4-6 includes two pallet beams that are simulated with shell elements and a rigid pallet supported by them. The contact between pallet and the pallet beams is simulated by appropriate contact elements of Coulomb type with a specified friction coefficient (Figure 4-7). At their ends, the pallet beams are considered as fixed in vertical plane to represent rigid connections to the uprights and pinned in horizontal plane. In practice the connections in vertical plane are not rigid, but this was a simplification not to add more parameters in the study. The pallet's weight and the horizontal load are applied to the centroid of the pallet. The influence of important parameters like the mass eccentricity, the beam's stiffness and the position of the pallet along the beam is examined by three different case studies. It should be said that the two latter parameters do not enter in the analytical formulae, so it is of interest to examine if they actually do influence the pallet forces. The type of analysis is linear elastic but non-linear in terms of geometry. The pallet weight is applied first in order to develop friction and activate the contact elements. Subsequently a horizontal force is applied at the centroid of the pallet and is gradually increased up to the point where the pallet starts to slide. At this point the horizontal forces on the two pallet beams, provided by the sum of the corresponding beam reactions, are recorded and compared to those derived analytically by equations Eq. (4-15) and Eq. (4-19).

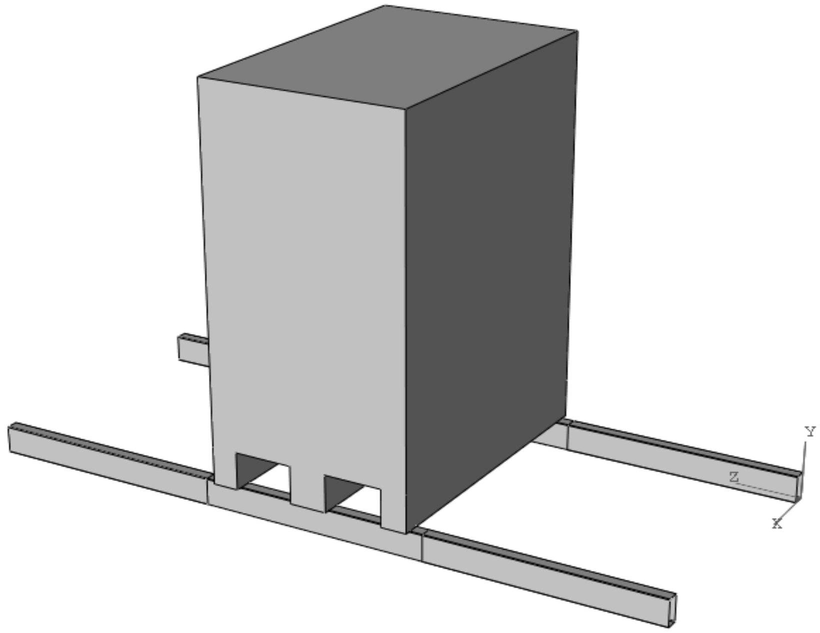

Figure 4-6 Numerical model with a rigid pallet on the middle part of the pallet beams

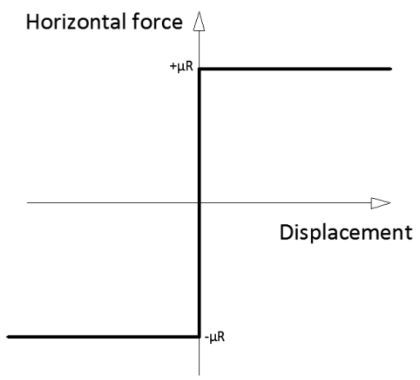

Figure 4-7 Adopted friction law of Coulomb type

4.2.4 Case study 1

The pallet beams have a rectangular hollow section with dimensions 120X40X2 mm, their distance is b = 1.1 m, the pallet mass is V = 800 kg, the friction coefficient is taken as μ = 0.375, adopted from [25] where μ = 0.37 is proposed as friction coefficient between steel beams and wooden pallet. The pallet has dimensions 800X1100X1500 mm, typical for a EUROPALLET and it is placed in the middle of the pallet-beams. The parameter that is varied is the eccentricity of the mass e which corresponds to half of the height of goods and takes values 0, 0.065, 0.43, 0.8, 1.31, 1.385 and 1.46 m.

Figure 4-8 compares the sliding forces on the two beams as provided by the numerical analysis, the analytical formulae and the Code [25]. It may be seen that the numerical results are very close to the analytical ones. It may also be seen that the additional safety factor $C_{\mu H}$ = 1.5 proposed in [24] and [25] does not cover larger loading eccentricities. This factor was not supposed to cover this effect but other uncertainties, e.g. in regard to the value of the friction coefficient etc. It may be observed that the analytical formulae predict correctly the horizontal seismic forces on the pallet beams and that the Code predictions underestimate the forces that are directed towards the exterior of the rack.

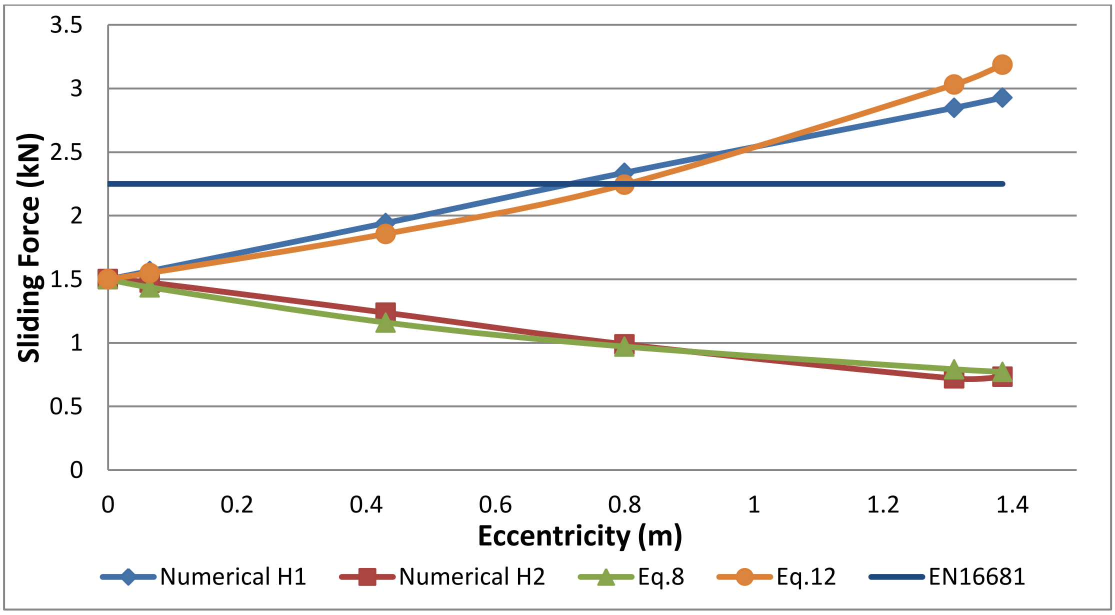

Figure 4-8 Sliding forces on pallet beams for one pallet in the middle of the beams

4.2.5 Case study 2

This case study investigates the influence of the beam-stiffness on the system. For this purpose a stiffer cross section is applied to the pallet beams. More specifically a hollow rectangular section 120X40X10 mm is used, which has a moment of inertia 3.8 times higher than the section 120x40x2, used in case study 1. Figure 4-9 shows the results that extend the observations of the previous case study to stiff pallet beams.

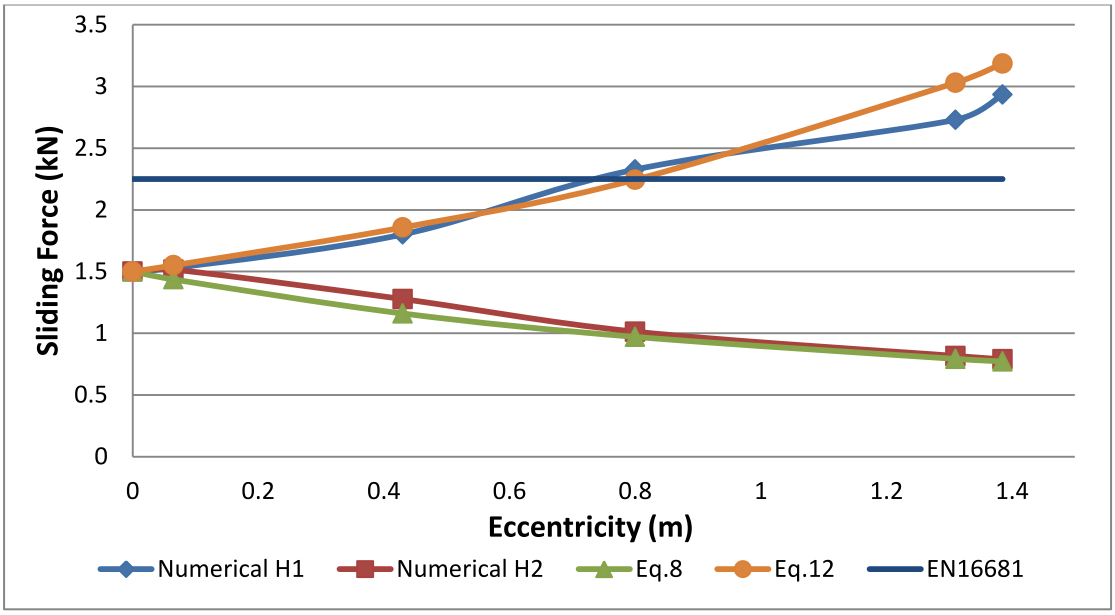

Figure 4-9 Sliding forces on stiff pallet beams for one pallet in the middle of the beams

4.2.6 Case study 3

This case study examines the influence of the pallet's position on the ultimate sliding force. The difference to case study 1 is that the rigid pallet is placed on the right side of the pallet-beams. Figure 4-10 shows that this effect does not influence the seismic forces on the pallet beams.

Based on the previous investigations it may be concluded that the horizontal seismic forces on the pallet beams at pallet sliding are influenced by the elevation of the pallet mass in respect to the top flange of the pallet beams. The forces on the two beams become unequal with increasing mass eccentricity with the rear beam subjected to a larger force that is directed towards the outside of the rack.

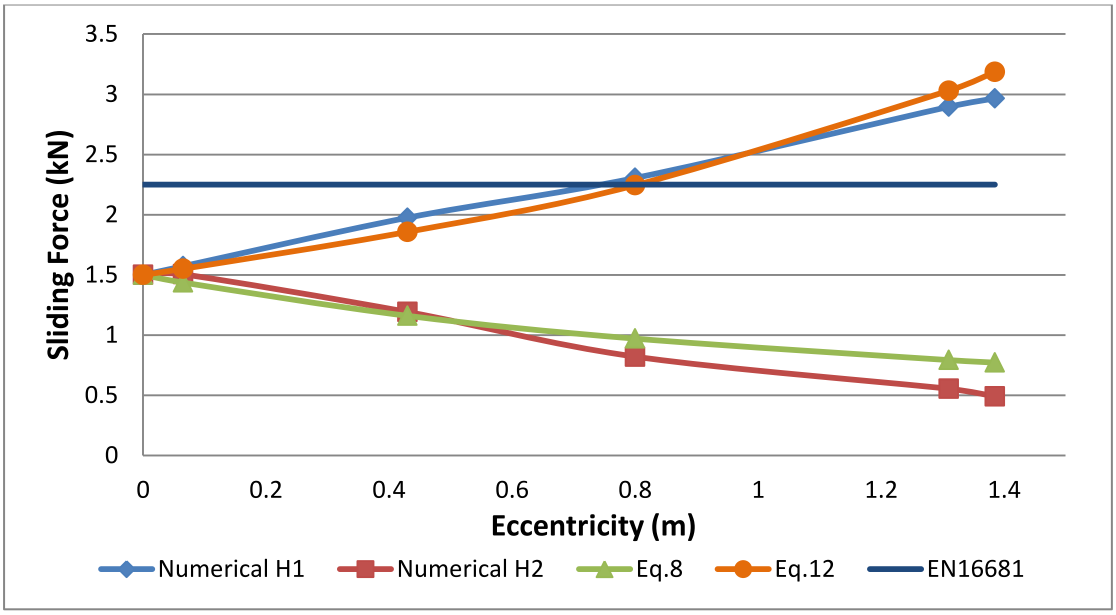

Figure 4-10 Sliding forces on pallet beams for one pallet at the right side of the pallet beams

4.3 Horizontal bending moments in pallet beams

The horizontal seismic loads in cross aisle direction introduce bending moments in the pallet beams that act on their minor axis. These loads are considered, like the vertical live loads, as uniformly distributed where a pallet exists. However, due to friction the pallets may act as a diaphragm to the pallet beams distributing more evenly horizontal loads over the entire beam's length. The resulting bending moments may be thus less than the corresponding ones derived from global analysis. This is taken into account in EN16681 by introduction of correction coefficients to the bending moments as shown in Table 4-1. Obviously the diaphragmatic action, if any, exists up to the point where sliding of the pallets occurs and is lost after sliding. This section presents a numerical study where these effects are investigated.

Line	Number of unit loads per compartment	Single span beams
1	n out of n	0 (completely restrained)
2	1 out of 2	0.6
3	1 at mid span out of 3	1.0
4	2 out of 3	0.6
5	2 at mid span out of 4	0.7
6	3 out of 4	0.5

Table 4-1 Correction coefficients for horizontal bending, excerpt from EN16681

The numerical model is as simple as possible and consists of 2 independent pallet beams loaded with up to 3 out of 3 pallets. The pallet beams are considered deformable in the vertical plane and they retain their actual flexibility in all directions; the pallets are considered rigid in the horizontal plane and the transverse vertical plane (perpendicular to the pallet beams), but flexible in the longitudinal vertical plane (parallel to the pallet beams). A number of important parameters that are introduced later were taken into consideration. Other parameters such as the eccentricity of the support conditions, the eccentricity of the horizontal loads on the pallet beams (applied on the upper flange), the flexibility of the pallet beams and/or that of the pallets were not examined here, as their influence in the specific problem is considered to be of minor importance.

The numerical model in the ABAQUS Code is presented in Figure 4-11. The pallet beams are represented by beam elements assigned with a general section with user defined properties. The inertial and geometric properties of this section are the nominal values for an RHS 120X50X2 (typical pallet-beam section). The beams are fixed in vertical plane and pinned in horizontal plane. The pallets are simulated as three rigid surfaces in contact with the pallet beams (Figure 4-12).

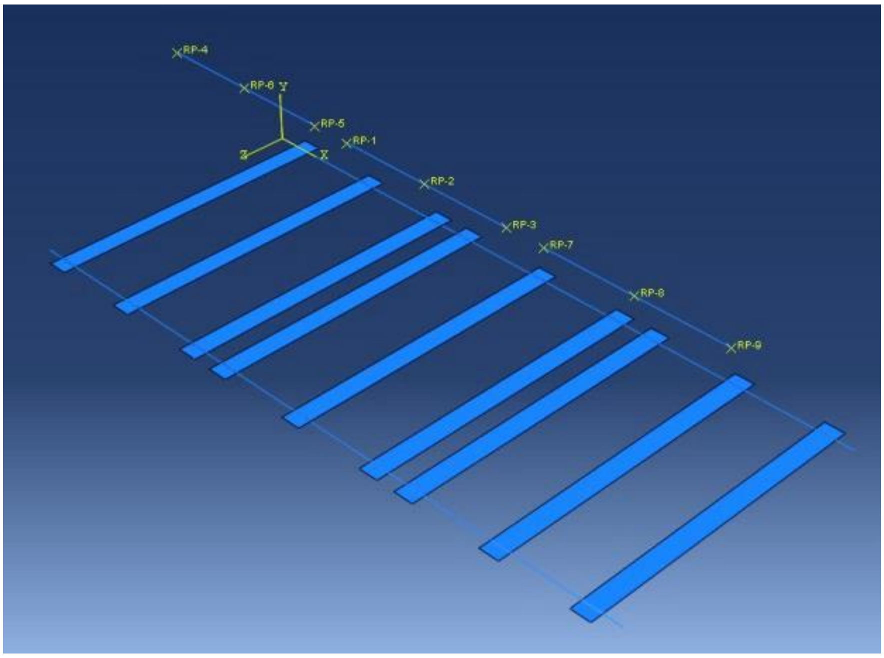

Figure 4-11 The numerical model in ABAQUS for 3 pallets in a compartment

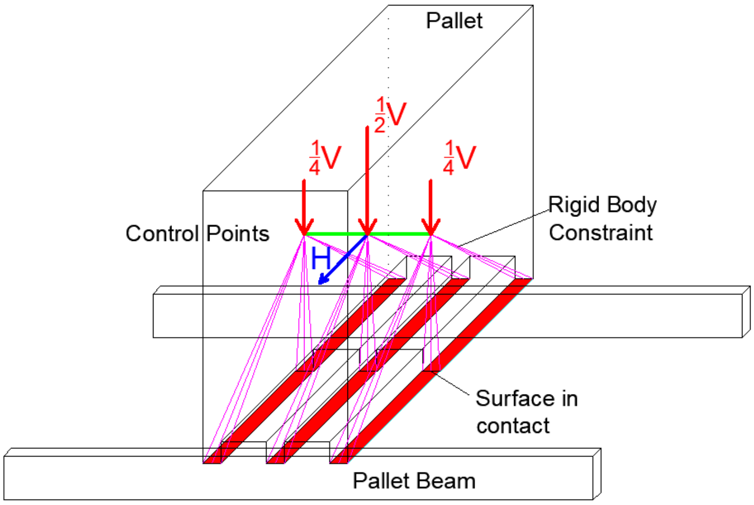

Figure 4-12 Simulated configuration of pallets and pallet beams

Each surface is tied to a given point (control point) which lies on the level of the pallets' center of mass (CM), taking into consideration the mass-eccentricity. These control points, and consequently the respective three surfaces, are constrained to each other to all degrees of freedom except the vertical translation, in order to let the pallet deform in that plane. Contact- friction elements were introduced between pallets and pallet beams to simulate their interaction. The loads are applied directly to the control points in two steps as following: in the first step the vertical load is applied in order to activate the contact-friction elements and in the second step the horizontal loading is gradually increased up to the point where the pallet starts to slide. The vertical load is applied with a distribution ¼, ½, ¼ to the three control points of each pallet and the horizontal load is applied entirely on the middle control point. The analyses were elastic and geometrically nonlinear. From each analysis the bending moments of the pallet beams during the application of the horizontal load were recorded and compared to the theoretical values.

Although the problem has been simplified, several parameters are taken into account such as the friction coefficient between the pallet and the pallet beam, the elevation of the pallets centroid, the pallet's nominal weight (Q_p) and the position and number of pallets on the compartment. More specifically following values of the parameters were considered, see Table 4-2:

- For the friction coefficient μ the values 0.1, 0.3 and 0.5.
- For the elevation of the pallets (mass eccentricity) the values 0.35, 0.625 and 0.9 m
- For the pallet's nominal weight Q_p = 4, 8 and 12 kN.
- For the number and position of the pallets five different loading cases.

The loading cases examined have some correspondence with the cases considered in Table 4-1. Case B corresponds to line 3, cases C and D to line 4 and case E to line 1. The total number of scenarios is 3x3x3x5 = 135. However, only 11x5 = 55 different analyses as highlighted with bolt in Table 4-3 were performed, ensuring that the influence of each parameter is examined at least once, while the other parameters remain constant. The length of the pallet beams was taken here as L=2700mm.

Case	Configuration	Loading	Theoretical moment M*
A		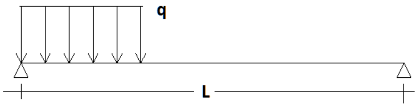	$25/648\ qL^2$
B		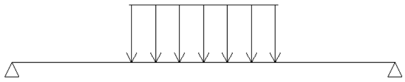	$5/72\ qL^2$
C	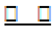	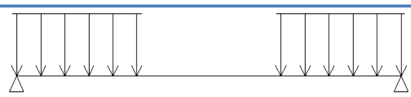	$1/18\ qL^2$
D		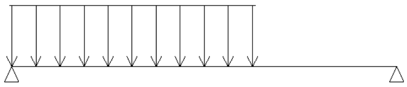	$8/81\ qL^2$
E		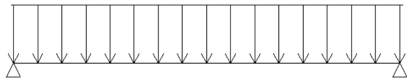	$1/8\ qL^2$

Table 4-2 Loading configurations of the numerical study (boxes represent the pallets) and corresponding theoretical bending moments M*

No of case study	Friction coefficient μ	Pallet Weight Qp	Eccentricity of mass e
1	0.1	4	0.9
2	0.1	4	0.625
3	0.1	4	0.35
4	**0.1**	**8**	**0.9**
5	**0.1**	**8**	**0.625**
6	**0.1**	**8**	**0.35**
7	0.1	12	0.9
8	0.1	12	0.625
9	0.1	12	0.35
10	0.3	4	0.9
11	**0.3**	**4**	**0.625**
12	0.3	4	0.35
13	**0.3**	**8**	**0.9**
14	**0.3**	**8**	**0.625**

15	**0.3**	**8**	**0.35**
16	0.3	12	0.9
17	**0.3**	**12**	**0.625**
18	0.3	12	0.35
19	0.5	4	0.9
20	0.5	4	0.625
21	0.5	4	0.35
22	**0.5**	**8**	**0.9**
23	**0.5**	**8**	**0.625**
24	**0.5**	**8**	**0.35**
25	0.5	12	0.9
26	0.5	12	0.625
27	0.5	12	0.35

Table 4-3 Total number of variations and examined cases of the numerical study

The theoretical bending moments M* for each loading configuration are shown in Table 4-2. The results of the analyses in dimensionless form are presented in Figure 4-13 to Figure 4-17. The horizontal axis denotes the ratio H/Q_p, where H is the horizontal force on the front/rear beam and Q_p the corresponding total vertical force from all pallets resting on each of them. The maximum value of the ratio H/Q_p is the friction coefficient μ employed in each case study after which the pallets slide and do not offer any diaphragm action. The vertical axis presents the ratio M/M*, where M is the maximum bending moment of the pallet beam from the nonlinear analysis and M* the corresponding theoretical moment according to Table 4-2, when the front and rear beam are loaded by half of the total force H/2. The vertical axis, the ratio M/M*, actually presents the investigated correction coefficient for bending moments.

Figure 4-13 shows the results for fully loaded compartment, Table 4-2 case E. It may be seen that the results may be grouped in three categories in accordance to the friction coefficient – 0.1 (dotted lines), 0.3 (dashed lines), 0.5 (continuous lines) – employed.

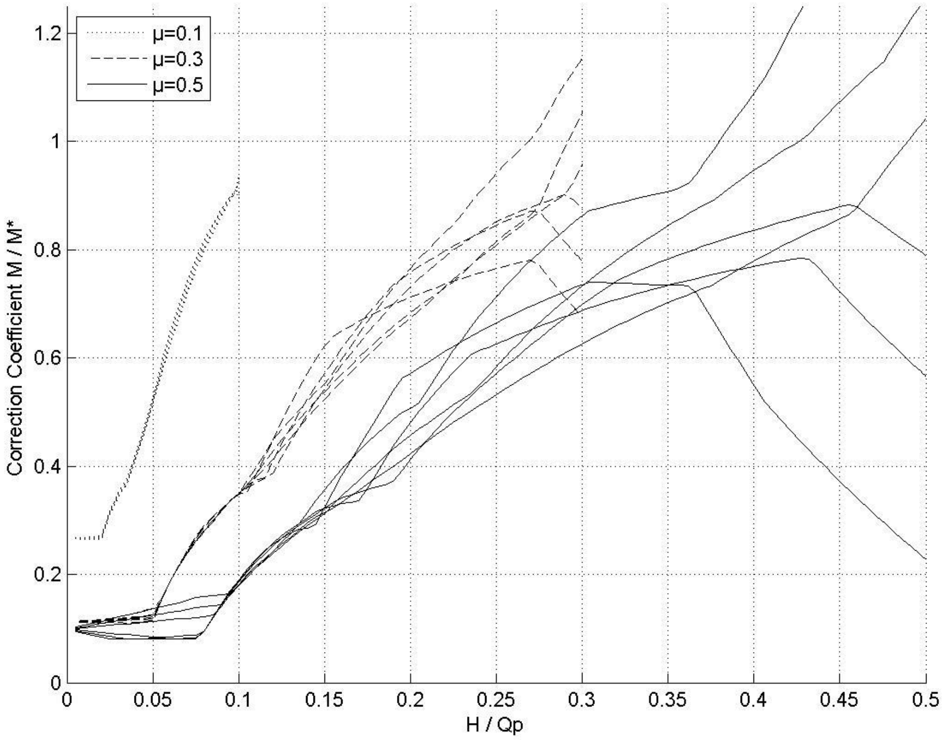

Figure 4-13 Results for 3 unit loads out of 3 per compartment (case E)

Figure 4-14 and Figure 4-15 show the results for 2 unit loads out of 3 in the compartment, Table 4-2 cases C and D. The results may also be grouped in three categories as before according to μ. For μ = 0.5 and 0.3 it is observed that the moments of the rear beams are larger than those of the front beams from the very beginning of the analyses. Graphically it is depicted at the point, where each group of curves broadens. The curves that tend upwards are those of the rear beams as they are more intensively being loaded, while the curves that tend downwards are those that correspond to the front beams which are gradually being unloaded. This contradicts the regularly used assumption of equally sharing of the horizontal seismic forces between the two beams. Accordingly, the conclusion of the previous paragraph that the forces of the rear beams are larger than those of the front beams is once more confirmed. That happens when the pallet starts to slide over the front beam, and the point where the curves broaden depicts also the beginning of the sliding effect. At the end steps of the curves an intense divergence of the curves is observed, which is due to the beginning of the sliding over the rear beam as well.

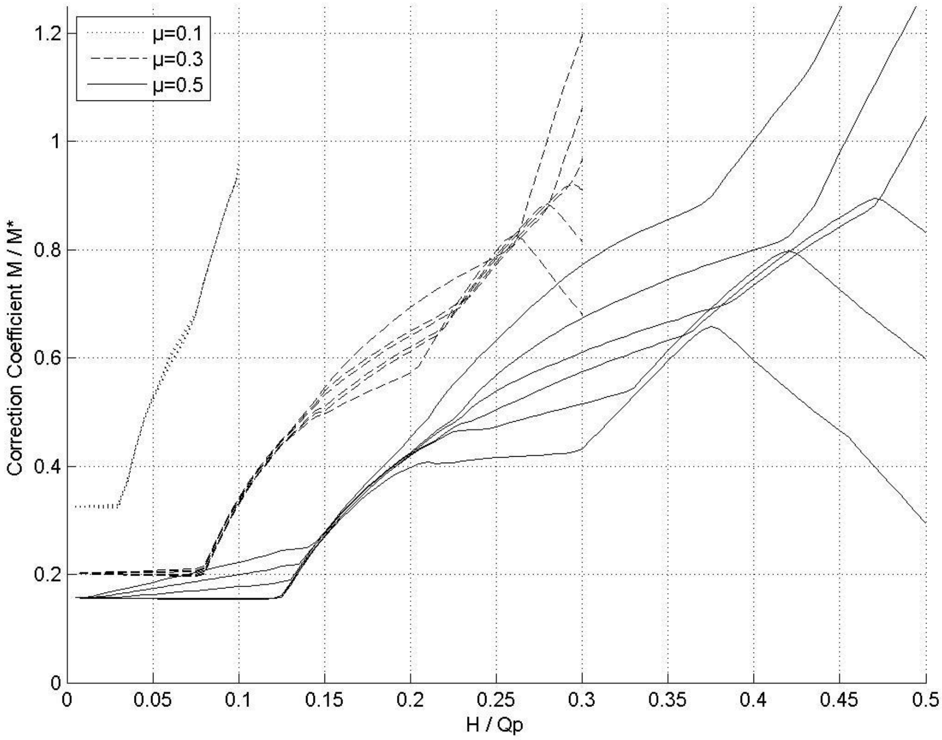

Figure 4-14 Results for 2 unit loads out of 3 per compartment (case C)

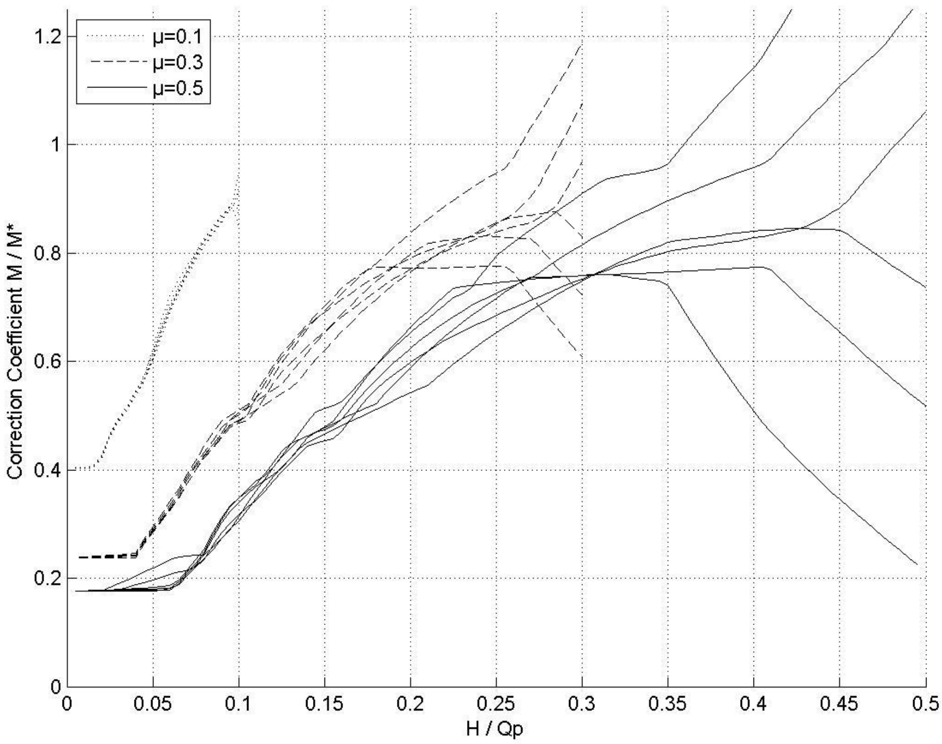

Figure 4-15 Results for 2 unit loads out of 3 per compartment (case D)

Finally, Figure 4-16 shows the results for one unit-load at mid-span, Table 4-2 case B and Figure 4-17 for one unit-load at the extremity of the pallet beams, Table 4-2 case A, respectively. The observations made before in respect to the grouping in friction coefficients and the larger forces of the rear beams are also valid here. It may be seen that pallets at mid-span provide some diaphragm action for a long range of horizontal forces providing a correction coefficient with a stable value of 0.8. The M/M*-ratio increases in the rear beams beyond 0.8 at larger horizontal forces. However, this effect is balanced if the horizontal forces are not equally shared between the two pallet beams as was seen in the previous section of this chapter.

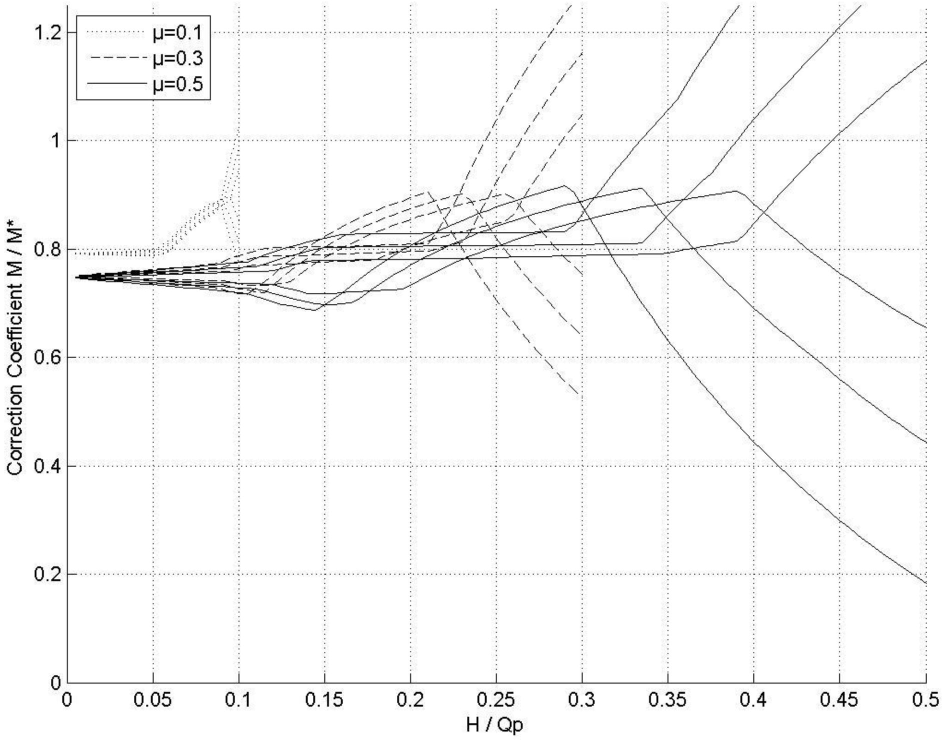

Figure 4-16 Results for 1 unit-load at mid span out of 3 per compartment (case B)

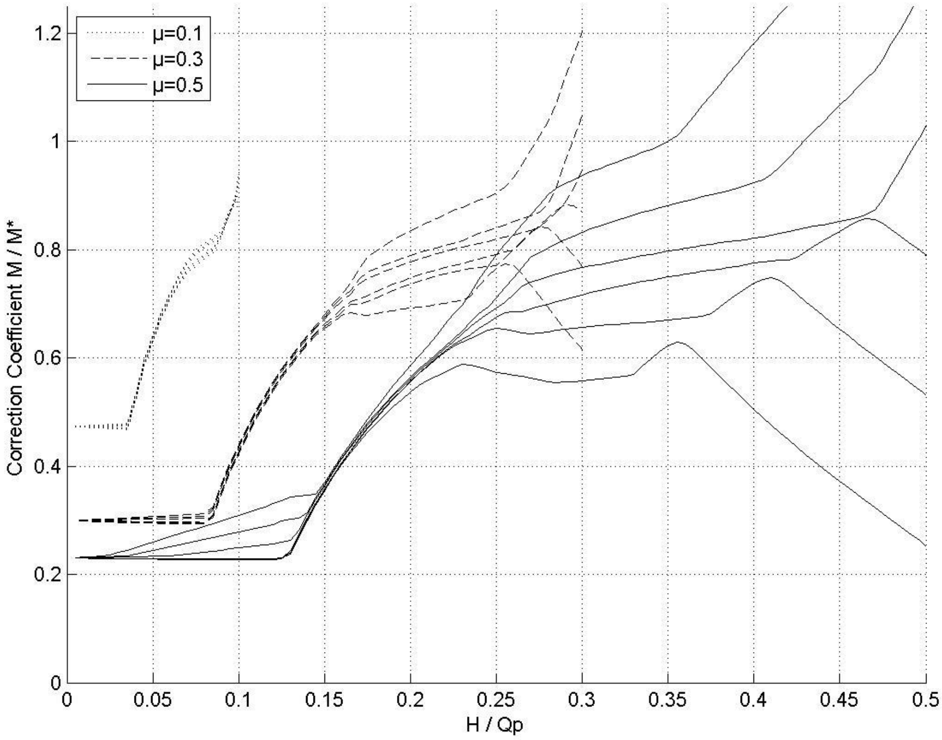

Figure 4-17 Results for 1 unit-load at the extremity out of 3 per compartment (case A)

In order to clarify the influence of the pallets on the pallet beams' minor axis bending, moments diagrams are presented that depict the bending moment diagram along the pallet-beams for different steps of the nonlinear (multistep) analyses. Two extreme situations are presented, that is cases 6 and 22 of Table 4-3. The extreme situations refer to the friction coefficients (0.1 vs. 0.5) and the eccentricity of masses (0.35m vs. 0.9m) that intensifies the rocking effect and consequently the loading difference between the two pallet beams. Figure 4-18 (A to E) present the bending moment diagrams of case study 6 and for loading cases A to E. Red shows the moments for the more intensively loaded rear beam and black the less loaded front beam. The different lines depict the moments at increasing loading steps. It may be seen that the bending moments of the two pallet beams are quite similar from the first steps even until some steps before the sliding of the pallet. This happens for all cases A to E. However after sliding the moments at the front beam (black line) do not increase anymore, while they increase further at the rear beams (red line). This confirms that the sliding starts at the front beams and that the forces after sliding do not increase any more.

A

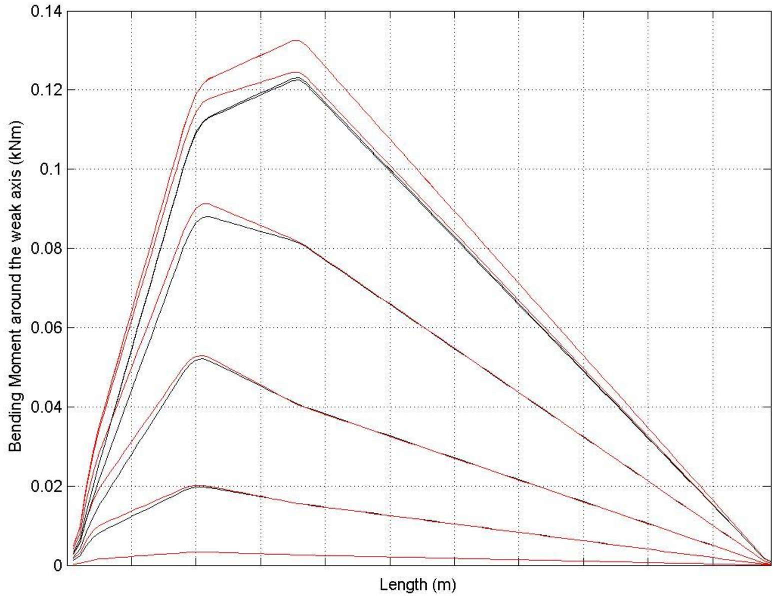
0.14
0.12
0.1
0.08
0.06
0.04
0.02
0
Bending Moment around the weak axis (kNm)
Length (m)

B

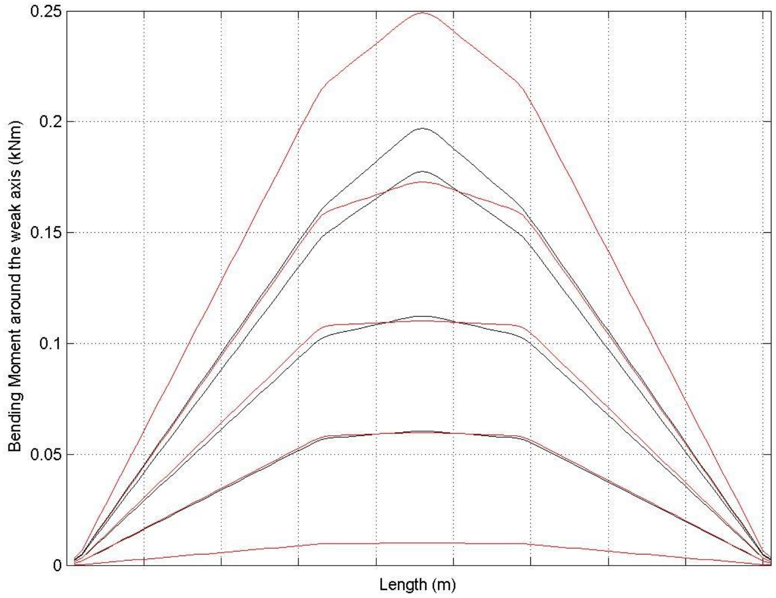
0.25
0.2
0.15
0.1
0.05
0
Bending Moment around the weak axis (kNm)
Length (m)

C

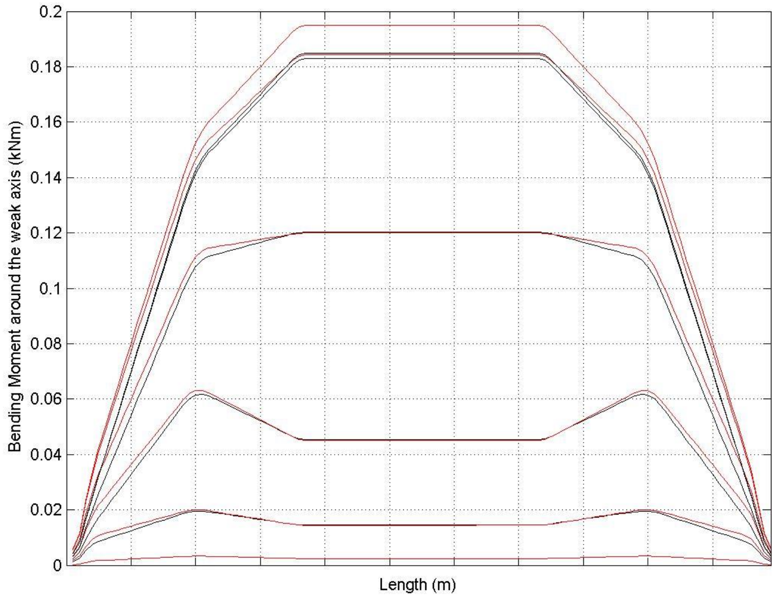
Bending Moment around the weak axis (kNm)
Length (m)
0
0.02
0.04
0.06
0.08
0.1
0.12
0.14
0.16
0.18
0.2

D

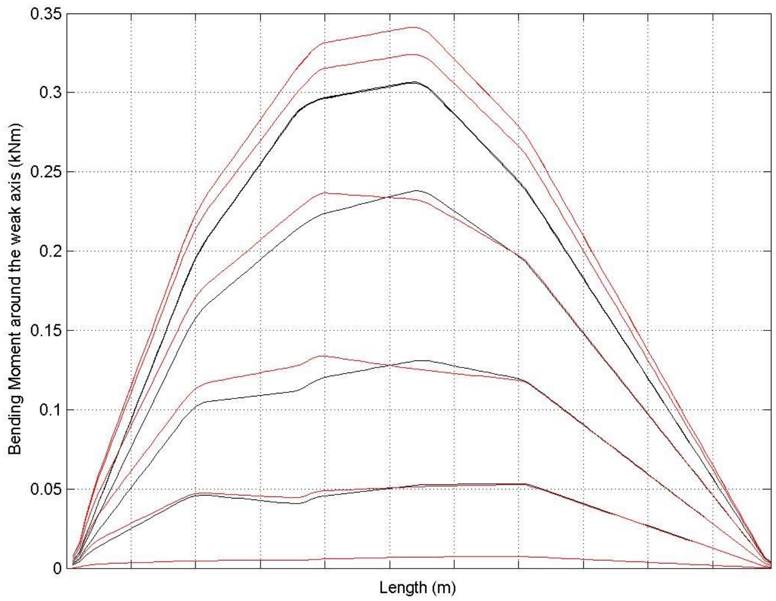
Bending Moment around the weak axis (kNm)
Length (m)
0
0.05
0.1
0.15
0.2
0.25
0.3
0.35

E

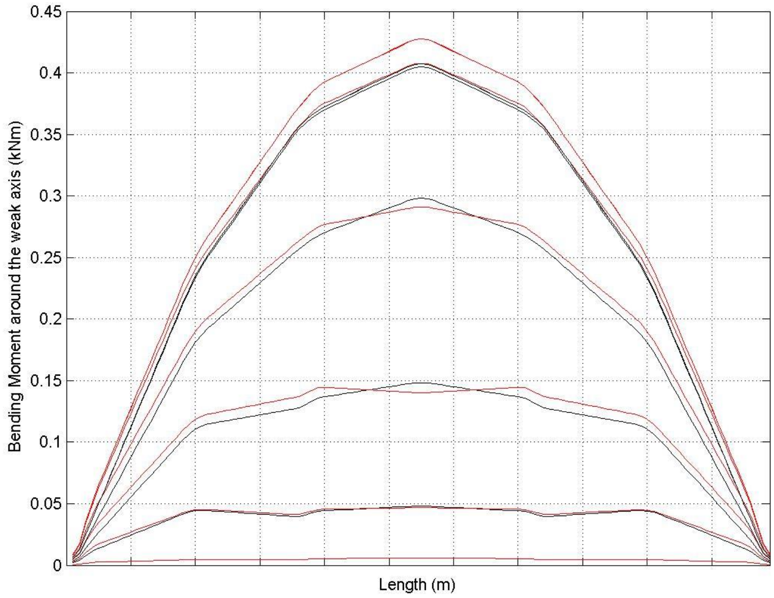

Figure 4-18 Weak axis moment distribution for the front (black) and the rear (red) pallet beams at increasing loading steps, case study 6, cases A to E

Figure 4-19 presents the corresponding curves for case study 22 of Table 4-3. The observations made before are valid here too. However, the rocking effect is intensified at higher eccentricity and higher friction coefficient. The pallet is starting to overturn earlier and thus the bending moments of the two pallet beams deviate more than before.

A

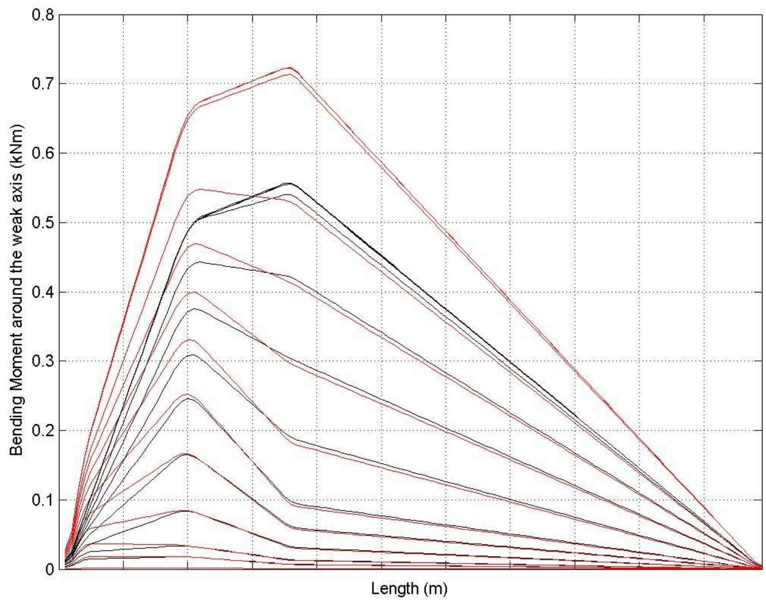

B

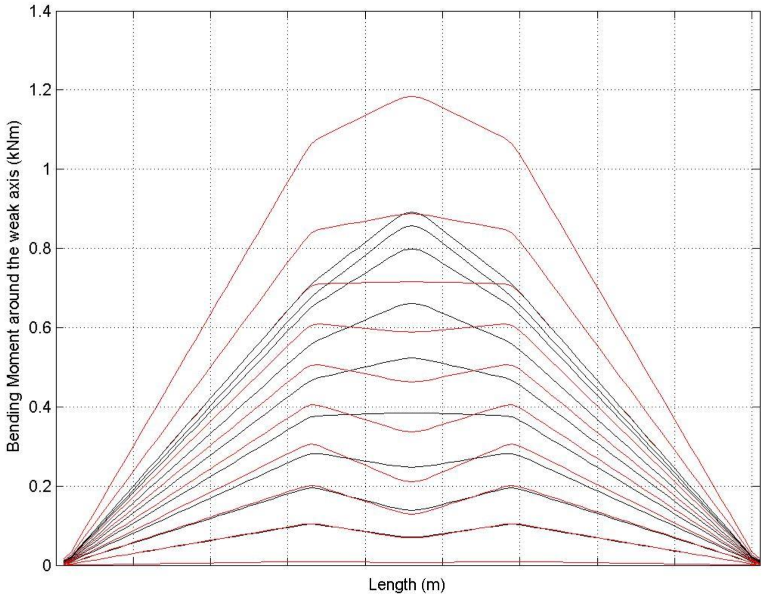
1.4
1.2
1
0.8
0.6
0.4
0.2
0
Bending Moment around the weak axis (kNm)
Length (m)

C

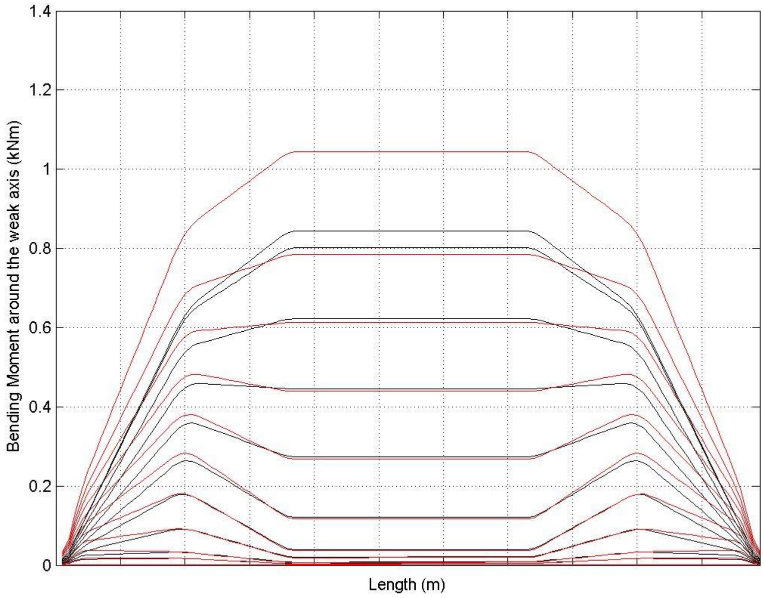
1.4
1.2
1
0.8
0.6
0.4
0.2
0
Bending Moment around the weak axis (kNm)
Length (m)

D

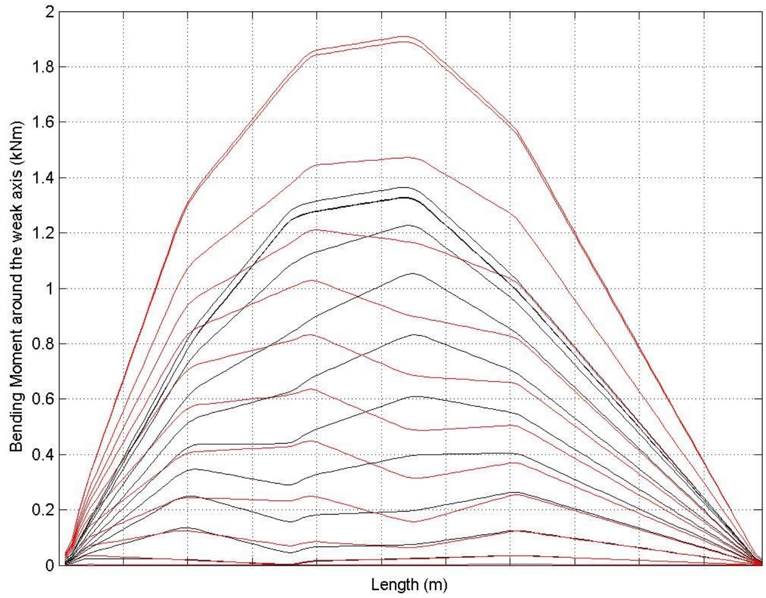

E

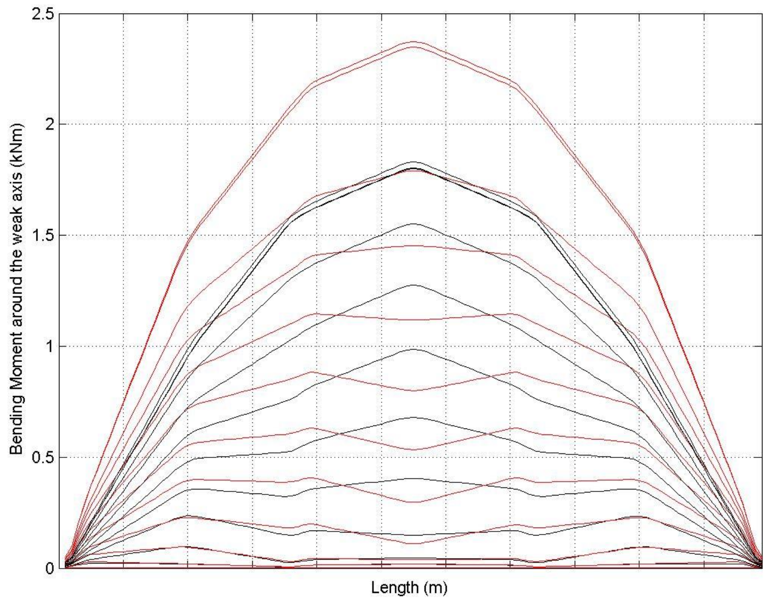

Figure 4-19 Weak axis moment distribution for the front (black) and the rear (red) pallet beams at increasing loading steps, case study 22, cases A to E

4.4 Buckling Length of Pallet Beams in Horizontal plane

Pallet beams may be subjected to high axial forces, especially if they are part of the vertical bracing system. Accordingly, they must be checked against buckling in both directions though the pallets act through the friction forces like a diaphragm between the two pallet beams. This might reduce the buckling length in horizontal plane and therefore increase the buckling resistance of the beams. EN16681 considers this phenomenon, proposing reduced buckling length factors that depend on the number and position of the pallets on the pallet beams as shown in Table 4-4. This proposed reduction is numerically investigated in this section.

Line	Number of unit loads per compartment	K for single span beams
1	n out of n	0
2	1 out of 2	0.6
3	1 at mid span out of 3	1.0
4	2 out of 3	0.6
5	2 at mid span out of 4	0.7
6	3 out of 4	0.5

Table 4-4 Buckling length factor K for pallet beams in horizontal plane, excerpt from [25]

The numerical model employed is the same as in the previous paragraph as shown in Figure 4-11 and Figure 4-12. The parameters considered here are:

a) The friction coefficient μ with values 0.1, 0.3, 0.5 and 100, the latter representing a theoretical case in which the pallets are fixed to the pallet beams.
b) The pallet's nominal weight Qp = 8 and 12 kN.
c) The number and position of the pallets according to Table 4-2.
d) The elevation of the pallets (mass eccentricity) was taken as 0.625m.
e) The length of the pallet beams was fixed and equal to L = 2.7 m.

The analyses are performed in 3 steps. In the first step, the pallet beams are subjected to a horizontal uniformly distributed load, in order to create an initial deflection of a bow-like shape, thus introducing an out-of-plane initial imperfection on the pallet beams. In the second step, the vertical loads are applied to the pallets in order to create the reactions on the pallet beams and to activate the friction-contact elements of the model. In the third step, both the pallet beams are subjected to an equal axial compression loading until the load cannot increase substantially.

The system's response is expressed by applied compression force – mid-span deflection curves as shown in Figure 4-20 (Qp=8kN) and Figure 4-21 (Qp=12kN). Two curves are also added in the figures:

The Euler buckling load of the beams for buckling length factor K = 1, designated as "Euler", and the numerically determined by geometrically non-linear elastic analysis load-deflection curve of a single pallet beam subjected to compression with a horizontal imperfection 13.5 mm (L/200), provided by Eurocode 3 [29] for buckling curve c, designated as “Single”.

The other curves are denoted by a capital letter and a figure. The letter denotes the loading configuration according to Table 4-2, while the figure the value of the friction coefficient. For example, B-0.3 represents the case (B) of loading by one pallet positioned in the middle of the beam and a friction coefficient of 0.3.

The results show very high resistances for B-100 and E-100, indicating that if the pallets are mechanically connected with the beams, no buckling would occur since the pallets would laterally restrain the beams or at least the middle part of it. For clarity reasons, the envelope of the curves is presented as a grey shaded area; this area is bounded by the cases B-0.1 and A-100. It is observed that the shaded area that refers to realistic conditions of the friction coefficient and the placement of pallets on the beam is bounded by the Euler buckling load and the curve of the beam with initial imperfections. This indicates that the presence of the pallets offers some diaphragm action and makes the system stiffer; however this increase in stiffness is not sufficient to reduce the buckling length so that all beams ultimately fail in the first buckling mode. In relation to Table 4-4 it may be said that the proposed values of the buckling length reduction factor K are not confirmed by the present study.

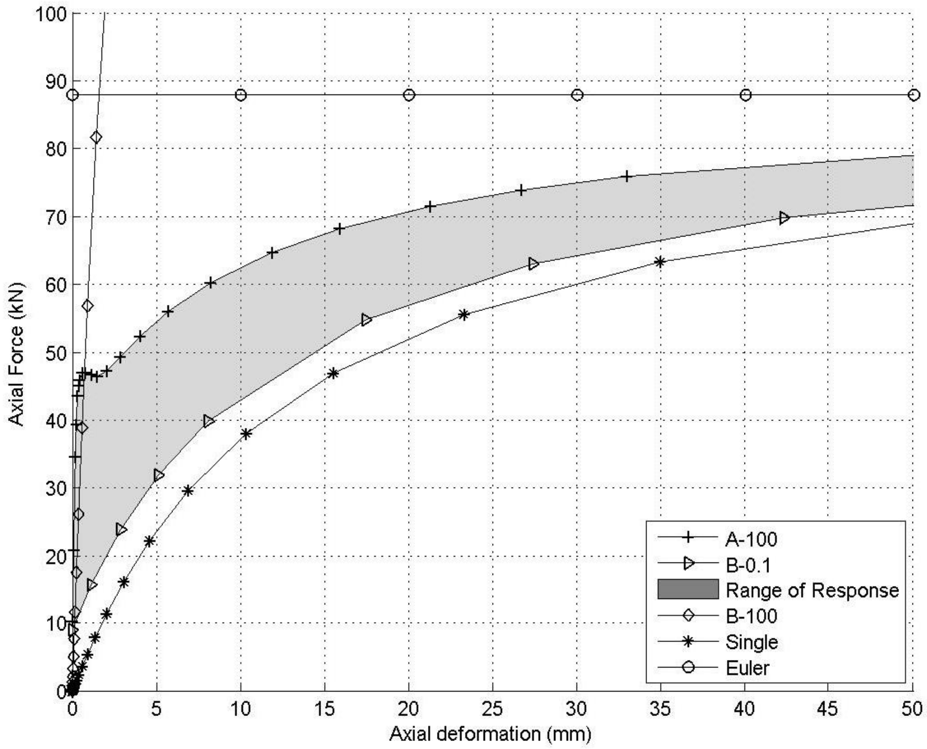

Figure 4-20 Load vs. deformation curve for pallet weight 8 kN

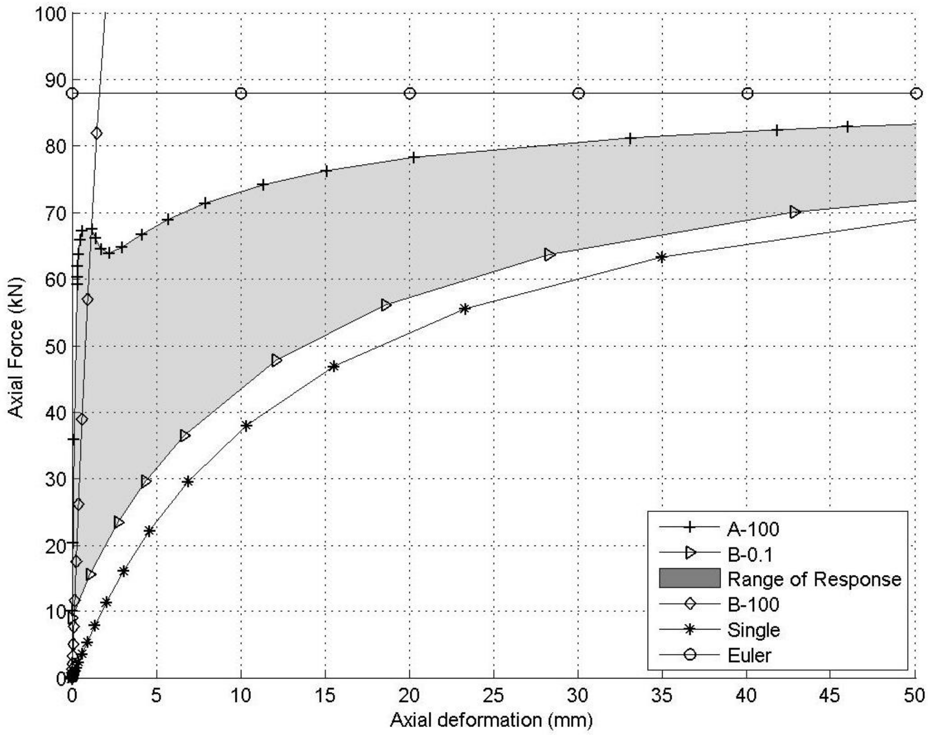

Figure 4-21 Load vs. deformation curve for pallet weight 12 kN

4.5 Conclusions

This paper deals with steel storage racking systems in seismic areas and more specifically with the seismic design of their pallet beams. Employing analytical and numerical methods, the provisions of the current European Codes were examined and reassessed. The conclusions with respect to the investigated issues are here summarized.

Regarding the lateral forces on pallet beams, it was found that:

- Unlike the Code provisions the lateral forces are not equally distributed between the two supporting pallet beams.
- The distribution of the lateral forces is strongly influenced by the elevation of the pallet mass, in respect to the beam top flanges, as well as by the friction coefficient and the width of the rack.
- The beam forces directed towards the outside of the rack are higher than those predicted by the Codes and it is strongly recommended to determine them according to Eq. (4-19)

- The latter explicates why the permanent deformations of some beams, after strong earthquakes are always directed towards outside the rack. (see Figure 4-2 and Figure 4-3)

Concerning the influence of the pallets, through a diaphragmatic action, on reducing the horizontal bending moments of the beams, it was found that:

- Reduction coefficients for the horizontal bending moments were confirmed only before and at the very beginning of the sliding effect.
- It is therefore proposed instead of using correction-reduction factors on the horizontal bending moments, to determine these based on the lateral seismic forces, as defined by Eq. (4-15) and Eq. (4-19).

Finally, about the buckling length of the beams in the horizontal plane, it was found that:

- The frictional forces, due to the presence of pallets on a beam, could not prevent sufficiently the beams from buckling according to the dominant buckling mode
- The buckling length should be equal to the beam’s length, if no mechanical connection between the two opposite beams is used.

4.6 References

1. Gilbert, B. P., Teh, L. H., Badet, R. X., Rasmussen, K. J. R. The influence of pallets on the behaviour and design of drive-in steel storage racks – Part I Behaviour. Fifth International Conference on Structural Engineering, Mechanics and Computation, 2013a Cape Town, South Africa.
2. Gilbert, B. P., Teh, L. H., Badet, R. X., Rasmussen, K. J. R. (2013). The influence of pallets on the behaviour and design of steel drive-in storage racks - Part II Design. Research and Applications in Structural Engineering, Mechanics and Computation - Proceedings of the 5th International Conference on Structural Engineering, Mechanics and Computation, SEMC 2013 (pp. 1285-1290). CRC Press.
3. Hua V., Rasmussen K. J. R. (2010), Static friction coefficient between pallets and beam rails and pallet shear stiffness tests, Research Report 914, School of Civil Engineering, The University of Sydney, Australia.
4. Castiglioni C. A., et al., (2007), Storage Racks In Seismic Areas (SEISRACKS), Research Programme of the Research Fund for Coal and Steel RTD, Final Report, May 2007
5. Coulomb C. A, (1776), Essai sur une application des regles de maximis et minimis a quelques problemes relatifs a l'architecture, Memoires de Mathematique et de Physique (Vol. 7, pp.343-382). Academie Royale des Sciences, Paris.
6. Morin A. J., 1833, New friction experiments carried out at Metz in 1831-1833. In Proceedings of the French Royale Academy of Sciences (Vol.4, pp. 1-128)
7. Stribeck, R. (1902): "Die Wesentlichen Eigenschaften der Gleit- und Rollenlager – The Key Qualities of Sliding and Roller Bearings." Zeitschrift des Vereines Deutscher Ingenieure, 46:38,39, pp. 1342– 48,1432–37.
8. Karnopp D., 1985, Computer simulation of stick-slip friction in mechanical dynamic systems, journal of Dynamc systems, Measurment and control, 107(1), 100-103
9. Armstrong B., Dupont P., Canudas de Wit C., 1994, A survey of models, analysis tools and compensation methods for the control of machines with friction Journal Automatica (Journal of IFAC Volume 30 Issue 7, July 1994 Pages 1083-1138

10. Olsson H., Astrom K. J., Canudas de Wit C., Gäfvert M., Lischinsky P., 1998, Friction models and friction compensation. European Journal of Control, 4(12), 176-195.
11. Yang Z., Zhang H. P., Marder M., Dynamics of static friction between steel and silicon, Proceedings of the National Academy of Sciences, 2008
12. Dahl P. R., (1968). A solid Friction Model, The Aerospace Corporation, El Segundo, CA, Technical Report, TOR-0158(3107-18)
13. Dahl P. R., (1975). Solid friction damping of spacecraft oscillations. In AIAA Guidance and Control Conference. AIAA Paper NO. 75-1104, Boston, USA
14. Dahl P. R., (1976). Solid friction damping of mechanical vibrations. AIAA Journal, 14(12), 1675-1682
15. Bliman, P. A. and Sorine M., (1991): “Friction Modelling by Hysteresis Operators. Application to Dahl, Sticktion and Stribeck Effects.” In Proceedings of the Conference “Models of Hysteresis”, Trento, Italy.
16. Bliman P. A. and Sorine M., (1993): “A System-Theoretic Approach of Systems with Hysteresis. Application to Friction Modelling and Compensation.” In Proceedings of the second European Control Conference, pp. 1844–49, Groningen, The Netherlands.
17. Bliman, P. A. and Sorine M., (1995): “Easy-to-use Realistic Dry Friction Models for Automatic Control.” In Proceedings of 3rd European Control Conference, Rome, Italy, pp. 3788–3794.
18. Rabinowicz, E., (1951): “The Nature of the Static and Kinetic Coefficients of Friction.” Journal of Applied Physics, 22:11, pp. 1373–79.
19. Degée H., Denoël V., (2006), “An investigation on the sliding of pallets on storage racks subjected to earthquake”. Proc. 7th National Congress on Theoretical and Applied Mechanics, Faculté Polytechnique de Mons, Belgium.
20. Yang F., 1996, Vibrations of cable-stayed bridges under moving vehicles (Ph.D thesis, University of Liege)
21. Bournas, D., Negro, P., Taucer, F., (2013), “The Emilia earthquakes: report and analysis on the behavior of precast industrial buildings from a field mission”, Papadrakakis, M. et al (ed.), Proc. COMPDYN 2013 Conf.,Kos, Greece
22. Castiglioni, C. A., (2016), Seismic behavior of steel storage pallet racking systems, Springer International Publishing, Switzerland.

23. ITSAK (2008). “The earthquake of Achaia-Ilia 8.6.2008”. Institute of Technical Seismology and Aseismic Structures, Thessaloniki, Greece
24. FEM 10.2.08 (2011), Recommendations for the design of static steel pallet racks in seismic conditions, Version 1.04, 2011, FEM- European Racking Federation.
25. EN 16681:2016. Steel static storage systems — Adjustable pallet racking systems — Principles for seismic design, CEN, Brussels, Belgium.
26. ABAQUS (2008). ABAQUS User’s Manual. Version 6.8 EF-2, Dassault Systèmes Simulia Corp., Providence, RI, USA.
27. Adamakos K., Vayas I. (2014). “Tragverhalten von Palettenregalsystemen unter Erdbebenbeanspruchung.” Stahlbau, Ernst & Sohn, 83 (1), p.36-46.
28. Castiglioni, C. A., et al, (2014), EUR 27583 EN: Seismic behavior of steel storage pallet racking systems (SEISRACKS2), Final Report, RFSR-CT-2011-00031, European Commission, DG Research, Brussels, Belgium.
29. EN 1993-1-1 (2003): Eurocode 3. Design of Steel Structures, Part 1-1: General rules and rules for buildings, European Committee for Standardization.
30. EN 1993: Eurocode 3: Design of Steel Structures, European Committee for Standardization, Brussels, Belgium.
31. EN 15512 (2009). "Steel static storage systems - Adjustable pallet racking systems - Principles for structural design." European Committee for Standardization (CEN), Brussels, Belgium.
32. EN 1998-1-1 (2004). Eurocode 8. Earthquake resistant design of structures. Part 1-1 General rules and rules for buildings, European Committee for Standardization (CEN), Brussels, Belgium.
33. FEM 10.2.02 (2000). The Design of Static Steel Pallet Racking, Federation Europeenne de la Manutention Section X Equipment et Proceedes de Stockage.

5. Conclusion, scientific contribution and proposals for further research

5.1 Conclusions

The conclusions of the present dissertation refer to two different issues: First the seismic response and seismic design of racks and second the interaction between pallets and pallet beams that affect the final design not only of a pallet beam but also of a whole system.

The conclusions on the seismic design and response of racking systems are summarized as following:

a) Numerical simulations of racking systems based on nominal values for the component members and assemblies are very often not realistic and cannot predict adequately the actual dynamic properties of the systems. As a result they should be supported by experimental tests on the level of subassemblies.
b) Nonlinear static, pushover, analyses that are based exclusively on theoretical and/or numerical data overestimate the ductility of the system, leading to very high values of the behavior factors
c) Nonlinear dynamic analyses indicate that the available ductility of the systems is usually limited
d) Values of the behavior factors employed in design practice are notably lower than the proposed ones by the norm, however, they seem to be more realistic
e) The available ductility of the systems has its main source to the overstrength
f) Since the large portion of the behavior factor determined by pushover analyses is derived from the overstrength, it indicates the need for an alternative q factor definition, different than the usual one for buildings, especially for racks.
g) The application of a complete capacity design for racking systems is necessary, in order to achieve a progressive failure mechanism that would result in the safe use of the proposed by the norm or even higher values of the

behavior factor with confident, and that would lead to lighter structures and more economic solutions

The conclusions on the seismic design of pallet beams may be summarized as following, where reference is made to European codes:

a) The normative documents describe well, but in a static manner, the global sliding event
b) Pallet beams are subjected to horizontal seismic forces that are sometimes much higher than the described ones by the codes
c) The parameters that found to influence the maximum developed horizontal forces on a pallet beam in case of sliding are the elevation of the center of mass of the pallet, the distance between the faced pallet beams, the friction coefficient and the weight of the pallet
d) The normative provisions of EN16681 concerning the reduction of the out-of-plane bending moments on the pallet beams were not confirmed
e) In case of pallets' sliding, the existence of the pallets on the pallet beams was found not to offer a diaphragm action on the system
f) The buckling length of the pallet beams should not be reduced due to the existence of the pallets, as the initiating of the buckling enforces local sliding and the initially partial diaphragm is suspended.

5.2 Scientific contribution

The present thesis is one of the few researches about steel storage pallet racking systems against seismic actions. There are surely many published works about them, but they are still few in comparison to the conventional structures. There are two main parts in this thesis; the one concerns the evaluation of the seismic response of conventional racks in a global response-level and the second one is the investigation of the seismic actions on the pallet beams, from a local point of view.

The first part of the thesis could contribute in the research concerning racking systems providing a guideline for the application of static nonlinear analyses in these systems. A step by step methodology is presented about how to run pushover analyses and numerous numerical result are presented for real case studies provided by real manufactures, comparing also the numerical results with experimental full scale test that were performed in other collaborated universities. The maximum available behavior factor for each different system is given, categorizing the results depending on the different types of configurations. Moreover, this first part of the thesis provides also the guidelines for the performance of dynamic analyses, or even incremental dynamic analyses, accompanying by a rough probabilistic analysis and a final evaluation of the dynamic behavior of racks that are designed according to the latest European norms. The thesis is one of the first ones that present results of an Incremental dynamic analyses applied to racking systems, providing a completed evaluation of the seismic response of those systems and proposing specific values of the behavior factor for unbraced racks in the down and cross aisle direction.

The second part of the thesis eliminates the doubts around the design of the pallet beams under seismic actions. Although the present norms are extensively referred to the pallet beams, the herein included reports and pictures show a lot of cases of failure at the pallet beams. Chapter 4 investigates the influence of the pallets on the pallet beams during an earthquake event and mainly proposes new formulas for the pallet beams' horizontal actions that result in the sliding of the pallet and in bending moments around the minor axis of the beams; facts that many times have led to partial collapse of the racks, or even, fall of the pallets down to the floor. This part amends also the proposed tables (by the European norm EN16681) that are referred to the out of plane bending of the pallet beams, their buckling length and generally gives an answer to a question of major importance that concerns many researchers; whether or not the existence of the pallet could offer a diaphragm action on the pallet beams, making the system stiffer, and able to redistribute the forces, in case of local failures.

5.3 Proposals for further research

Although the present study includes numerous analyses and investigates many of the hot topics around the steel storage pallet racks, there are apparently many other issues that are related to the research of the present thesis and that were not investigated. Thus, some interesting issues for further research are proposed for investigation.

A first aspect that would support the present research would be the performance of incremental dynamic analyses for braced racks. It requires very special and complicated numerical models that should be based on experimental results.

Application of the proposed methodology of chapter 3 to braced models could verify and propose the appropriate values of the behavior factor for these systems.

Next, a capacity design should be organized and proposed in order to avoid such brittle collapse modes, as exhibited by the experiments and the numerical results. The use of low values of the behavior factor does not oblige the engineers to perform a capacity design for the system. However, since the racks do not allocate high levels of ductility, there are many cases that the most brittle mechanisms (i.e. the shear failure of connected bolts) are firstly developed. Thus, a capacity design is highly proposed to be settled, in order to be able to provide more sufficient inelastic behavior in these systems.

Finally, a proposal for further research could be the dynamic investigation of the sliding event on the pallet beams. Chapter 4 of the present thesis presents results for a pseudo static investigation of the interaction that exist between pallets and pallet beams. Dynamic models tested under harmonic loading or even better under real earthquake excitations could be the most accurate to describe the whole phenomenon with completeness, evaluating dynamically the proposed formulas presented in chapter 4.

6. Appendix A

Post-testing calibration of numerical models to experimental tests

6.1 Introduction

The objective of this appendix is to present a method for calibration of numerical models to experimental investigations such as those performed during the SEISRACKS2 for racks of the industrial partners. The components where tests were performed and calibrations done were the beam-end-connectors, the base-plates and the upright sections.

The behavior in down aisle direction is highly influenced by the properties of the beam-end-connectors, of the base-plates, the existence of the vertical bracings and the upright sections in respect to bending around their major axis. The cross aisle direction is governed by the behavior of the diagonal members, the upright sections in respect to bending around their minor axis, and generally the global shear stiffness of the upright frames. The latter is apparently directly affected by all previous components, although the shear stiffness determined experimentally is less than the calculated one when the latter is based on the analytical formulae. This is due to the looseness of either the single bolts or the hooked connections. This is the reason why both normative documents FEM10.02.08 and EN16681 require the execution of experimental tests for each different configuration that appears in the market.

Experimental tests during SEISRACKS2 were performed in three Universities and in particular in the University of Liege for tests on the shear stiffness of uprights frames, under monotonic and cyclic loading, in RWTH Aachen for tests on base-plates, beam-end-connectors and in Politecnino di Milano on complete racking systems.

The post testing calibration procedure presented here refers to monotonic and cyclic tests and was used to define reliable numerical models to be used in nonlinear static and dynamic analyses. In addition to experimental results, results of detailed numerical analyses on upright members to bending with axial force were introduced in global numerical models using Opensees [1].

6.2 Beam-end-connectors

Experimental monotonic and cyclic tests have been performed in down aisle direction for different pay load levels in order to identify the properties of the semi-rigid beam-to-column type connections, the so called beam-end-connectors. The cyclic tests detected a hysteretic behavior that included pinching strength and stiffness degradation. The tests for a fully loaded configuration (3 pallets of 800kg per compartment) were used for calibration as they represent the most severe condition in the global model.

All tests have been simulated using the exact geometry, the loading protocol, the used cross sections and the constraints or restrains of the system. Figure A- 1 shows a sketch of the experimental configuration. In order to distribute uniformly the horizontal applied load, a horizontal rigid beam, indicated in red, is installed as extension of the jack. This is simulated constraining the two top nodes in the longitudinal direction.

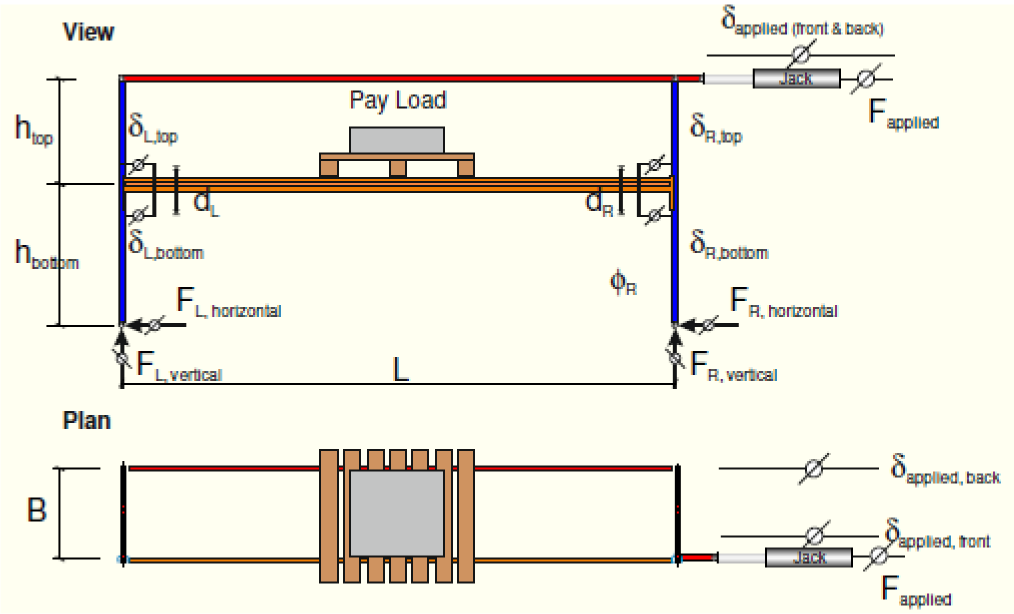

Figure A- 1 Experimental configuration for the characterization of the beam-end-connectors performed in RWTH Aachen

The beam-end-connectors are hooked-in semi-rigid connections and they are conventionally simulated with rotational springs, either linear or nonlinear with one or two nodes (depending on the software). In the current case the springs are governed by a cyclic non-linear moment-rotation law. The selected material mode provided by Opensees is the Hysteretic Material. This is defined by a positive and a negative skeleton curve and four additional parameters that influence the loading and unloading stiffness of the connector, strength degradation the pinching. The hooks of the connector need severe tolerance in the corresponding holes in order to be easy-installed; this tolerance makes the stiffness gradually zero when the assembly is almost unloaded, creating looseness and as a result the pinching phenomenon. During the cycles of the loading history and when the connector is highly loaded, the hooks deforms plastically, the perforations of the upright are becoming bigger and bigger and thus the degradation and the pinching intensify.

Figure A- 3 and Figure A- 4 present experimental and numerical results for the different tested configurations. It may be seen that the calibration procedure was adequate to produce a high similarity between experimental and numerical predictions. The calibration took place selecting the appropriate parameters for the hysteretic model defined graphically in Figure A- 2. The calibrated values of the parameters are shown in Table A- 1. The diagrams present the curves in terms of bending moment (M) over yield moment at the first significant yielding point of the connector (My) in the vertical axes and rotation (r) over the corresponding rotation at the first significant yield (ry).

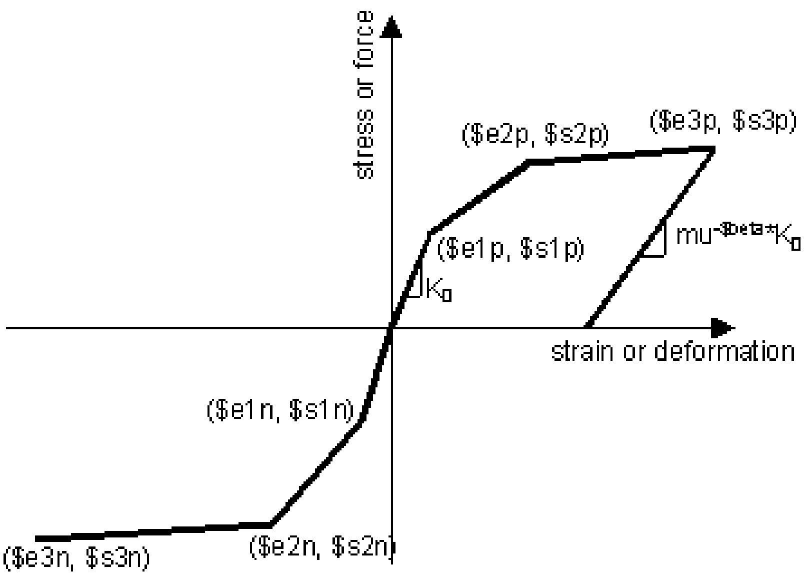

Figure A- 2 Skeleton curve of the spring elements used in Opensees

Industrial partner	A		B		C		D	
$e1p-$s1p	1	1	1	1	1	1	1	1
$e2p-$s2p	1.07	2.3	1.5	3.33	1.4	3	1.16	3.2
$e3p-$s3p	0.24	6	0.73	11.33	1.3	15	0.5	6
$e1n-$s1n	-0.95	-1	-1	-1	-1	-1	-0.93	-0.84
$e2n-$s2n	-1	-2.5	-1.33	-3.33	-1.63	-7.5	-1.06	-3.2
$e3n-$s3n	-0.38	-6	-0.73	-11.33	-1.3	-18	-0.5	-6
$pinchX	0.8		0.8		0.8		0.8	
$pinchY	0.5		0.5		0.5		0.5	
$damage1	0		0		0		0	
$damage2	0		0		0.1		0	
$beta	0		0.3		0		0	

Table A- 1 Values of the hysteretic spring parameters for the beam-to-column connections

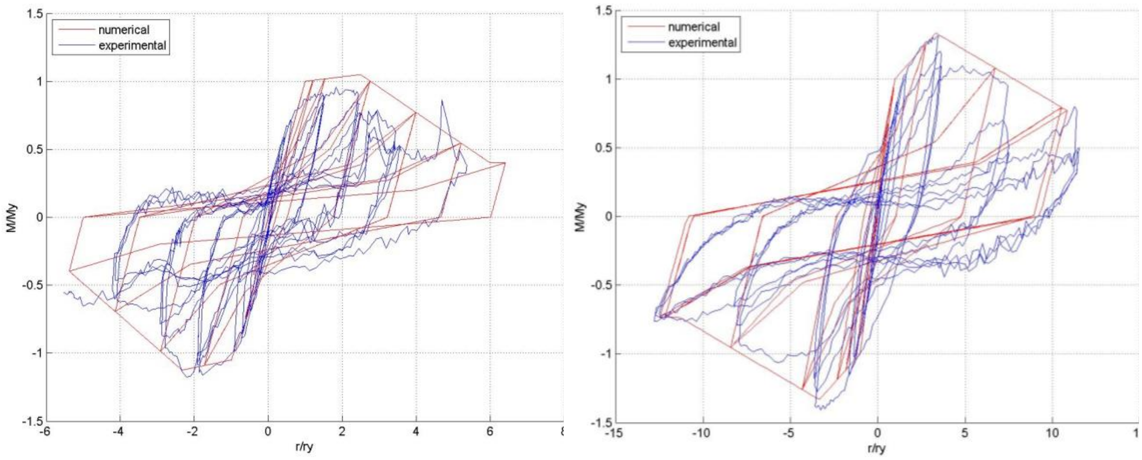

Figure A- 3 Moment-rotation diagram for a) BEC provided by IP-A, b) BEC provided by IP-B

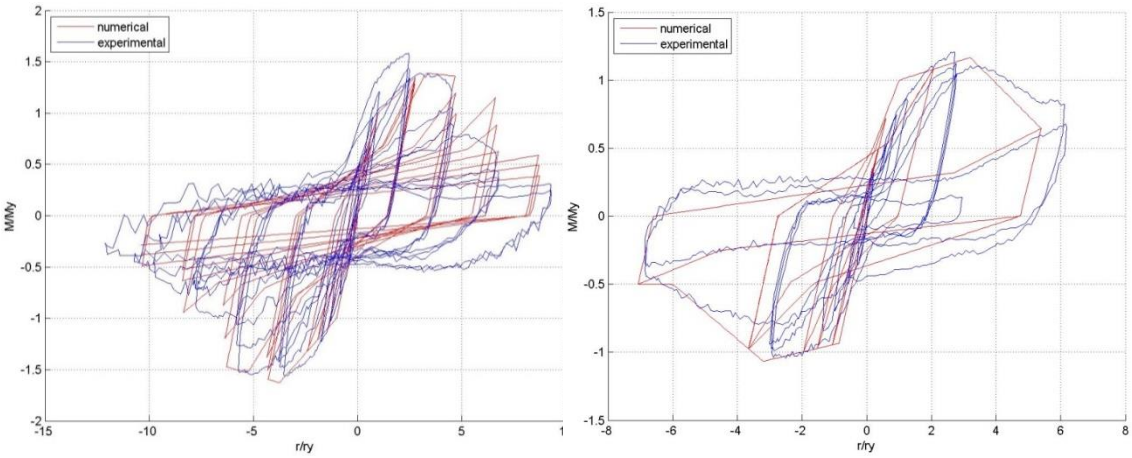

Figure A- 4 Moment-rotation diagram for a) BEC provided by IP-C, b) BEC provided by IP-D

6.3 Base-plates

Tests on base-plate connections were performed using a single upright member supported on a base-plate and then on a rigid steel plate, representing a stiff concrete slab. The uprights are short, about 45cm, and extended by a rigid member. On the top they were pinned as depicted in Figure A- 5. The specific tests have the objective to determine the rotational stiffness of the connection to monotonic and cyclic loading, as well as the moment capacity and the moment-rotation law of the assembly. The upright members were loaded on the top with an imposed horizontal displacement, under a simultaneous constant axial load of 48 kN. The numerical model consists of a single beam element that is connected to a rotational non-linear spring at the base-plate and is pinned on the top. The spring's moment rotation law is defined by the same hysteretic material of Opensees as presented before in Figure A- 2. Figure A- 6 and Figure A- 7 present graphically the results of the calibrated numerical models and the corresponding experimental ones. It may be seen that the hysteretic model and the selected values of the parameters are appropriate for the description of the base-plate behavior.

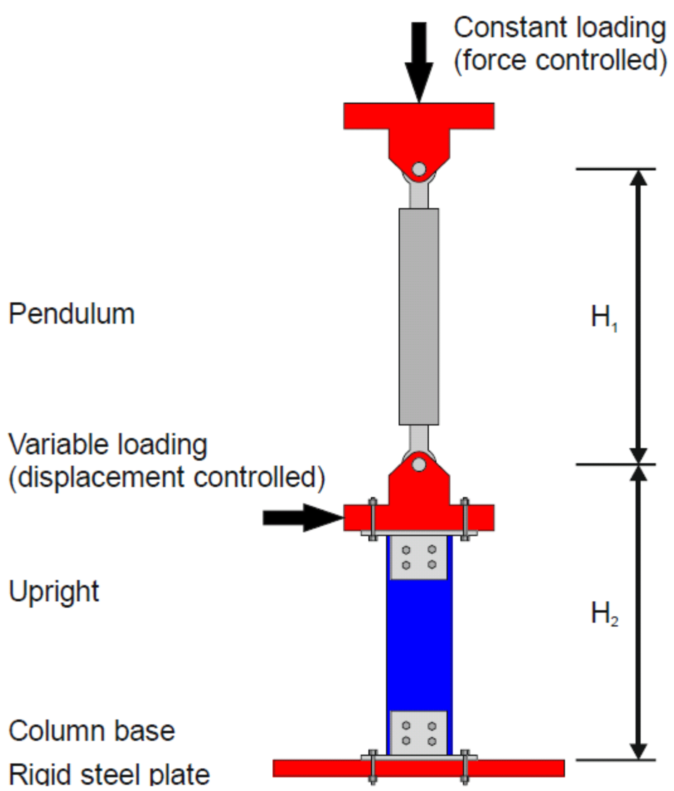

Figure A- 5 Experimental configuration for tests on the base-plates (RWTH Aachen)

Industrial partner	A		B		C		D	
$e1p-$s1p	1	1	1	1	1	1	1	1
$e2p-$s2p	1.56	8.57	1.25	4.54	1.02	5	1.18	7.5
$e3p-$s3p	0.8	21.4	0.5	13.6	0.67	16.6	0.3	25
$pinchX	0.35		0		1		0	
$pinchY	0.15		0		0.4		0.1	
$damage1	0		0		0		0	
$damage2	0		0		0		0	
$beta	0		0		0.4		0	

Table A- 2 Values of the hysteretic spring parameters for the base plate

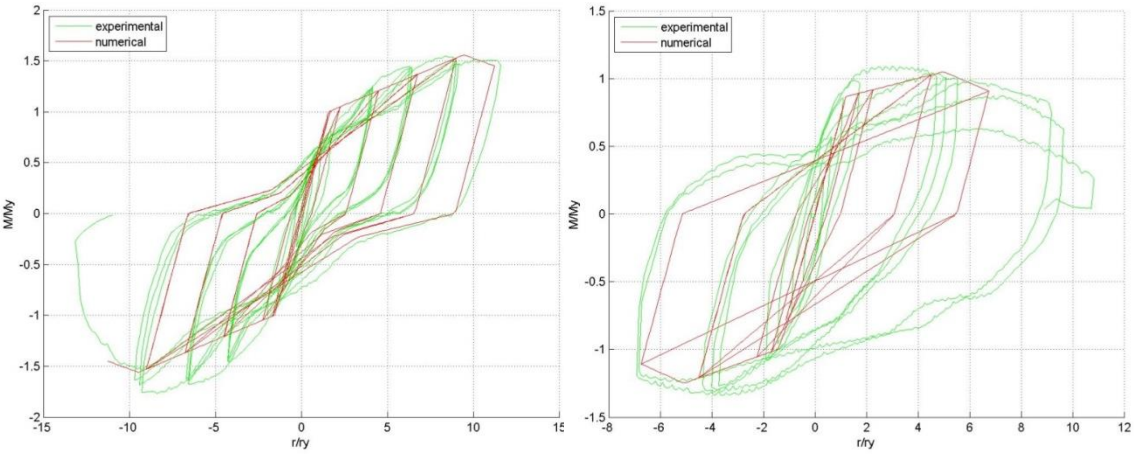

Figure A- 6 Moment-rotation diagram for a) BP provided by IP-A, b) BP provided by IP-B

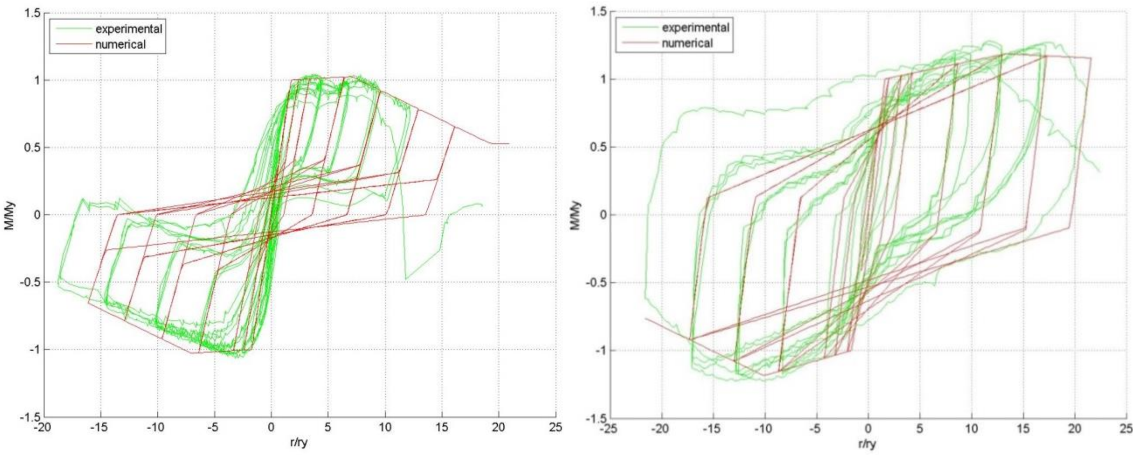

Figure A- 7 Moment-rotation diagram for a) BP provided by IP-C, b) BP provided by IP-D

6.4 Upright's behavior

The uprights are composed of perforated open, thin walled sections. The prediction of the behavior of such members is remarkable difficult by analytical methods. Therefore, experimental and/or detailed numerical methods should apply to define the behavior to cyclic loading. Experimental tests on isolated uprights were not scheduled in the frame of SEISRACSK2, so their response to cyclic loading has to be determined by application of numerical tools. Abaqus software [2] was used to simulate a single upright member of 1m, with shell elements and the exact geometry provided by the industrial partners. The uprights' behavior is investigated separately for the major and minor axis. An axial loading of 48 kN (corresponds to a middle upright of a fully loaded configuration) is applied and a non-linear monotonic analysis is performed in order to define the yield displacement of each examined upright for each direction. Subsequently the cyclic response is studied applying cyclic displacements ±δy, ±2δy, ±3δy, ±4δy. Analyses are material- and geometry-non-linear. The material law takes into account hardening of steel, supposing that due to cold-forming the material has no distinct yield point, plateau region etc. Accordingly, the material follows a continuous bilinear stress strain law.

The required diagrams to introduce in Opensees software for global analyses are moment-curvature curves that describe the plastic-hinge's properties for the upright members. The plastic-hinge cyclic behavior is described by the hysteretic model presented in Figure A- 2. This is accomplished using Eq.(A.1) which describes the relation between plastic rotation and plastic curvature as proposed by Naderpour, 2007 [3].

$$\theta_p = \int_0^{l_y} [\varphi(\chi) - \varphi_y]\, dx \qquad \text{(A-1)}$$

In Eq. (A-1) θp is the plastic hinge rotation on each side, ly is the length of the beam over which the bending moment is larger than the yielding moment, φ(x) is the curvature at a distance x from the critical section and φy is the yielding curvature. Using Eq. (A-1) one can easily calculate the relation between the rotation and the curvature of a critical section of a plastic hinge. A simplified expression of the above equation is given by Eq. (A-2):

$$\theta_p = (\varphi_u - \varphi_y) l_p = \varphi_p l_p \tag{A-2}$$

where, φu and φy is the curvatures at the ultimate load and yielding, respectively and φp is the plastic hinge curvature.

The plastic hinge length was derived by the analysis, measuring the length over which the von Mises stress is higher than the equivalent nominal yield stress. This length is depicted with grey in Figure A- 8 and Figure A- 9.

As the objective is to define an equivalent reliable and calibrated model in Opensees software, a model was created in Opensees, using beam elements, with distributed plasticity in a length equal to the previously defined l_p. The nominal inertial and geometric properties are used for the beam model, which is loaded exactly as in Abaqus model. The supports of the two models are exactly the same; in particular, the base point is pinned and the top point is fixed with releases for the translation on the two loading directions (axial direction and one of the two other horizontal directions). Figure A- 8 and Figure A- 9 show the behavior of a typical upright cyclic loaded on the major and minor axis respectively as exported from Abaqus. It should be mentioned that the plastic hinge forms due to local buckling of the section, while outside it the compression stress does not exceed the yield stress.

In the Abaqus model bending moments at the base point and member rotation are directly recorded, while in Opensees they are calculated, using the displacement and the imposed load of the top node. The bending moment is equal to M=Fl, the member's rotation to θ=Δ/l, where F is the imposed force, Δ is the top displacement and l the examined length. Figure A- 10 to Figure A- 15 present moment-rotation curves from the previously described Abaqus-analyses in comparison to the calibrated Opensees-results, using Eq.(A-2) and the parameters for the uprights of each IP, presented in Table A- 3, Table A- 4 and Table A- 5.

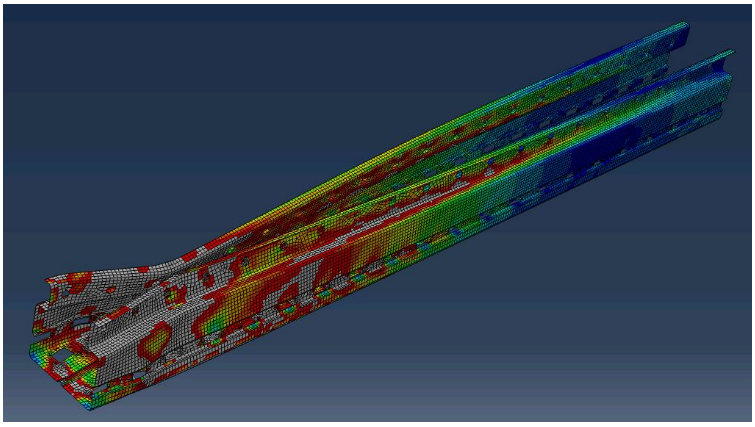

Figure A- 8 Failure mode of upright for bending around the major axis

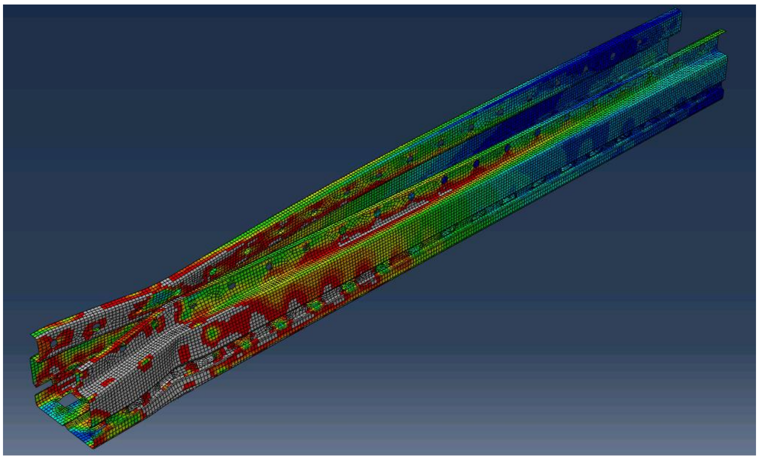

Figure A- 9 Failure mode of upright for bending around the minor axis

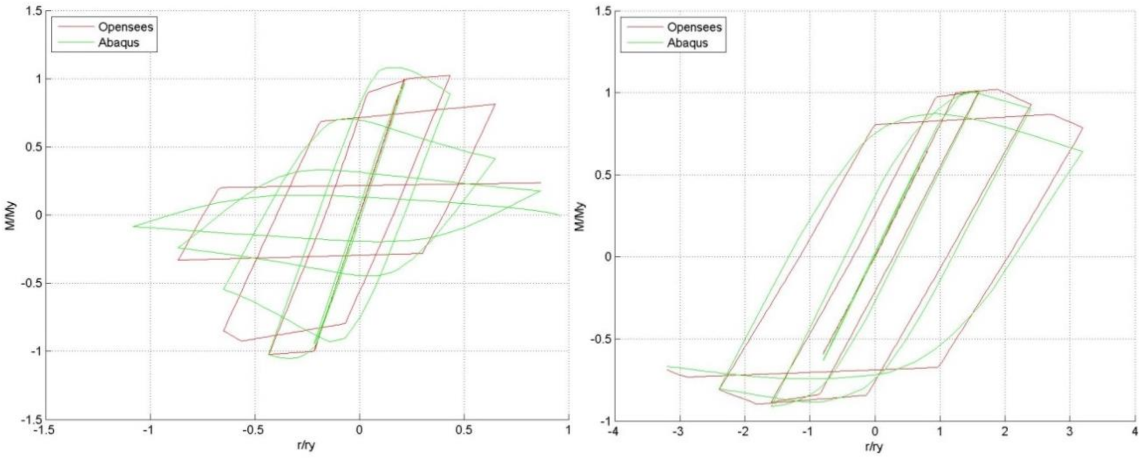

Figure A- 10 Moment-curvature diagram for IP-A

a) Major axis bending **b) minor axis bending**

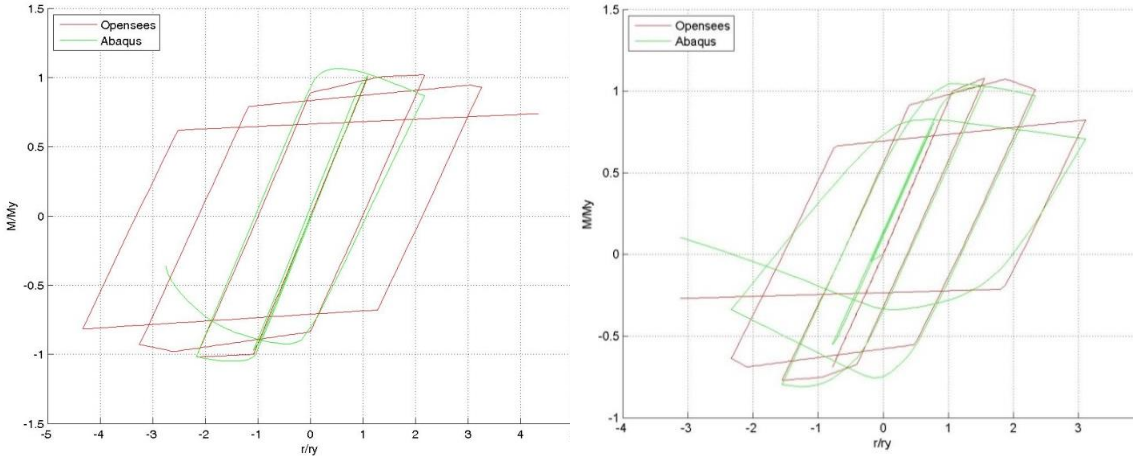

Figure A- 11 Moment-curvature diagram for IP-B

a) Major axis bending **b) minor axis bending**

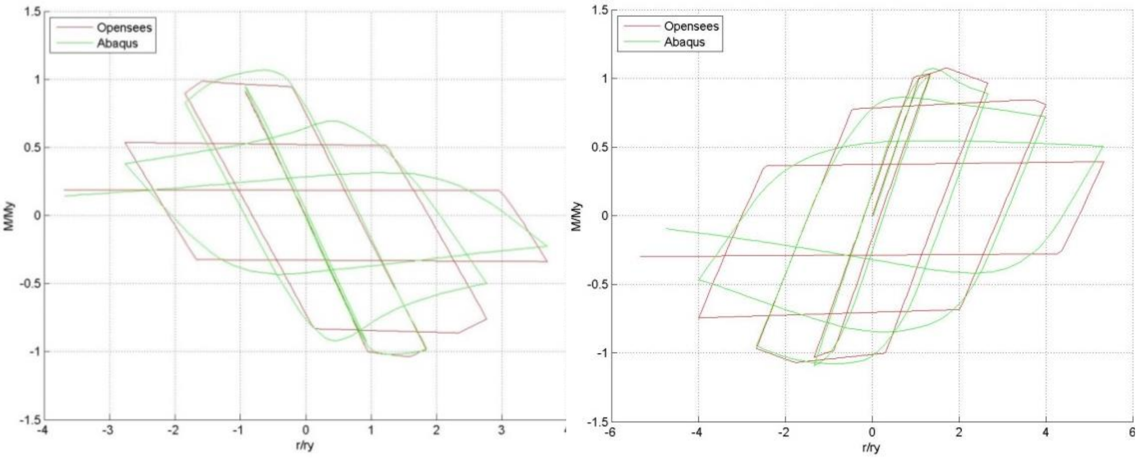

Figure A- 12 Moment-curvature diagram for IP-C for the high seismicity configuration

a) Major axis bending **b) minor axis bending**

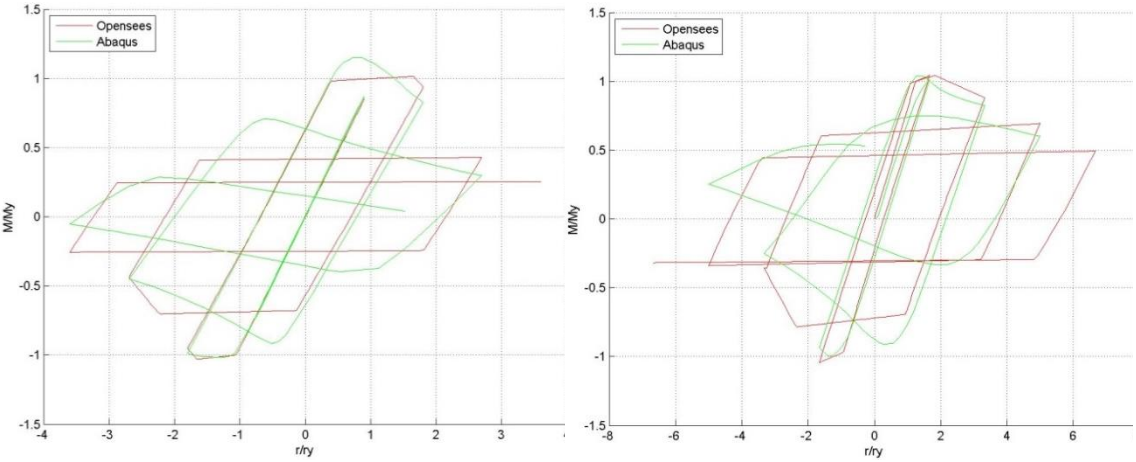

Figure A- 13 Moment-curvature diagram for IP-C for the medium seismicity configuration

a) Major axis bending **b) minor axis bending**

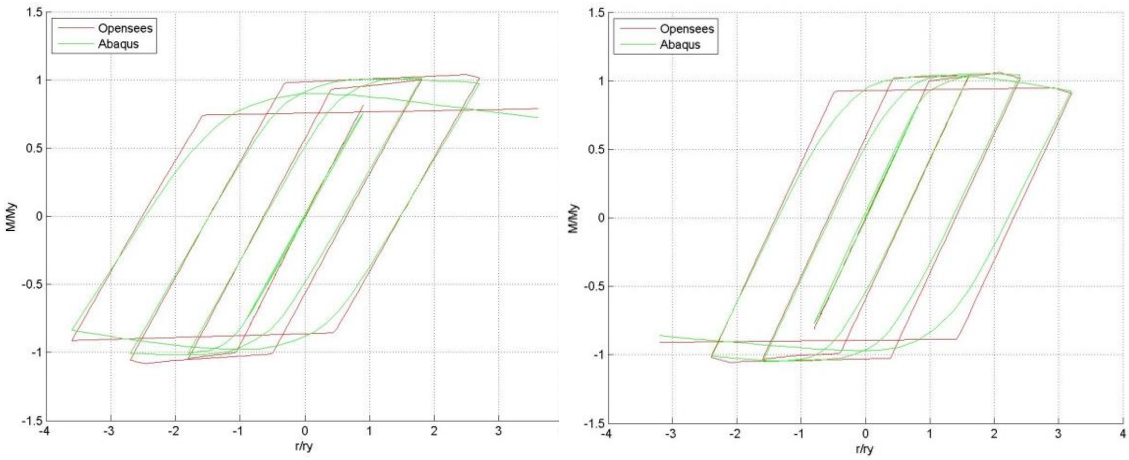

Figure A- 14 Moment-curvature diagram for IP-D for the high and medium seismicity configuration

a) Major axis bending **b) minor axis bending**

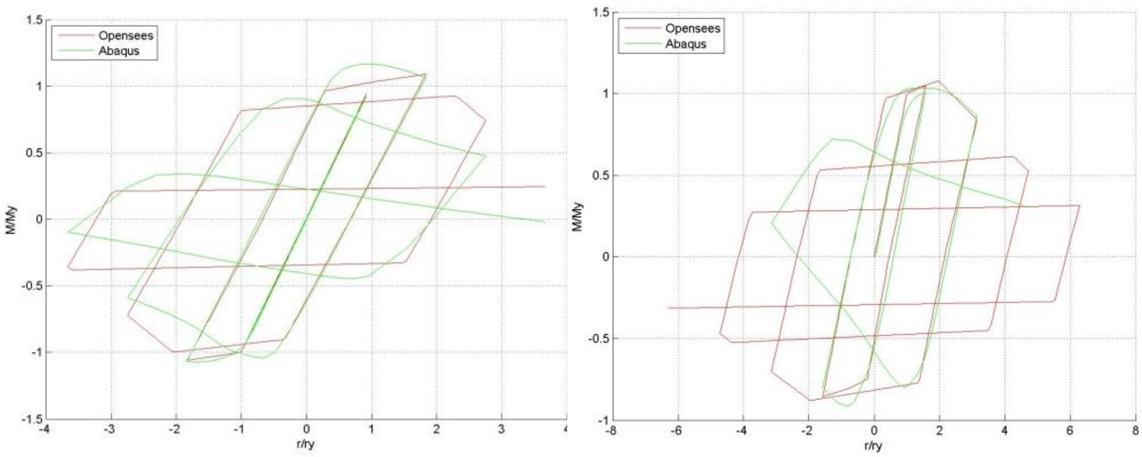

Figure A- 15 Moment-curvature diagram for IP-D for the low seismicity configuration

a) Major axis bending **b) minor axis bending**

Industrial partner	A				B			
	Low/High				Low/High			
	Major		Minor		Major		Minor	
$e1p-$s1p	1	1	1	1	1	1	1	1
$e2p-$s2p	1.02	2.16	1.02	1.58	1.02	2	1.1	1.6
$e3p-$s3p	0.25	6.67	0.2	5.88	0.19	12	0.75	4
$e1n-$s1n			-0.85	-1			-0.75	-0.8
$e2n-$s2n			-0.89	-1.53			-0.77	-1.6
$e3n-$s3n			-0.2	-5.88			-0.25	-4
$pinchX	0		0		0		0	
$pinchY	0.9		0.9		0.8		0.75	
$damage1	0.05		0.1		0.2		0.2	

$damage2	0.9	0.05	0	0.2
$beta	0.3	0.18	0.1	0.1

Table A- 3 Used hysteretic parameters for the uprights for each IP and each direction (notation as in Figure A- 2)

Industrial partner	C							
	Medium				High			
	Major		Minor		Major		Minor	
$e1p-$s1p	1	1	1	1	1	1	1	1
$e2p-$s2p	1.03	1.6	1.05	1.43	1.03	1.72	1.07	1.6
$e3p-$s3p	0.26	3	0.52	4	0.32	5.17	0.3	5
$e1n-$s1n					-0.96	-1.03		
$e2n-$s2n					-0.98	-1.72		
$e3n-$s3n					-0.19	-043		
$pinchX	0	0			0		0	
$pinchY	0.95	0.85			0.95		0.9	
$damage1	0.2	0.2			0.2		0.2	
$damage2	0.2	0.2			0.2		0.2	
$beta	0.2	0.25			0.2		0.15	

Table A- 4 Used hysteretic parameters for the uprights for each IP and each direction (notation as in Figure A- 2)

Industrial partner	D											
	Low				Medium				High			
	Major		Minor		Major		Minor		Major		Minor	
$e1p-$s1p	1	1	1	1	1	1	1	1	1	1	1	1
$e2p-$s2p	1.02	1.93	1.13	1.71	1.2	1.8	1.16	2.85	1.08	2.4	1.06	2.5
$e3p-$s3p	0.15	4.38	0.22	4.28	0.25	5.4	0.33	7.14	0.41	8	0.47	7.5
$e1n-$s1n												
$e2n-$s2n												
$e3n-$s3n												
$pinchX	0		0		0		0		0		0	
$pinchY	0.85		0.85		0.92		0.97		0.92		0.96	
$damage1	0.1		0.1		0.2		0.1		0.2		0.1	
$damage2	0.1		0		0.2		0.1		0.2		0.1	
$beta	0.15		0.15		0.09		0		0.09		0	

Table A- 5 Used hysteretic parameters for the uprights for each IP and each direction (notation as in Figure A- 2)

Although the uprights are mainly subjected to bending moments and/or axial forces there are some configurations for which the shear forces are significantly high and the experiments showed failure due to these extreme shear forces. Such cases were also studied with Abaqus especially for IP-B by a non-linear static analysis. High shear forces develop in the uprights due to fact that the consecutive diagonals are not connected at the same perforation of the upright, but at two different consecutive perforations. Accordingly, their axes do not meet at the same point of the upright's axis, but eccentrically resulting in significant shear forces. The uprights are simulated in ABAQUS using elements with an extra fine mess. The material law is bilinear elastic-plastic with hardening. A constant axial force 48kN is applied, and two opposite diagonal forces to two consecutive perforations are applied monotonically in the direction of the diagonal members. The deformed shape of the upright and the von Mises stresses in the vicinity of the eccentricity are illustrated in Figure A- 16, while Figure A- 17 show the applied shear force vs. the transverse displacement. In Opensees software a linearized diagram is introduced.

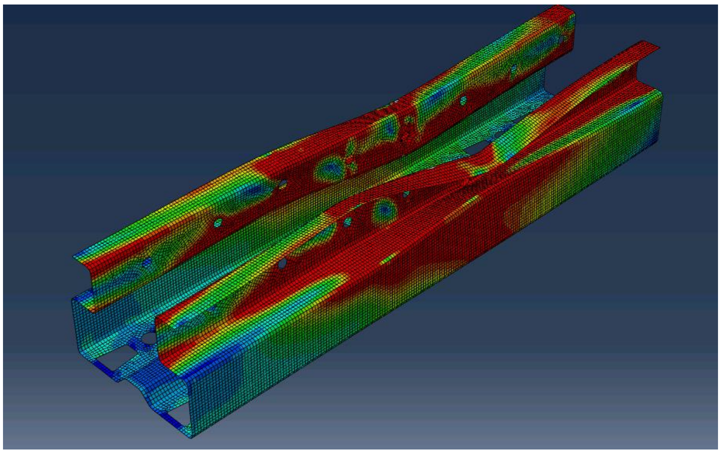

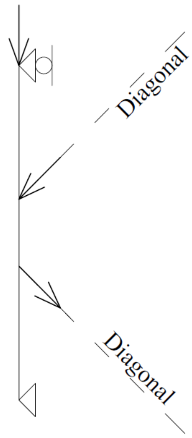

Figure A- 16 Deformed shape of upright member under shear force and examined equivalent static model

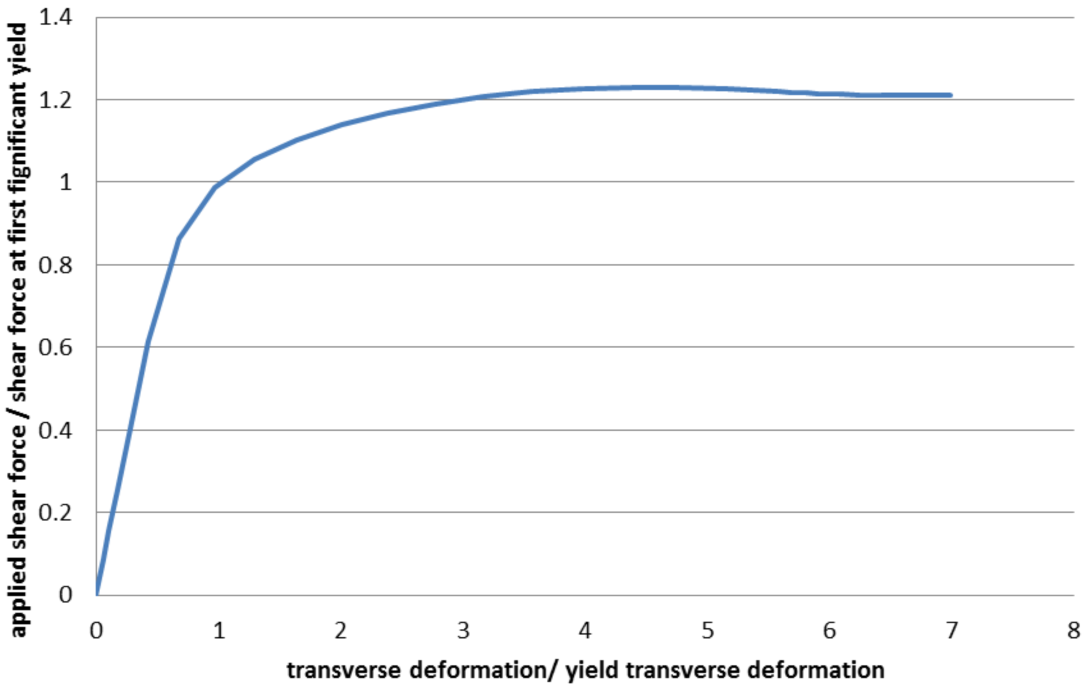

Figure A- 17 Shear force- transverse deformations for upright member of IP-B

6.5 Upright frames

Complete full scale upright frames were tested in the University of Liege in order to identify the structural response in cross aisle direction. Seven configurations provided by the four industrial SEISRACKS2 partners, were tested. Lateral forces were applied along the height in a triangular shape, as presented in Figure A- 18. Such tests are necessary to determine experimentally the shear stiffness of upright frames and assign an equivalent cross-sectional area for the diagonal members, in analysis that provides the same shear stiffness in cross aisle direction. In this research not only the elastic/ initially linear shear stiffness is of interest, but also the pre- and post- failure behavior as well as the maximum capacity and ductility of the systems. Thus, numerical models in Opensees were developed to simulate these tests, calibrate the values of the parameters that provide and use these values in subsequent nonlinear static and dynamic analyses. The numerical models use beam elements with nonlinear properties for the uprights and truss elements with nonlinear properties for the diagonals. The uprights properties were already calibrated as described in paragraph A-4 of this appendix. The properties of the diagonal members are here calibrated to fit as possible to the experimental curves. The previously described hysteretic model of

Opensees is again used for both upright and diagonal nonlinear properties, where the latter are expressed in terms of axial force vs. axial displacement and are given in Table A- 6. Figure A- 19 to Figure A- 22 show the experimental and numerical results, after calibration. The curves are presented in dimensionless form in terms of Vy and dy, which correspond to the “yield” values of the base shear and top displacement, as determined by Eurocode 3.

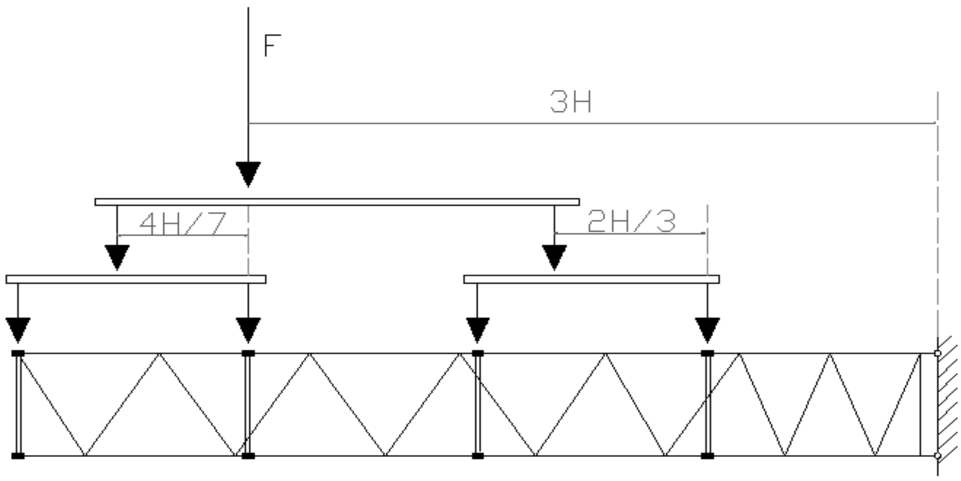

Figure A- 18 Experimental configuration for the upright frames in cross aisle direction for tests performed in Uliege

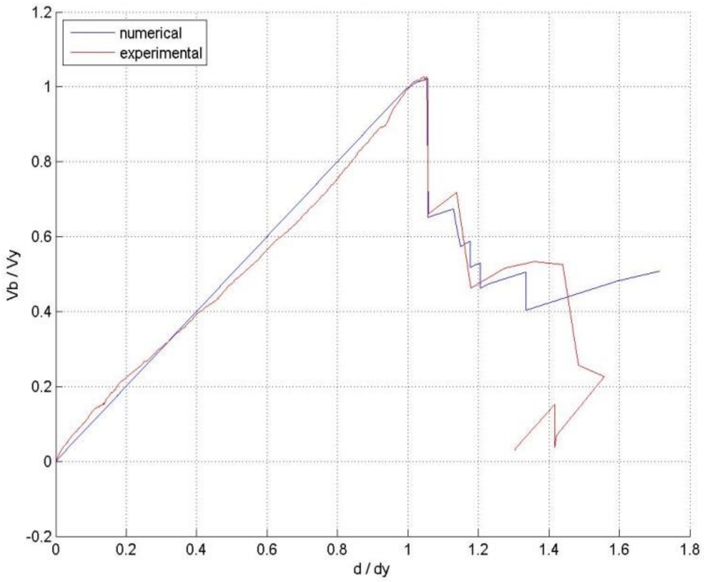

Figure A- 19 Base Shear- Top displacement curves for IP-A

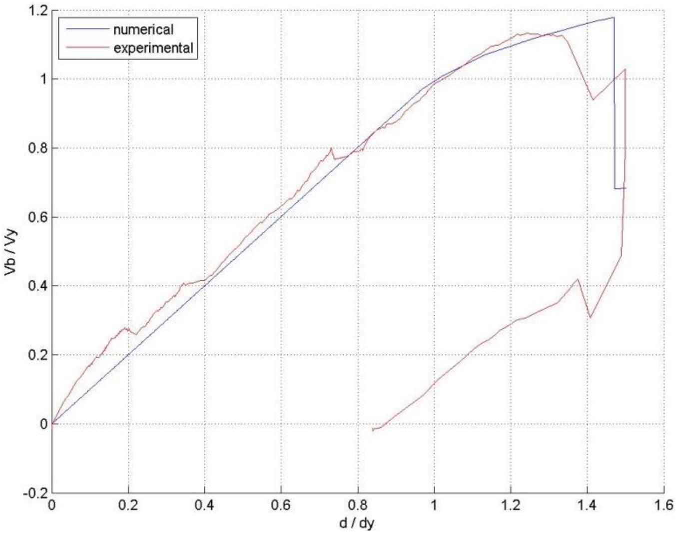

Figure A- 20 Base Shear- Top displacement curves for IP-B

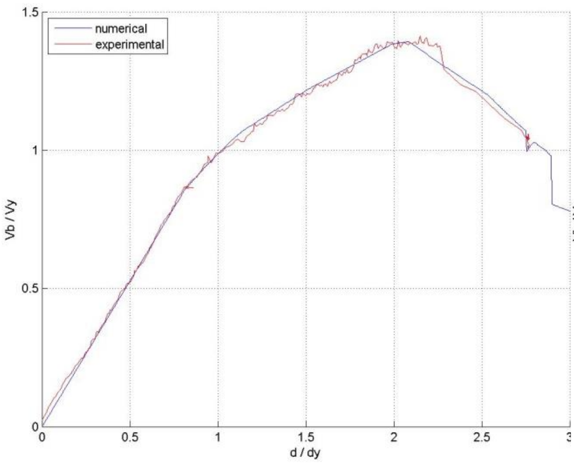

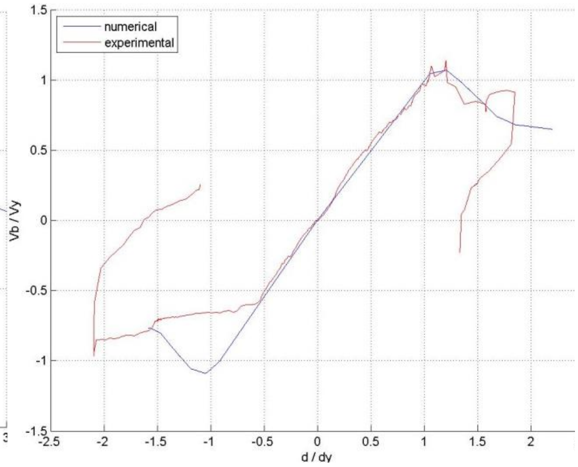

Figure A- 21 Base Shear- Top displacement curves for IP-C

a) configuration for high seismicity **b) configuration for medium seismicity**

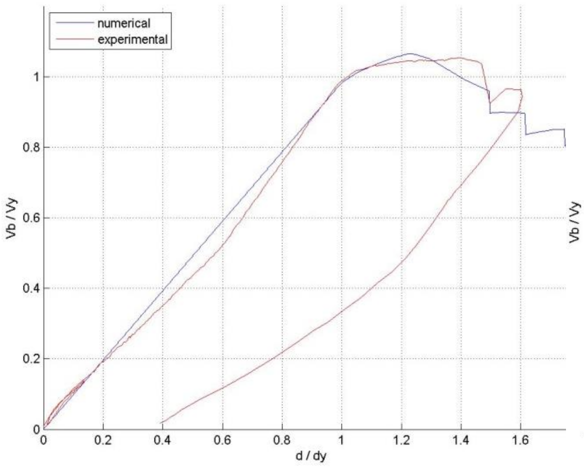

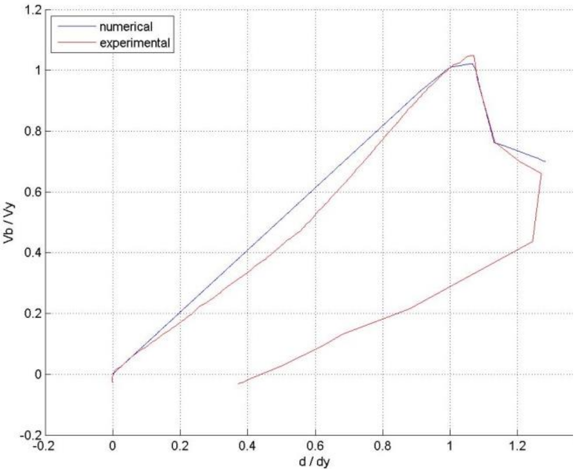

Figure A- 22 Base Shear- Top displacement curves for IP-D

c) configuration for high seismicity **d) configuration for medium seismicity**

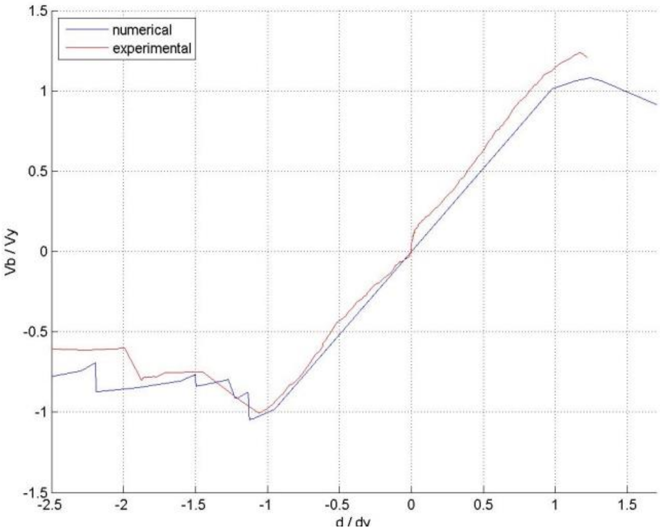

e) configuration for low seismicity

Industrial partner	A		B		C				D					
	-		-		High		Medium		High		Medium		Low	
$e1p-$s1p	1.00	1.00	1.00	1.00	1.00	1.00	1.00	1.00	1.00	1.00	1.00	1.00	1.00	1.00
$e2p-$s2p	1.00	1.07	1.12	2.00	1.55	3.00	1.00	3.00	1.00	1.76	1.00	2.14	1.05	2.14
$e3p-$s3p	0.22	2.86	0.20	3.00	0.64	10.00	0.42	10.00	0.37	5.88	0.80	2.86	0.19	2.86
$e1n-$s1n	-	-	-	-	-	-	-	-	-0.78	-0.88	-0.92	-0.71	-	-
$e2n-$s2n	-	-	-	-	-	-	-	-	-0.78	-1.76	-0.96	-1.43	-	-
$e3n-$s3n	-	-	-	-	-	-	-	-	-0.37	-5.88	-0.32	-4.29	-	-

Table A- 6 Used hysteretic parameters for the diagonals with notation from Figure A- 2

6.6 Calibration of full-scale systems

Using the data from the calibration of the specimen-tests (subassemblies) a numerical model is formed for each configuration of the IPs. The full scale configurations are composed of 2 bays and 4 storeys, fully loaded by 3 pallets of 800kg per compartment. Pushover analyses are performed for each model, following the same loading protocol (triangular distribution) as the full scale tests. The initial model for two braced and two unbraced racks present a very good match to the experimental results. However, the numerical models for two unbraced and two braced racks presented a completely different response than the corresponding experimental ones. These models were considered unreliable and were not further investigated. Figure A- 23 to Figure A- 26 present the fitted numerical results to the experimental ones. The presented configurations are the ones that are investigated in chapter 3 for dynamic analyses.

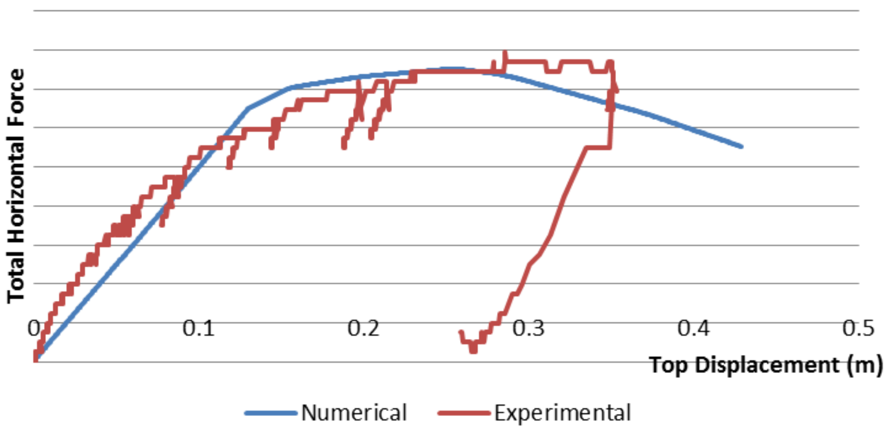

Figure A- 23 Total horizontal force vs. top displacement for the unbraced configuration IP A

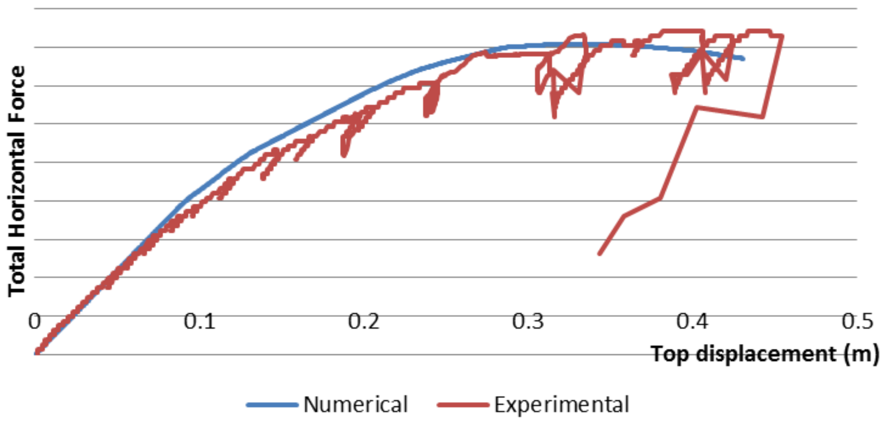

Figure A- 24 Total horizontal force vs. top displacement for the unbraced configuration IP B

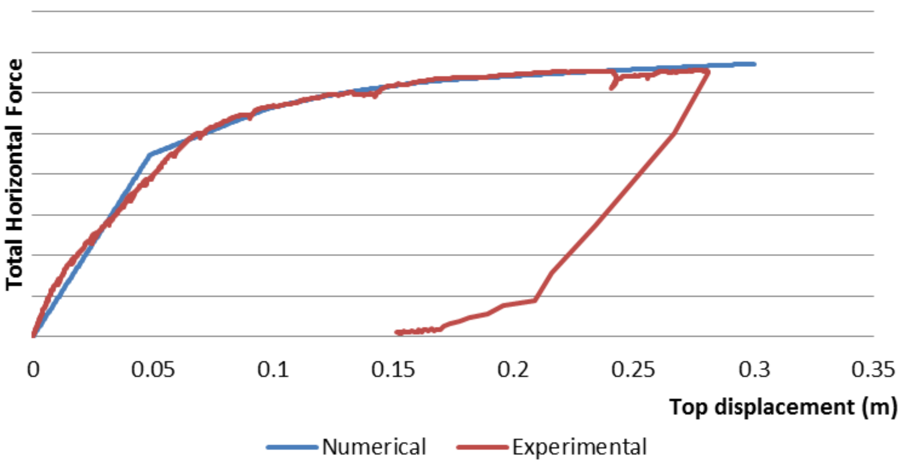

Figure A- 25 Total horizontal force vs. top displacement for the braced configuration IP A

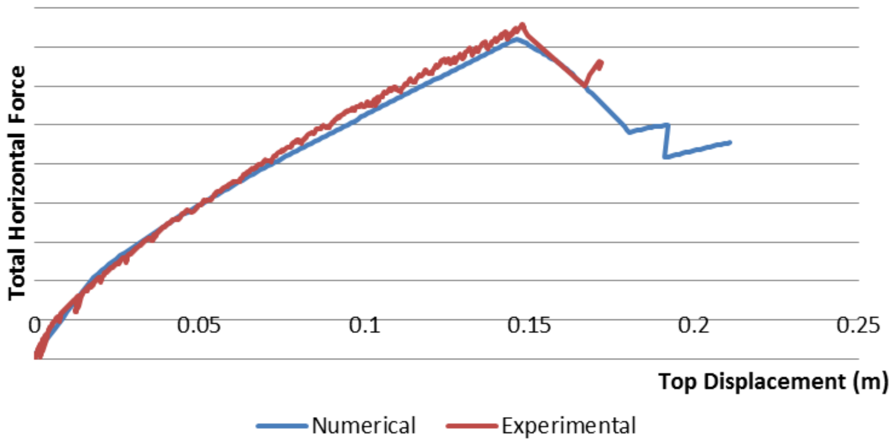

Figure A- 26 Total horizontal force vs. top displacement for the braced configuration IP D

6.7 Conclusions

The conclusion is that although the individual elements of the numerical models have been calibrated separately to the tests on subassemblies, when these elements are fitted together in a global model, they do not always provide similar results to the experimental ones of the full scale tests on complete racks. The major discrepancy presented at the initial-elastic stiffness of the experimental full scale models. Consequently, the dynamic characteristics of the systems could not always be reliably predicted and so the spectral accelerations too.

6.8 References

1. McKenna, F., Fenves, G. L., Scott, M. H., and Jeremic, B., (2000). Open System for Earthquake Engineering Simulation (OpenSees). Pacific Earthquake Engineering Research Center, University of California, Berkeley, CA.
2. ABAQUS/Standard User's Manual, Vol. I & II (ver. 5.4), (1994). Hibbit, Karlsson &Sorensen, Inc., Pawtucket, Rhode Island.
3. Naderpour, K. A. (2007)." Plastic hinge rotation capacity of reinforced concrete beams". International Journal of Civil Engineering, Vol. 5 No. 1, 30-47